Summary Final Report

Objective Operational Utilization of Satellite Microwave Scatterometer Observations of Tropical Cyclones

Vincent J. Cardone and Andrew T. Cox
Oceanweather Inc.
5 River Road
Cos Cob, CT 06807
Phone: 203-661-3091 fax: 203-661-6809 email: oceanwx@oceanweather.com
NASA/MSFC Order No. H-29389D of December 31, 1997

Submitted to

NASA MSFC
Attn: HR20
Marshall Space Flight Center, AL 35812

NASA/MSFC Order No. H-29389D of December 31, 1997

August 31, 2000

1. INTRODUCTION

This report summarizes research supported at Oceanweather Inc. and carried out nominally over a two-year period beginning in early 1999 and comprising a collaborative effort involving research teams at three institutions: Dr. Vincent J. Cardone and co-investigator Andrew T. Cox from Oceanweather Inc., Dr. W. Linwood Jones and co-investigators at the University of Central Florida (UCF), and Dr. Willard J. Pierson and co-investigators at the City College of City University of New York (CUNY). The research addresses two general problems: (1) the demonstration and improvement of scatterometer surface wind retrievals in tropical cyclones; (2) diagnosis of tropical cyclone planetary boundary layer (PBL) wind fields using a combination of high resolution NASA Scatterometer (NSCAT and its successor QuickScat) retrievals and a primitive equation vortex PBL numerical model. This research addresses the objectives of the US Weather Research Program (USWRP) related to improving hurricane forecasts near landfall including nowcasting storm intensity and tendency and prediction of hazards such as extreme winds and storm surge in coastal areas. The ultimate goal is to provide operational facilities, such as the NOAA Tropical Prediction Center, with improved methods for analyzing hurricanes and forecasting their movement and impact.

This report focuses on the contributions of Oceanweather Inc. to the collaborative program. Later this year an integrated team report will be submitted upon the termination of the part of program supported at CUNY.

The specific problems that must be solved to achieve the long-range goal may be stated as follows.

1. Demonstrate that high-resolution scatterometer measurements over tropical storms and other high-marine surface wind regimes when processed through an appropriate geophysical model function possess sufficient accuracy and dynamic range to be useful indicators of cyclone intensity and surface wind structure.

2. Develop a method which utilizes the high resolution scatterometer (from NSCAT and is successor

QuickScat) data acquired in a single pass over a tropical cyclone (TC) in a consistent way to diagnose basic storm intensity and size in terms of parameters routinely used by warning centers including maximum sustained surface wind, V_{mx}, and the radii of 35 and 50 knots sustained winds, R_{35} and R_{50}.

3. Utilize scatterometer data acquired in a succession of passes over a TC in a consistent way to specify the complete time and space evolution of the surface wind field over the sea suitable to drive ocean response and wind damage loss models thereby improving predictions of hazards to life and property from extreme winds, storm surge and coastal surf.

These objectives have been substantially demonstrated in the research completed to date as summarized in the next sections and documented in detail in publications and presentations supported by this program and additional papers in preparation. In addition, an important first step has been taken to implement the results of this research operationally by integrating the analysis methods developed in this study into a major team program initiated in 1999 under the Navy Ocean Partnership Program (NOPP) organized by Prof. H. C. Graber at the University of Miami. This NOPP program is entitled: "Real Time Forecasting of Winds, Waves, and Surges in Tropical Cyclone". The program includes the endorsement and participation of the NOAA Tropical Prediction Center and the NOAA/AOML Hurricane Research Division. Oceanweather Inc. are a critical member of the NOPP and are primarily responsible for developing the module to be used for operational analysis and prediction of the tropical cyclone wind fields. The early results of this program (a four-year NOPP program is planned) are to be reported in a paper in preparation for the AMS Annual Meeting, January 2001 (Abstract attached as Appendix D). Finally, we should note that the success of the early results of our research has evidently stimulated significant interest in the scientific community on the utilization of scatterometer data to study tropical cyclones.

2. DEVELOPMENT AND TESTING OF A NEW SCATTEROMETER GEOPHYSICAL MODEL FUNCTION AND WIND RETRIEVAL METHOD

2.1 Analysis of NSCAT in Typhoon Violet.

The model function development work was carried out mainly by Professor Jones and his colleagues after it was found that the NSCAT Project Baseline geophysical model function, NSCAT1, yielded wind speeds in tropical cyclones which were too low. As part of an early test of the new function Oceanweather developed a wind field for typhoon Violet in three NSCAT passes to develop the comparison database for the NSCAT evaluations. The wind fields utilized all conventional data available for those cases and its PBL vortex model. The new model function was developed from aircraft scatterometer data in a tropical cyclone and other supplementary data that indicated that the backscatter values measured in a tropical cyclone are much lower for a given wind speed and direction than the backscatter values were used in NSCAT-1. The new model function, called a neural net geophysical model function, was found to yield improved wind speeds in Typhoon Violet when applied with a Spatial Adaptive Retrieval Algorithm (SARA) which uses a-priori wind directions derived from Oceanweather's PBL model analysis, and a goodness of fit algorithm to filter out possible rain contaminated cells. SARA allows each individual backscatter value to be used to retrieve a wind speed.

The analysis of the validation wind field in Typhoon Violet and the SARA algorithm evaluation is documented in the following paper which appeared in the Journal of Geophysical Research special issue:

Jones, W.L., V. J. Cardone, W.J. Pierson, J. Zec, L.P.Rice, A.T. Cox, W.B. Sylvester, 1999: NSCAT High Resolution Surface Winds Measurements in Typhoon Violet. J. Geophys. Res., NSCAT Special Issue, 104,C5, 11247-11259.

This paper presented the analysis of NSCAT data in Revs. 478 and 485 which sampled much of the

circulation of Western North Pacific Typhoon Violet, a tropical cyclone that earlier had attained super-typhoon intensity but that at the time of these revs was of lower intensity with maximum sustained wind speeds of 90 knots. In the absence of aircraft reconnaissance data, the analysis of the surface wind "ground truth" relied on conventional data and the PBL model. The only use of NSCAT data in the surface wind analysis was a slight repositioning of the eye based on analysis of NSCAT sigma-0 profiles along constant incident angles by the CUNY group and research carried out by Mladen Susanj of the UCF team as described in more detail in the UCF report on this project.

The NSCAT data compared in Violet benefited from three new analysis features. First, the geophysical model function (called NMGMF at the time) was refitted and improved over the standard NSCAT-1 function by using backscatter measurements and coincident aircraft measurements of wind in hurricanes reduced to the surface using empirical flight-level 10 m reduction factors (Donnelly et al., 1998). According to the new function, the sigma-0 backscatter values are lower than NSCAT-1 for wind speeds greater than about 25 m/s but they increase very slowly with increasing wind speed even to wind speeds up to 40 m/s.

The second novel analysis feature is the Spatial Adaptive Retrieval Algorithm (SARA). Whereas the normal NSCAT processing produces wind vectors located on 50 km centers from groups of NSCAT cells, SARA recovers wind vectors at the intrinsic resolution of each sigma-0 cell, namely 8 km x 35 km cells sampled on 25 km centers along the satellite track. The wind direction alias removal step is averted because the field of vector wind direction is tightly constrained about a tropical cyclone and may be specified from a first guess PBL model solution as solved from conventional data only.

The third feature was the application of a "goodness of fit" algorithm to flag retrievals probably contaminated by heavy rain. Basically, this algorithm examines the anisotropy of four nearest neighbors of sigma-0 to determine whether one or more of the measurements are inconsistent within a 25 km grouping because of rain. This algorithm is described by Jones et al. (1999). The application of this algorithm to Violet indicated that even close to the main inner core of the circulation there are cells successfully retrieved because the beam is able to penetrate to the surface in areas of relatively

light rain or clouds between the spiral rain bands.

Figures 1 shows the retrieved wind field plots and Figure 2 shows scatter plot comparisons of retrieved and analyzed surface winds in the two Violet revs with the best coverage of NSCAT data. The field plots indicate that the SARA algorithm provides significant improvement in spatial sampling over the standard NSCAT processing over the high wind areas near the center. The scatter plots show that at least qualitatively, the PBL model winds are in good agreement with the new NSCAT retrievals with winds recovered with little bias up to wind speeds to 35 m/s although the NSCAT wind speeds still slightly underestimate the model winds above about 30 m/s. These plots refer to wind speeds as the "average" wind at 10 meters. Operational warning centers classify tropical cyclones in terms of "sustained" wind speeds, which are about 25% greater than the average wind speed. Our study of NSCAT in Violet demonstrates, therefore, that the "sustained" winds up to perhaps 45 m/s or about 90 knots may be sensed even close to the center.

2.2 Analysis of Hurricane Lili

The analysis of the PBL wind field in Typhoon Violet for the selected passes in October, 1996 could not benefit from the best in-situ wind data, namely reconnaissance aircraft data, because since 1986 there has been no aircraft reconnaissance of North Pacific Ocean tropical cyclones. During the formulation of this project in the Spring of 1997, it was expected that NSCAT would acquire data in several North Atlantic hurricanes during the 1997 season coincident with aircraft data. However, the early demise of NSCAT on June 30, 1997 precluded this prospect. Therefore, a thorough search was made for potentially useful NSCAT data acquired over tropical cyclones during its lifetime.

Oceanweather carried out this search using all available meteorological data and the outputs of various warning centers while UCF scanned the NSCAT data set. We were pleasantly surprised during this search to find a number of potentially interesting cases in the North Atlantic Ocean, including Gulf of Mexico and Caribbean Sea, including Tropical Cyclone Josephine, October 4-9, 1996 and Hurricane Lili, October 15-21, 1996. Because Tropical Cyclone Josephine exhibited

properties of extratropical structure, Hurricane Lili was selected for further analysis.

Hurricane Lili developed in the western Caribbean and moved across Cuba and into the southwest North Atlantic Ocean. Lili reached Category 3 intensity while under aircraft surveillance south of Bermuda with central pressure of 960 mb and maximum flight level wind speeds of 110 knots. A search of NSCAT data showed that Hurricane Lili was an excellent case for analysis and it was agreed by the team that Oceanweather should proceed to an intensive analysis of the PBL winds in this storm at the times of Revs 900 (0342 UTC, October 19), Rev 907 (1432 UTC October 19) and Rev 914 (0314 UTC October 20). The best-documented rev was rev 900 on October 19, 1996 because of the wealth of aircraft data. Figure 3 (a-d) shows the coverage of aircraft data within +/-6 hours of this rev and gives a comparison of the aircraft data and modeled winds for four different flight level-10 m reduction algorithms. The analysis of NSCAT data in this rev is presented in the following paper:

Cardone, V.J., A.T. Cox, W. J. Pierson, W. B. Sylvester, W.L. Jones and J. Zec.: NSCAT Scatterometer High Resolution Wind Fields for Hurricane Lili. IEEE IGARRS'99, Hamburg, Germany, June 28-July 2, 1999, 1509-1513.

Figure 4 (from this paper) shows the modeled wind field solution and the retrieved winds using a new Tropical Cyclone Geophysical Model Function (TC-GMF) (Zec and Jones, 1999) and the SARA algorithm. Figure 5 shows the comparison of the retrieved winds speeds and the model wind speeds at each SARA cell which passed the rain filter. This comparison confirms the basic properties of the NSCAT winds with the new model function, namely good wind speed sensitivity up to wind speeds of at least 20 m/s and a small bias above 25 m/s. Above 25 m/s, the bias in the retrieved wind speeds is only 0.1 m/s or TC-GMF compared to a bias of –5.32 m/s or NSCAT-1b.

2.3 North Sea NSCAT vs. Offshore Platform High Wind Speeds

The new model function used for the analyses summarized above was derived from the assumption that the NSCAT-1 model function is correct in the low to moderate wind speed range and used aircraft scatterometer data sets at higher wind speeds (up to 35 m/s). Beyond 35 m/s the new l function is an extrapolation. An important difficulty is this approach is that the aircraft winds are reduced to 10 m from flight level using an empirical algorithm. This process introduces an uncertainty and potential bias in the reference 10 m wind speeds above about 20 m/s. Meanwhile, the validation of scatterometer winds have generally utilized comparison data sets assembled from data buoys and research vessels that are generally limited to 10- m neutral wind speeds of 20 m/s or less. For example, Freilich and Dunbar (1999) found only 184 out of 56,000 NSCAT-buoy collocations with 10-m buoy winds exceeding 18 m/s and virtually none above 22 m/s. Validation is further complicated by evidence that buoy wind speeds may be biased low in high sea states. Our evaluation of the sensitivity and accuracy of scatterometer winds above 20 m/s or so by comparison of winds from the cyclone PBL model in tropical cyclones is encouraging; however, the lack of high-wind speed in-situ data sets coincident with NSCAT and QuickScat hampers further refinements of the backscatter model function.

To ameliorate this lack of in-situ data at very high wind speeds, as part of this research program we assembled a unique comparison database for NSCAT wind validation at high wind speeds. This data set utilized winds measured from offshore platforms in the open Northern North Sea and Southern Norwegian Sea. Of the dozens of platforms which make and report synoptic observations in this region, we selected only nine platforms at each of which a calibrated anemometer is well exposed at the top of the drilling derrick (the height range is 86-m to 143-m) and quality-controlled continuous time average wind samples are archived by and available from European weather centers. Collocation of the NSCAT 25-km database with the platform database yielded 3663 (2773) matches for separation distances of 25-km and time offsets up to 1.5 (0.5) hours. Using Liu's reduction to 10-m equivalent neutral wind, 110 matches are found for wind speeds above 20 m/s and 37 matches for wind speed above 24 m/s. However, because in some regimes the anemometer may be above the

surface boundary layer, four different stability-dependent wind profile models were used in the analysis, including a model that extends the wind profiles into the Ekman layer. The data were analyzed and reported to the AGU 2000 Spring Meeting, May 30-June 3, 2000, Washington, DC (Cardone et al., 2000).

The NSCAT-platform winds were compared in terms of scatter plots, regressions on bin-averaged data and comparisons of wind speed and platform wind speed distributions in terms of quantile-quantile scatter plots. For a selected set of 58 passes during particularly intense storms, the number of collocations was greatly expanded (about 10,000 matches) by analyzing the platform data into a continuous field using the natural neighbor objective analysis system. Figure 6 shows one of these high-wind speed revs (February 16, 1997, 2100 GMT) and Figure 7 shows the time history of measured winds at one site (drill-ship "Polar Pioneer"). Average wind speeds up to 45 m/s were measured at anemometer height of 92 m in this event and were reduced to 10 m using the four different profile forms noted above. Figure 8 shows the NSCAT (using NSCAT-1 model function) versus platform wind speeds over all available comparisons (all revs in the mission). The standard deviation of the difference in wind speeds is only 1.5 m/s but there is a clear low bias in the NSCAT-1 winds above about 15 m/s. This high wind speed negative bias is also shown in the distributional comparisons (quantile-quantile plots) given in Figure 9 for the difference profile forms. This pilot study confirms that North Sea platform data may be used to supplement cyclone aircraft data to refine the model function at high wind speeds. Unfortunately, the four different profile forms used do not yield the same 10-m wind speeds for a given stability and anemometer level measurement. Experiments are underway in Canada to resolve the difference between platform and buoy derived estimates of the 10-m wind and in the UK to study the flow distortion (if any) contribution to winds measured from offshore platforms.

During the Northern Hemisphere winter sensed by QuickScat, 1999/2000, a number of very intense and damaging storms crossed from the North Atlantic Ocean over the North Sea and into NW Europe and it is therefore possible to produce a data set such as assembled here for validation of QuickScat and further refinement of the model function.

Appendix A gives copies of key viewgraphs presented the AGU conference. A paper is being prepared for submission to the next JGR special issue as follows:

Accuracy of Scatterometer Winds Assessed from In-Situ Measured Wind Data Up to 32 m/s

V.J.Cardone, E.A. Ceccacci, A.T. Cox, J. G. Greenwood

3. INVERSE MODELING OF TROPICAL CYCLONE WIND FIELD FROM QUICKSCAT

3.1 Approach

The inverse model developed and tested in this study to diagnose the inner core structure of a tropical cyclone from scatterometer data utilizes the most recent update of Oceanweather's tropical cyclone PBL model (Thompson and Cardone, 1996) hereinafter TC96. This model solves the primitive equations of motion representing the vertically integrated PBL on a nested rectangular grid in a moving coordinate system centered on the storm. Vertical and lateral friction are included. The model resolution of the inner core structure on the inner grid nest is 2 km . The model is driven by a specification of the following parameters (see TC96, p. 202 for a theoretical description of the model and its initialization):

V_{spd}, V_{dir}	speed and direction of vortex motion
V_{gs}, D_{gs}	equivalent geostrophic flow of the ambient PBL pressure field in which the vortex propagates
D_p	total storm pressure anomaly
dp1	pressure anomaly associated with the first component of the exponential radial pressure profile
R_{p1}, R_{p2}	scale radii of the up to two components of the exponential radial pressure profile
B_1, B_2	Holland's (1980) profile peakedness parameter for each component

The problem may be posed as follows. Given only scatterometer winds acquired in a pass over the TC, standard warning center satellite derived Dvorak estimates of intensity (as a first guess) at the time of the pass, and conventional synoptic data available on the periphery of the circulation, how may TC96 be used in an "inverse" sense to develop refined estimates of storm intensity (i.e. maximum sustained eye-wall wind speeds) and size, namely R_{p1}, $R_{p2, R35}$, $R_{50.}$ By inverse modeling, we mean an objective algorithm that seeks and selects the optimum TC96 forcing variables above,

which when applied to TC96, return a surface wind field that exhibits minimum difference, in a least squares sense, between the model winds and the scatterometer winds. Such an inverse modeling procedure has already been constructed (Cardone et al. 1994) for the case when only dropsonde central pressure and the radial profile of the flight level wind as measured by an aircraft are known. That problem is somewhat simpler than the scatterometer problem because in the scatterometer case the maximum eye-wall wind speed is not known if the wind speed is in the model function saturation range. We assume here that rain contamination and possibly model function saturation for the more intense storms prevents direct retrieval of this quantity (it is approximated by the Dvorak estimate), whereas when there is aircraft reconnaissance of a cyclone, the aircraft almost always penetrates the eye-wall on a radial leg and accurately measures the flight level wind in the eye-wall.

The preliminary results carried out with the neural net algorithm summarized above suggests that average wind speeds up to 25 m/s may be routinely retrieved with little bias in tropical cyclones, but it is not yet clear that wind speeds above 30 m/s will be retrievable. Therefore, we have developed a preliminary design for an inverse model which seeks to find solutions of TC96 which best match the azimuthally averaged scatterometer wind field in areas of wind speeds of less than 20 m/s (1-hour average at 10 m, not sustained). This part of the circulation includes the areas of the operationally significant radius of the 35 knot and 50 knot sustained winds. The inverse model required the generation of over 30,000 TC96 model solutions covering the following model parameter (single exponential only) space:

Latitude	20 degrees
V_{spd}, V_{dir}	stationary
V_{gs}, D_{gs}	stationary
D_p	2 to 120 mb in 2 mb increments
R_p	5 nm to 120 nm in 4 nm increments
B	1 to 2.5 in 0.1 increments
H	500 m (boundary layer depth)
Dif	-2 C (air-sea temperature)

For each solution the following information was saved:

Maximum surface wind
Radius of maximum wind
Azimuthally averaged wind speed in 5 nm bins
Radius (maximum) of 35 knot winds
Radius (maximum) of 50 knot winds

A preliminary working algorithm was applied which matched only scatterometer and model radii of 35 and 50 knot winds but we found a better solution was obtained by matching the entire azimuthally averaged wind profile over the valid range of wind speeds in an rms sense.

3.2 Application of Inverse Model to Floyd (1999) using QuickScat

3.2.1 General History of Floyd

Floyd was a large and very intense Cape Verde type hurricane that formed on September 7, 1999 in the eastern North Atlantic and later seriously threatened the southeast US coast triggering evacuations of millions of people. Floyd attained the high-end of Category 4 status with peak sustained winds of 135 knots east of the Bahamas on September 13, 1999. The system weakened slowly thereafter and induced immense flooding as it entered North Carolina on September 16 with peak sustained wind speeds of about 90 knots. Floyd caused 56 deaths and 3-6 billion dollars of property damage in the United States.

Almost continuous aircraft monitoring of Floyd from September 8 through the 16th defined the position, central pressure, maximum eye-wall wind speed and two-dimensional wind field structure of the storm. Those data allowed the NOAA AOML Hurricane Research Division to construct 31 "snapshots" between September 9 and 16 of the sustained wind field at 10 m over water using a

method (Powell et al., 1998) which consists of objective analysis of mainly surface winds extrapolated from the aircraft flight level winds using empirical reduction factors. Figure 10 for 1330 UTC 13 September gives an example of these wind fields. We have used these snapshots to construct a time and space continuous representation of the wind field to serve as a basis for the evaluation of wind fields inverse modeled from the QuickScat data.

3.2.2 Inverse Model Fits

All QuickScat passes over the North Atlantic between September 8 and 16 were downloaded from the JPL distribution center. It was found that because of the wide swath of QuickScat, at least part of the storm circulation was viewed at least twice per day, with pass times typically near 00, 09, 12 and 21 UTC. Appendix B shows the coverage of the QuickScat data for each of the 32 data swaths for which there was data within about 360 nm of the center of the storm. For about half of these passes, the center of Floyd and its entire inner core circulation are well sampled except, of course, for the gaps which indicate the rain flag was set (we used the preliminary QuickScat processing for this study, not the more recently reprocessed data which only became available during summer of 2000).

The QuickScat data were azimuthally averaged within 360 nm of the center in 5 nm bins (we used the official fix, though in a case without aircraft data, satellite images or the sophisticated processing of the scatterometer data developed at UCF may be used to infer a center). Since we are using standard processed QuickScat data that uses essentially the old NSCAT-1 model function there is the possibility of attenuation/saturation of the winds speeds above 20 m/s. Only QuickScat bins with azimuthally averaged wind speed less than 20 m/s were used as a conservative way to omit QuickScat data which might have saturated. Also, passes for which no data were retrieved within 150 nm of the center were discarded. Only 7 of the passes were discarded for this reason.

As noted above, the simple inverse model developed involves matching the azimuthally averaged QuickScat radial wind speed profile with precomputed TC96 model azimuthally averaged radial wind speed profiles in a least squares minimization sense given only the location of the center and the

equivalent Dvorak estimate of eye-pressure. Figure 11 shows the best match near 0000 September 10, early in the life of Floyd when wind speeds even near the center were less than 20 m/s (hourly average). The profile radius and shape parameters selected are indicated on this plot. Figure 12 is an example match near 2100 UTC September 11. In this case even though the azimuthally averaged QuickScat winds greater than 20 m/s were not used, the best- matched profile gives azimuthally average peak winds of about 29 m/s at a radius of maximum wind (Rmx) of about 35 nm. Interestingly, the QuickScat data in the vicinity of Rmx also average to about 30 m/s. However, the case for Floyd near peak intensity shown in Figure 13 indicates that the inverse model provides maximum azimuthally average wind speeds of 47 m/s while the QuickScat wind speeds there average only to about 30 m/s. In fact, it would appear that within 120 nm the of the center, the QuickScat winds in this pass are biased low but there is sufficient information in the profile outside that radius to allow the inverse model to recover the inner-core structure. All of the inverse model fits developed are included in Appendix B.

Each of the inverse model fits provides the critical model "snapshot" profile parameters. To these must added the storm motion vector (taken from the past track) and the background pressure field (taken from standard large scale NOAA NWP fields). Then the TC96 model is solved for each snapshot of the actual wind fields and these snapshots are interpolated to a regular grid of spacing of 0.125 degree and to 30-minute time intervals using OWI's standard software for this purpose.

3.2.3 Comparison of Inverse Model Wind Fields and QuickScat Winds

The snapshots wind fields corresponding to each QuickScat pass may be compared to the individual QuickScat retrieved winds. This direct comparison is shown in Figure 14 for all snapshots recovered. As expected, the higher QuickScat winds are lower than the model winds. Over these 13,502 comparisons, the mean difference (Quickscat inverse model field – QuickScat individual retrievals) is 0.81 m/s and the standard deviation of the difference is 3.63 m/s and much of this scatter arises in data pairs above 20 m/s in which range the QuickScat data are biased and relatively inaccurate.

3.2.4 Comparison of Inverse Model Wind Fields and HRD Wind Fields

While the HRD winds do not constitute an absolute standard for verification, they do provide a measure of the success of our inverse model to utilize QuickScat data to diagnose the complete two-dimensional surface wind field in a severe tropical cyclone. Comparisons of HRD derived wind fields and inverse model wind fields are presented at the times of the 24 HRD snapshots in Appendix C between September 11 and September 16. Each wind is shown as a vector and wind speed differences are color-coded. The statistical differences between the HRD and inverse model winds speeds and directions over the domains shown and for the times shown in Appendix C are given in Table 1. There are generally between 6000 and 7000 grid point comparisons for each snapshot. For example, near the peak of the storm on September 13 there are four snapshot comparisons at around 00UTC, 13UTC, 19UTC and 22 UTC. The mean differences in wind speed (Inverse model-HRD) are 3.23 m/s, -.2.31 m/s, 0.61 m/s and 1.00 m/s respectively. The standard deviations of the wind speed differences are: 2.34 m/s, 4.38 m/s, 2.70 m/s and 2.57 m/s while the correlation coefficients for wind speed are .94, .80, .91, and .92. The mean wind direction differences are -.75 deg, -3.29 deg, -8.36, -11.42. These differences are in the sense that there is more inflow in the model winds than in the reduced aircraft winds and this may well reflect insufficient turning of the aircraft winds toward the surface in the HRD analyses. Over all snapshots, the differences are:

Wind speed bias (QuickScat inverse model-HRD)	2.79 m/s
Wind speed difference standard deviation	2.63 m/s
Wind speed scatter index	.17
Wind speed correlation coefficient	.92
Wind direction mean difference	-5.6 degrees
Wind direction difference standard deviation	16. Degrees

These statistics indicate a close statistical match between the QuickScat derived inverse model winds and the HRD aircraft derived winds. The difference plots of Appendix C indicate that the wind differences within a given snapshot display occasionally large spatially coherent differences, and

these may arise from a number of causes including: (1) failure of the TC96 model to simulate smaller scale spiral bands which are indeed sensed by the aircraft; (2) HRD wind errors in storm quadrants which might not have been probed by the aircraft in the composite of data used for a given snapshot; (3) slight positioning differences of wind field features which have been qualitatively well modeled in both field. What is encouraging, however, is that the coherent spatial differences appear not to have much coherency in time from snapshot to snapshot, suggesting that such errors will have minimal impact on ocean response models forced by the QuickScat winds.

4. CONCLUSIONS AND RECOMMENDATIONS FOR FURTHER RESEARCH

We may now restate the specific problems addressed and summarize the results achieved.

Demonstrate that high-resolution scatterometer measurements over tropical storms and other high-marine surface wind regimes when processed through an appropriate geophysical model function possess sufficient accuracy and dynamic range to be useful indicators of cyclone intensity and surface wind structure.

The analysis of NSCAT data sets in Typhoon Violet and Hurricane Lily have demonstrated that accurate scatterometer measurements of surface wind are possible even near the inner core of intense tropical cyclones for wind speeds up to about 35 m/s, but this dynamic range requires a geophysical model function different in its tuning at high winds than used operationally for NSCAT and QuickScat, and a spatial adaptive retrieval algorithm which utilizes the fact that the vector wind direction is so tightly constrained in the inner core of mature tropical cyclones that wind direction can be assumed to be prescribed accurately independently of the remote sensing data and utilized to resolve surface winds at the highest spatial resolution allowed by the scatterometer cell footprint. The filtering of rain-contaminated cells remains a daunting problem but the UCF goodness of fit algorithm used in this study allows useful high wind retrievals even near the cyclone center. However, operational NSCAT and QuickScat winds remain biased low at wind speeds above about 20 m/s and we recommend additional studies to develop a more accurate model function at high wind speeds. A pilot study using North Sea platforms to validate NSCAT data during the winter 1996/97 suggests that such data may be used to refine the QuickScat model function.

Develop a method which utilizes the high resolution scatterometer (from NSCAT and is successor QuickScat) data acquired in a single pass over a tropical cyclone (TC) in a consistent way to diagnose the surface wind field in the inner core and far-field.

The coupling of a highly tuned and proven dynamical model of the cyclone PBL (TC96) with the operational QuickScat data has led to an inverse model which recovers a snapshot of the asymmetric surface wind field from a QuickScat pass over a cyclone provided the circulation within 150 km of the center is included in the swath. The wind field including the eyewall region is recovered with wind speed bias and scatter of about 2.5 m/s and wind direction bias and scatter of about 5 Degrees and 15 Degrees respectively, all relative to a reference wind field snapshot derived objectively from copious aircraft flight level winds reduced to 10 m.. The wind field allows accurate recovery of the storm intensity and size parameters routinely used by warning centers including maximum sustained surface wind, V_{mx}, and radii of 35 and 50 knots sustained winds, R_{35} and R_{50}. In addition to the QuickScat data, the method requires knowledge of the position of eye of the storm, and an accurate Dvorak type estimate of intensity from which may be specified an estimate of eye pressure. We suggest that reprocessing of QuickScat with the improved model function developed at UCF will yield an even greater dynamic wind speed range and even more accurate inverse model parameters. We recommend the analysis of additional tropical cyclones after the improved model function is implemented.

Utilize scatterometer data acquired in a succession of passes over a TC in a consistent way to specify the complete time and space evolution of the surface wind field over the sea suitable to drive ocean response and wind damage loss models thereby improving predictions of hazards to life and property from extreme winds, storm surge and coastal surf.

It has been demonstrated through our Hurricane Floyd case study that QuickScat data may be used to inverse model the complete life-cycle of the surface wind field in a typical very intense North Atlantic hurricane. We recommend study of additional cases of this type, including application of the derived wind fields to force ocean response models for surface waves, continental shelf currents and coastal storm surge and validation of the ocean response predictions against measurements.

This study represents an important first step toward the operational implementation of the analysis methods developed in this study. The operational aspects of this work are being continued under a

major team program initiated in 1999 under the Navy Ocean Partnership Program (NOPP) entitled: "Real Time Forecasting of Winds, Waves, and Surges in Tropical Cyclones". The program includes the endorsement and participation of the NOAA Tropical Prediction Center and the NOAA/AOML Hurricane Research Division. The early results of this program are to be reported in a paper in preparation for the AMS Annual Meeting, January 2001.

REFERENCES

Cardone, V. J., A. T. Cox, J. A. Greenwood and E. F. Thompson (1994): Upgrade of the tropical cyclone surface wind model, Miscellaneous paper CRC-94-14, U. S. Army Engineers Waterways Experiment Station, Vicksburg, MS.

Cardone, V.J., A.T. Cox, W. J. Pierson, W. B. Sylvester, W.L. Jones and J. Zec.: NSCAT Scatterometer High Resolution Wind Fields for Hurricane Lili. IEEE IGARRS'99, Hamburg, Germany, June 28-July 2, 1999, 1509-1513.

Donnely, W.J., J. R. Carswell, R. E. Mcintosh, P. S. Chang, J. Wilkerson, F. Marks, and P. G. Black, 1999: Revised ocean backscatter models at C and Ku band under high-wind conditions. J. Geophys. Res., NSCAT Special Issue, 104,C5, 11485-11498

Jones, W.L., V. J. Cardone, W.J. Pierson, J. Zec, L.P.Rice, A.T. Cox, W.B. Sylvester, 1999: NSCAT High Resolution Surface Winds Measurements in Typhoon Violet. J. Geophys. Res., NSCAT Special Issue, 104,C5, 11247-11259.

Powell, M. D., S. H. Houston, L. R. Amat and N. Morriseau-Leroy, 1998: The HRD real time hurricane wind analysis system. J. Wind. Eng. and Industr. Aerodyn., 77&78, 53-64.

Thompson, E. F. and V. J. Cardone (1996): Practical modeling of hurricane surface wind fields, J. of Water. Port, Coast., and Ocean Eng.,122(4),195-205.

Zec, J. and W. L. Jones, 1999: Tropical cyclone geophysical model function for ocean surface wind retrievals from NASA scaterometer measurements at high wind speeds. IGARSS'99, Hamburg, Germany, june 28-July 2, 1999.

Table 1. Differences in Hurricane Floyd (1999) between OWI 10 m average wind fields inverse modeled from QuickScat and NOAA HRD 10 m average wind fields derived from aircraft data. QuickScat derived wind fields are interpolated in space and time to the grid and times of the 24 available HRD snapshots.

	Station	Grid Point	Number of Pts	Mean Meas	Mean Hind	Diff (H-M)	RMS Error	Stnd Dev	Scat Index	Ratio	Corr Coeff
Hindcast Period : 1999091101 to 1999091101											
Wind Spd. (m/s)	Combined	0	7055	16.30	17.02	0.72	2.33	2.22	0.14	0.60	0.88
Wind Dir. (deg)	Combined	0	7055	83.01	60.38	-7.83	N/A	9.51	0.03	N/A	N/A
Hindcast Period : 1999091113 to 1999091113											
Wind Spd. (m/s)	Combined	0	7055	16.99	20.44	3.44	4.15	2.31	0.14	0.96	0.93
Wind Dir. (deg)	Combined	0	7055	73.47	57.02	-7.03	N/A	9.88	0.03	N/A	N/A
Hindcast Period : 1999091119 to 1999091119											
Wind Spd. (m/s)	Combined	0	7055	10.99	13.94	2.94	3.64	2.14	0.19	0.89	0.91
Wind Dir. (deg)	Combined	0	7055	102.86	90.15	-20.49	N/A	12.35	0.03	N/A	N/A
Hindcast Period : 1999091201 to 1999091201											
Wind Spd. (m/s)	Combined	0	6723	13.51	14.72	1.21	2.13	1.75	0.13	0.77	0.94
Wind Dir. (deg)	Combined	0	6723	76.97	92.95	-7.98	N/A	13.44	0.04	N/A	N/A
Hindcast Period : 1999091213 to 1999091213											
Wind Spd. (m/s)	Combined	0	6723	20.60	23.48	2.88	3.67	2.28	0.11	0.88	0.89
Wind Dir. (deg)	Combined	0	6723	77.56	60.87	-14.16	N/A	8.24	0.02	N/A	N/A
Hindcast Period : 1999091219 to 1999091219											
Wind Spd. (m/s)	Combined	0	7055	12.94	16.02	3.08	3.77	2.18	0.17	0.96	0.94
Wind Dir. (deg)	Combined	0	7055	90.67	92.83	1.75	N/A	11.96	0.03	N/A	N/A
Hindcast Period : 1999091300 to 1999091300											
Wind Spd. (m/s)	Combined	0	6889	13.18	16.41	3.23	3.98	2.34	0.18	0.97	0.94
Wind Dir. (deg)	Combined	0	6889	97.05	102.55	-0.75	N/A	11.97	0.03	N/A	N/A
Hindcast Period : 1999091313 to 1999091313											
Wind Spd. (m/s)	Combined	0	7055	18.23	15.91	-2.31	4.96	4.38	0.24	0.23	0.80
Wind Dir. (deg)	Combined	0	7055	76.77	99.62	-3.29	N/A	13.49	0.04	N/A	N/A
Hindcast Period : 1999091319 to 1999091319											
Wind Spd. (m/s)	Combined	0	7055	16.04	16.64	0.61	2.77	2.70	0.17	0.56	0.91
Wind Dir. (deg)	Combined	0	7055	69.07	99.22	-8.36	N/A	11.54	0.03	N/A	N/A
Hindcast Period : 1999091322 to 1999091322											
Wind Spd. (m/s)	Combined	0	6723	16.13	17.13	1.00	2.76	2.57	0.16	0.76	0.92
Wind Dir. (deg)	Combined	0	6723	78.45	97.86	-11.42	N/A	11.30	0.03	N/A	N/A
Hindcast Period : 1999091401 to 1999091401											
Wind Spd. (m/s)	Combined	0	7055	14.49	16.88	2.40	3.18	2.09	0.14	0.87	0.96
Wind Dir. (deg)	Combined	0	7055	51.84	95.18	-0.61	N/A	15.91	0.04	N/A	N/A
Hindcast Period : 1999091416 to 1999091416											
Wind Spd. (m/s)	Combined	0	7055	15.58	18.38	2.80	3.57	2.21	0.14	0.91	0.95
Wind Dir. (deg)	Combined	0	7055	95.46	86.99	-11.83	N/A	11.94	0.03	N/A	N/A
Hindcast Period : 1999091419 to 1999091419											
Wind Spd. (m/s)	Combined	0	7055	14.88	18.58	3.70	4.27	2.14	0.14	0.96	0.95
Wind Dir. (deg)	Combined	0	7055	97.02	85.65	-10.20	N/A	10.69	0.03	N/A	N/A
Hindcast Period : 1999091501 to 1999091501											
Wind Spd. (m/s)	Combined	0	7055	14.46	19.08	4.62	5.28	2.57	0.18	0.98	0.93
Wind Dir. (deg)	Combined	0	7055	82.92	81.80	-9.10	N/A	12.47	0.03	N/A	N/A
Hindcast Period : 1999091504 to 1999091504											
Wind Spd. (m/s)	Combined	0	7055	14.88	18.95	4.07	4.80	2.55	0.17	0.98	0.93
Wind Dir. (deg)	Combined	0	7055	49.03	77.17	-4.82	N/A	18.76	0.05	N/A	N/A
Hindcast Period : 1999091507 to 1999091507											
Wind Spd. (m/s)	Combined	0	6640	15.68	19.39	3.72	4.16	1.88	0.12	0.98	0.96
Wind Dir. (deg)	Combined	0	6640	73.40	99.80	-7.39	N/A	17.12	0.05	N/A	N/A
Hindcast Period : 1999091510 to 1999091510											
Wind Spd. (m/s)	Combined	0	6308	15.81	19.62	3.82	4.67	2.69	0.17	0.96	0.92
Wind Dir. (deg)	Combined	0	6308	96.29	101.17	-6.12	N/A	16.13	0.04	N/A	N/A
Hindcast Period : 1999091513 to 1999091513											
Wind Spd. (m/s)	Combined	0	6225	16.19	19.58	3.40	4.12	2.33	0.14	0.92	0.94
Wind Dir. (deg)	Combined	0	6225	90.86	104.19	0.42	N/A	18.74	0.05	N/A	N/A
Hindcast Period : 1999091516 to 1999091516											
Wind Spd. (m/s)	Combined	0	6225	18.50	19.59	1.08	3.80	3.64	0.20	0.61	0.84
Wind Dir. (deg)	Combined	0	6225	172.97	113.17	-8.56	N/A	20.77	0.06	N/A	N/A
Hindcast Period : 1999091519 to 1999091519											
Wind Spd. (m/s)	Combined	0	5976	15.47	19.73	4.26	4.95	2.52	0.16	0.94	0.92
Wind Dir. (deg)	Combined	0	5976	135.74	112.81	-0.80	N/A	20.61	0.06	N/A	N/A
Hindcast Period : 1999091522 to 1999091522											
Wind Spd. (m/s)	Combined	0	6225	15.78	19.32	3.53	4.53	2.83	0.18	0.89	0.90
Wind Dir. (deg)	Combined	0	6225	135.52	106.76	-4.89	N/A	17.58	0.05	N/A	N/A
Hindcast Period : 1999091601 to 1999091601											
Wind Spd. (m/s)	Combined	0	6640	14.54	19.84	5.30	6.34	3.47	0.24	0.98	0.89
Wind Dir. (deg)	Combined	0	6640	114.15	98.00	-0.18	N/A	19.33	0.05	N/A	N/A
Hindcast Period : 1999091604 to 1999091604											
Wind Spd. (m/s)	Combined	0	6806	14.07	17.90	3.83	4.80	2.89	0.21	0.94	0.91
Wind Dir. (deg)	Combined	0	6806	155.29	95.88	4.42	N/A	28.09	0.08	N/A	N/A
Hindcast Period : 1999091607 to 1999091607											
Wind Spd. (m/s)	Combined	0	6723	14.00	17.76	3.77	4.81	2.98	0.21	0.97	0.90
Wind Dir. (deg)	Combined	0	6723	205.67	94.06	5.35	N/A	32.24	0.09	N/A	N/A

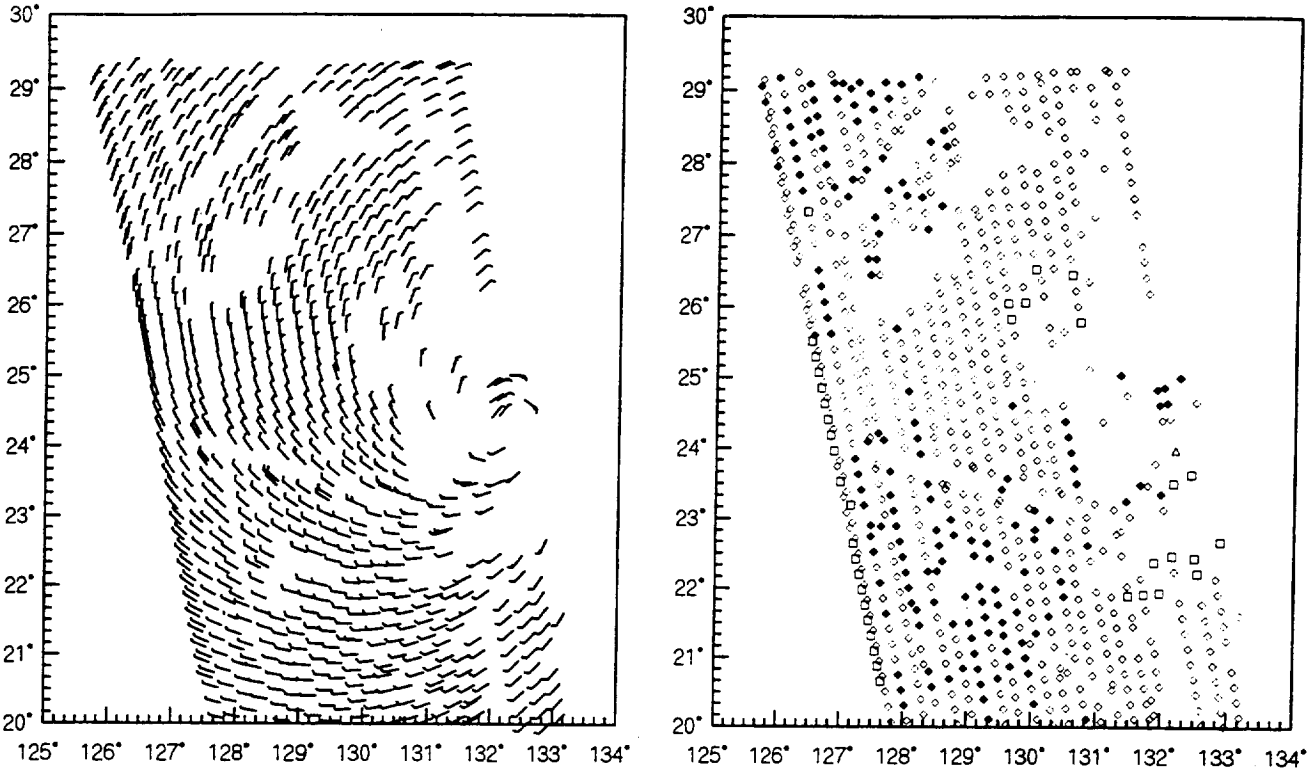

$SARA_{max}$ wind retrievals using NNGMF model function and TC96 wind directions for Violet revolution 478, showing (left) $SARA_{max}$ wind vectors and (right) wind speed differences between TC96 and $SARA_{max}$. Open triangle denote < -10 m s^{-1}, open squares represent -10 to -5 m s^{-1}, and open diamonds denote -5 to 0 m s^{-1}. Solid symbols correspond to positive differences.

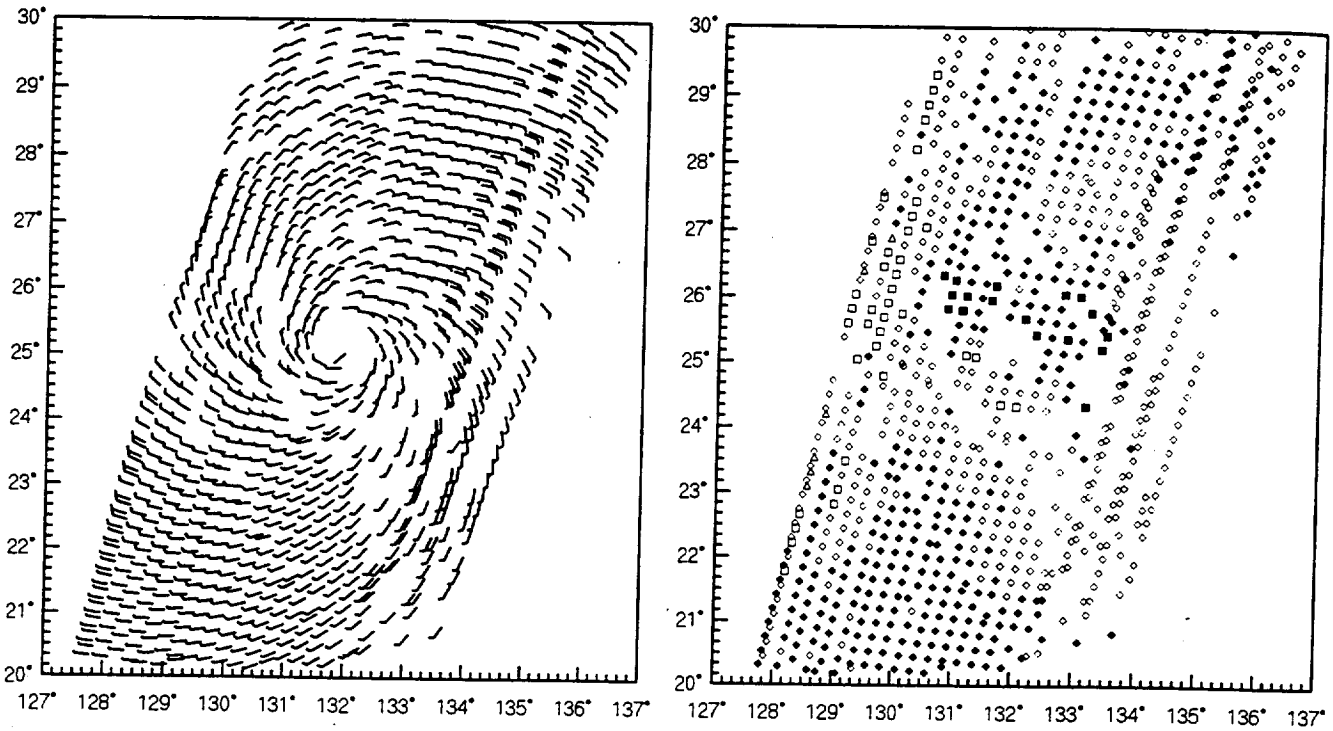

$SARA_{max}$ wind retrievals using NNGMF model function and TC96 wind directions for Violet revolution 485, showing (left) $SARA_{max}$ wind vectors and (right) wind speed differences between TC96 and $SARA_{max}$. Open triangles denote < -10 m s^{-1}, open squares represent -10 to -5 m s^{-1}, open diamonds denote -5 to 0 m s^{-1}. Solid symbols correspond to positive differences.

Figure 1

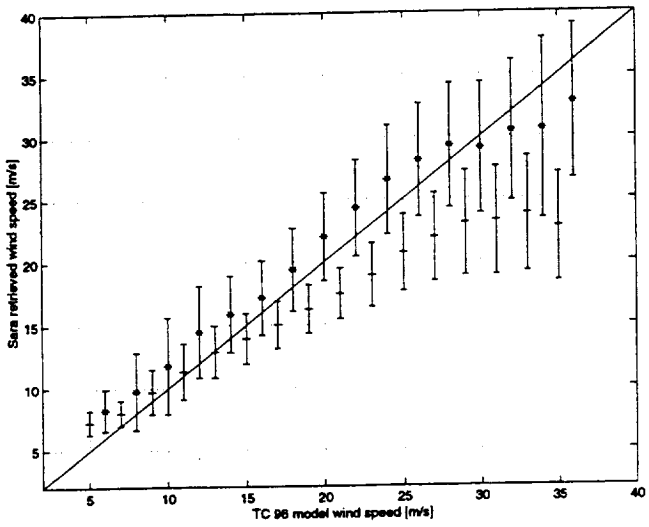

Comparison of the wind speeds recovered by $SARA_{max}$ with corresponding tropical cyclone model speeds (TC96) for revolution 478. Symbols are mean values for 5 m s^{-1} bins: asterisks denote NNGMF model function and minuses represent NSCAT 1 model function. Vertical lines show the standard deviations of the SARA retrievals about the means.

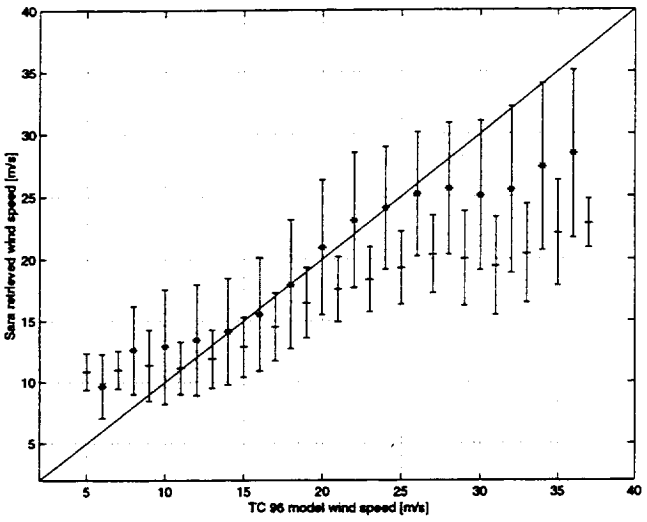

Comparison of the wind speeds recovered by $SARA_{max}$ with corresponding tropical cyclone model speeds (TC96) for revolution 485. Symbols are mean values for 5 m s^{-1} bins: asterisks denote NNGMF model function and minuses represent NSCAT 1 model function. Vertical lines show the standard deviations of the SARA retrievals about the means.

Figure 2

NSCAT/LILI 1996
OWI Model Winds vs. Flight Level Winds (adjusted)
.76*FLW to SFC Reduction Used
FLW +/-6 Hours from NSCAT Rev900 (October 19, 1996 4:00 GMT)

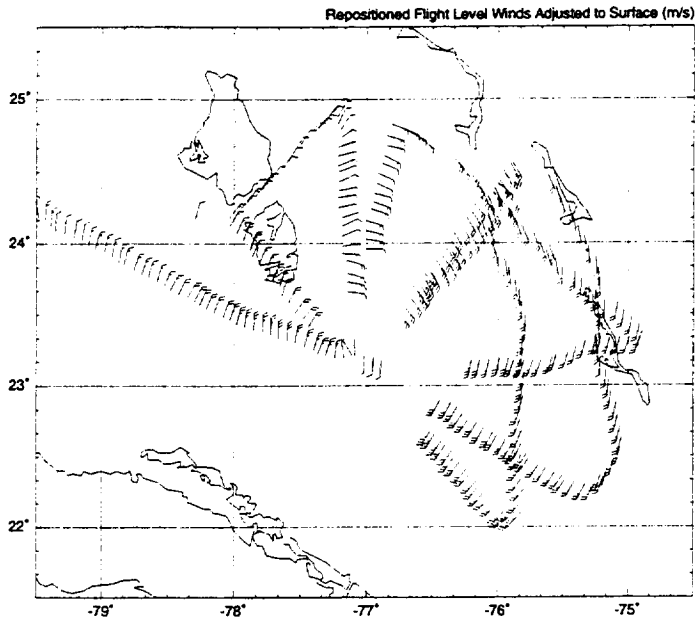

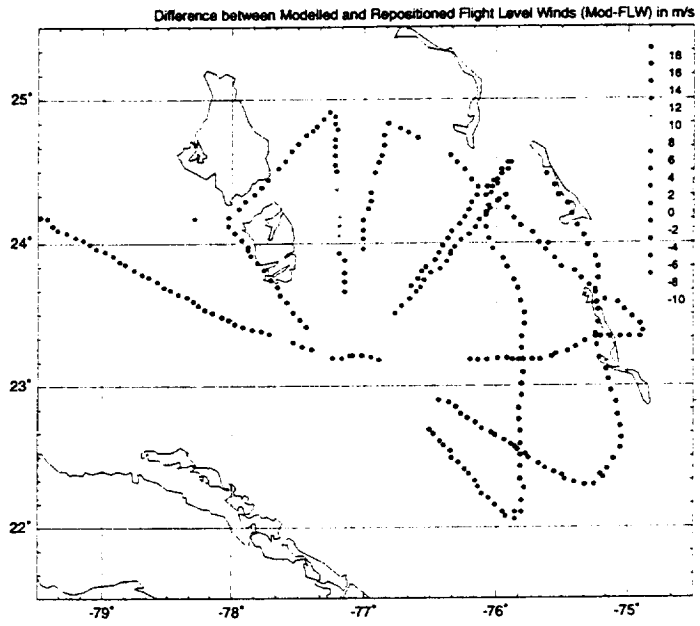

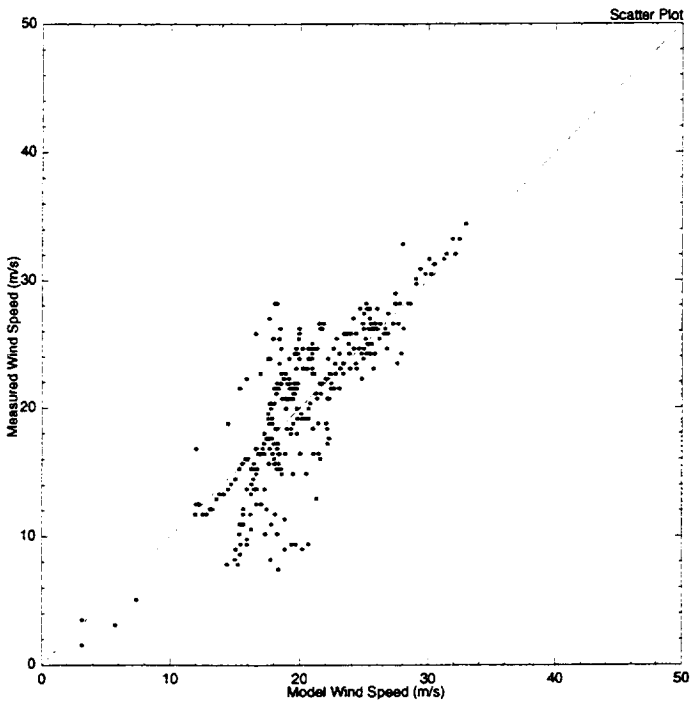

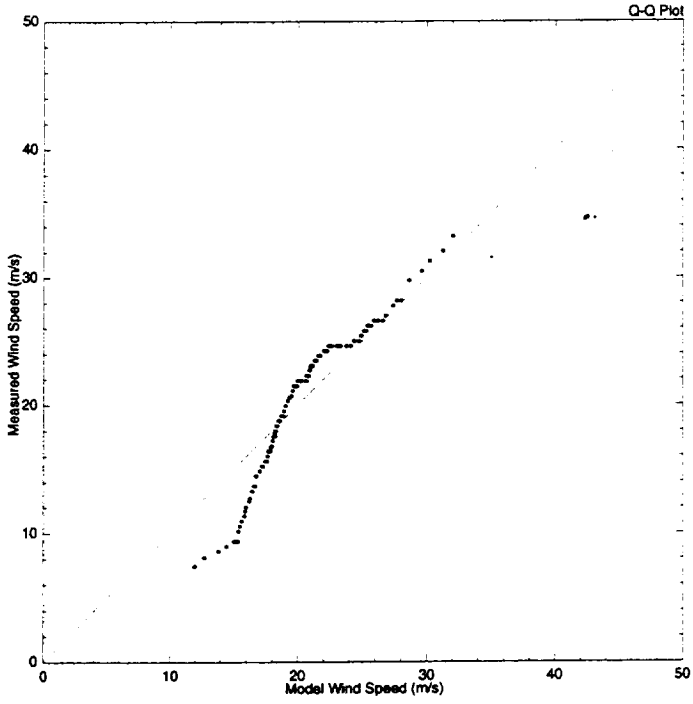

	Station	Grid Point	Number of Pts	Mean Meas	Mean Mind	Diff (H-M)	RMS Error	Stnd Dev	Scat Index	Ratio	Corr Coeff
Wind Spd. (m/s)	Combined	0	438	20.21	20.53	0.32	3.73	3.71	0.18	0.52	0.80
Wind Dir. (deg)	Combined	0	438	147.02	116.42	-19.27	N/A	26.02	0.07	N/A	N/A

Figure 3a

NSCAT/LILI 1996
OWI Model Winds vs. Flight Level Winds (adjusted)
GPS FLW to SFC Reduction Used
FLW +/-6 Hours from NSCAT Rev900 (October 19, 1996 4:00 GMT)

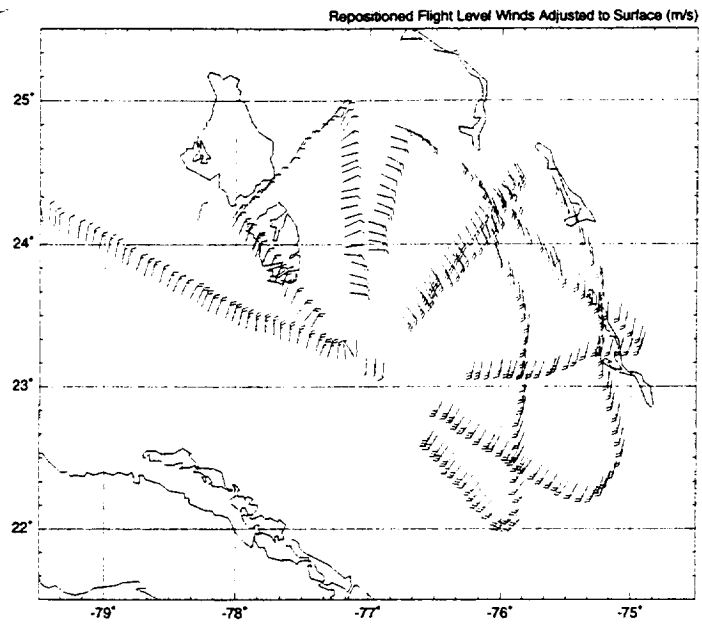

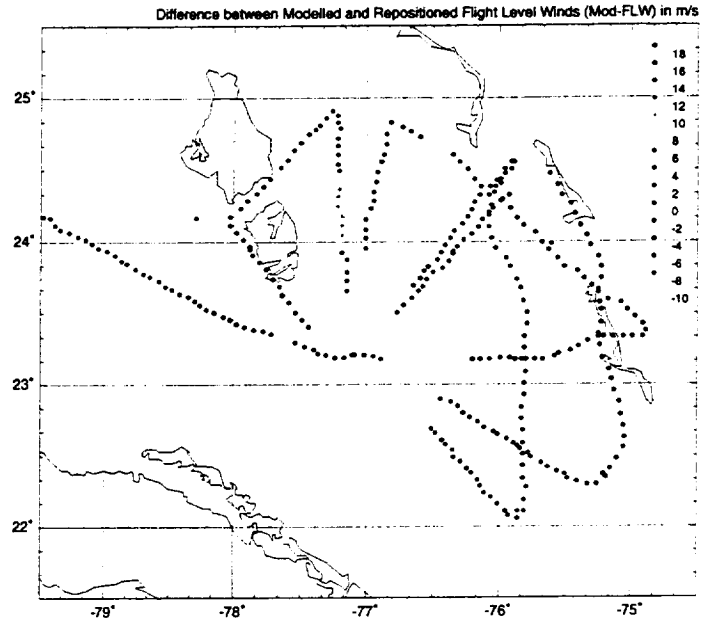

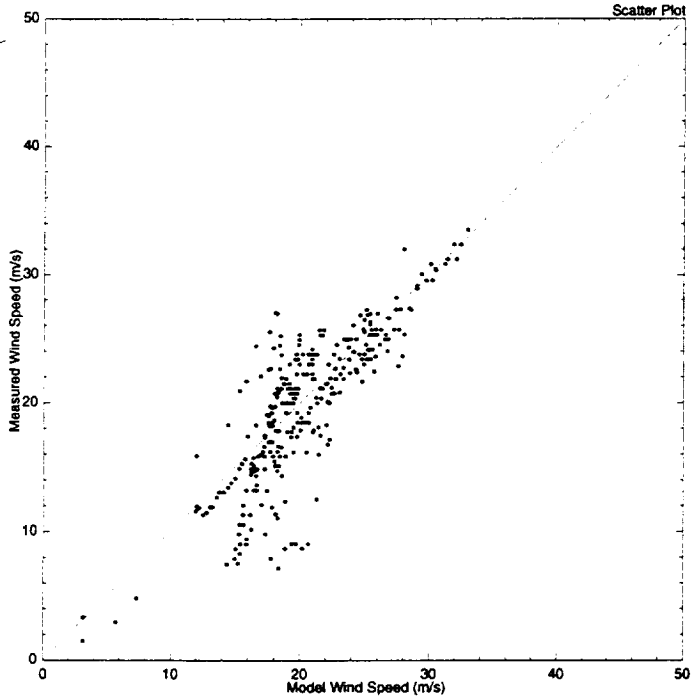

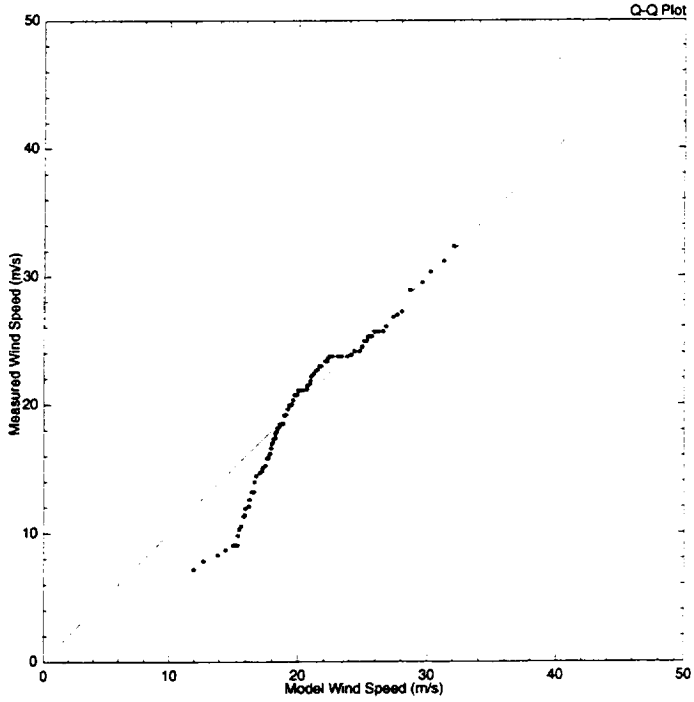

	Station	Grid Point	Number of Pts	Mean Meas	Mean Mind	Diff (H-M)	RMS Error	Stnd Dev	Scat Index	Ratio	Corr Coeff
Wind Spd. (m/s)	Combined	0	438	19.62	20.53	0.91	3.62	3.50	0.18	0.63	0.81
Wind Dir. (deg)	Combined	0	565	96.94	119.70	-16.92	N/A	54.99	0.15	N/A	N/A

Figure 3b

NSCAT/LILI 1996
OWI Model Winds vs. Flight Level Winds (adjusted)
GPS/BOUNDY FLW to SFC Reduction Used
FLW +/-6 Hours from NSCAT Rev900 (October 19, 1996 4:00 GMT)

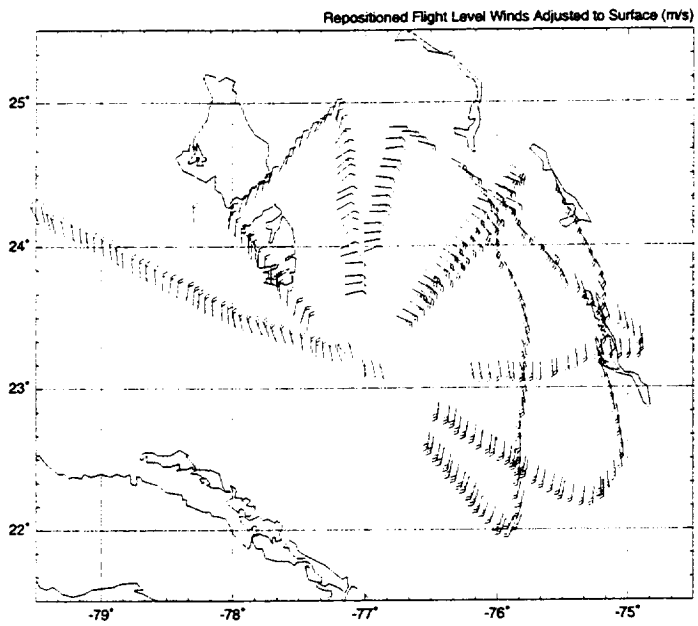

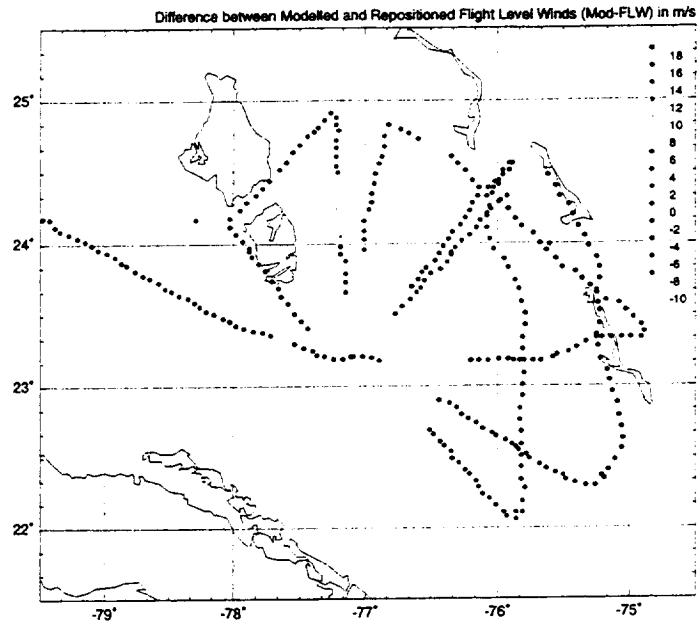

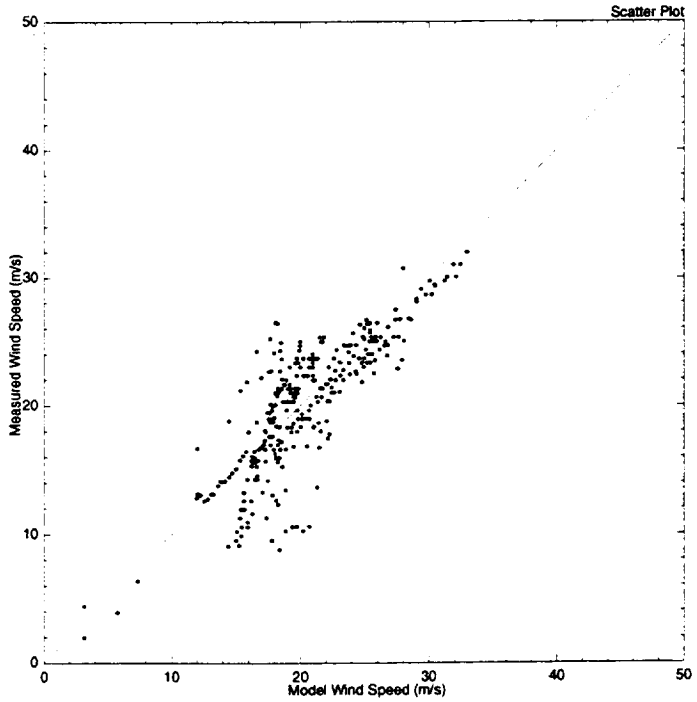

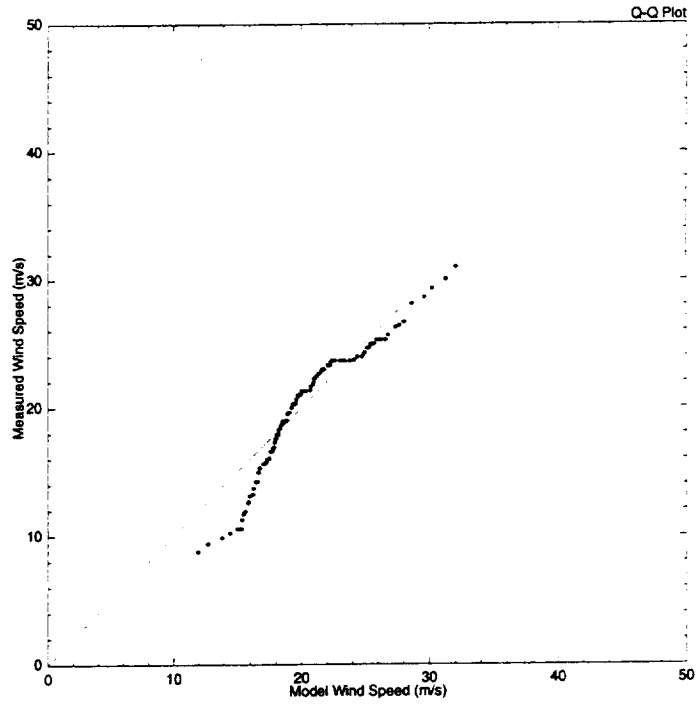

	Station	Grid Point	Number of Pts	Mean Meas	Mean Mind	Diff (H-M)	RMS Error	Stnd Dev	Scat Index	Ratio	Corr Coeff
Wind Spd. (m/s)	Combined	0	438	19.94	20.53	0.59	3.17	3.12	0.16	0.61	0.81
Wind Dir. (deg)	Combined	0	565	78.62	119.70	5.95	N/A	52.89	0.15	N/A	N/A

Figure 3c

NSCAT/LILI 1996
OWI Model Winds vs. Flight Level Winds (adjusted)
BOUNDY FLW to SFC Reduction Used
FLW +/-6 Hours from NSCAT Rev900 (October 19, 1996 4:00 GMT)

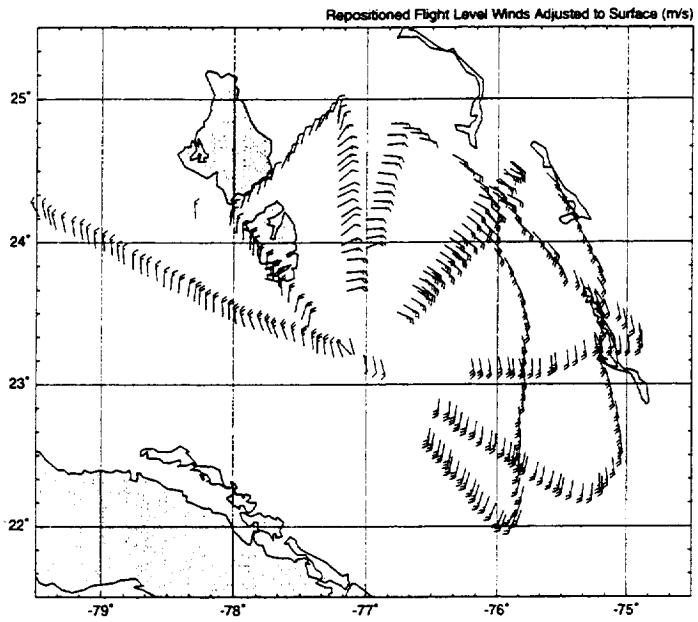

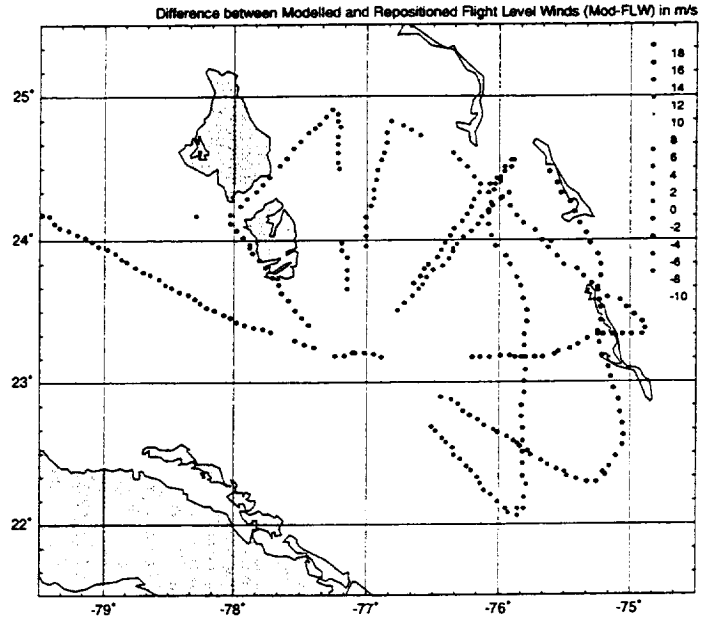

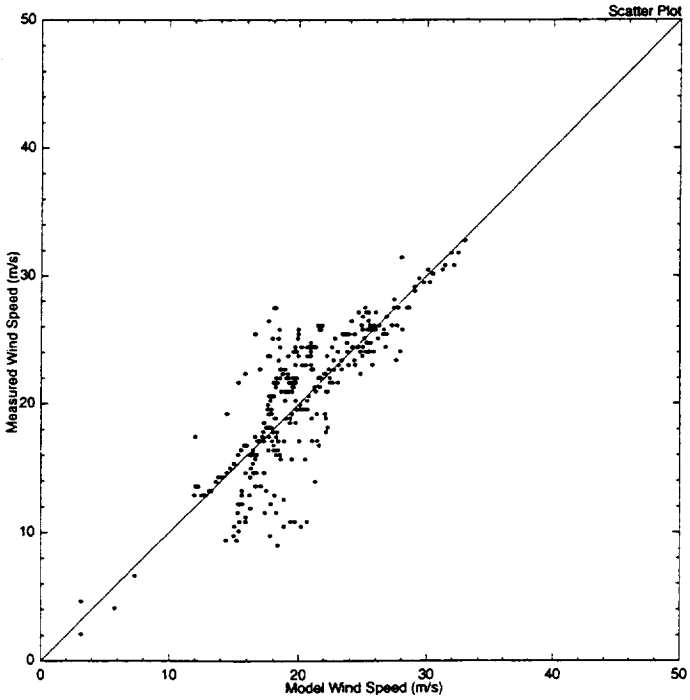

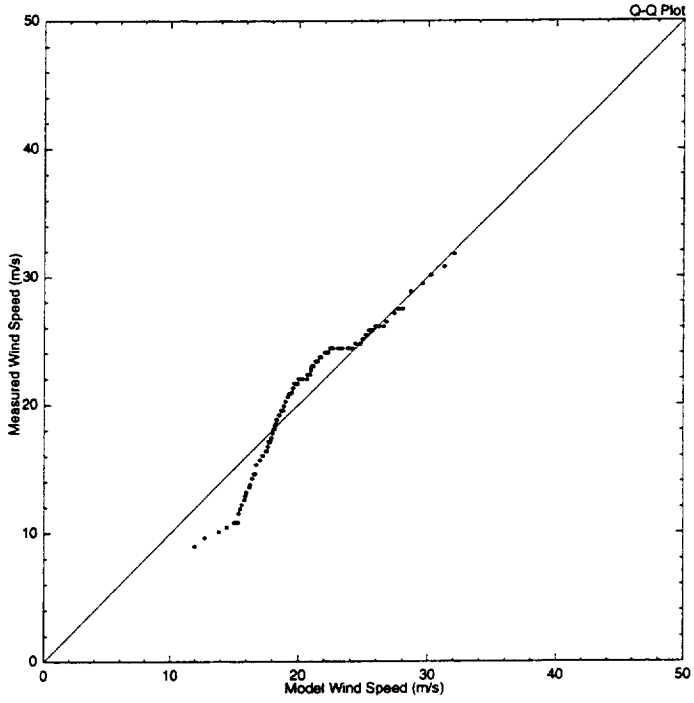

	Station	Grid Point	Number of Pts	Mean Meas	Mean Mind	Diff (H-M)	RMS Error	Stnd Dev	Scat Index	Ratio	Corr Coeff
Wind Spd. (m/s)	Combined	0	438	20.46	20.53	0.07	3.28	3.28	0.16	0.53	0.80
Wind Dir. (deg)	Combined	0	438	125.11	116.42	1.66	N/A	24.62	0.07	N/A	N/A

Figure 3d

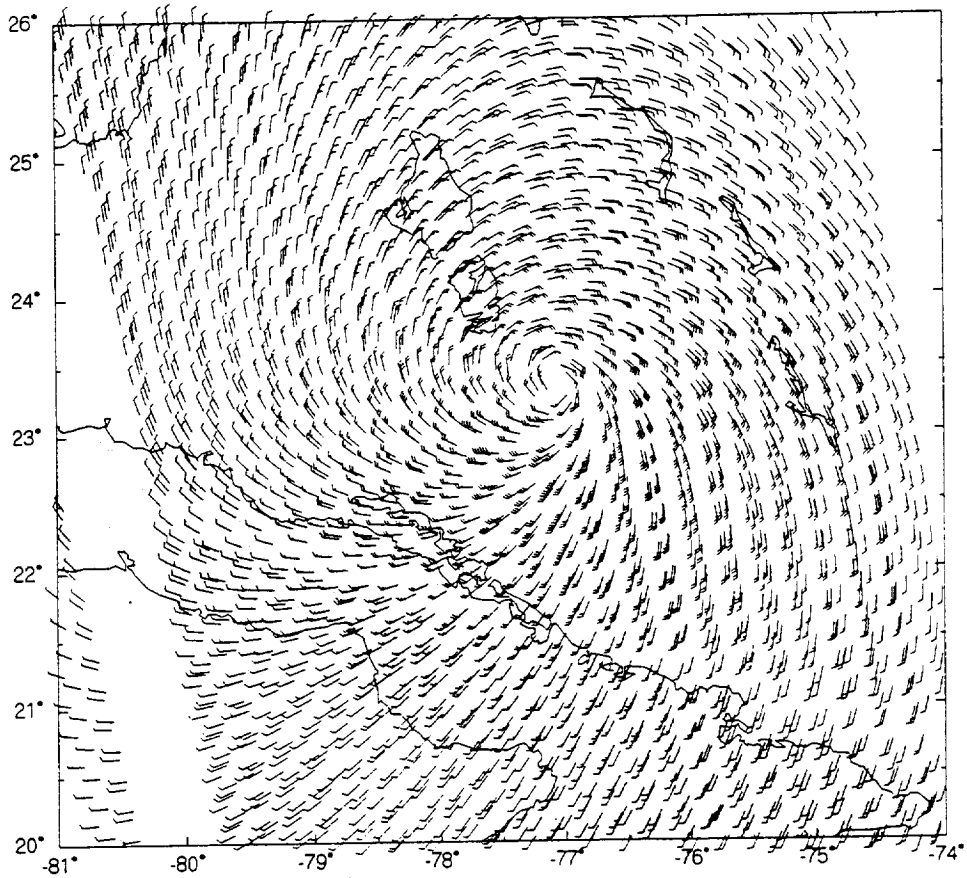

Fig. 1. Tropical cyclone PBL model surface winds from TC96 at 10 m elevation for Rev. 900. Wind barbs are shown at the corresponding NSCAT σ^o locations.

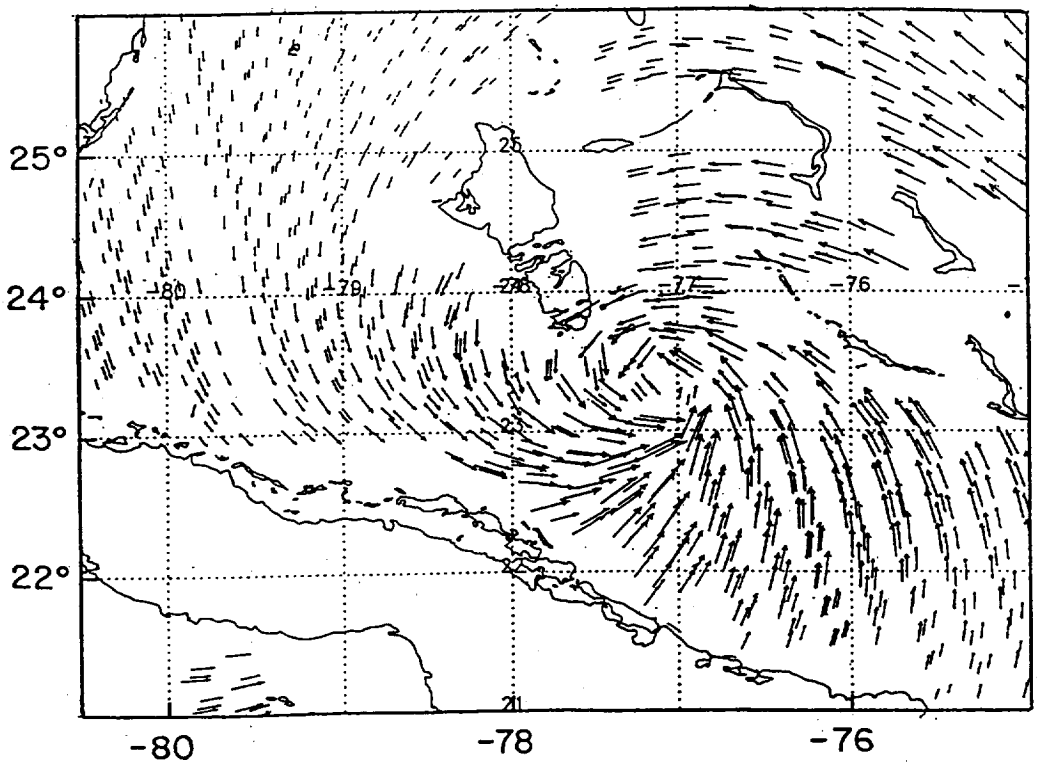

Fig. 2. NSCAT retrieved winds from the Tropical Cyclone Geophysical Model Function for Rev. 900.

Figure 4

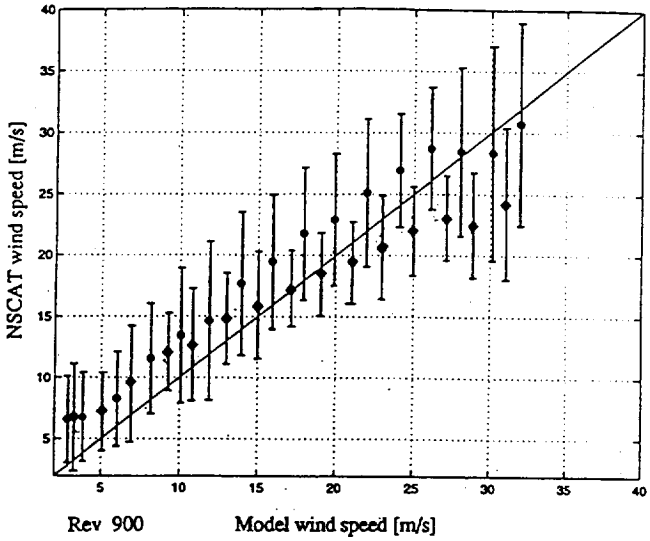

Fig. 3. Wind speed comparisons between the TC96 model and NSCAT retrieved winds for Rev. 900. The filled circles are for TCGMF and the tilted squares are for NSCAT-1b.

Figure 5

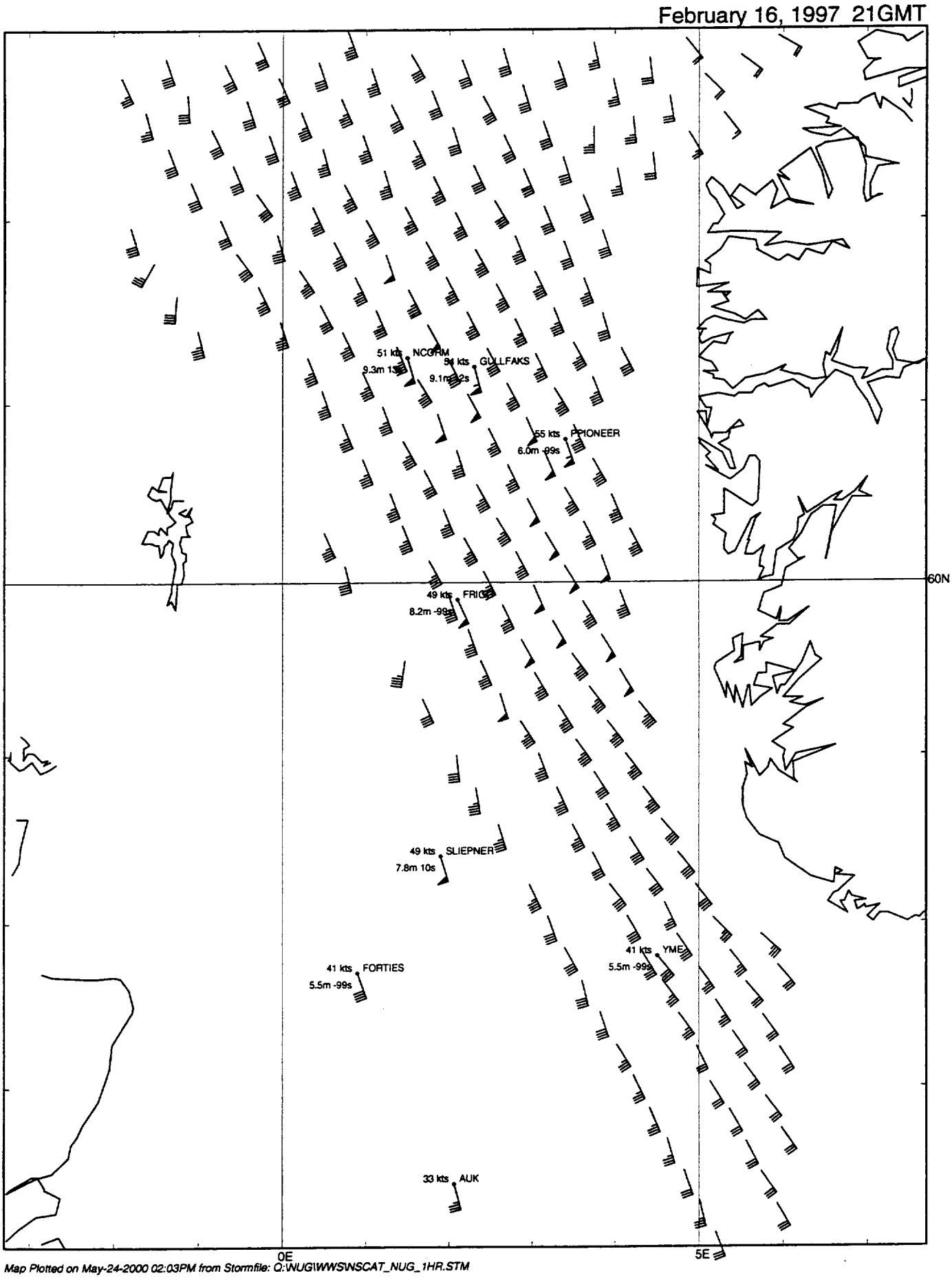
February 16, 1997 21GMT
51 kts NCORM
9.3m 1
54 kts GULLFAKS
9.1m 12s
55 kts PPIONEER
6.0m -99s
60N
49 kts FRIGG
8.2m -99s
49 kts SLIEPNER
7.8m 10s
41 kts FORTIES
5.5m -99s
41 kts YME
5.5m -99s
33 kts AUK
0E
5E
Map Plotted on May-24-2000 02:03PM from Stormfile: Q:\NUG\WWS\WSCAT_NUG_1HR.STM

Figure 6

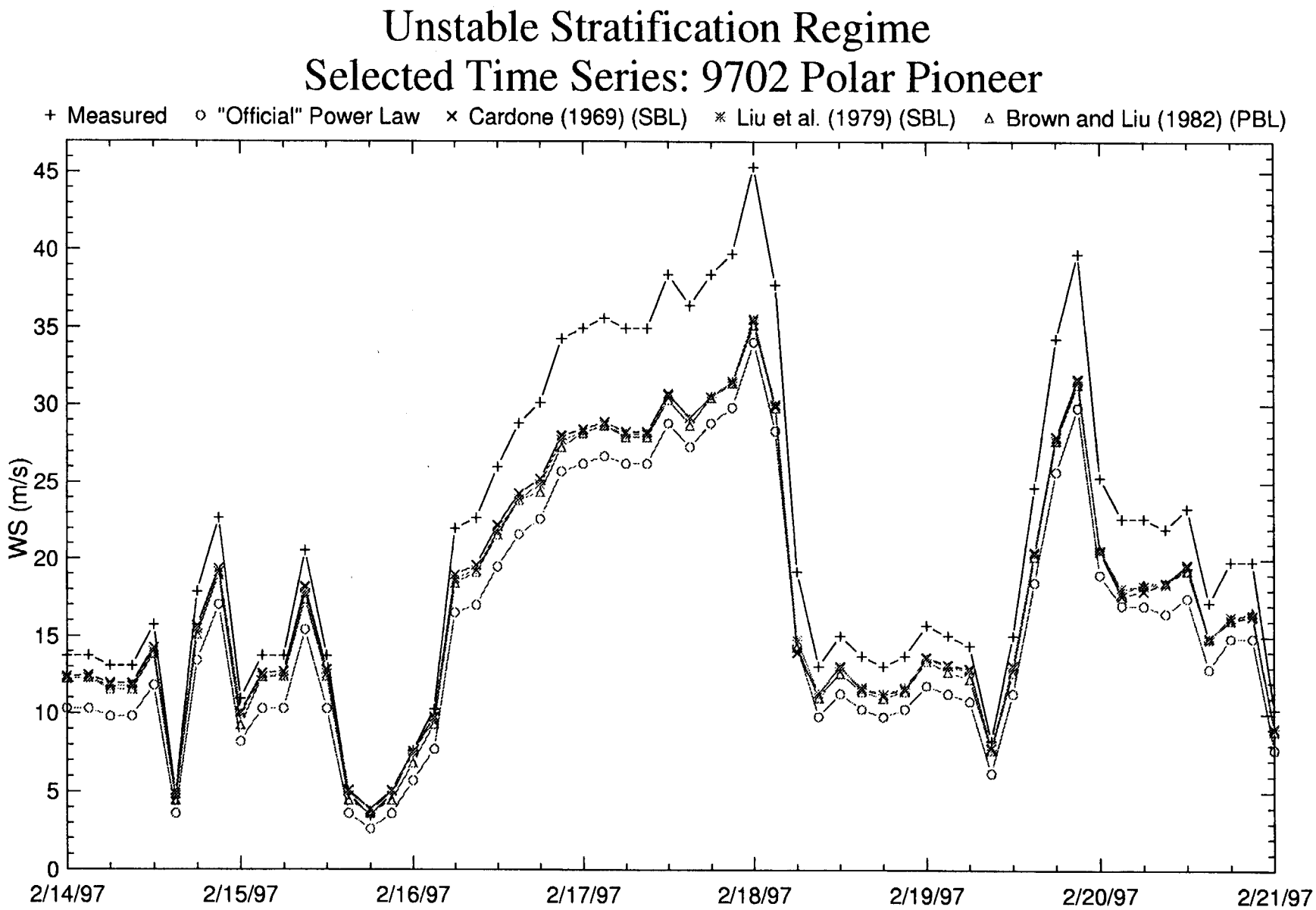
Unstable Stratification Regime
Selected Time Series: 9702 Polar Pioneer
+ Measured
o "Official" Power Law
× Cardone (1969) (SBL)
* Liu et al. (1979) (SBL)
△ Brown and Liu (1982) (PBL)
WS (m/s)
0
5
10
15
20
25
30
35
40
45
2/14/97
2/15/97
2/16/97
2/17/97
2/18/97
2/19/97
2/20/97
2/21/97

Figure 7

PLATFORMS vs. NSCAT COLLOCATED - 9609-9706

Using WindFN

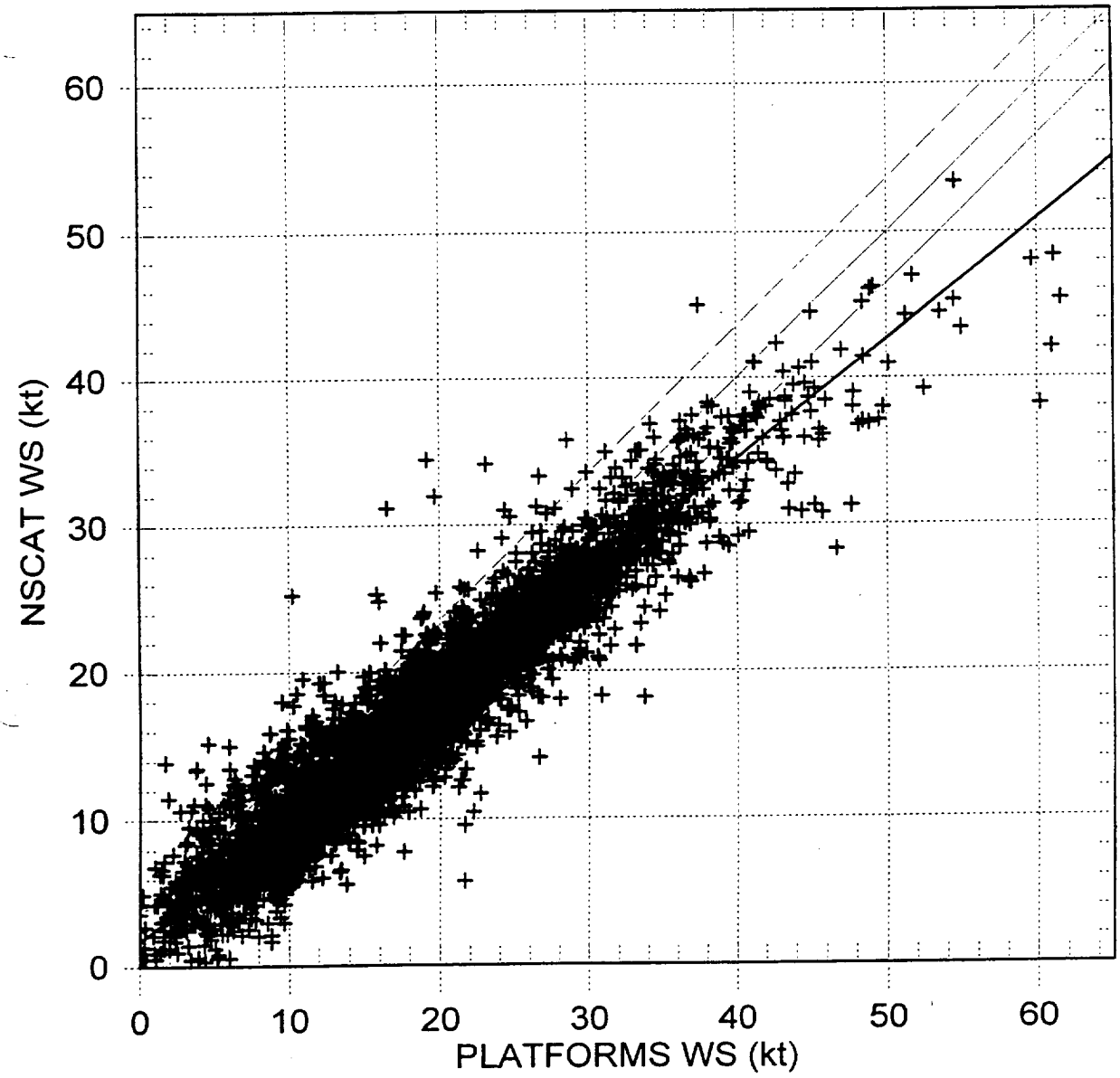

Best Fit: Y = 0.820X + 1.680	
Total Points:	3669
Mean X:	18.864
Mean Y:	17.143
Mean Diff:	-1.721
Root Mean Square:	3.537
Standard Dev.:	3.091
Scatter Index:	0.164
Ratio:	0.246
Correlation Coeff:	0.949

Quantile-Quantile Scatter Plots of Collocated NSCAT-North Sea Platform 10 m Wind Speed

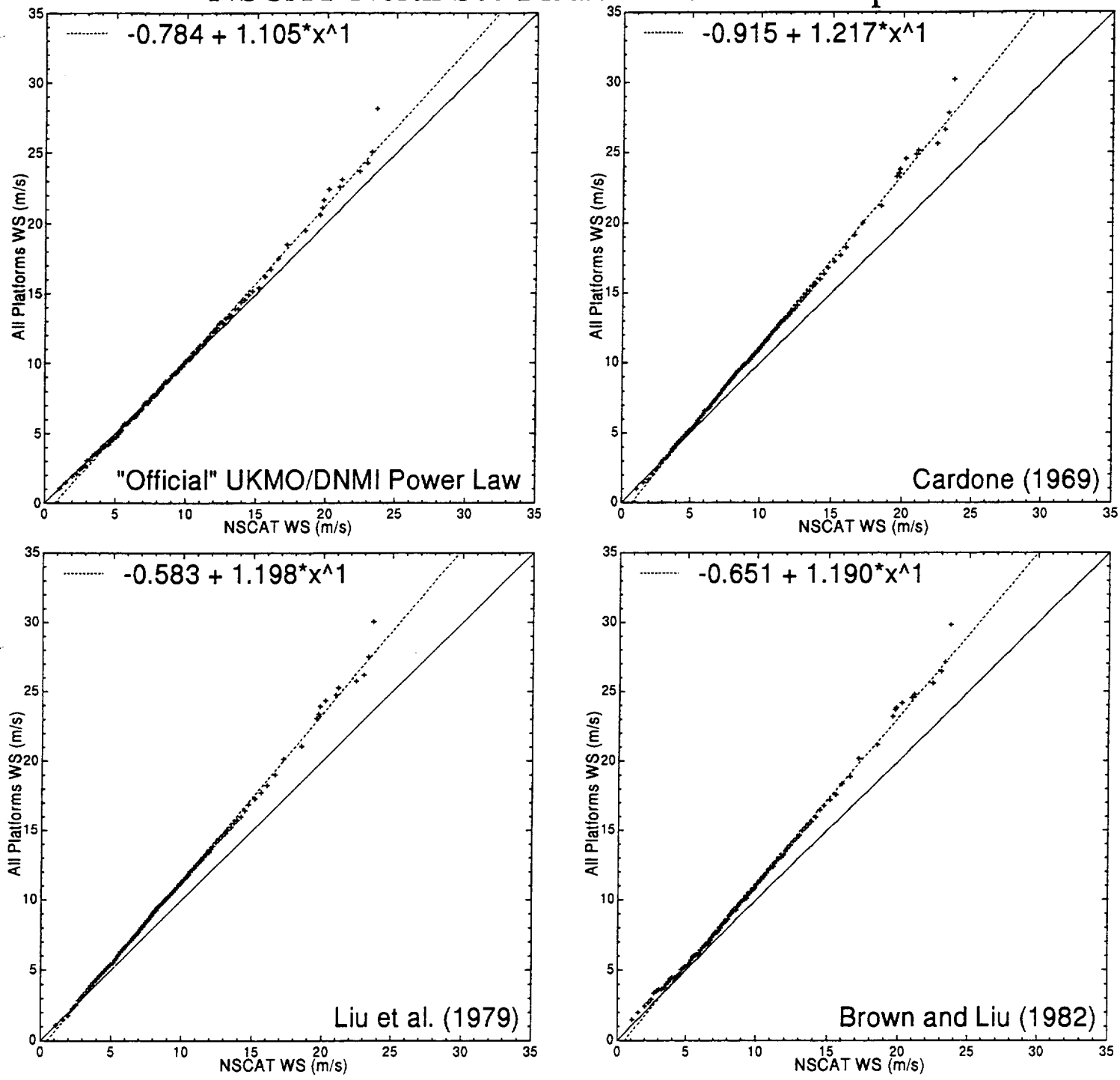

Figure 9

ATTENTION: HURRICANE SPECIALISTS

Hurricane Floyd 1330 UTC 13 Sept.1999

Max. 1-min sustained surface winds (kt) for marine exposure

Analysis based on US AFRES recon. 700 mb winds adj. to sfc: 0700-1154 z,
3 GPS dropwindsondes MBL adj to sfc: 0750, 0927, and 1115z
1330 z position extrapolated from 1121 z wind center fix assuming 280° @ 12 kt, mslp = 921 mb

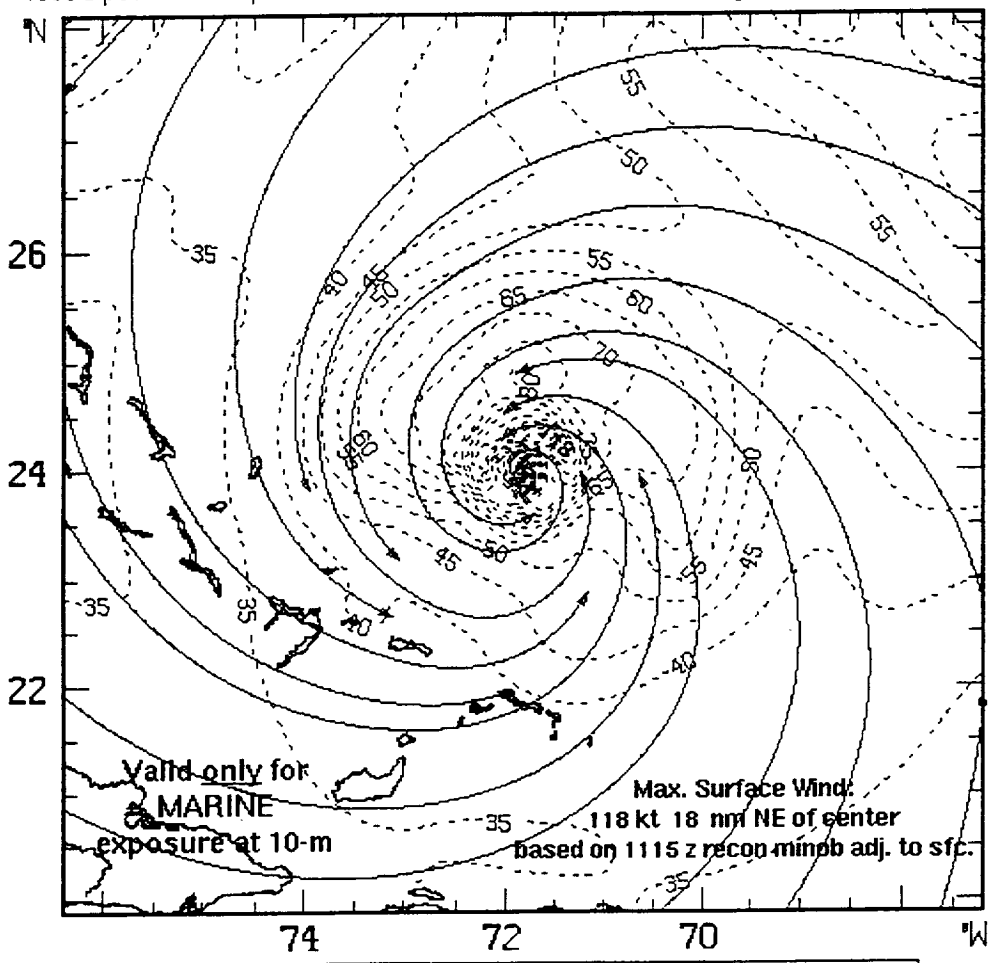

Experimental research product of :
NOAA / AOML / Hurricane Research Division

Figure 10

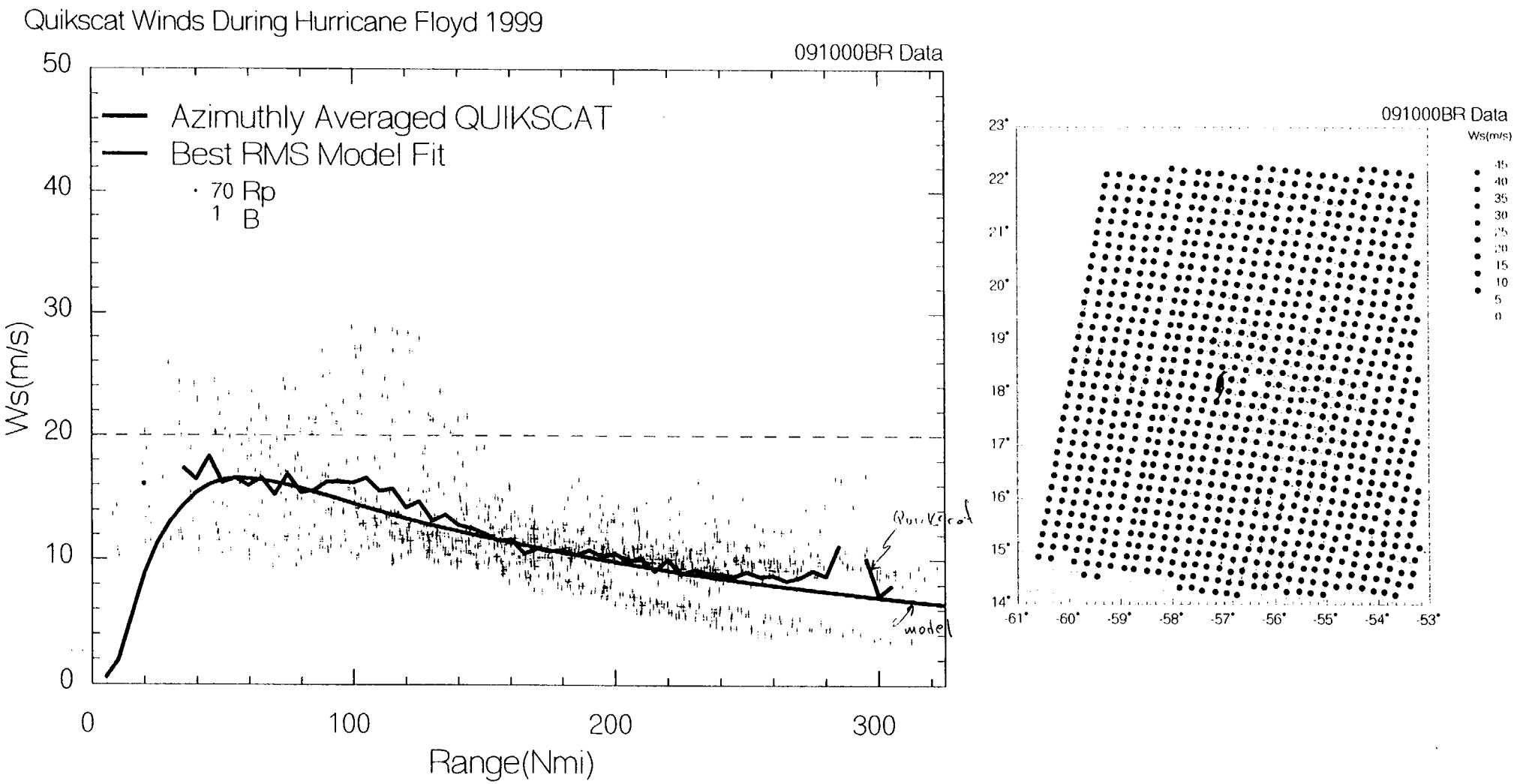
Quikscat Winds During Hurricane Floyd 1999
091000BR Data
Azimuthly Averaged QUIKSCAT
Best RMS Model Fit
70 Rp
1 B
Ws(m/s)
Range(Nmi)
0
10
20
30
40
50
0
100
200
300
model
091000BR Data
Ws(m/s)
45
40
35
30
25
20
15
10
5
0
23°
22°
21°
20°
19°
18°
17°
16°
15°
14°
-61°
-60°
-59°
-58°
-57°
-56°
-55°
-54°
-53°

Figure 11

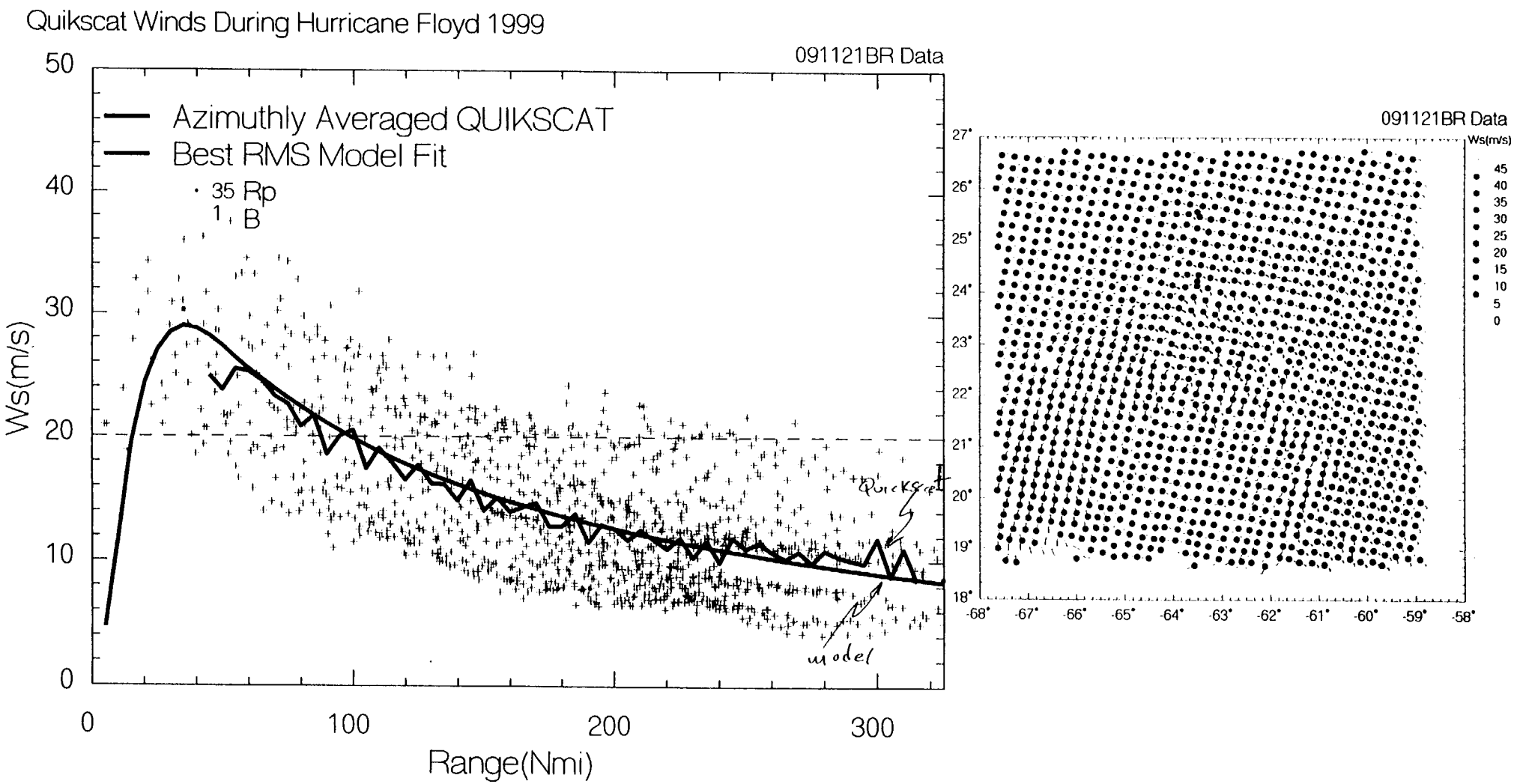
Quikscat Winds During Hurricane Floyd 1999
091121BR Data
Azimuthly Averaged QUIKSCAT
Best RMS Model Fit
35 Rp
1 B
Ws(m/s)
Range(Nmi)
0
10
20
30
40
50
0
100
200
300
model
091121BR Data
Ws(m/s)
45
40
35
30
25
20
15
10
5
0
27°
26°
25°
24°
23°
22°
21°
20°
19°
18°
-68°
-67°
-66°
-65°
-64°
-63°
-62°
-61°
-60°
-59°
-58°

Figure 12

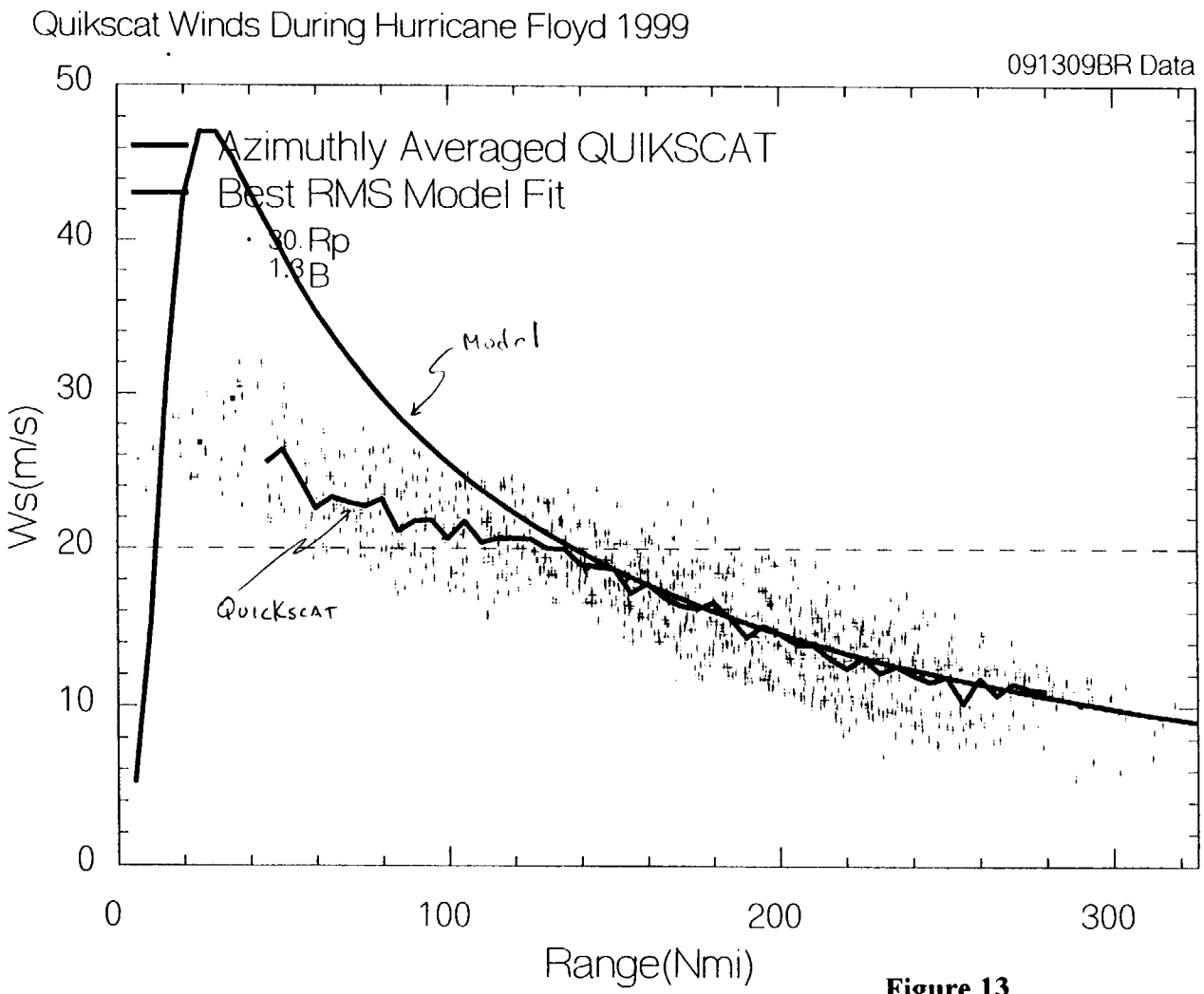
Quikscat Winds During Hurricane Floyd 1999
091309BR Data
Azimuthly Averaged QUIKSCAT
Best RMS Model Fit
Model
QuickScat
Ws(m/s)
Range(Nmi)
0
10
20
30
40
50
0
100
200
300

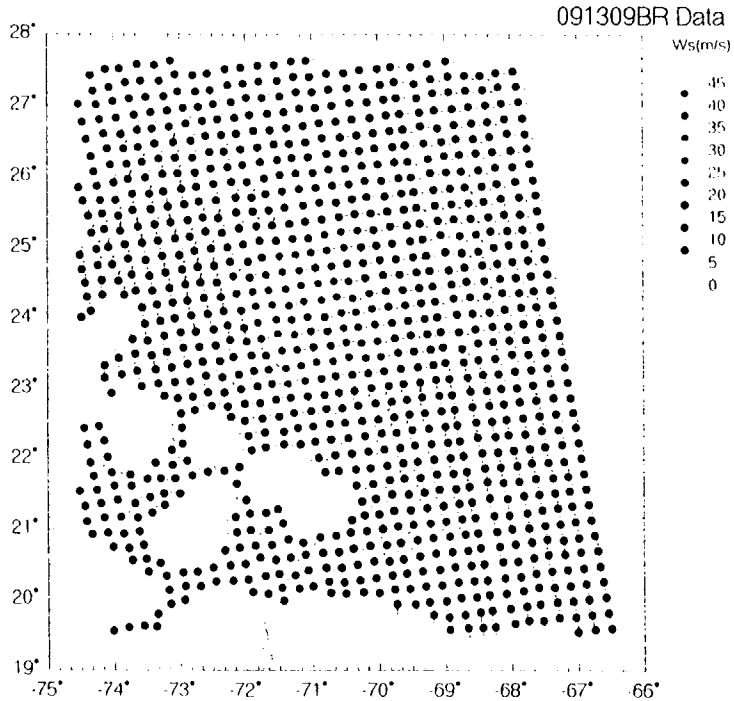
091309BR Data
Ws(m/s)
45
40
35
30
25
20
15
10
5
0
28°
27°
26°
25°
24°
23°
22°
21°
20°
19°
-75°
-74°
-73°
-72°
-71°
-70°
-69°
-68°
-67°
-66°

Figure 13

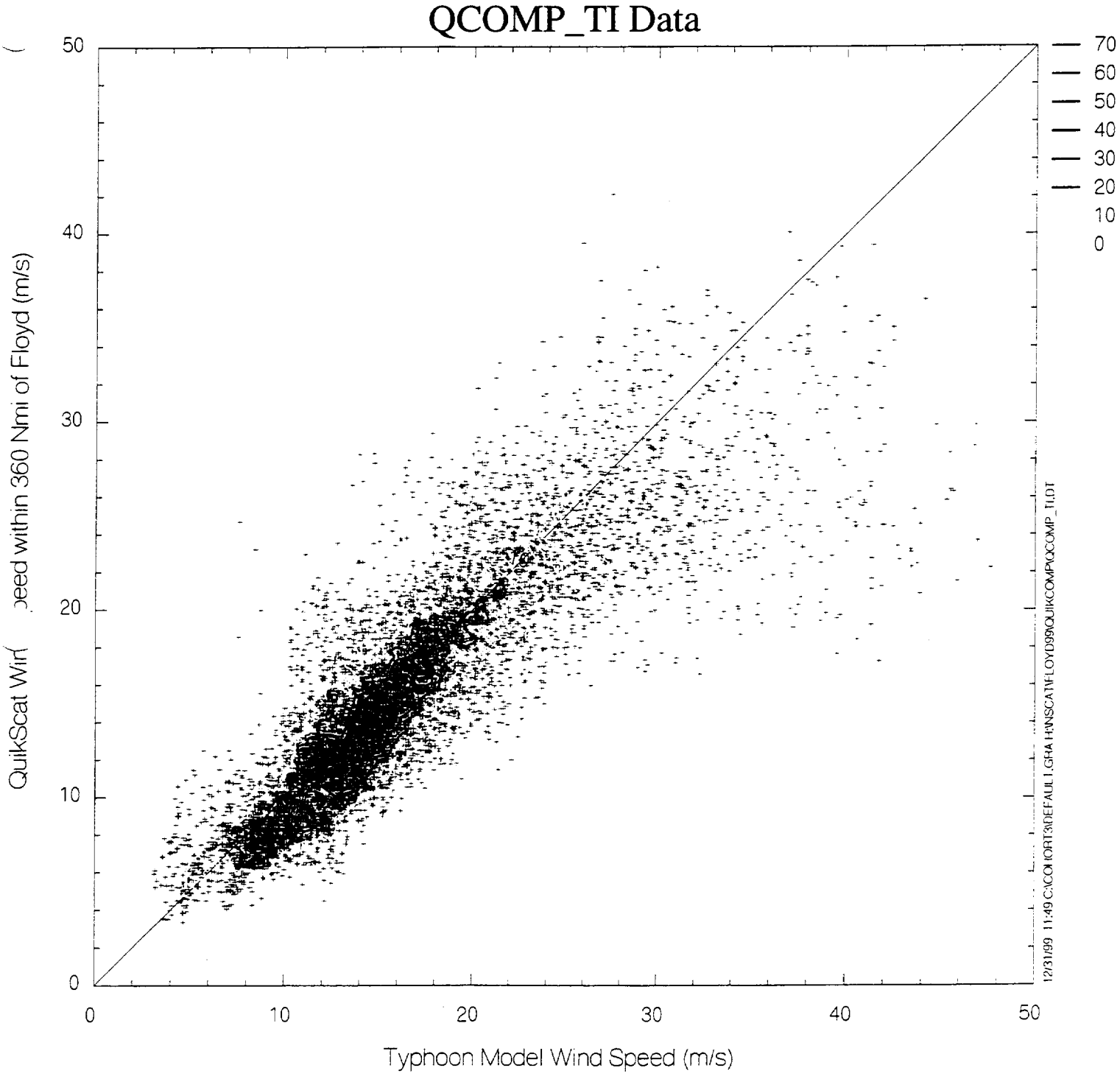
QCOMP_TI Data
QuikScat Wind Speed within 360 Nmi of Floyd (m/s)
Typhoon Model Wind Speed (m/s)
0
10
20
30
40
50
70
60
50
40
30
20
10
0
12/31/99 11:49 C:\QCOMP\ORT3\DEFAULT.GHA H4NSCATN-LOYD99\QUIKCOMP\QCOMP_TI.DT

Figure 14

Appendix A. Abstract and key slides of AGU Spring Meeting, 2000 Paper:

Accuracy of Scatterometer Winds Assessed from In-Situ Measured Wind Data up to 32 m/s

Accuracy of Scatterometer Winds Assessed from In-Situ Measured Wind Data Up to 32 m/s

V.J.Cardone, E.A. Ceccacci, A.T. Cox, J. G. Greenwood (Oceanweather Inc., Cos Cob, CT 06807, (203-661-3091) oceanwx@oceanweather.com,

Evaluations of the accuracy of scatterometer winds have generally utilized comparison data sets assembled from data buoys and research vessels that are generally limited to 10- m neutral wind speeds of 20 m/s or less. For example, Freilich and Dunbar (1999) found only 184 out of 56,000 NSCAT-buoy collocations with 10-m buoy winds exceeding 18 m/s and virtually none above 22 m/s. Validation is further complicated by evidence that buoy wind speeds may be biased low in high sea states. The scant evidence of the sensitivity and accuracy of scatterometer winds above 20 m/s or so has been provided to date only by comparison of winds from NWP systems or model generated wind fields in tropical cyclones. This lack of high-wind speed validation hampers scientific applications of existing data sets from NSCAT and QuickScat and further refinements of the backscatter model function.

We have assembled a unique comparison data base for NSCAT wind validation at high wind speeds, utilizing winds measured from offshore platforms in the open Northern North Sea and Southern Norwegian Seas. Of the dozens of platforms which make and report synoptic observations in this region, we selected only nine platforms at which a calibrated anemometer is well exposed at the top of the drilling derrick (the height range is 86-m to 143-m) and quality-controlled continuous time average wind samples are archived by and available from European centers. Collocation of the NSCAT 25-km database with the platform database yielded 3663 (2773) matches for separation distances of 25-km and time offsets up to 1.5 (0.5) hours. Using Liu's reduction to 10-m equivalent neutral wind, 110 matches are found for wind speeds above 20 m/s and 37 matches for wind speed above 24 m/s. However, because in some regimes the anemometer may be above the surface boundary layer, four different stability-dependent wind profile models were used in the analysis. The data are analyzed and will be reported in terms of scatter plots, regressions on bin-averaged data and comparisons of wind speed and platform wind speed distributions in terms of quantile-quantile scatter plots.

For a selected set of 58 passes during particularly intense storms, the number of collocations is greatly expanded (about 10,000 matches) by analyzing the platform data into a continuous field using the natural neighbor objective analysis system. These comparisons are reported as well. A similar analysis is planned using the reprocessed QuickScat following assembly of the platform data for the 99/00 winter.

Accuracy of Scatterometer Winds Assessed from In-Situ Measured Wind Data up to 32 m/sec

V. J. Cardone, E.A. Ceccacci,

A.T. Cox and J.G. Greenwood

Oceanweather Inc. - Cos Cob, CT

MOTIVATION

- SCAT (and ALT) backscatter wind validation and model function tuning heavily based on buoy (mainly NDBC) wind data and NWP model output

- NWP operational and reanalysis project marine surface winds DEFINITELY biased low above about 20 m/s
  (e.g. Swail and Cox, 2000, J. Atmos. Ocean. Tech. (April)

- Buoy winds increasingly indicted as biased low above about 20 m/s though field experiments and research underway to resolve this issue
  (for a recent review see Taylor et al., 1999, CLIMAR99)

PLATFORM WIND DATA

- Eight platforms and one drill ship in Norwegian and British sectors (map), all north of 56N, in deep water
- Calibrated instruments, top of derrick exposure, from quality controlled archives of UKMO and DNMI
- Anemometer heights: mean 106 m, range 86 m to 143 m
- "On-board" reduction to 10 m factors based on power law and vary by platform over .71 - .78, no stability variation
- Sampling rate varies from 20 minutes (3 sites), 1-hour (3 sites), and 3-hours (3 sites); averaging interval generally 10 min
- Owners: Shell, BP-Amoco, Phillips, Elf, Statoil, Norsk Hydro

Platform Locations and Anemometer Heights

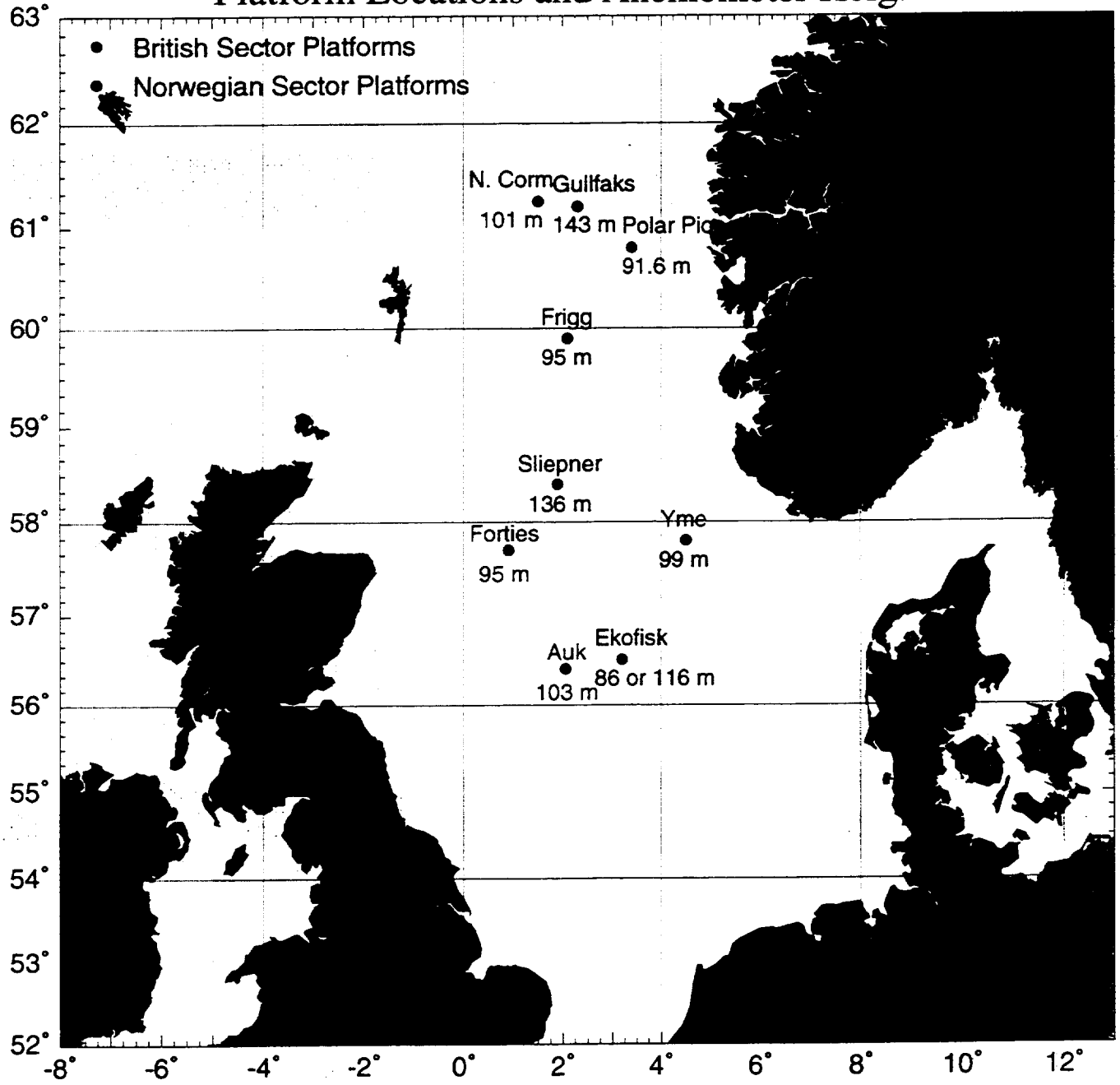

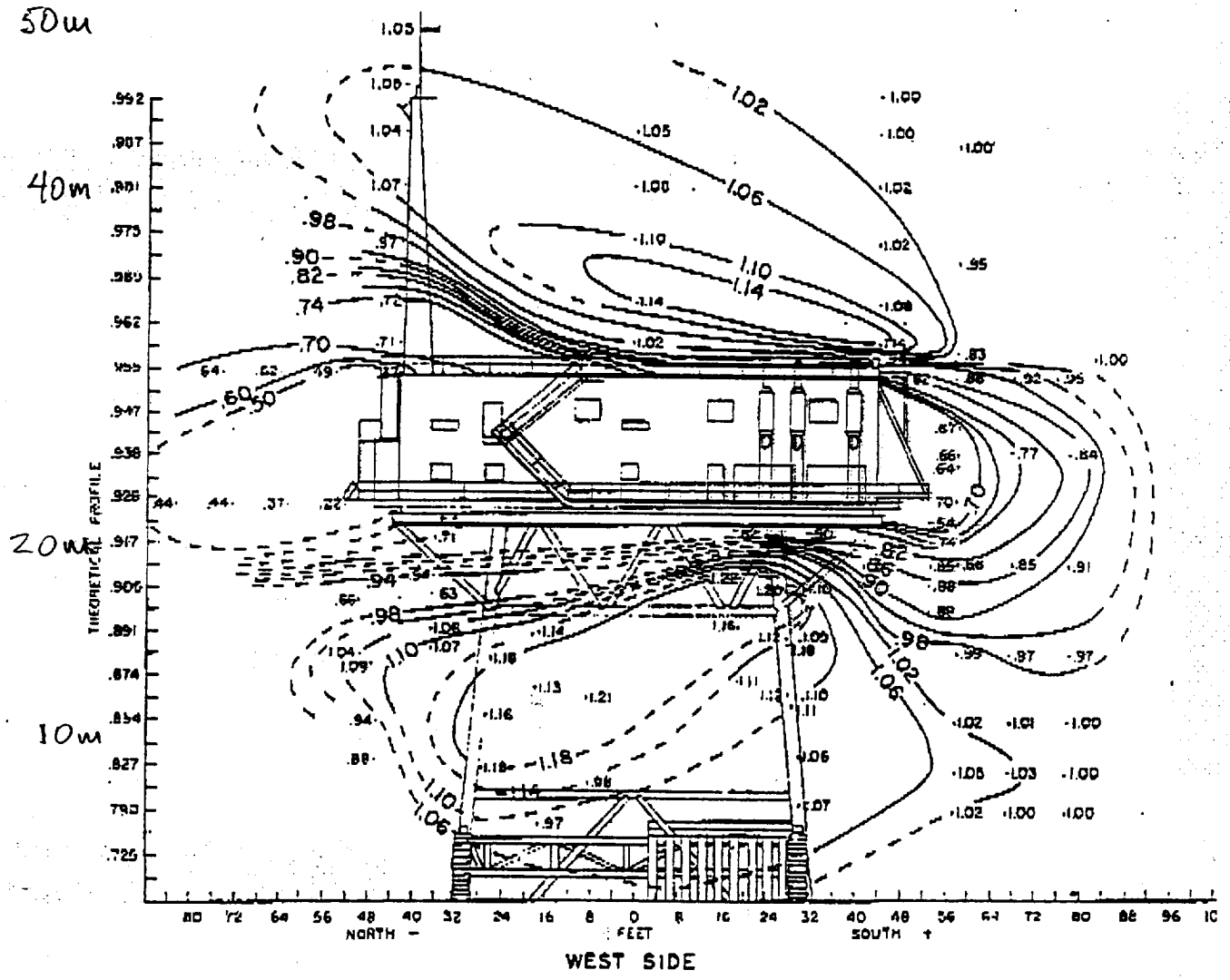

Fig. 1. Disturbed airflow around Argus Island for southerly flow expressed as ratio observed to assumed undisturbed wind speeds.

Platform Data Processing

- Platform data arrived already reduced to 10 meters using on-board power law factor.
- Three alternative reductions to 10m applied :

Cardone (1969) and Liu et al. (1979): inverted power law factor to restore wind speeds to anemometer height then computed 10 m neutral wind speed assuming 20 m air temperature sensor height (SST from platform or NCEP)

Brown and Liu (1982): fitted full pbl profile by finding nearest geostrophic wind (no curvature or baroclinicity) speed that would intercept measured wind speed given all the other variables, then computed 10 m neutral wind

Unstable Stratification Regime
Selected Time Series: 9702 Polar Pioneer

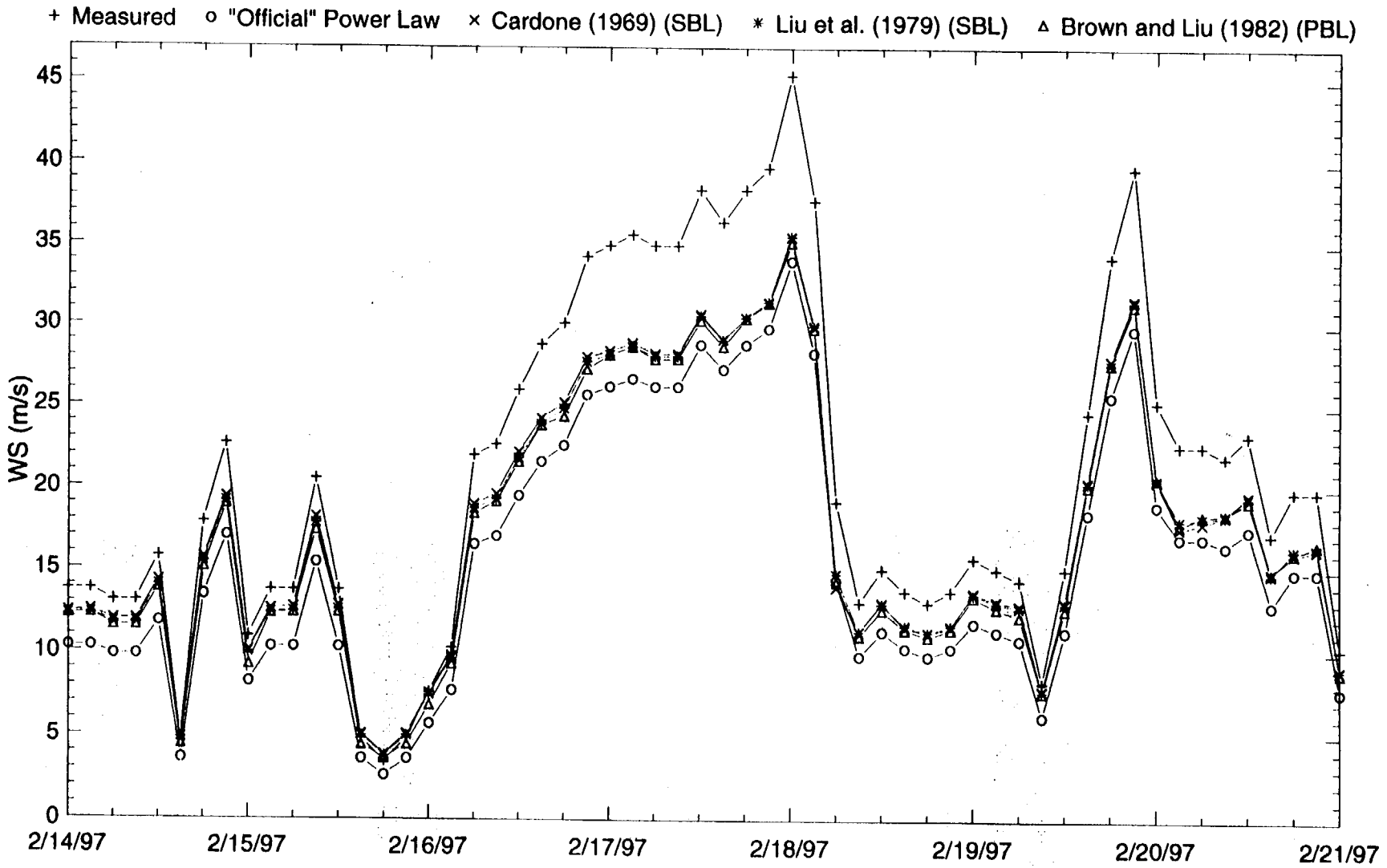

Stable Stratification Regime
Selected Time Series: 9706 Gullfaks "C"

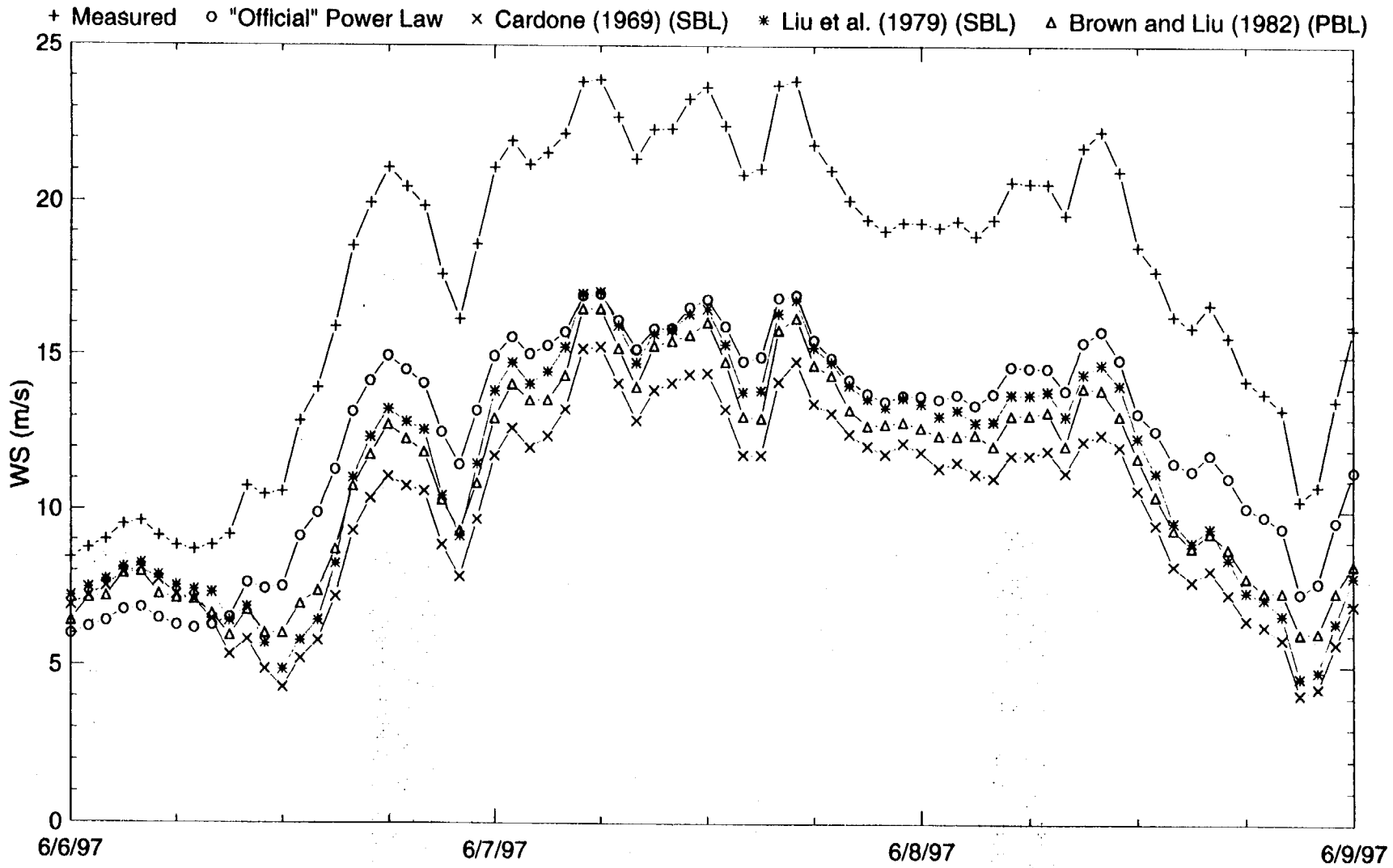

February 16, 1997 21GMT

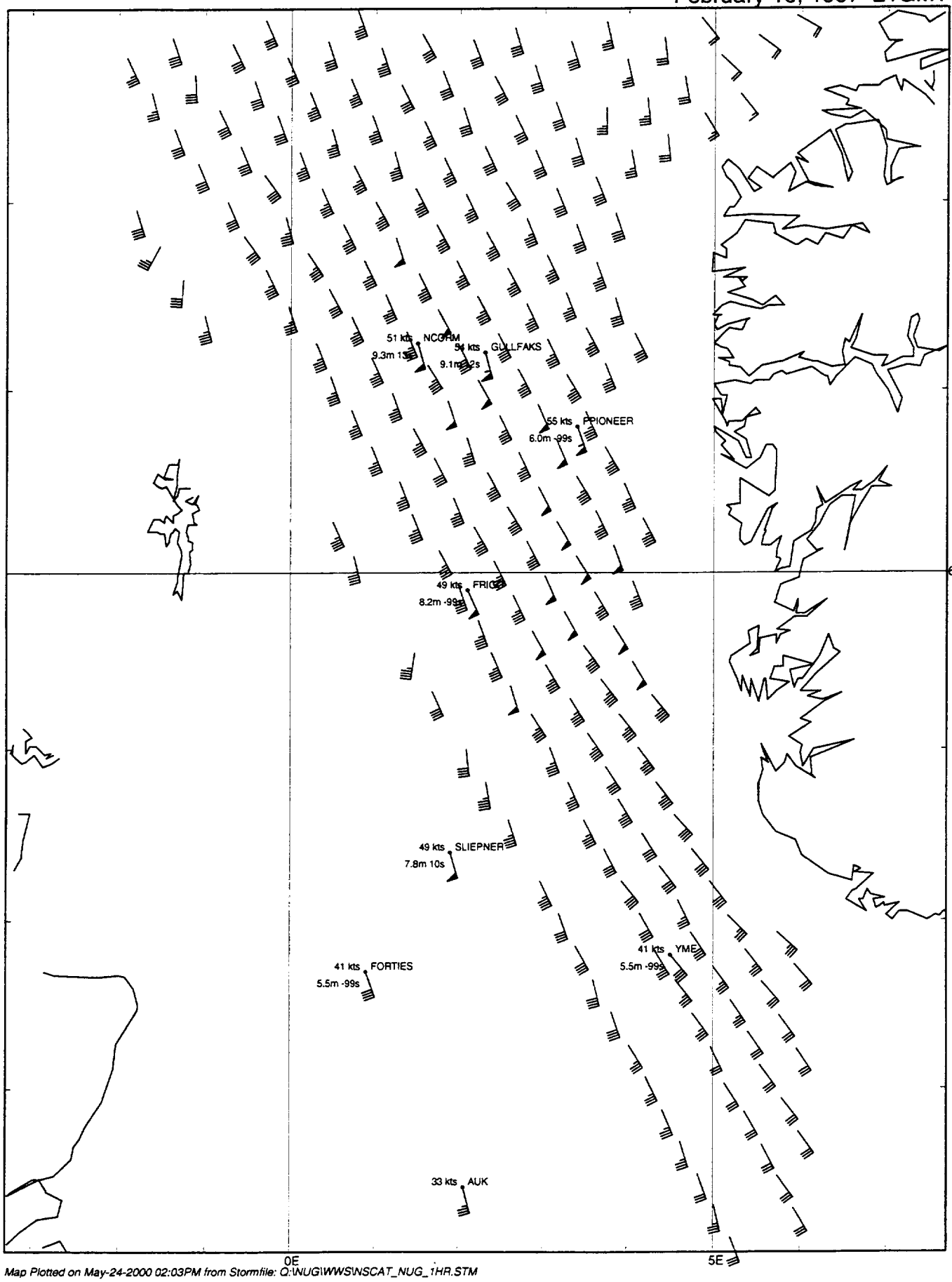

Map Plotted on May-24-2000 02:03PM from Stormfile: Q:\NUG\WWS\NSCAT_NUG_1HR.STM

Collocation Process

- Read 25-km NSCAT Selected Wind Vectors (SWV) over 9609-9706 from JPL PO.DAAC 11 CD-ROM data set
- Search for NSCAT SWVs within a 50-km box around each platform (box shifted slightly as Polar Pioneer relocated within Troll field)
- Impose time window of +/- 30 minutes for 1-hourly platform wind data (Auk, Forties, Frigg, Gullfaks, North Cormorant, and Sleipner)
- Impose time window of +/- 1.5 hours for 3-hourly platform wind data (Ekofisk, Polar Pioneer, and Yme)
- Always match single nearest 25 km SWV within time and space filter
- Found nearly 3,700 matches: 30% in stable regimes, 70% neutral or unstable regimes

FRIGG vs. NSCAT COLLOCATED - 9609-9706

Using WindBrown

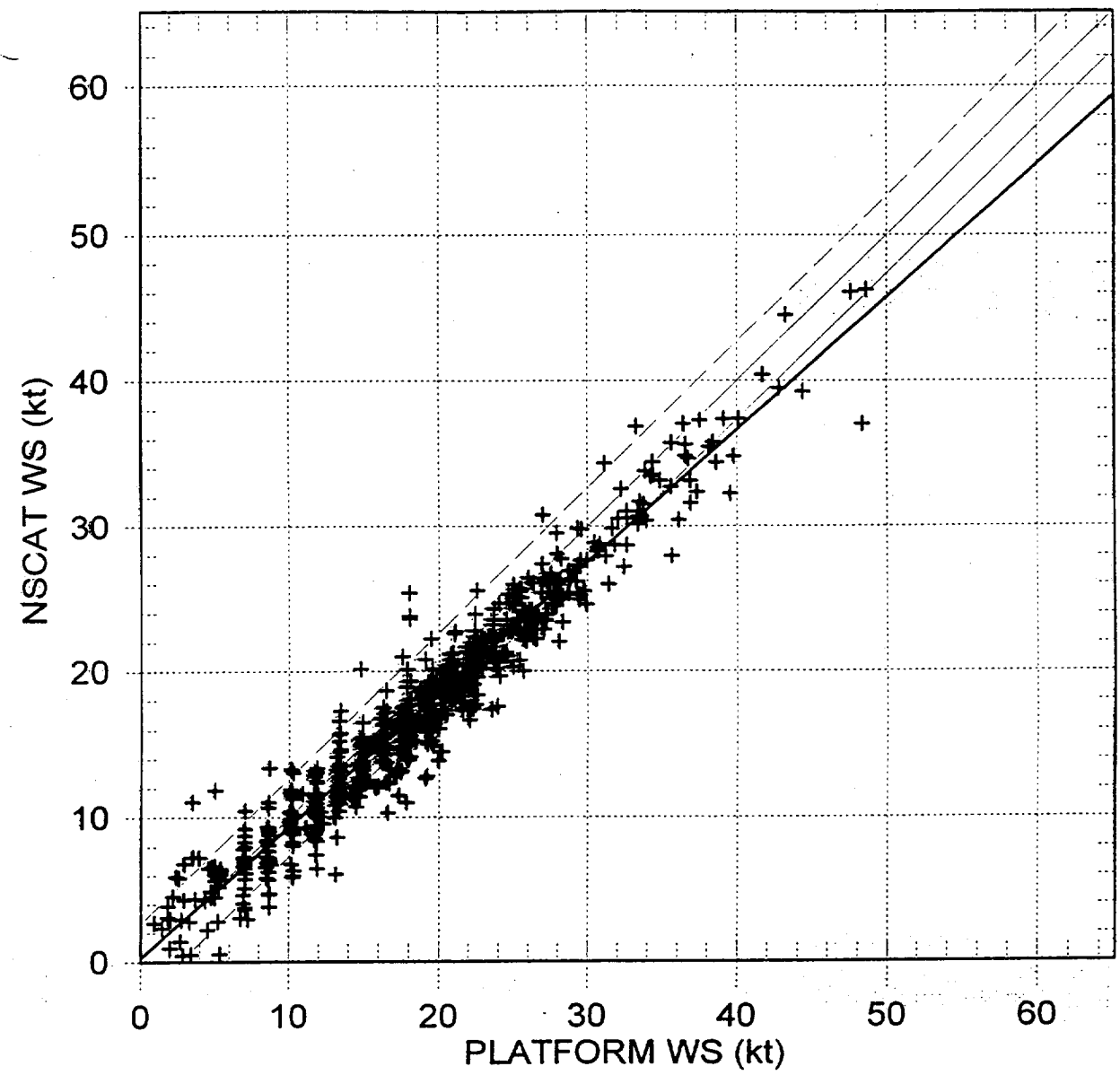

Best Fit: Y = 0.909X + 0.245	
Total Points:	549
Mean X:	18.342
Mean Y:	16.919
Mean Diff:	-1.423
Root Mean Square:	2.673
Standard Dev.:	2.263
Scatter Index:	0.123
Ratio:	0.233
Correlation Coeff:	0.969

PPIONEER vs. NSCAT COLLOCATED 9609-9706

Using WindBrown

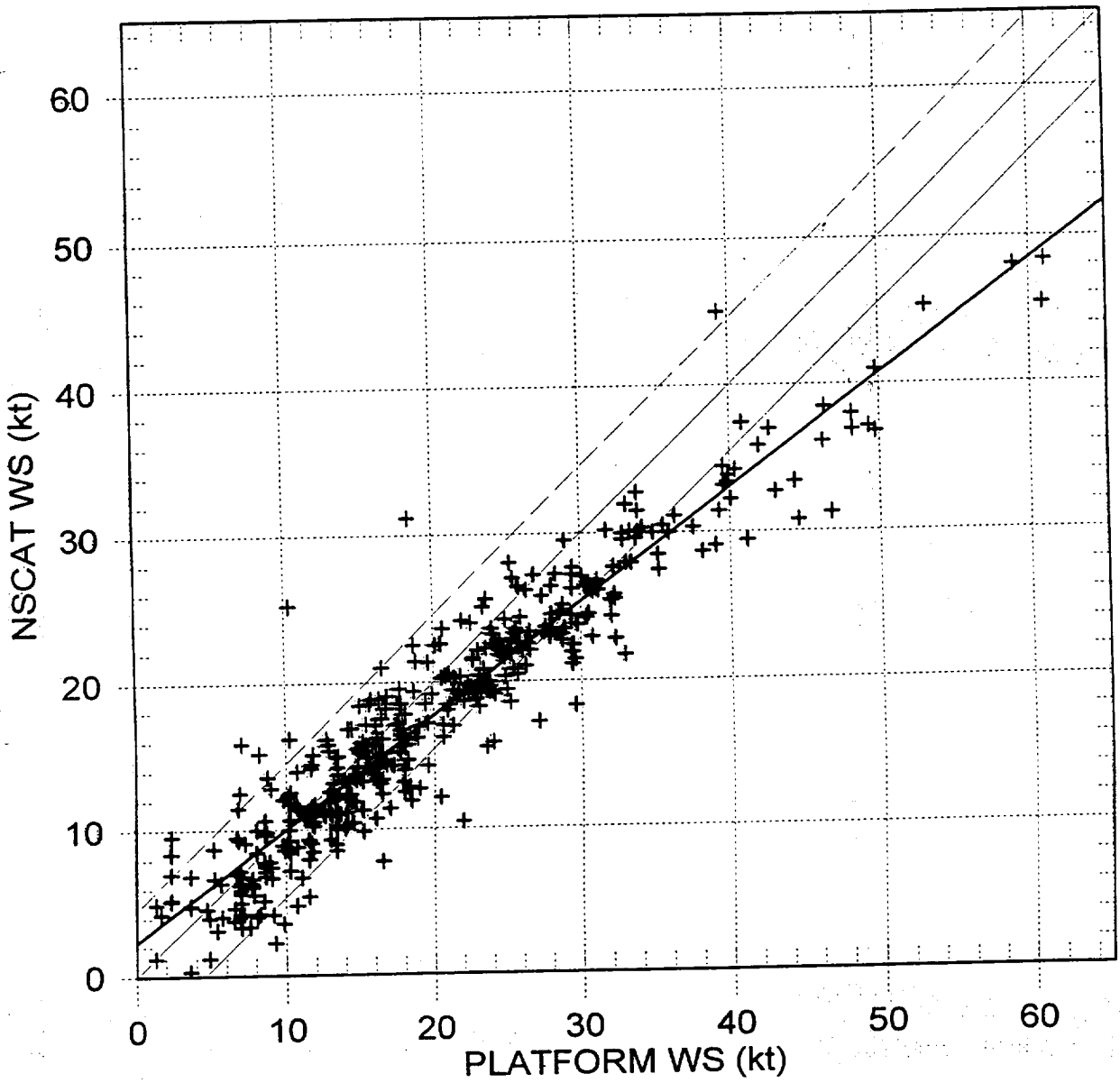

Best Fit: Y = 0.769X + 2.308	
Total Points:	381
Mean X:	19.840
Mean Y:	17.556
Mean Diff:	-2.283
Root Mean Square:	4.542
Standard Dev.:	3.926
Scatter Index:	0.198
Ratio:	0.239
Correlation Coeff:	0.945

PLATFORMS vs. NSCAT COLLOCATED - 9609-9706

Using WindFN

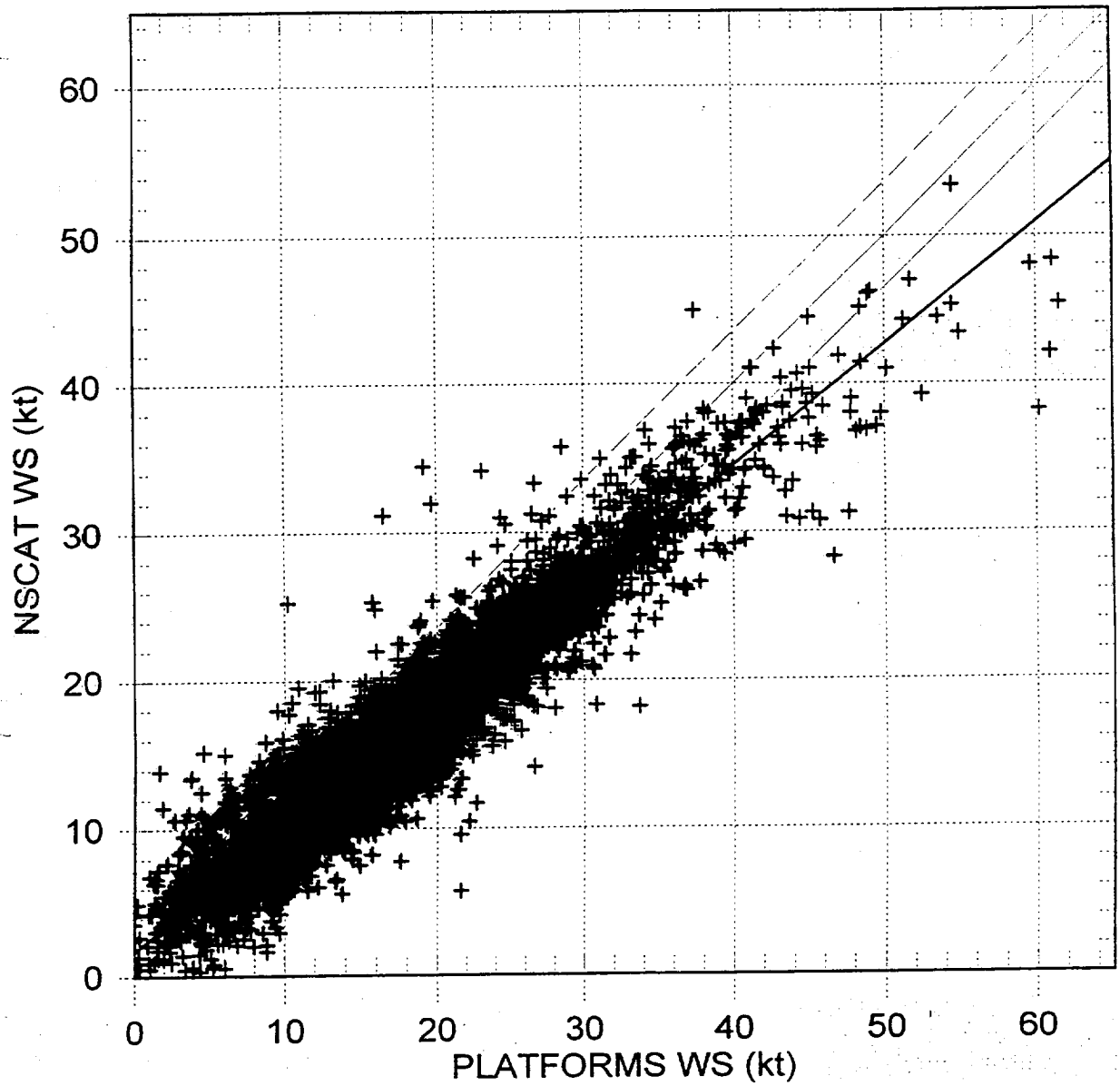

Best Fit: Y = 0.820X + 1.680	
Total Points:	3669
Mean X:	18.864
Mean Y:	17.143
Mean Diff:	-1.721
Root Mean Square:	3.537
Standard Dev.:	3.091
Scatter Index:	0.164
Ratio:	0.246
Correlation Coeff:	0.949

Collocated NSCAT/North Sea Platforms 10 m Wind Speed Plots Binned on 1 m/s Platform Winds

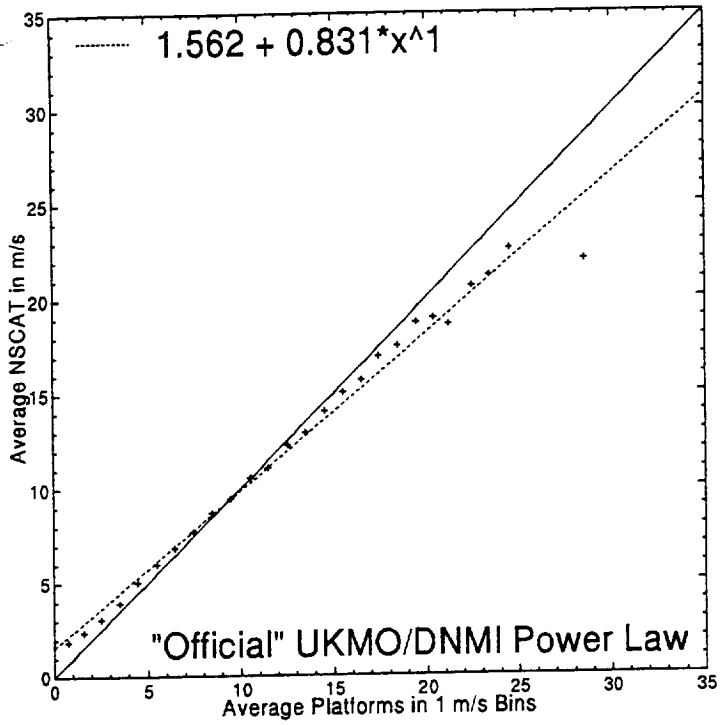

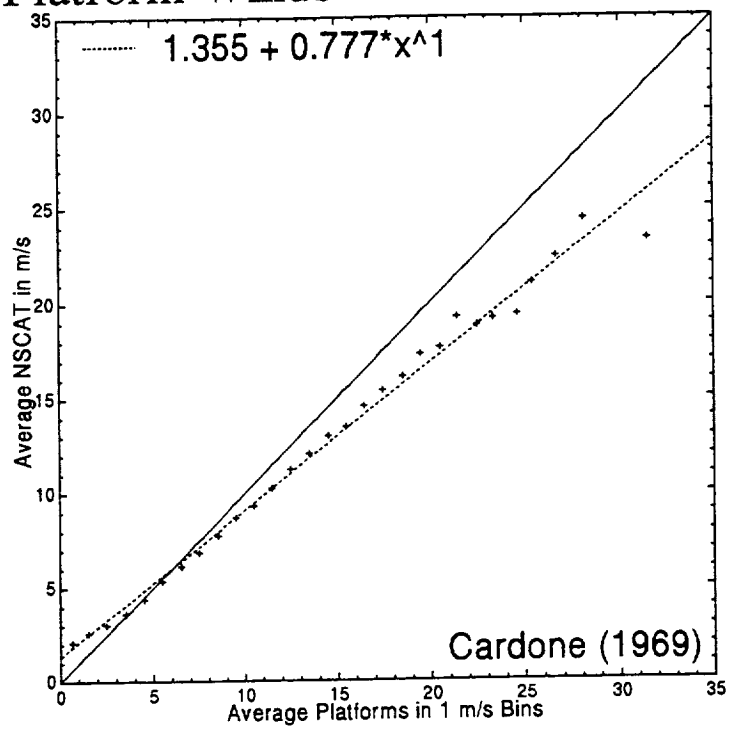

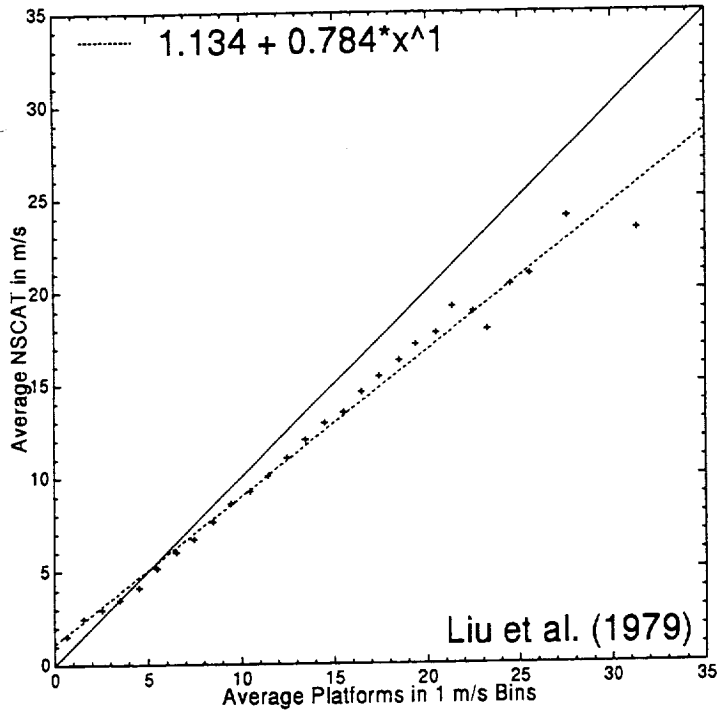

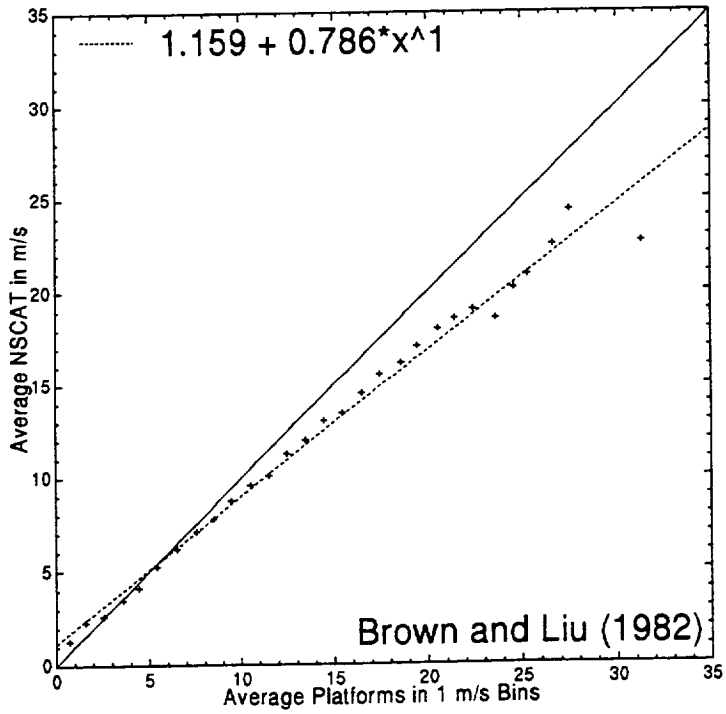

Quantile-Quantile Scatter Plots of Collocated NSCAT-North Sea Platform 10 m Wind Speed

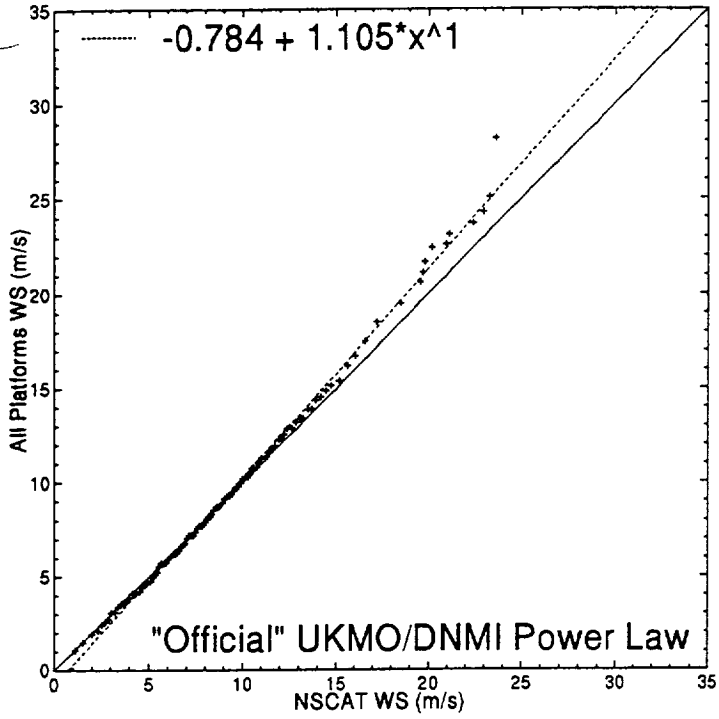

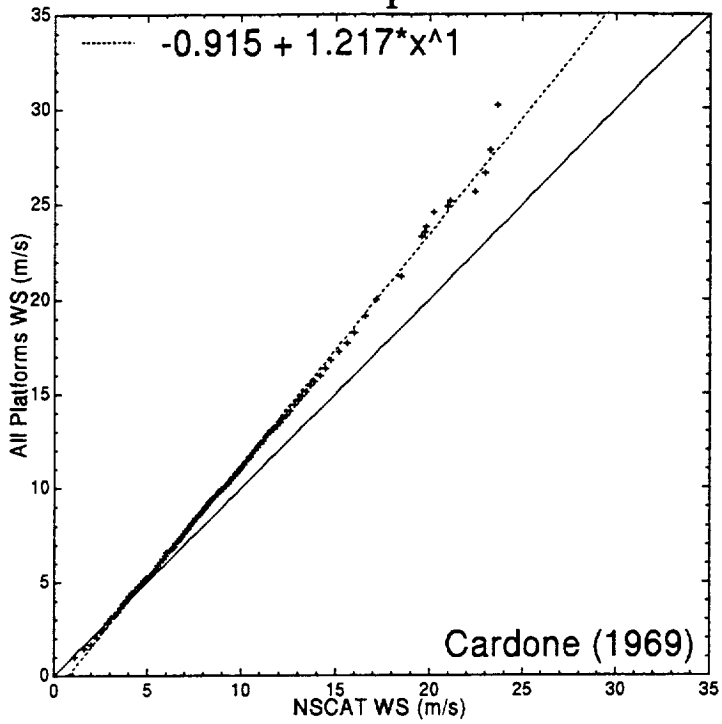

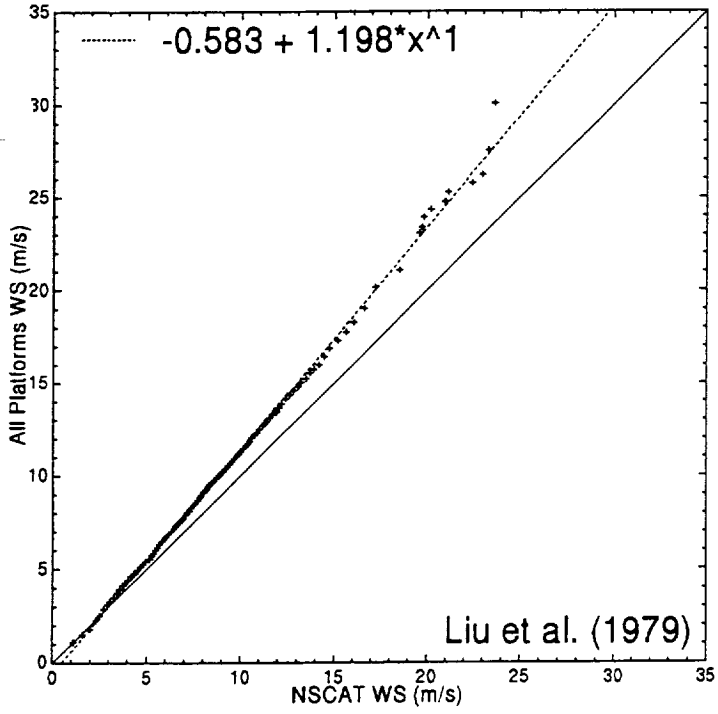

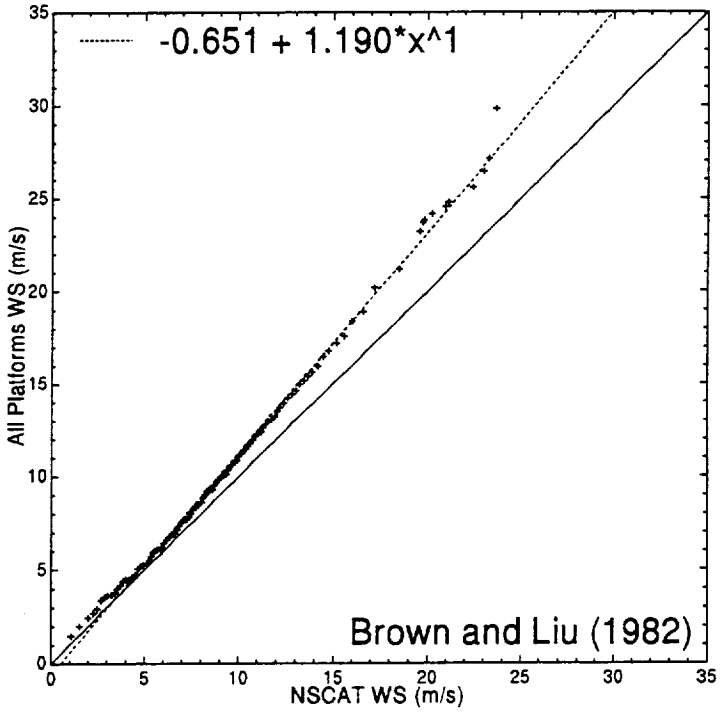

Mean Difference (Q-Q Regressions)
NSCAT - Platform (10 m)

	NSCAT=2-4 m/s		NSCAT=5-15 m/s		NSCAT=16-20 m/s		NSCAT=21-24 m/s	
Method	**Absolute**	**%**	**Absolute**	**%**	**Absolute**	**%**	**Absolute**	**%**
Power Law	0.469	22.93	-0.253	3.17	-1.106	5.76	-1.579	6.55
Cardone (1969)	0.264	14.17	-1.255	10.15	-2.991	14.23	-3.968	14.98
Liu et al. (1979)	-0.011	5.22	-1.397	11.66	-2.981	14.19	-3.872	14.68
Brown and Liu (1982)	0.081	7.03	-1.249	10.42	-2.769	13.31	-3.624	13.87
Freilich and Dunbar (1999)*	0.193	8.19	-0.185	1.78	-0.617	3.30	-0.860	3.68

* Based on regression of 30 NDBC Buoys

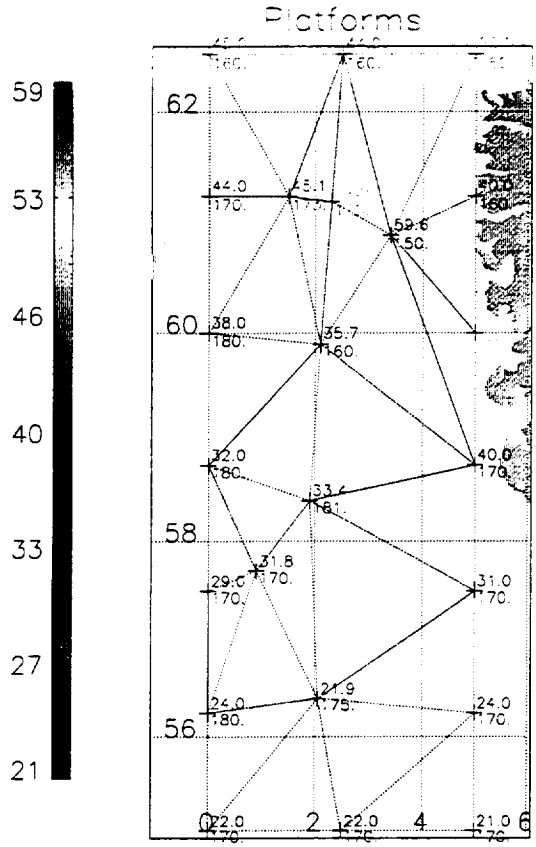

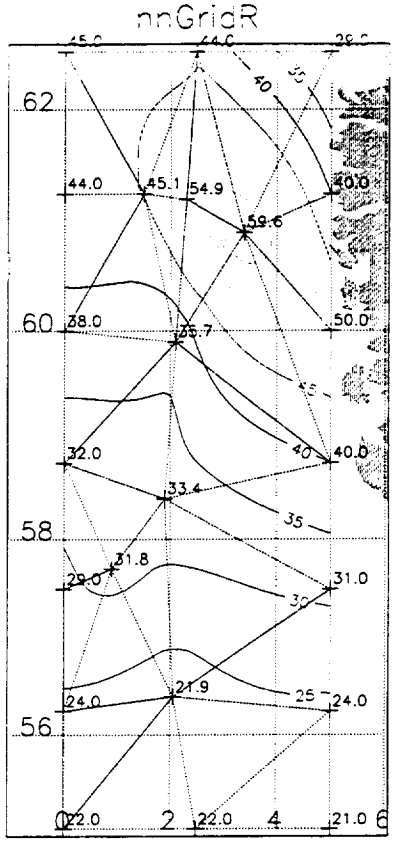

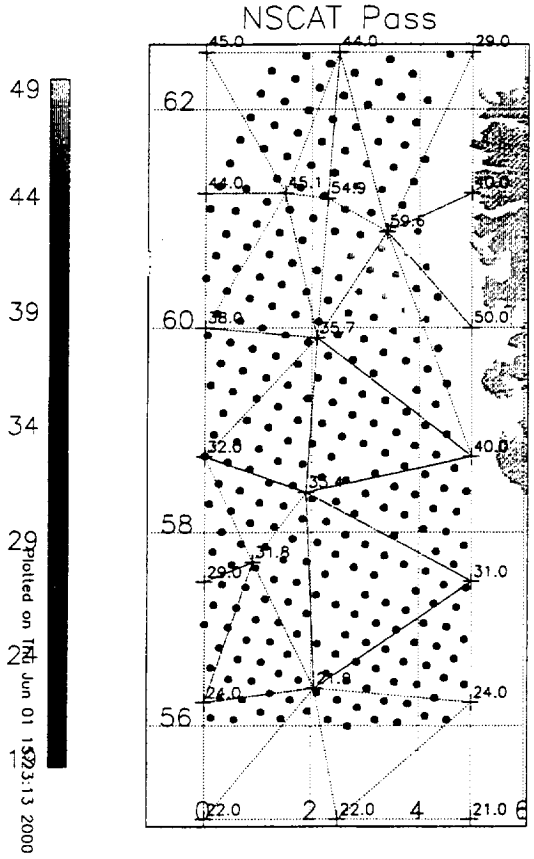

Best Fit: Y = 0.831X + 2.823
Total Points: 293
Mean X: 36.230
Mean Y: 32.913
Mean Diff (Y−X): −3.316
Root Mean Square: 4.714
Standard Deviation: 3.350
Scatter Index: 0.092
Ratio (Y>X): 0.171
Correlation Coeff: 0.926

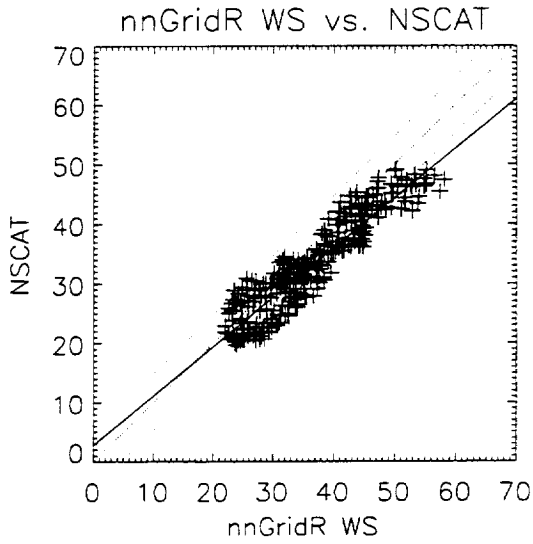

1997021712

All 58 Snapshots, WindFN adjusted with boundary

Best Fit: Y = 0.900X + 0.319
Total Points: 9992
Mean X: 32.056
Mean Y: 29.171
Mean Diff (Y−X): −2.885
Root Mean Square: 4.726
Standard Deviation: 3.744
Scatter Index: 0.117
Ratio (Y>X): 0.191
Correlation Coeff: 0.894

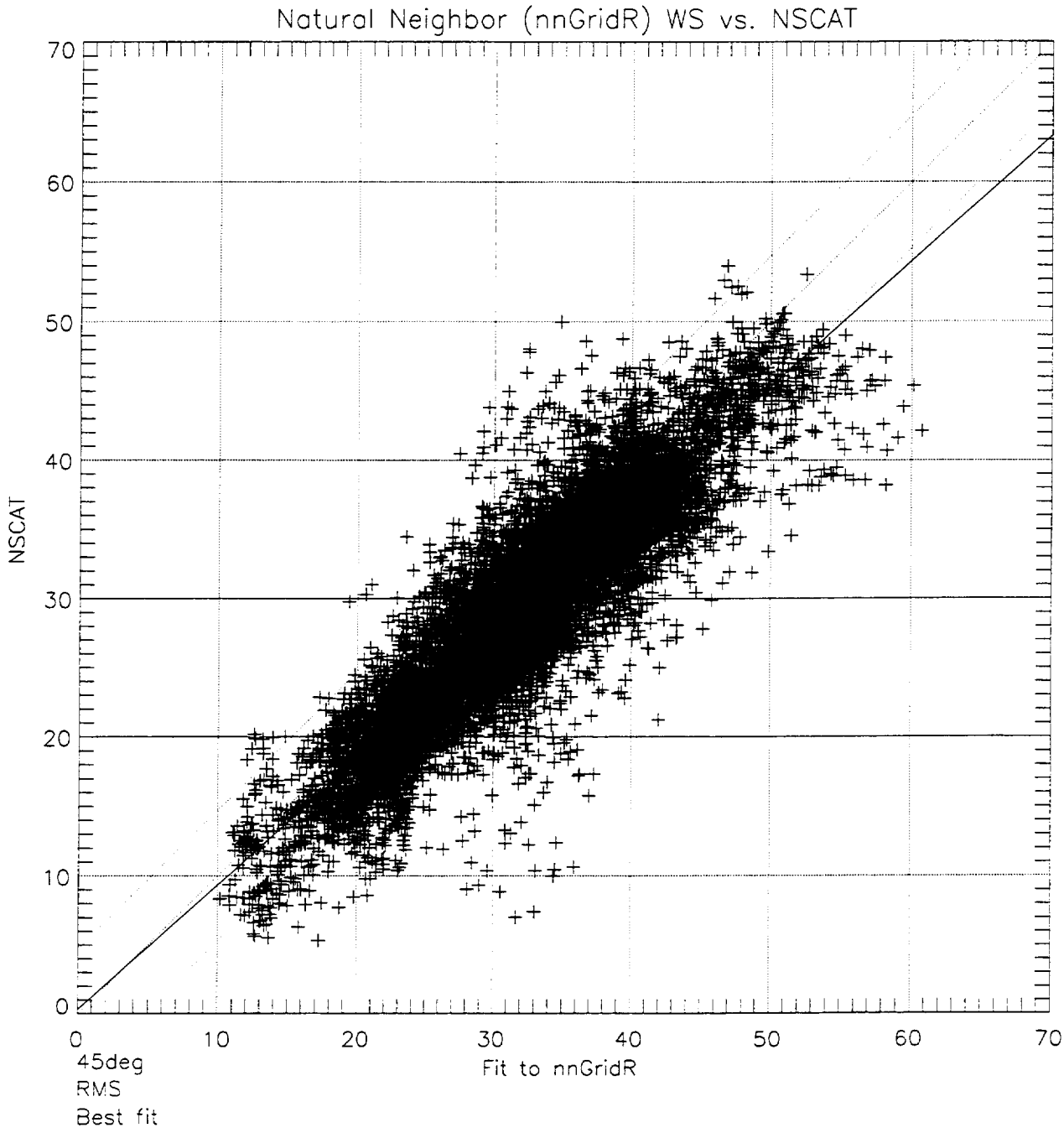

Plotted on Thu Jun 01 14:25:43 2000

SUMMARY

- Lack of clearly unbiased "reference" surface marine winds over whole dynamic range of interest (U10n of 0-40 m/s)
- North Sea platform array samples nearly entire dynamic range in one winter season and yields many thousands of Scat vs in-situ co-locations (50 km and 30 min filters)
- Platform winds perhaps two steps away from reference quality:
  1. definition of flow distortion effect: CFD program underway at Southampton Oceanography Center
  2. Resolution of wind profile 5 m – 150 m :platform-buoy comparison programs planned
- NSCAT sensitive to surface wind to at least 32 m/s with low bias of 5-15 % above 20 m/s

Appendix B. QuickScat data coverage of Hurricane Floyd (1999) and best fits of inverse model parameters to azimuthally averaged wind speed (average wind speed at 10 m)

Quikscat Winds During Hurricane Floyd 1999

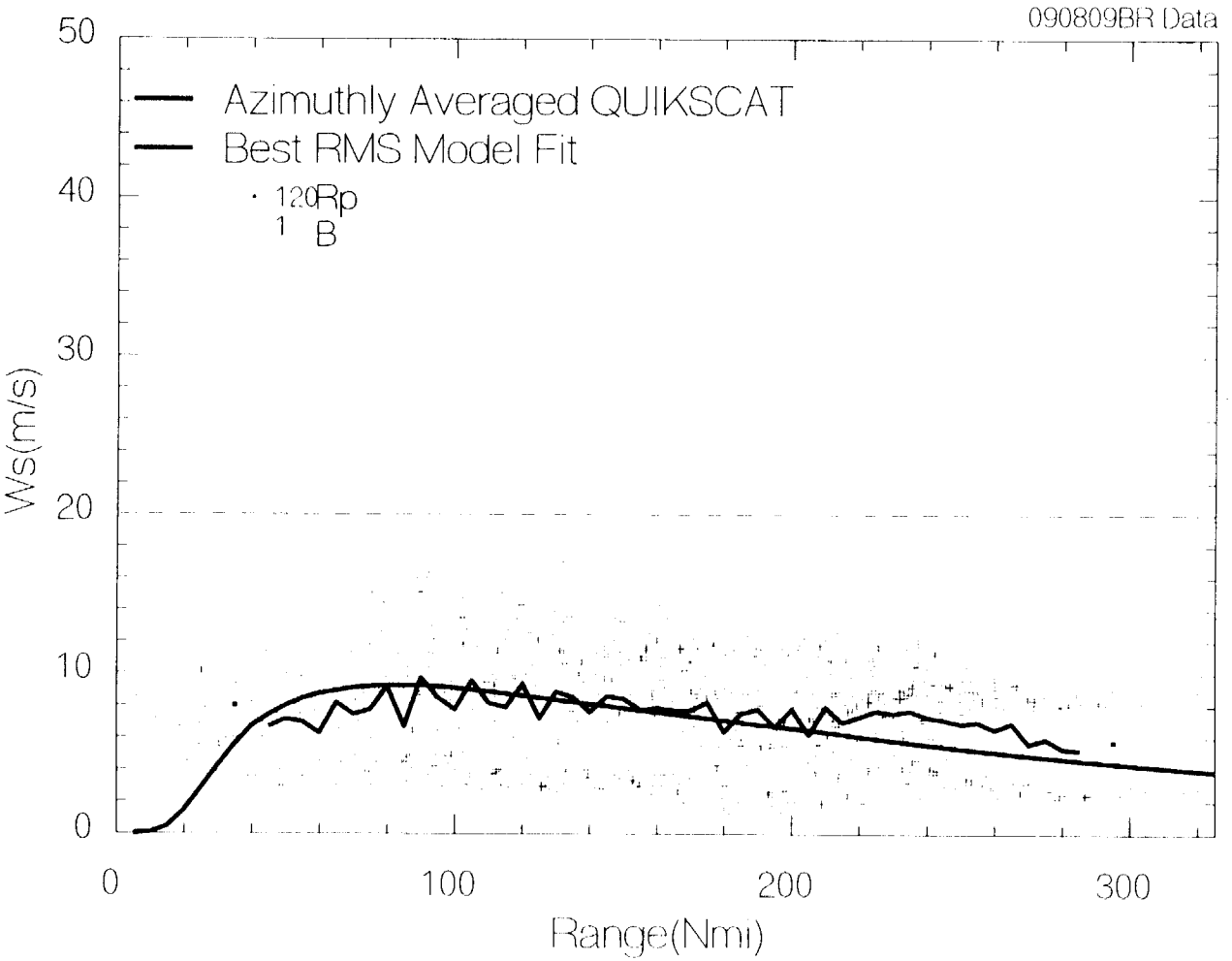

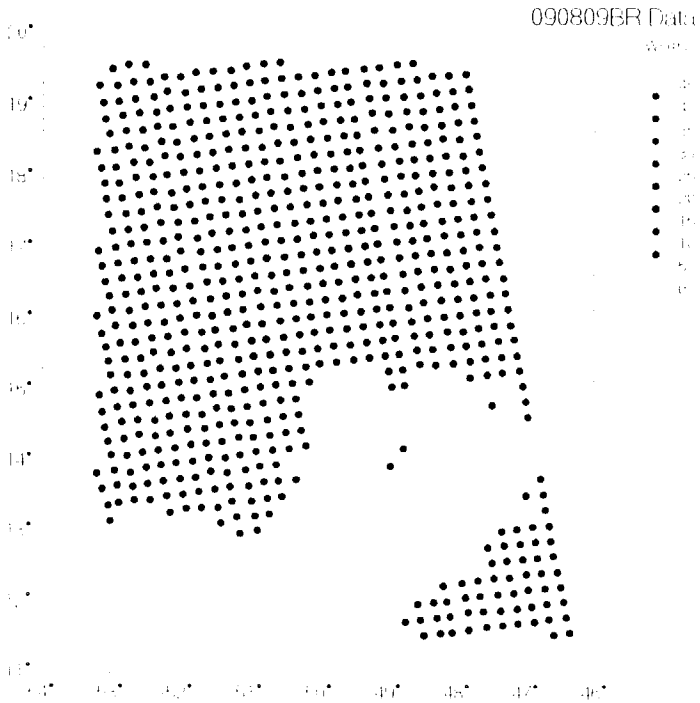

Quikscat Winds During Hurricane Floyd 1999

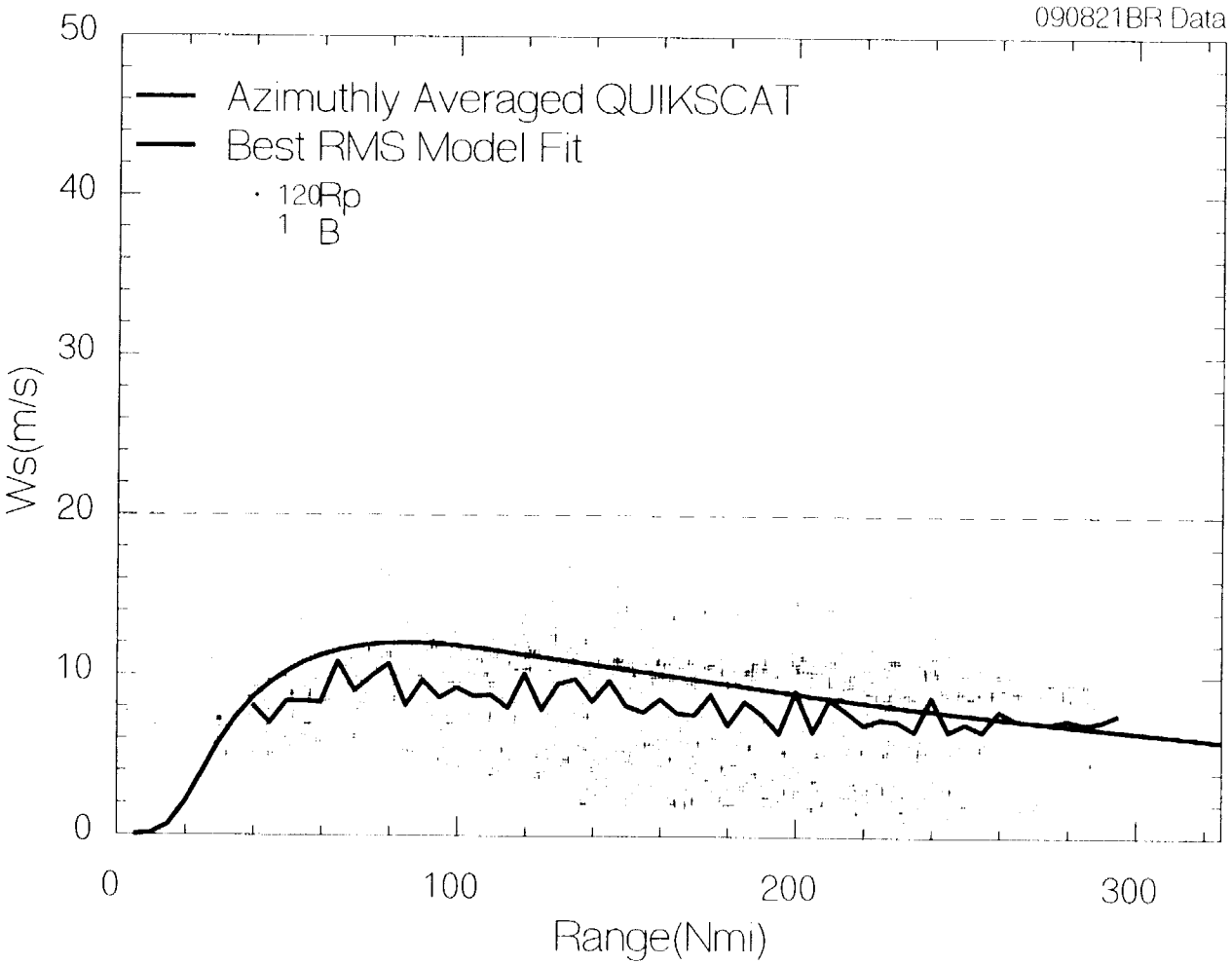

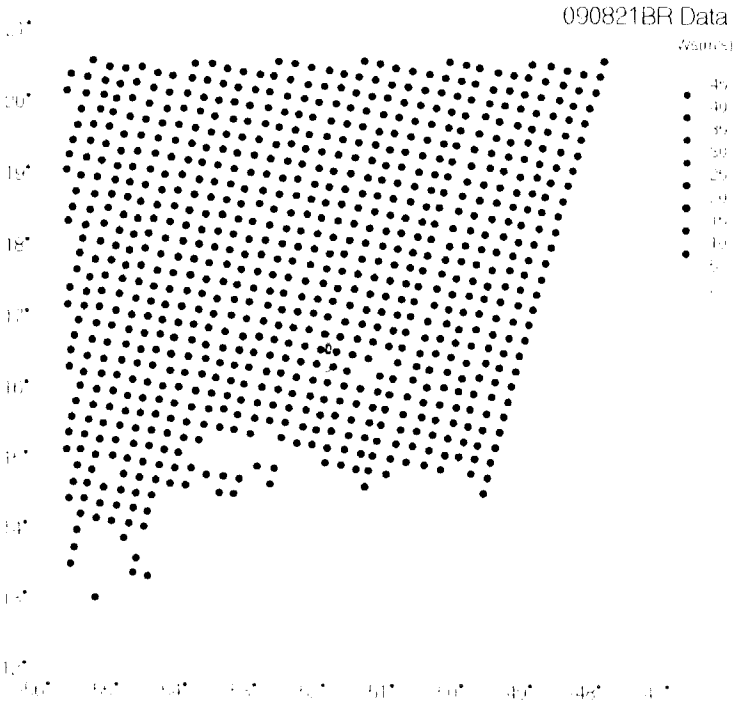

Quikscat Winds During Hurricane Floyd 1999

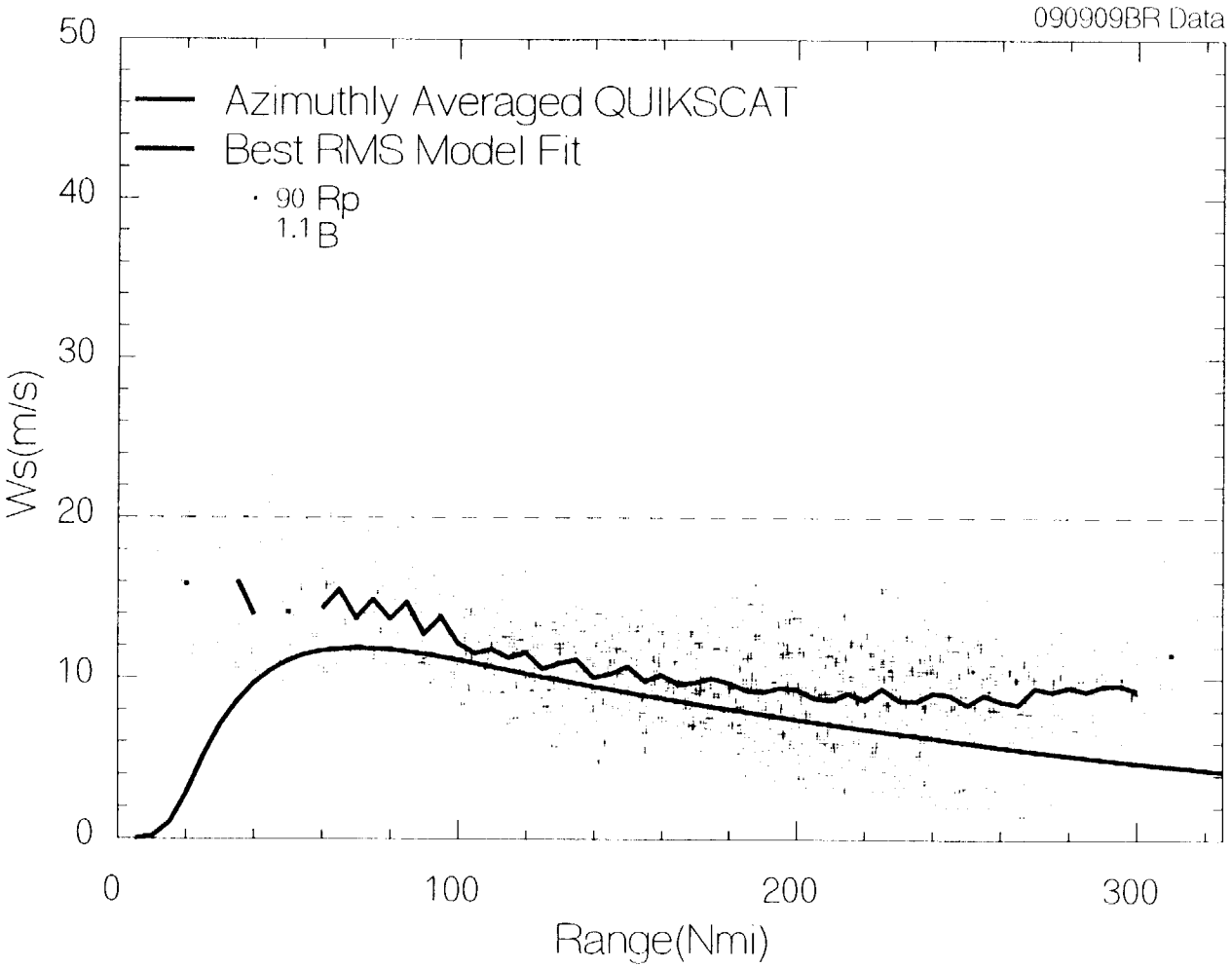

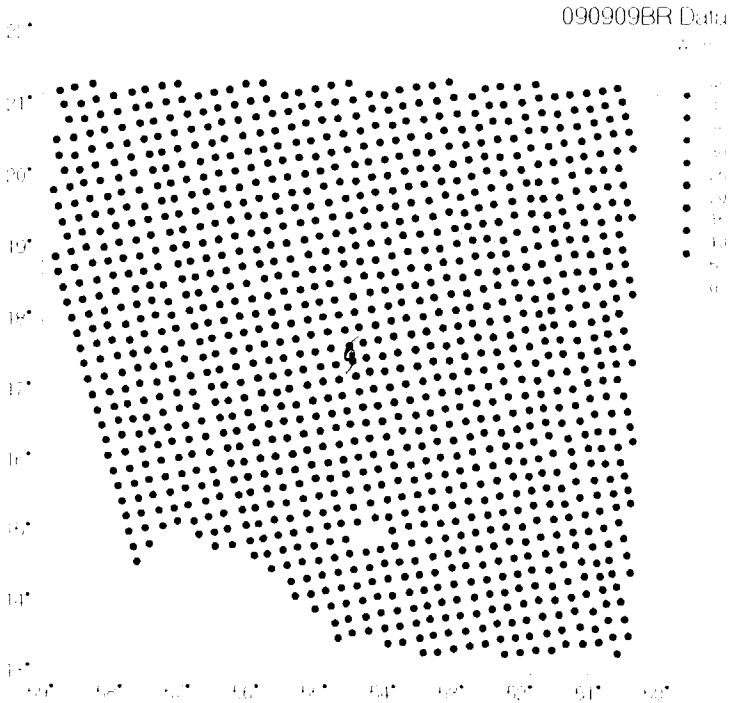

Quikscat Winds During Hurricane Floyd 1999

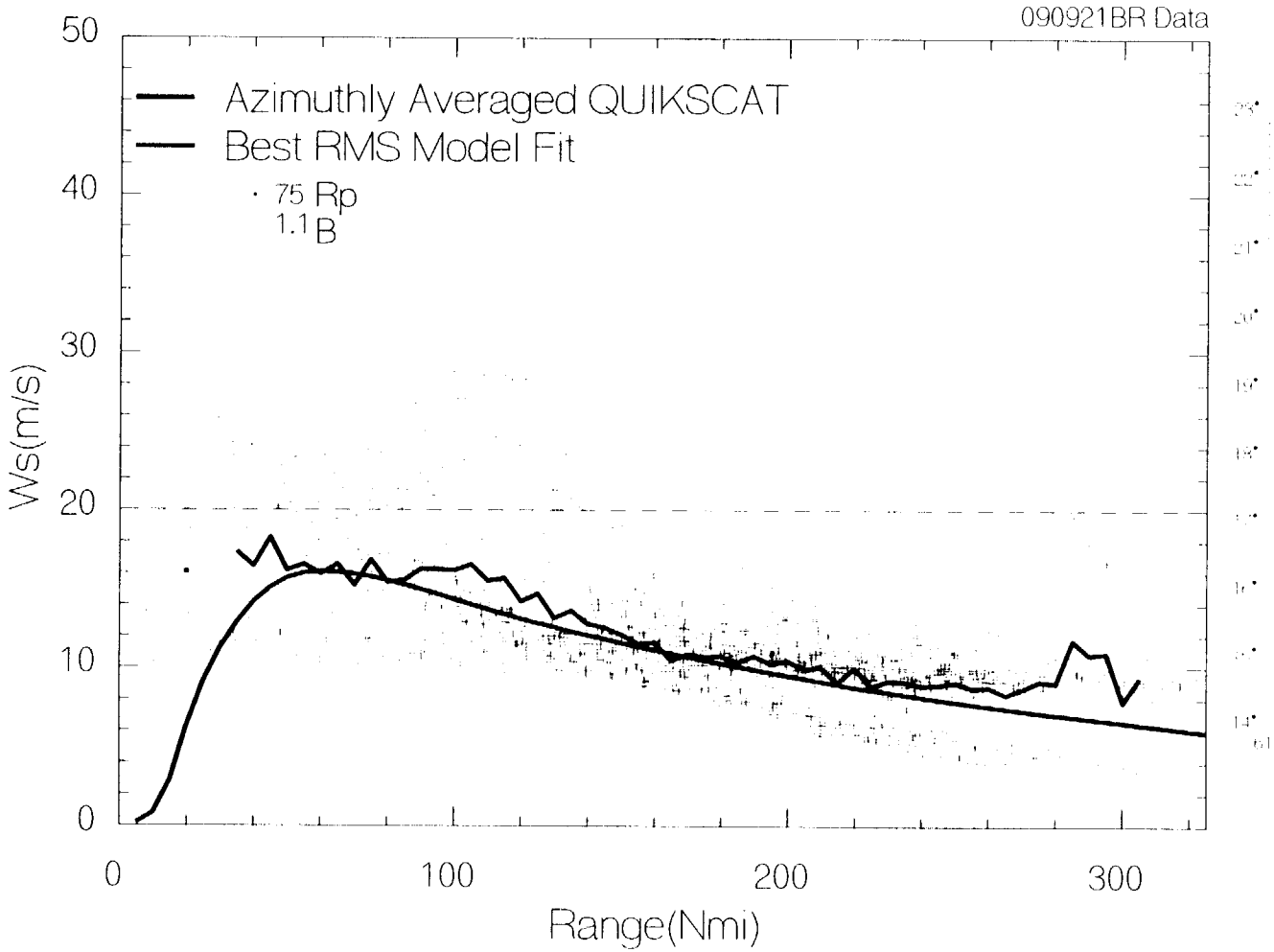

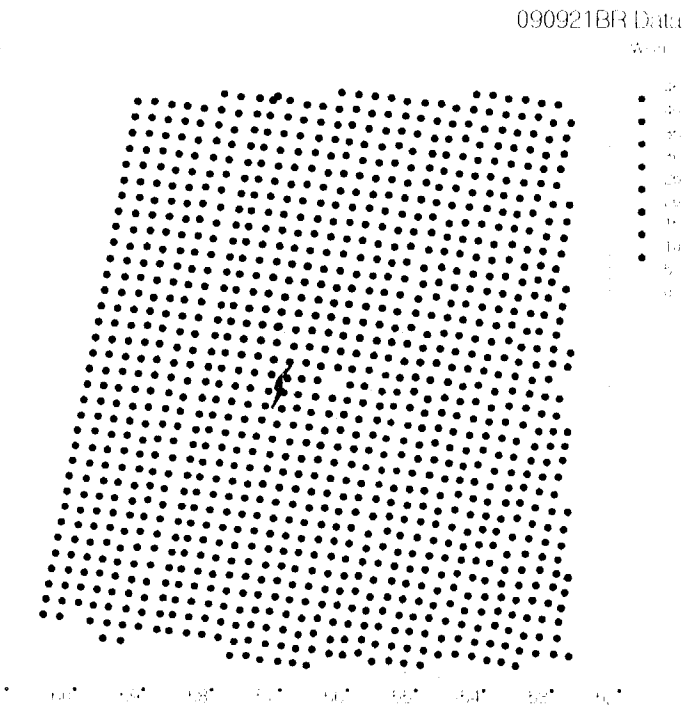

Quikscat Winds During Hurricane Floyd 1999

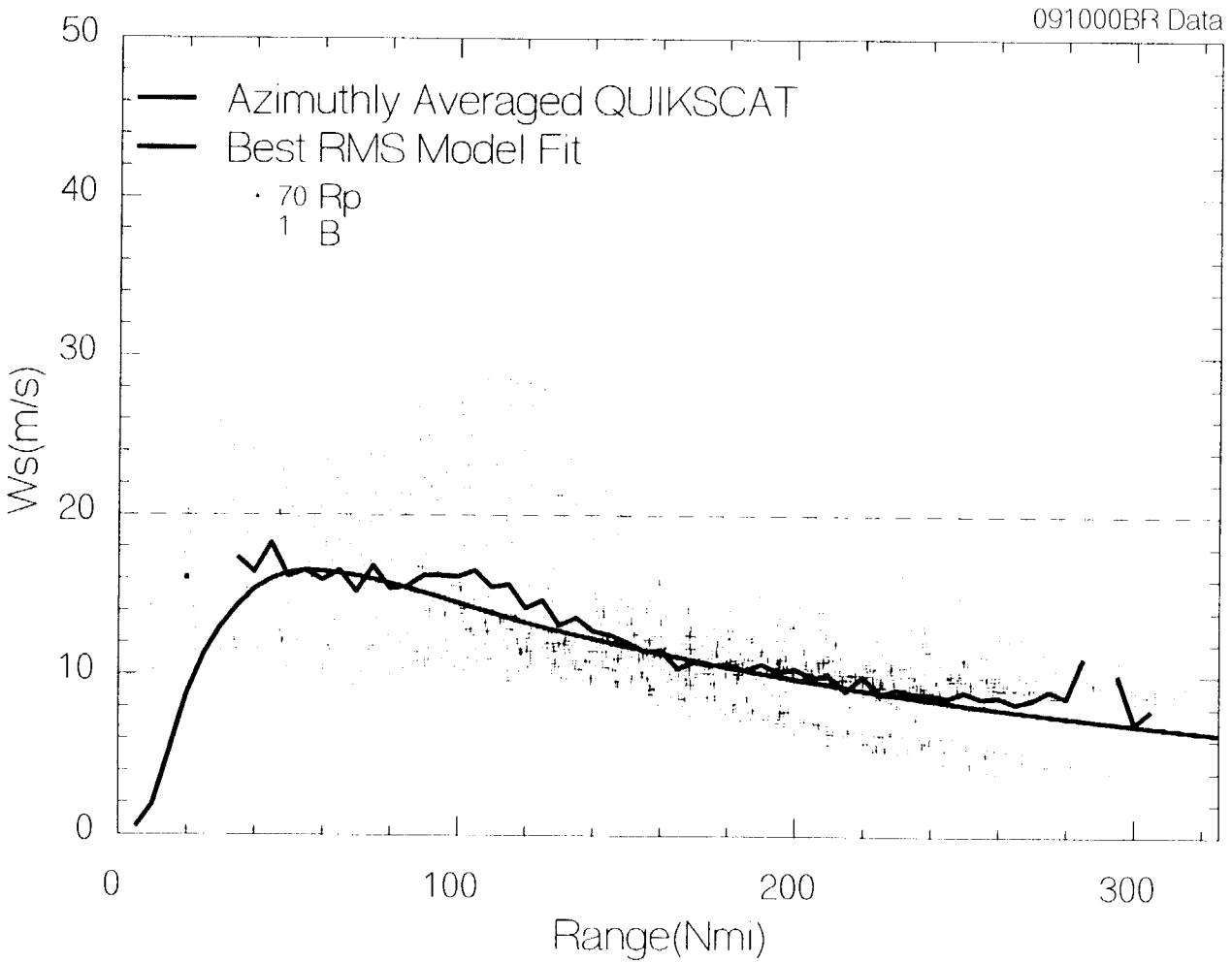

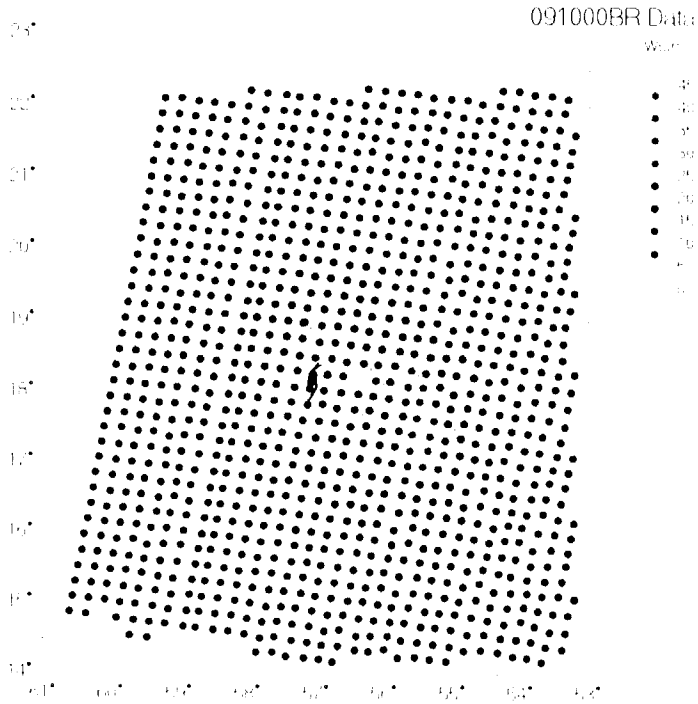

Quikscat Winds During Hurricane Floyd 1999

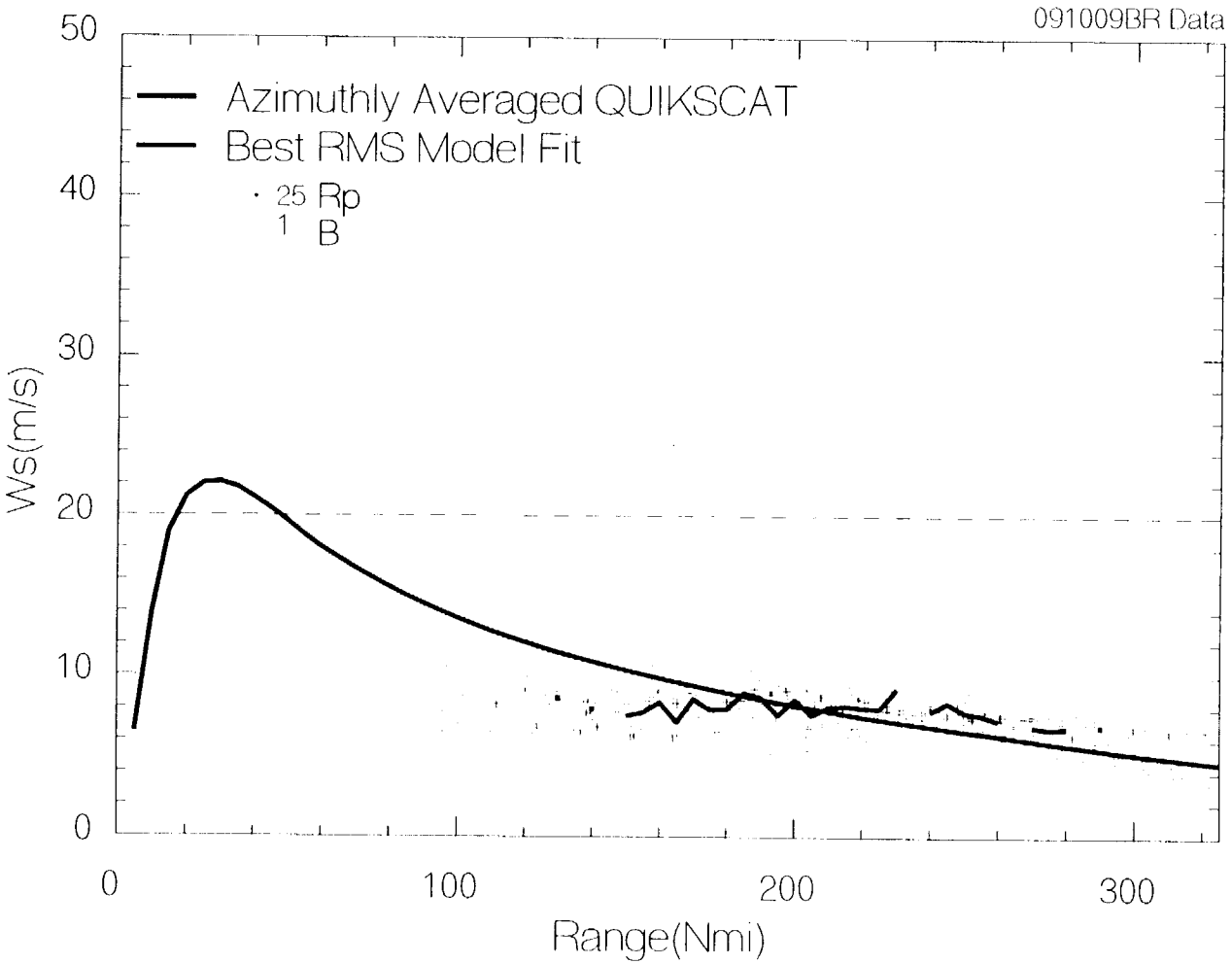

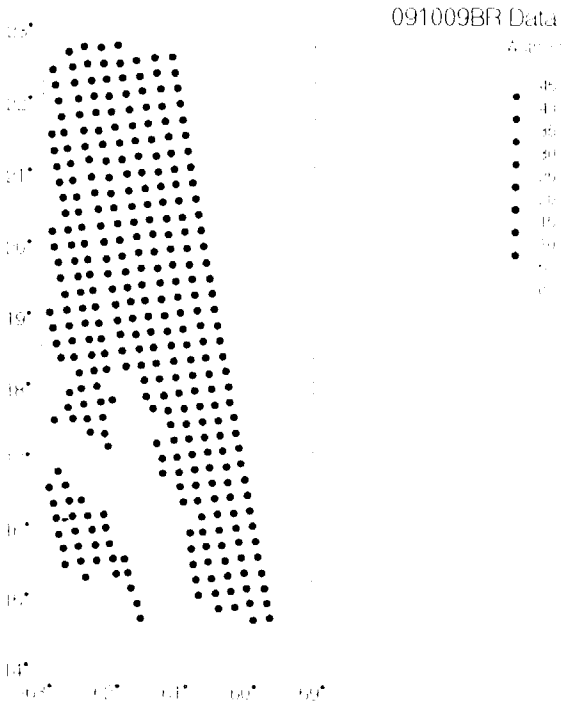

Quikscat Winds During Hurricane Floyd 1999

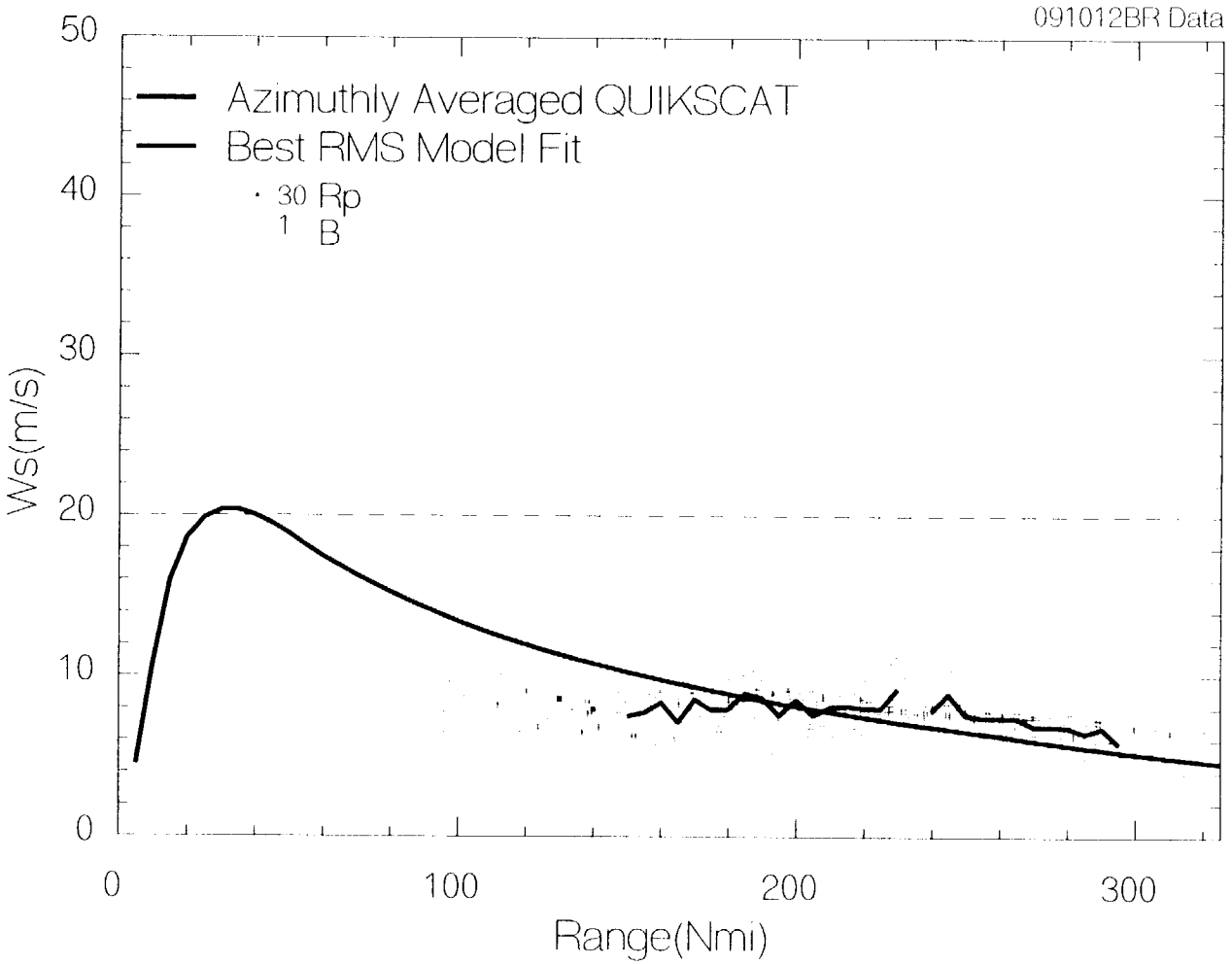

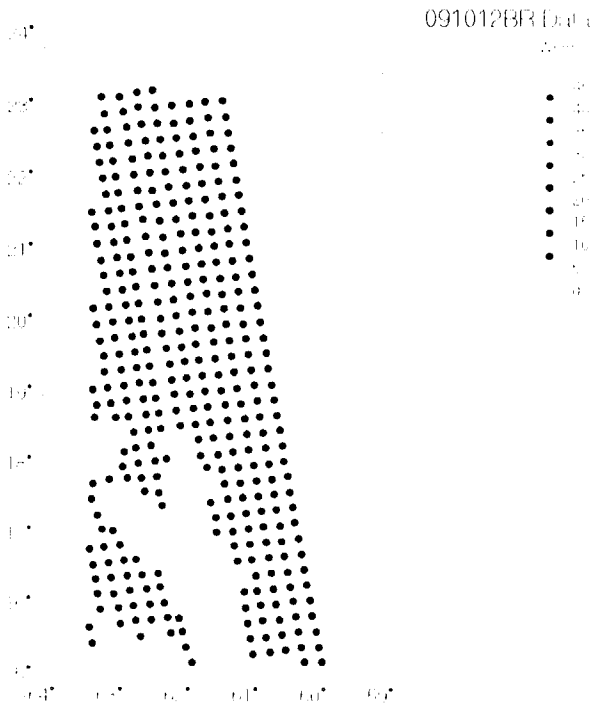

Quikscat Winds During Hurricane Floyd 1999

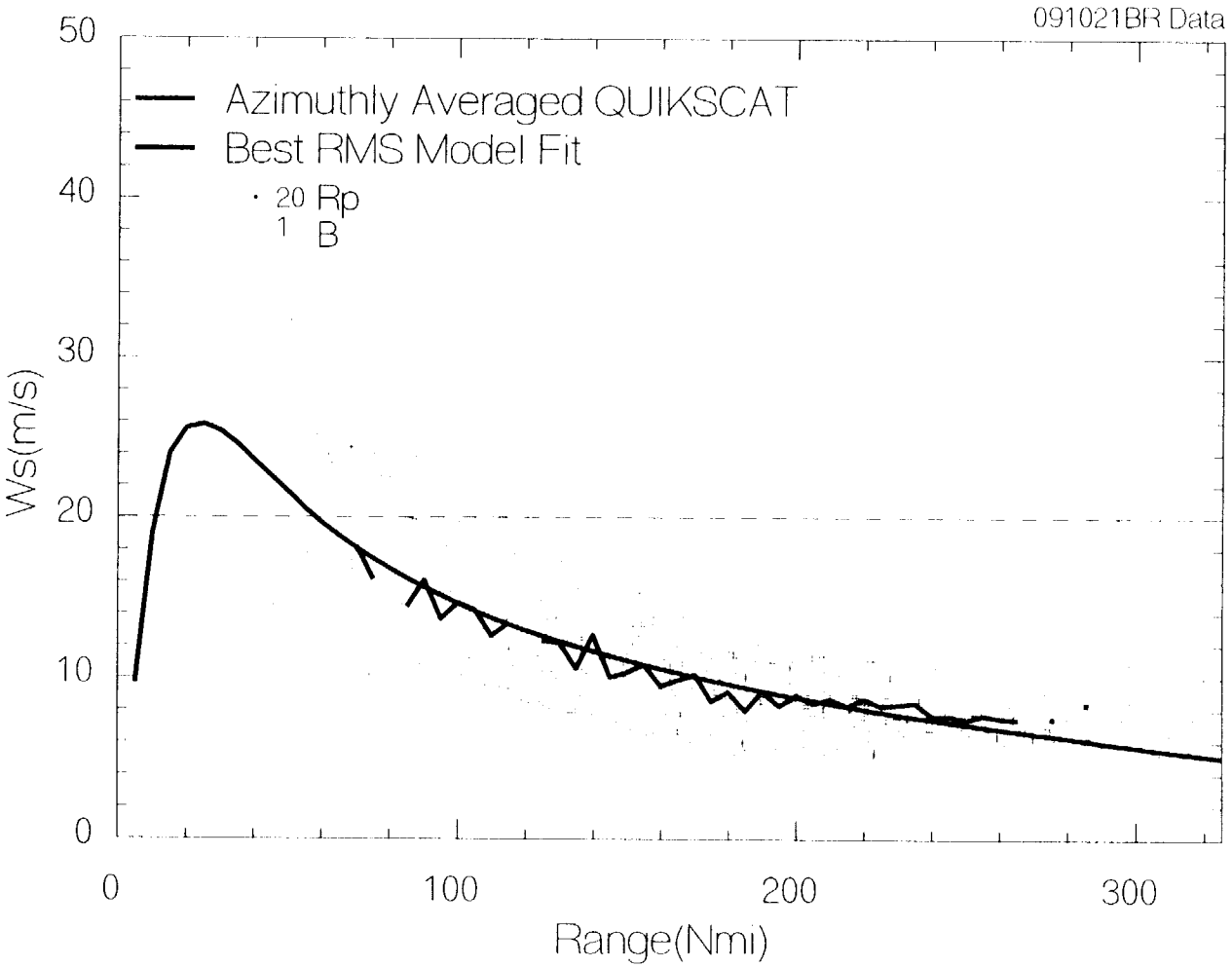

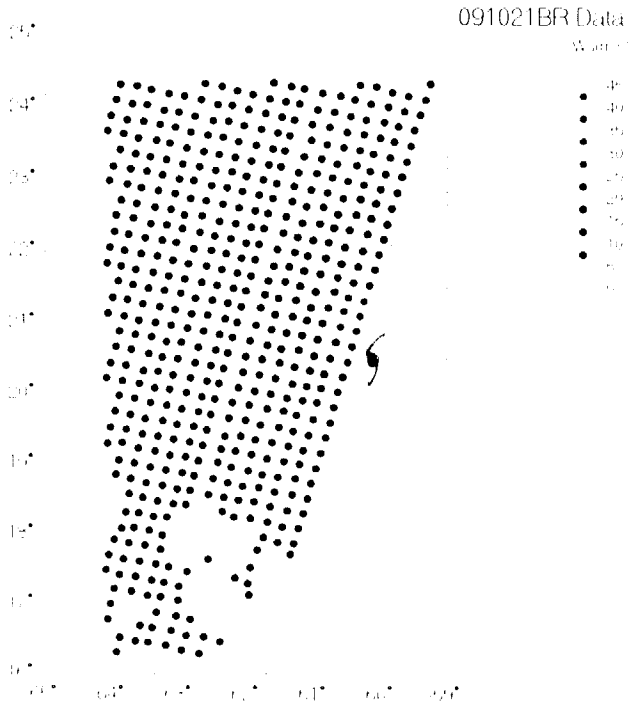

Quikscat Winds During Hurricane Floyd 1999

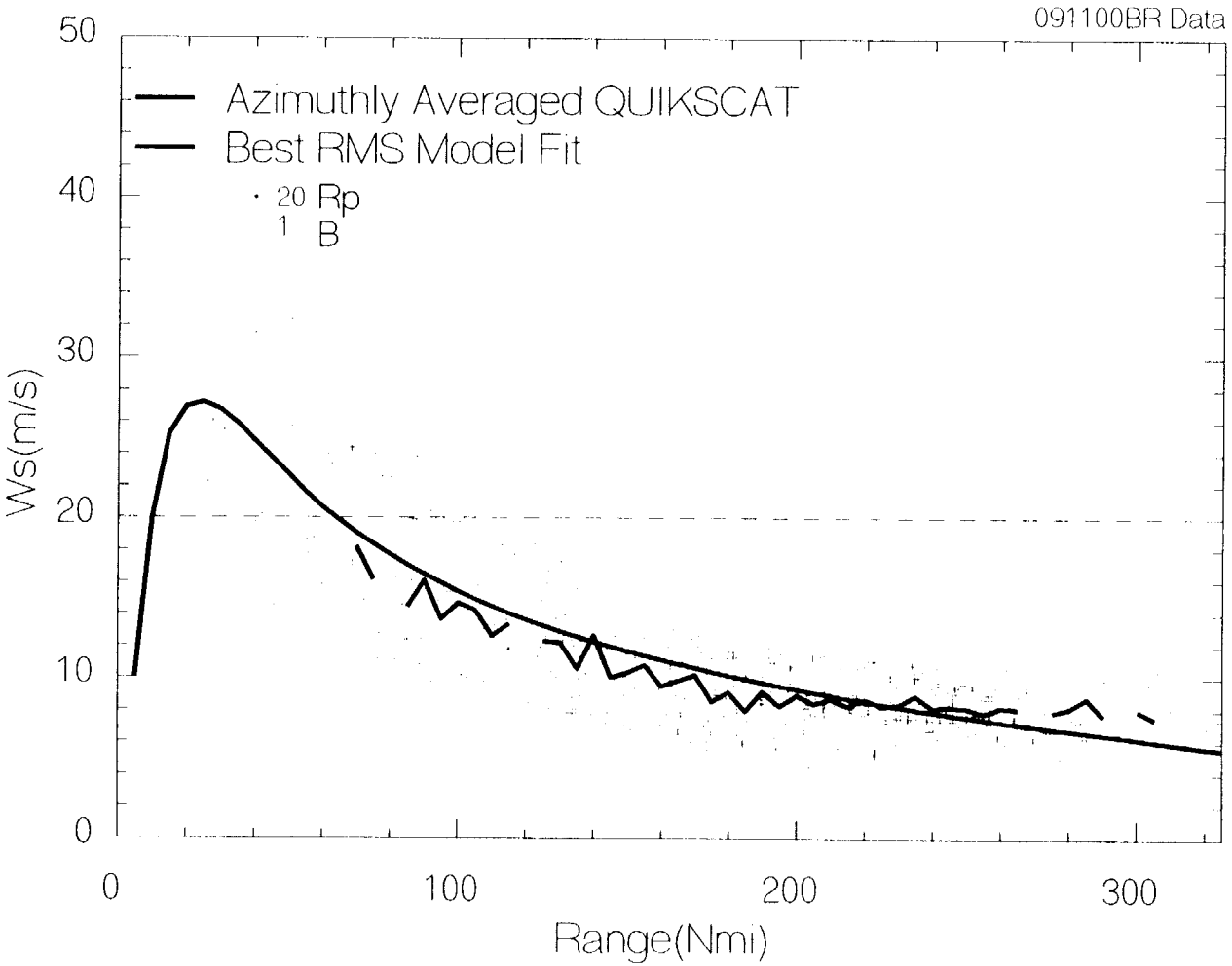

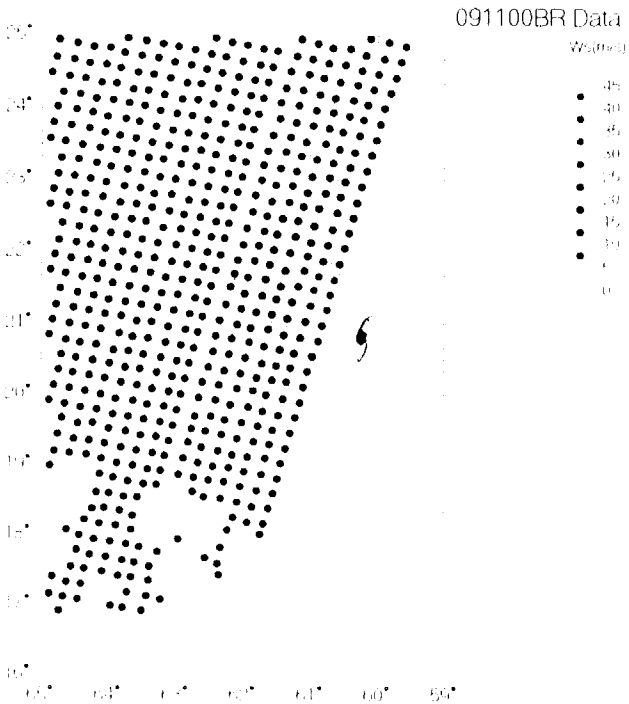

Quikscat Winds During Hurricane Floyd 1999

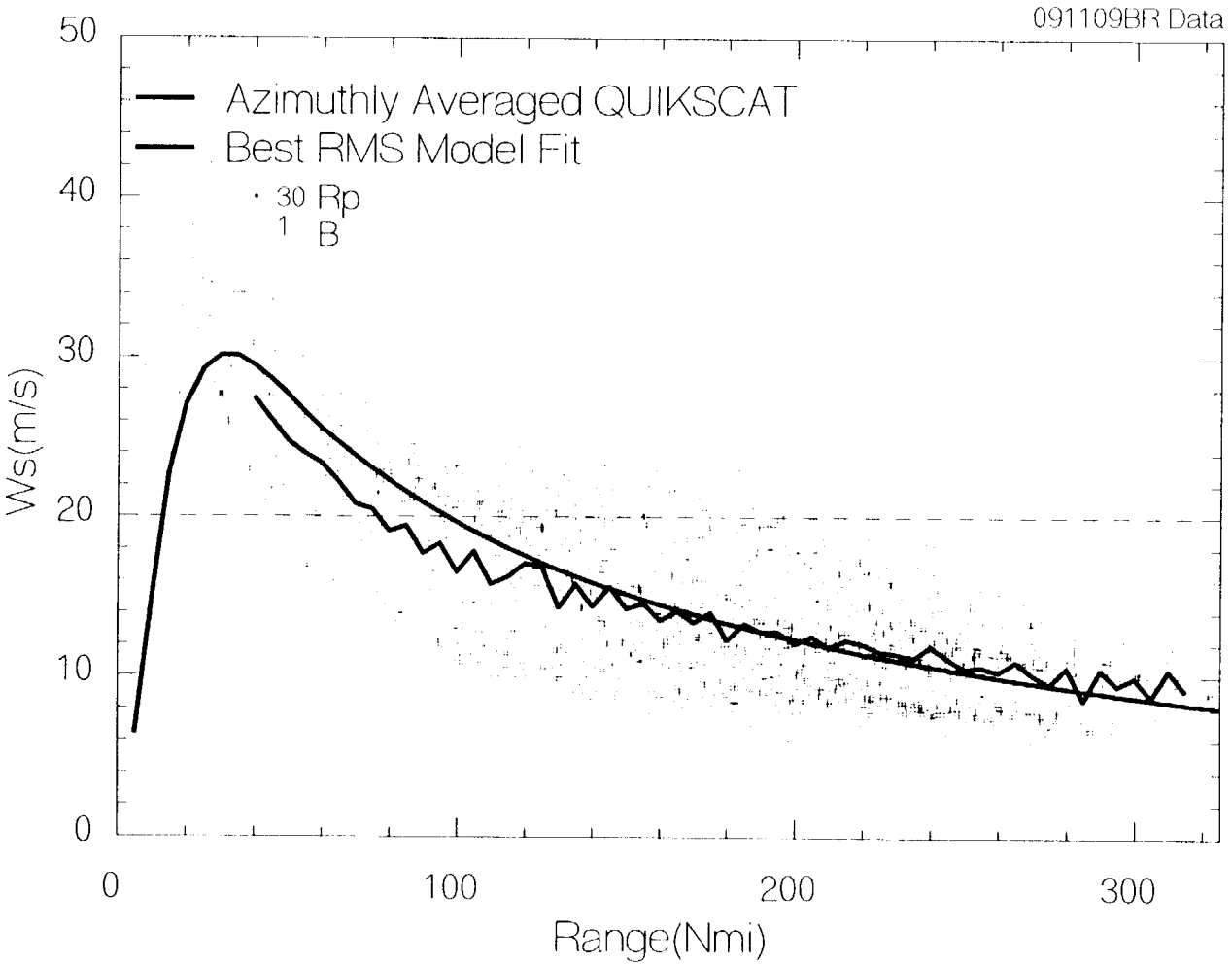

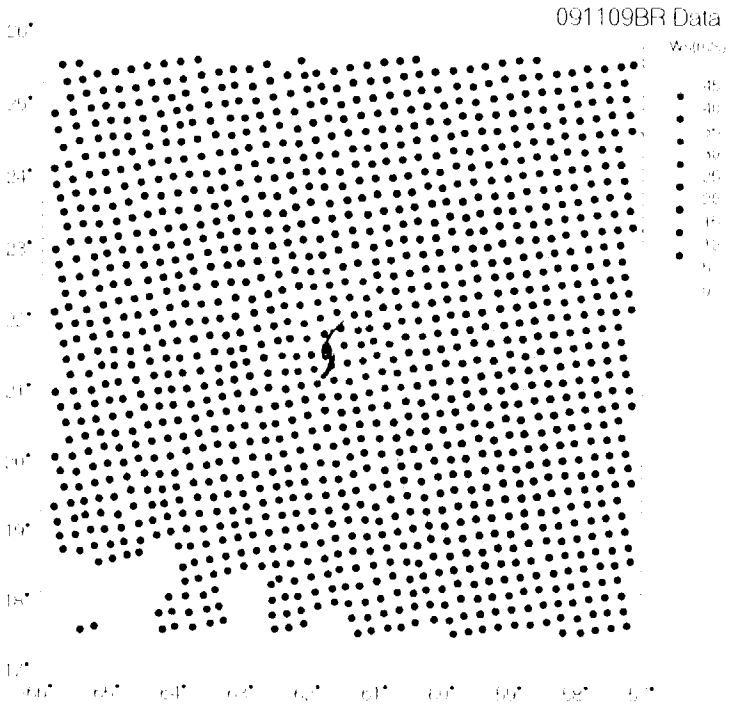

Quikscat Winds During Hurricane Floyd 1999

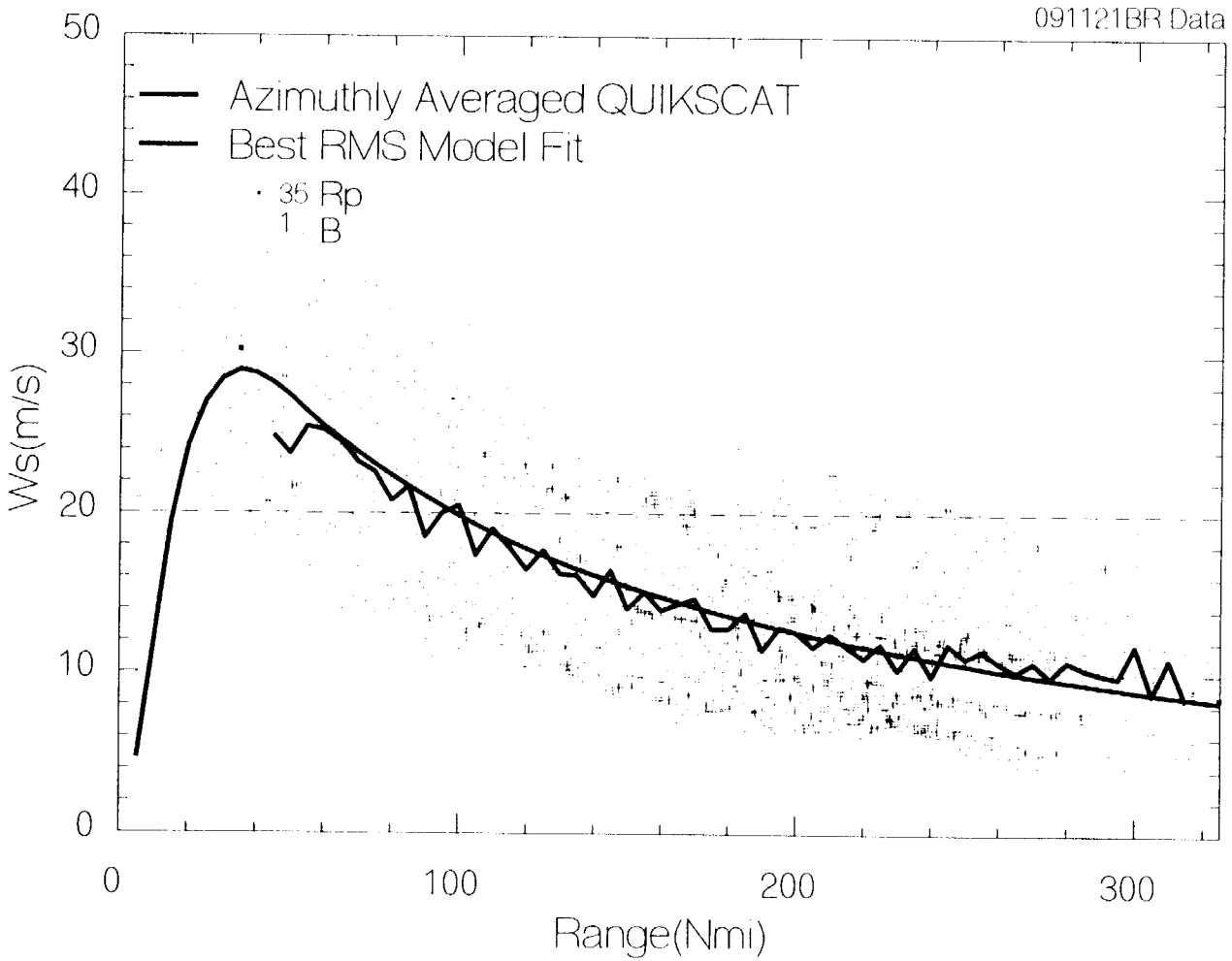

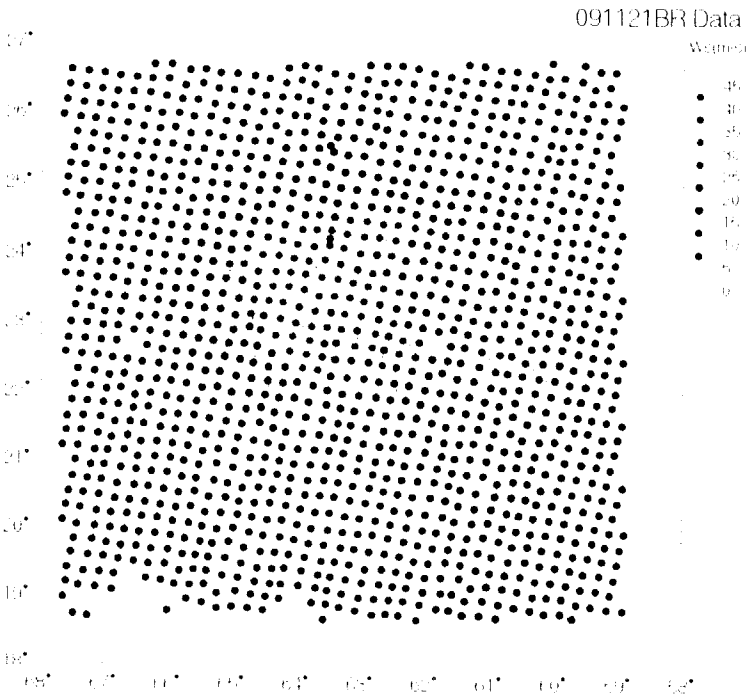

Quikscat Winds During Hurricane Floyd 1999

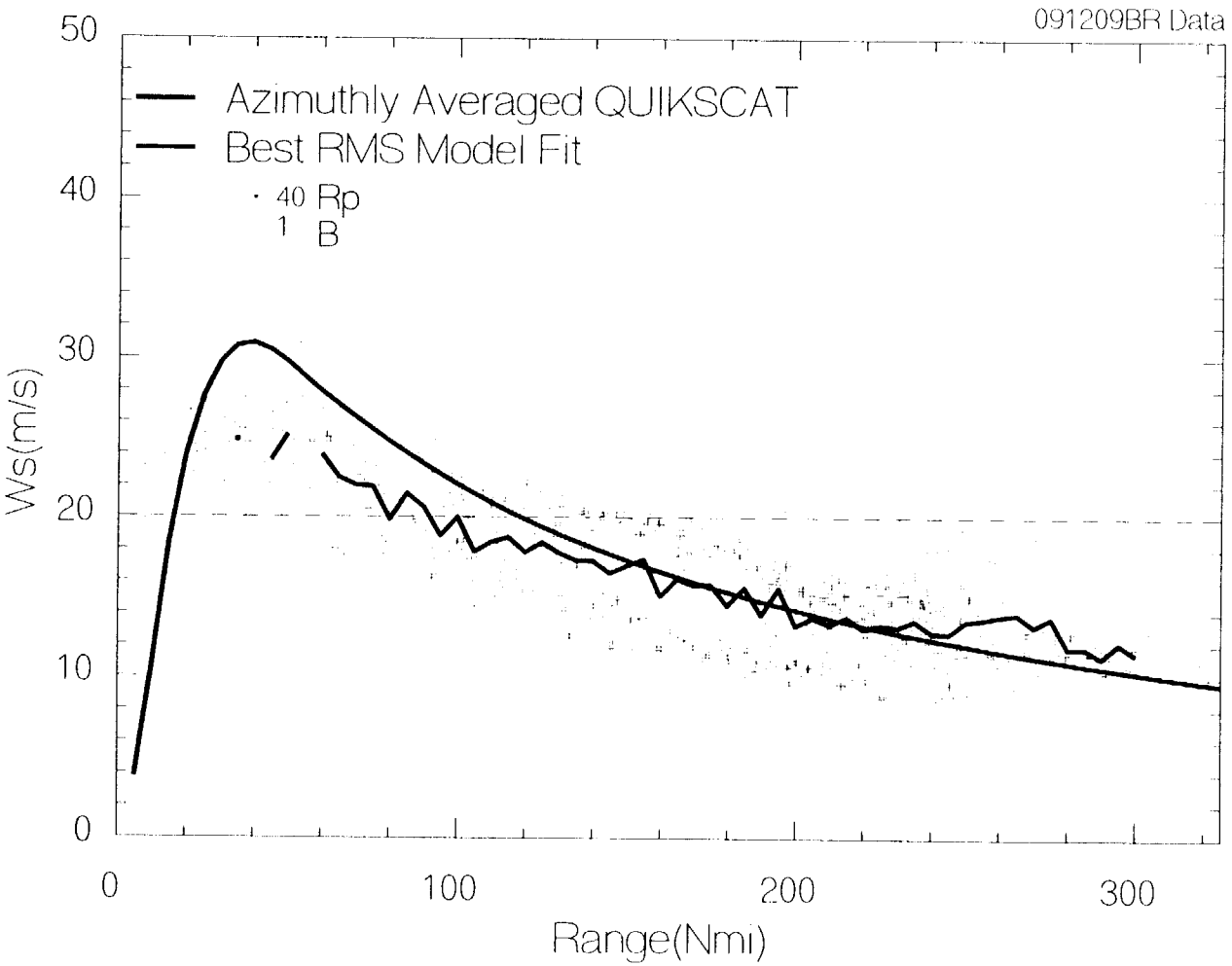

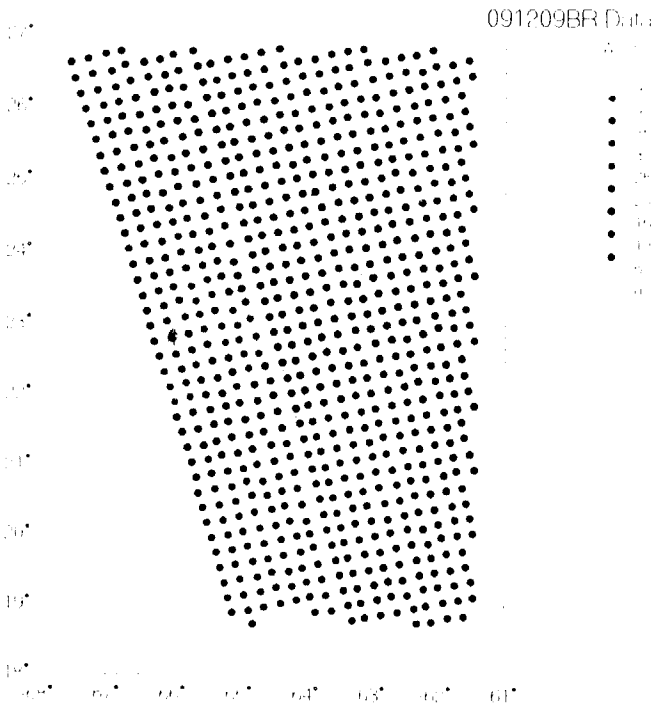

Quikscat Winds During Hurricane Floyd 1999

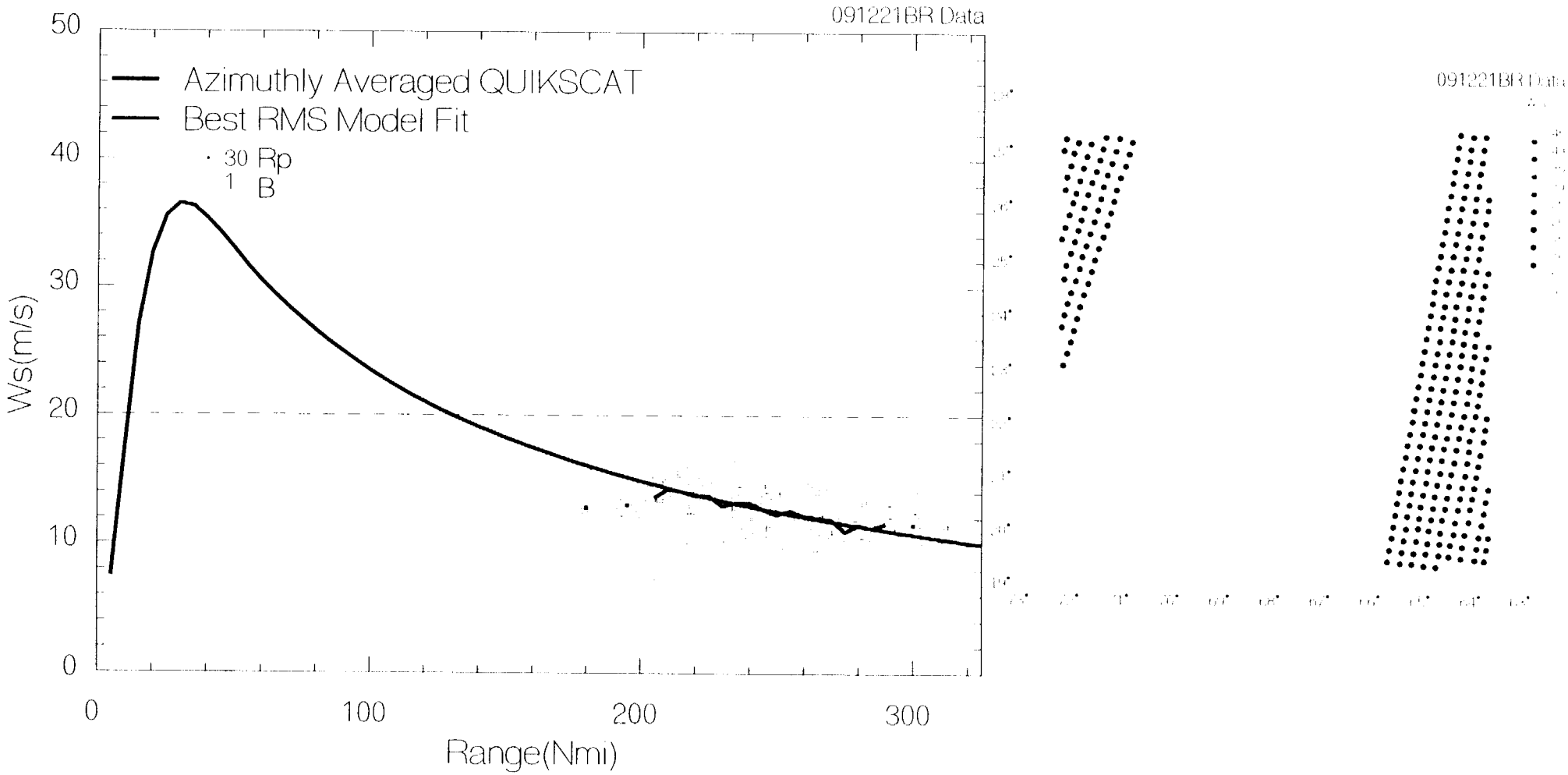

Quikscat Winds During Hurricane Floyd 1999

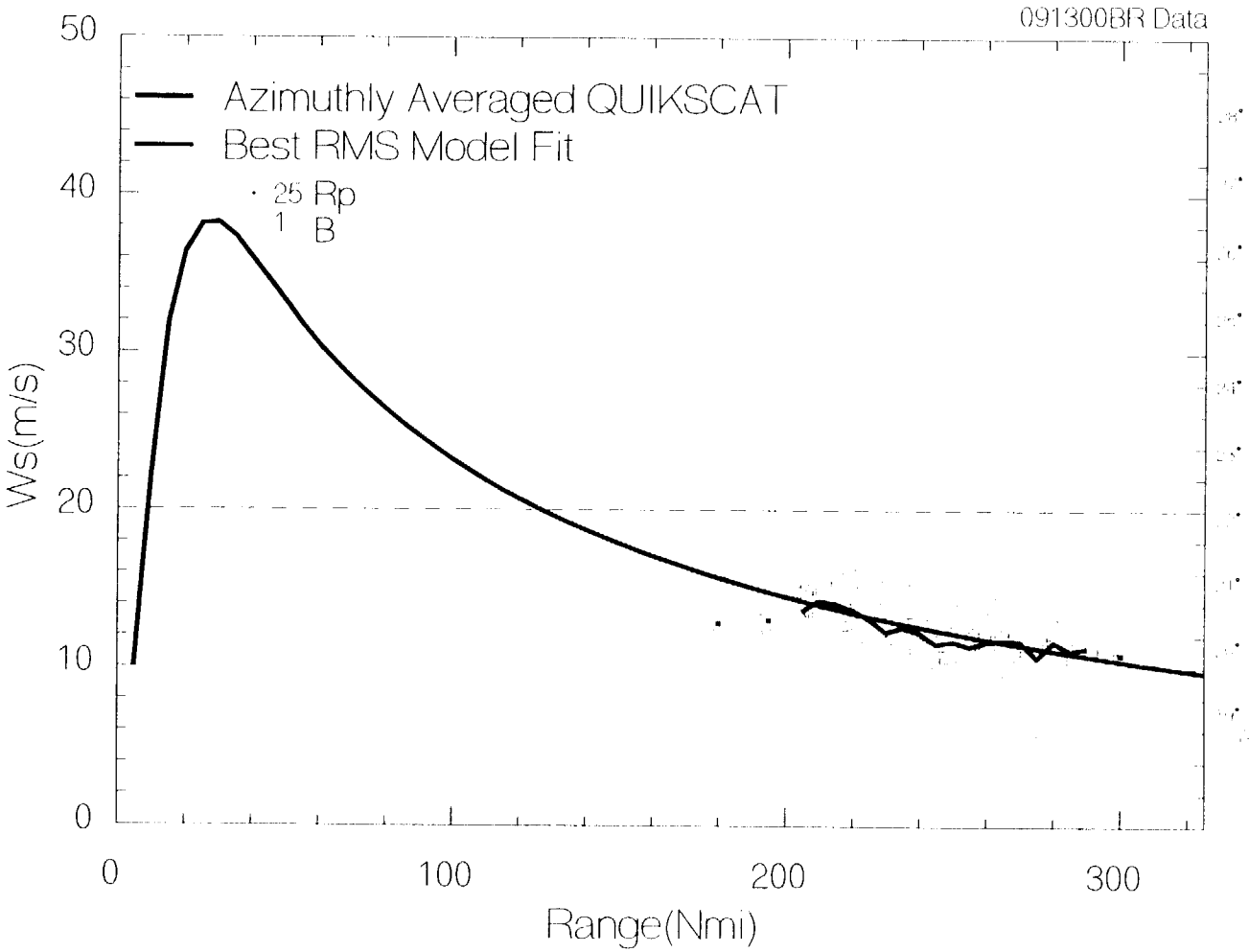

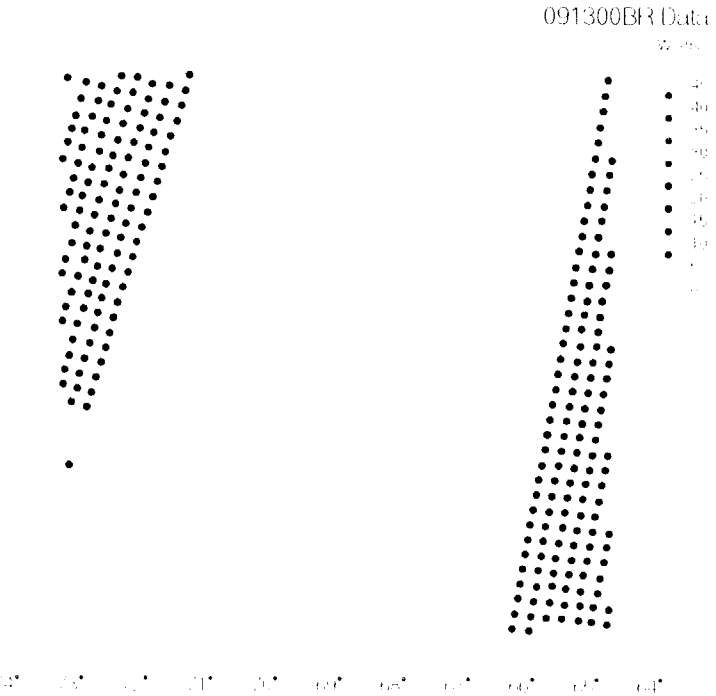

Quikscat Winds During Hurricane Floyd 1999

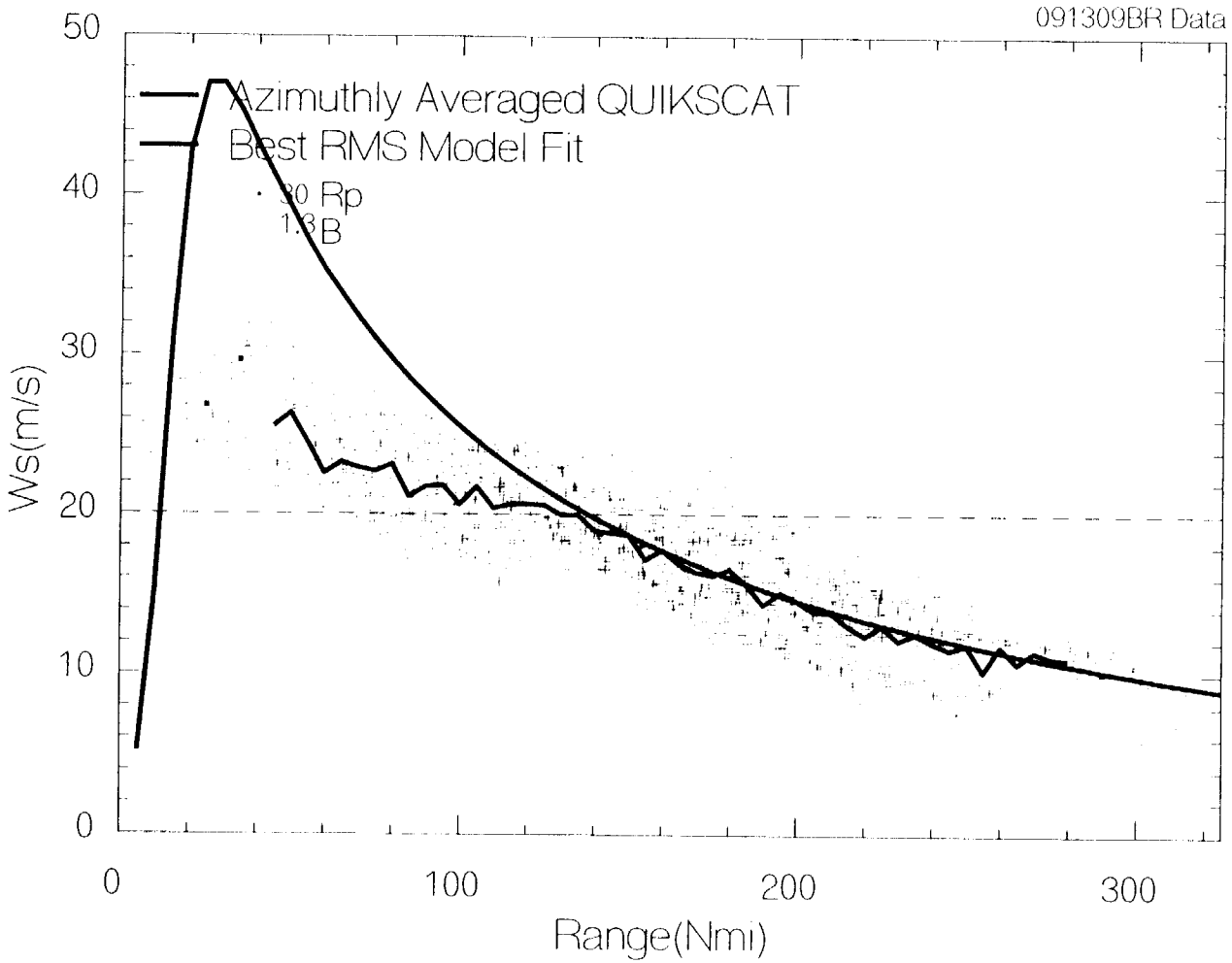

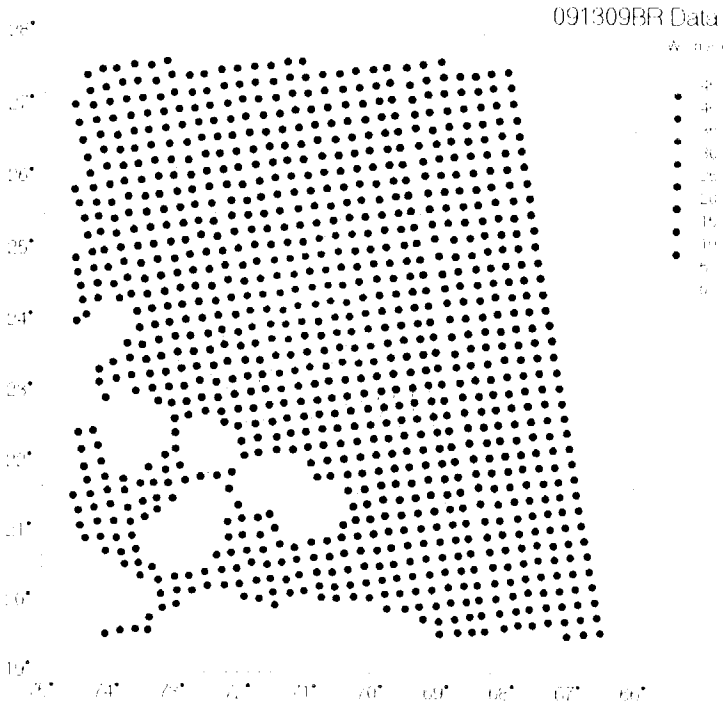

Quikscat Winds During Hurricane Floyd 1999

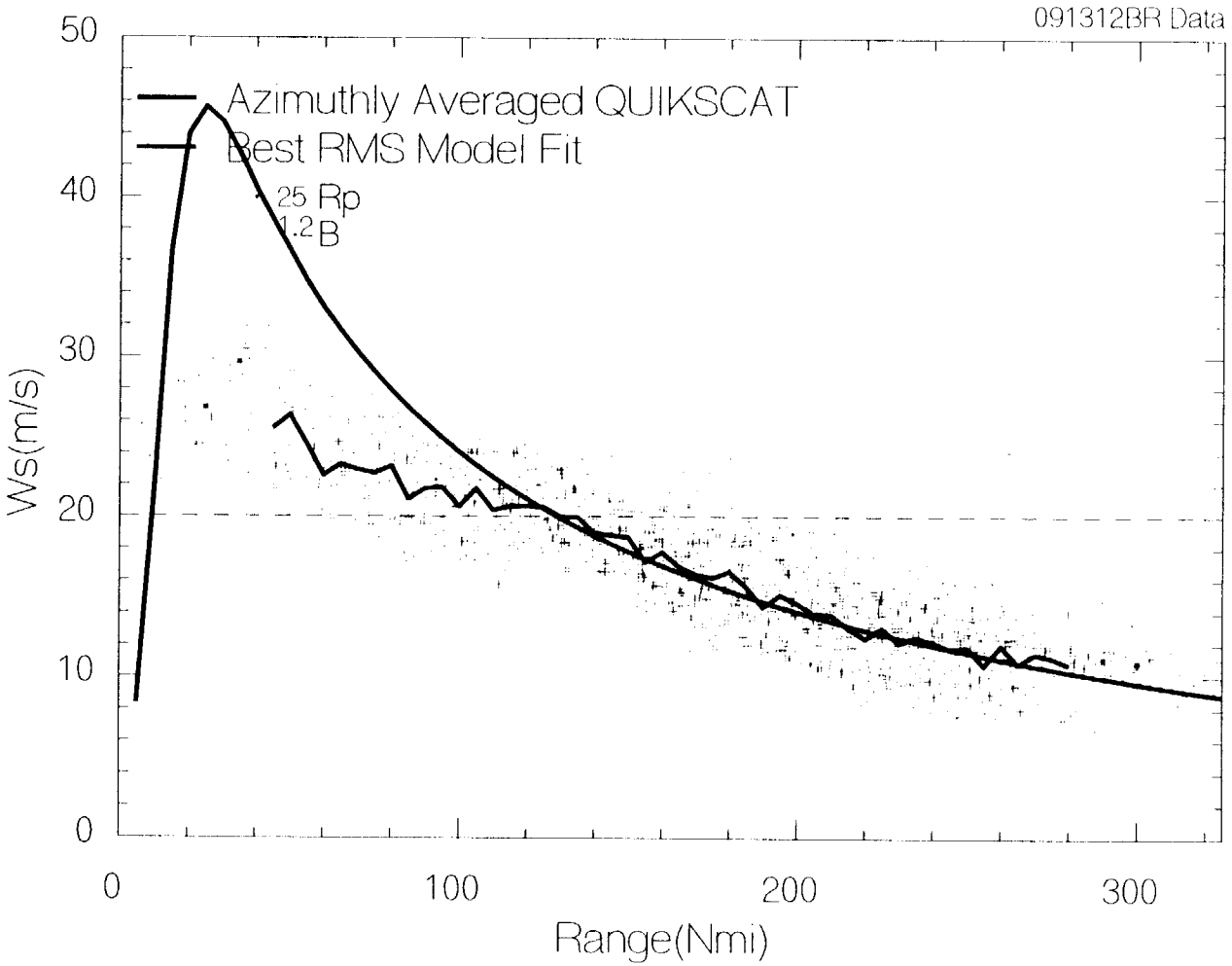

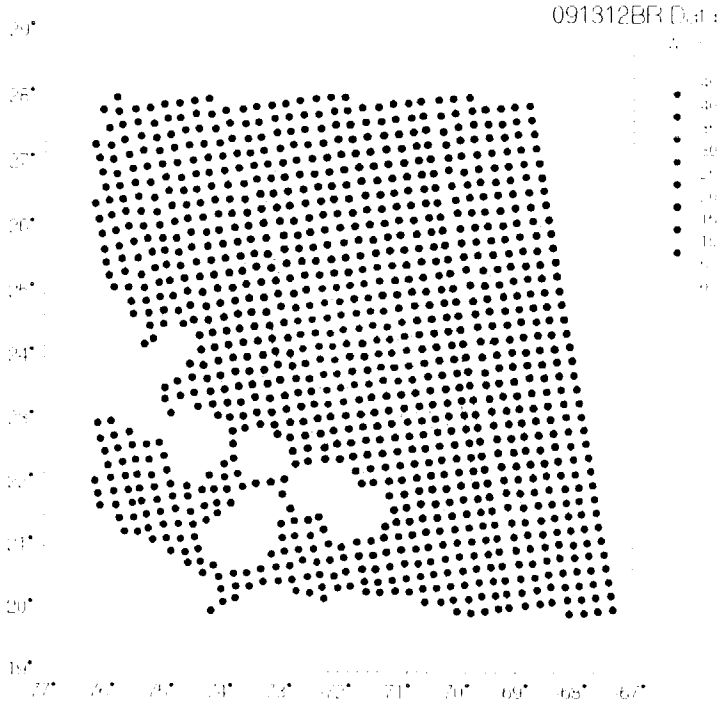

Quikscat Winds During Hurricane Floyd 1999

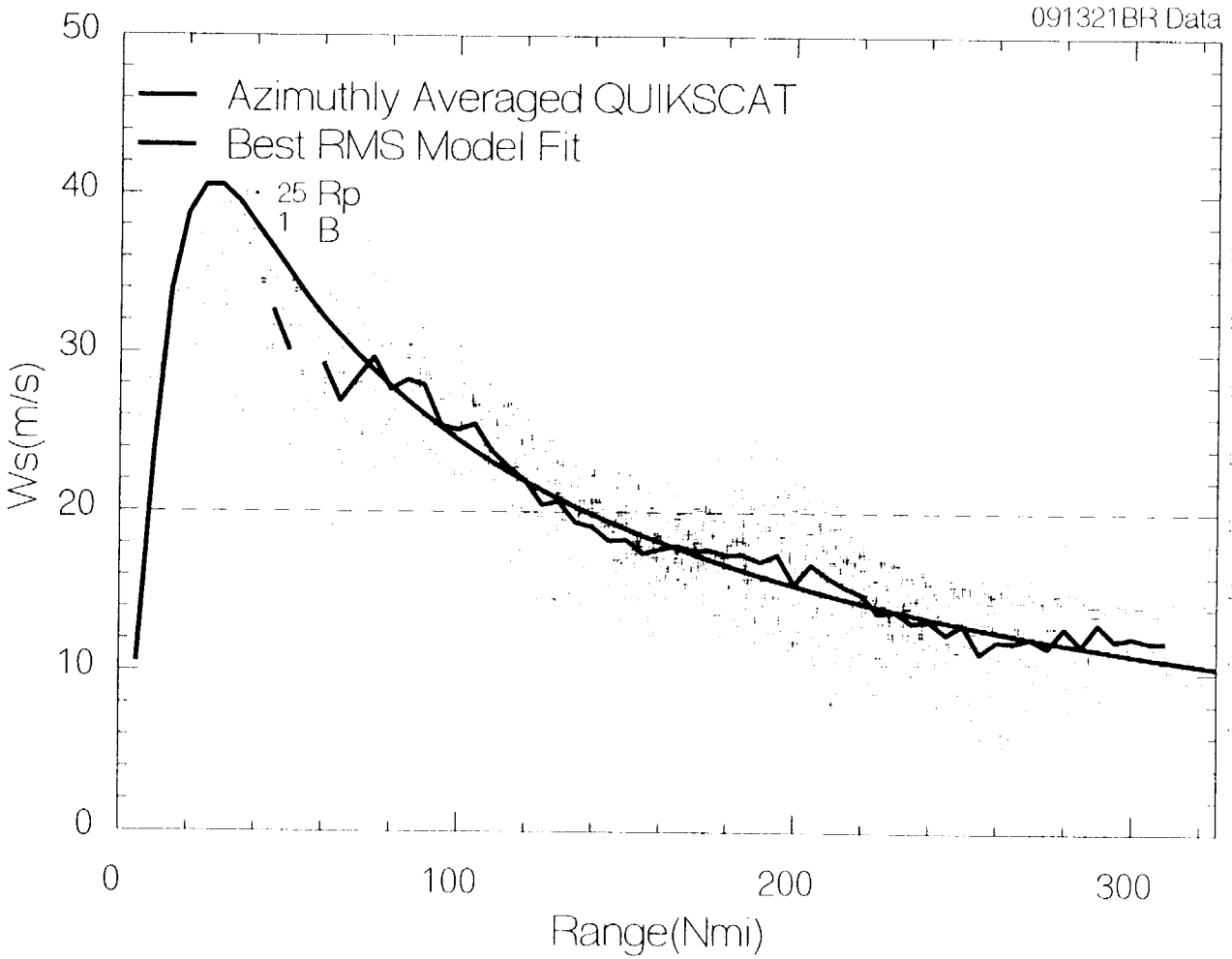

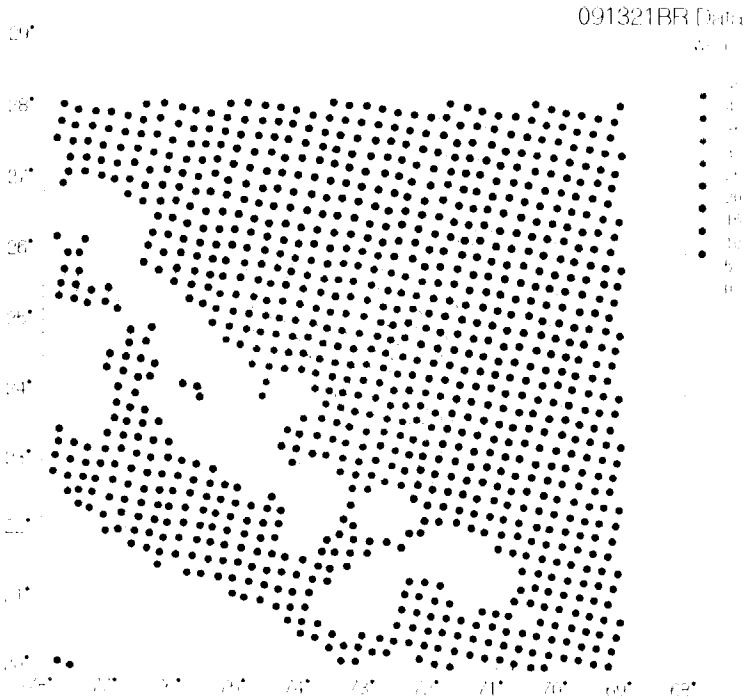

Quikscat Winds During Hurricane Floyd 1999

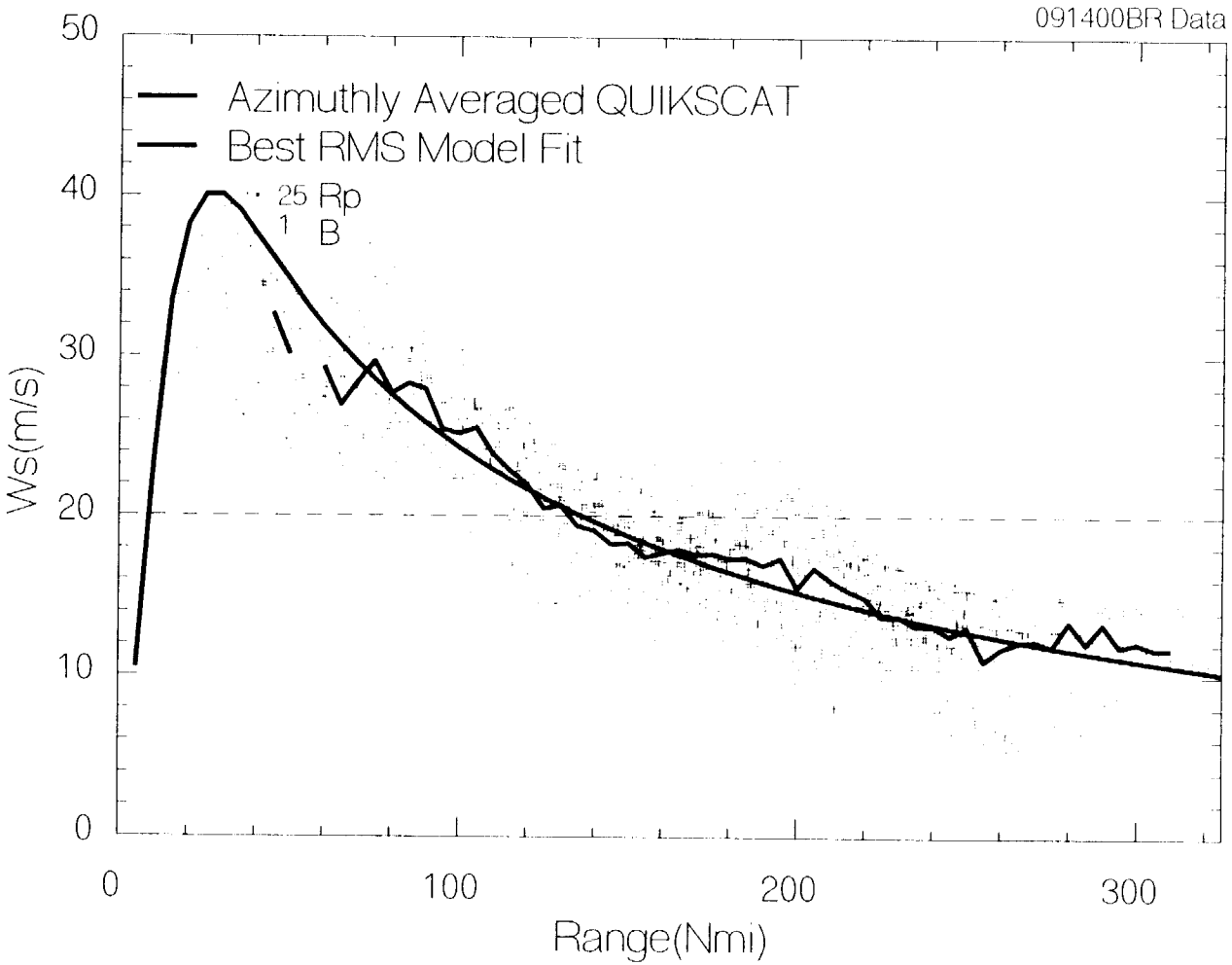

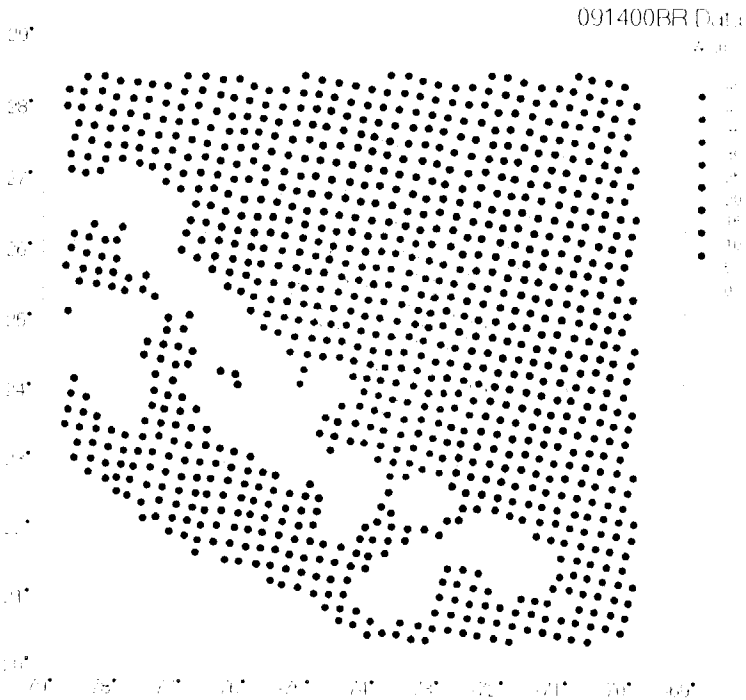

Quikscat Winds During Hurricane Floyd 1999

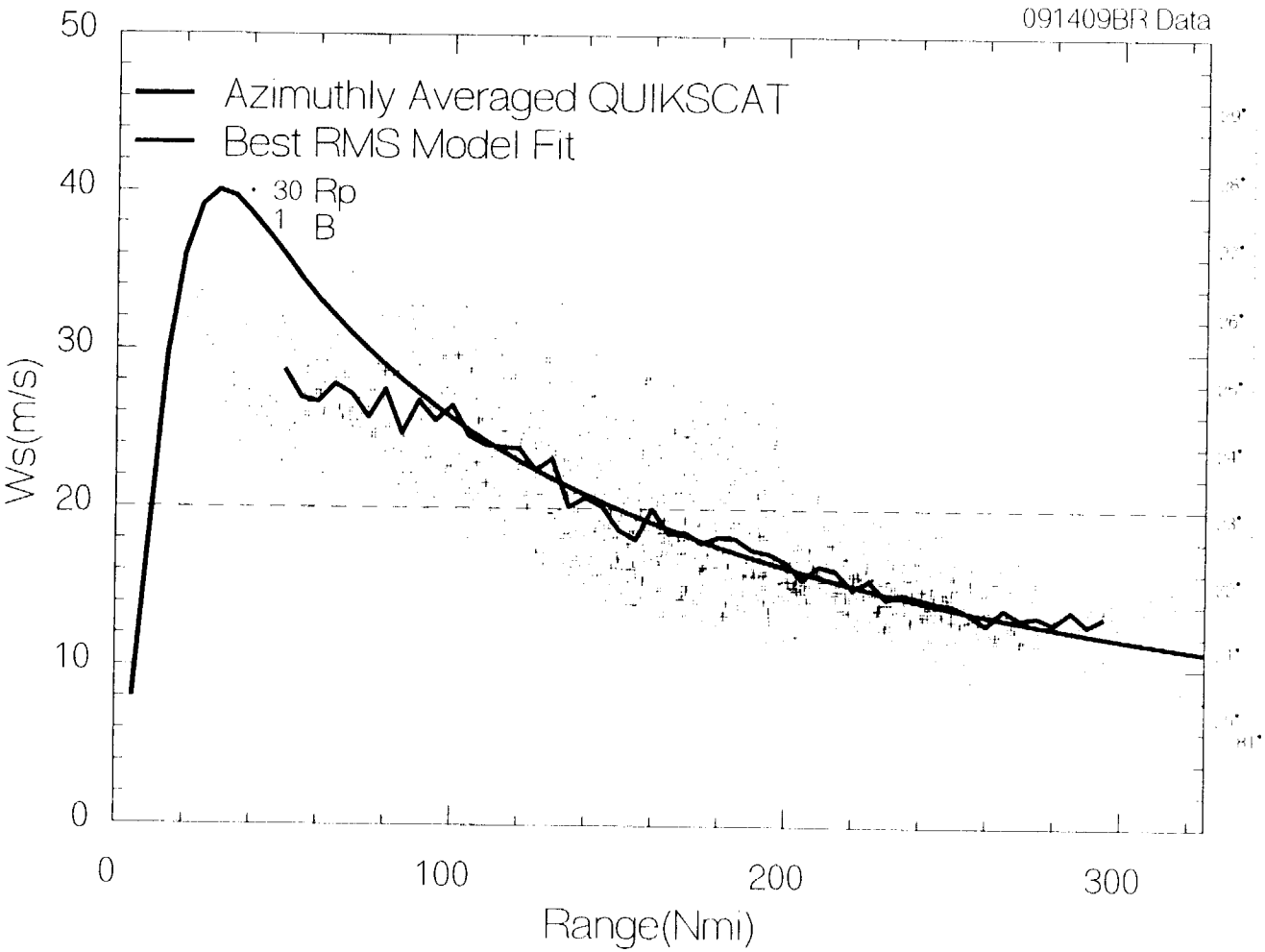

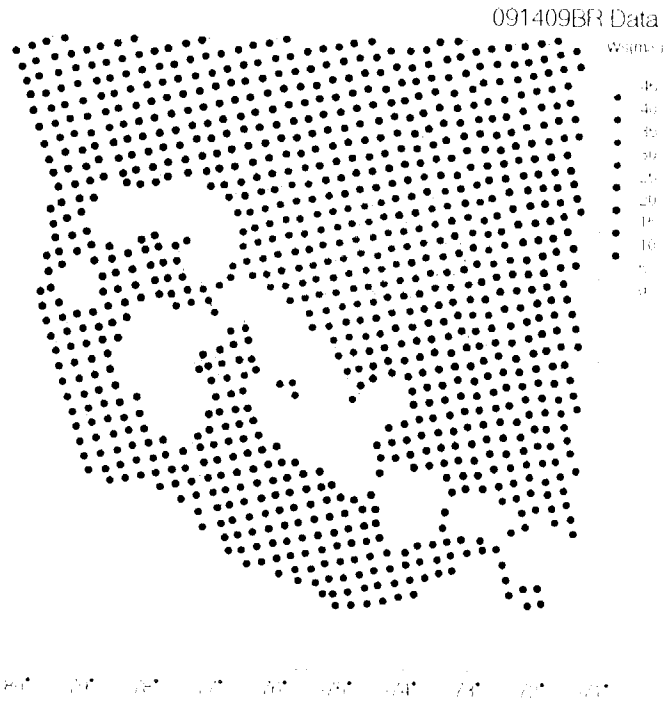

Quikscat Winds During Hurricane Floyd 1999

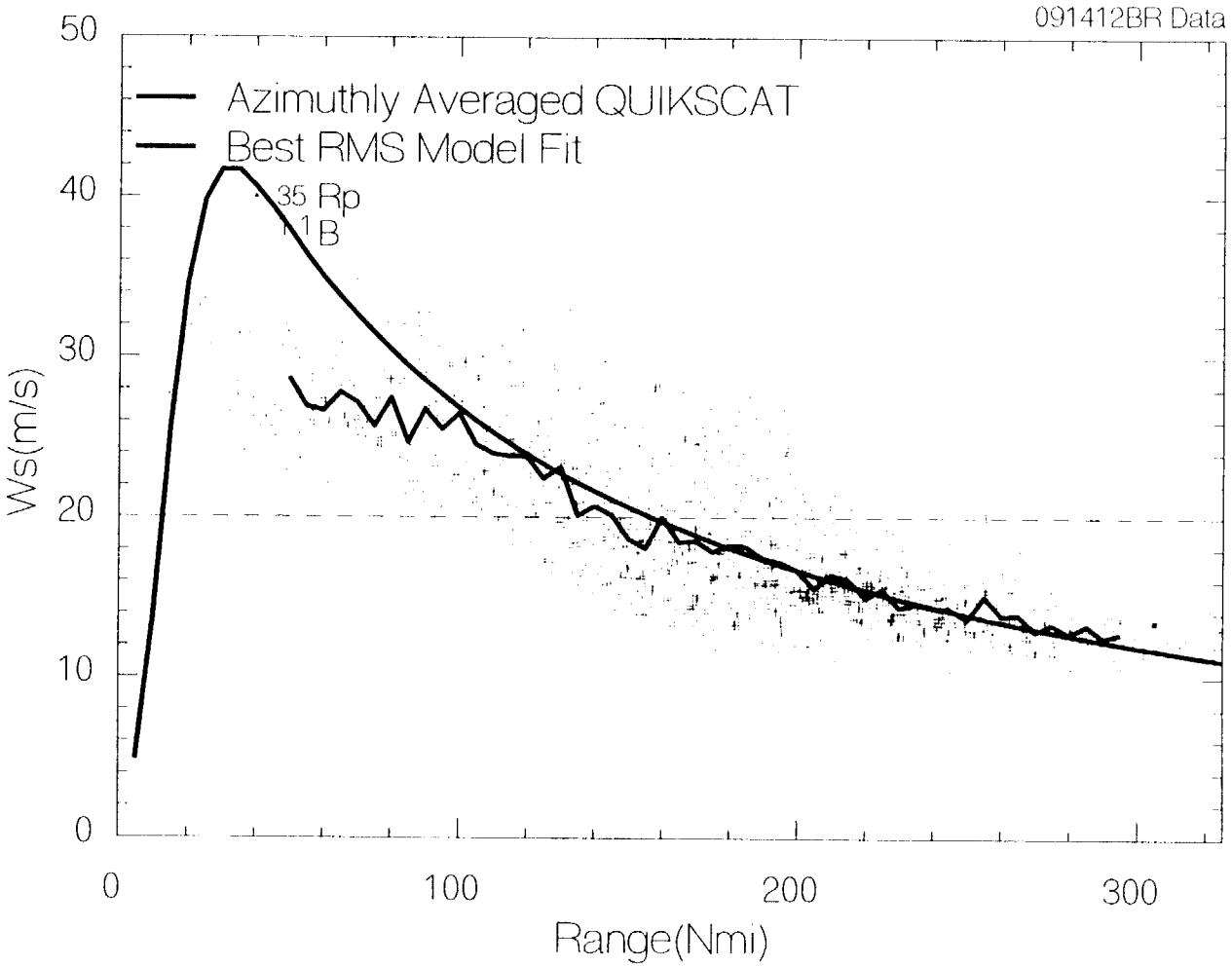

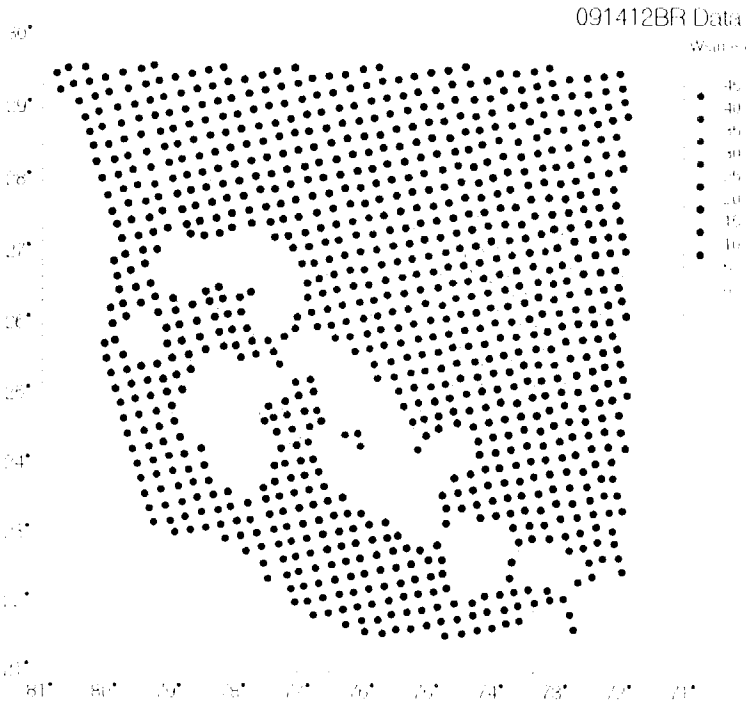

Quikscat Winds During Hurricane Floyd 1999

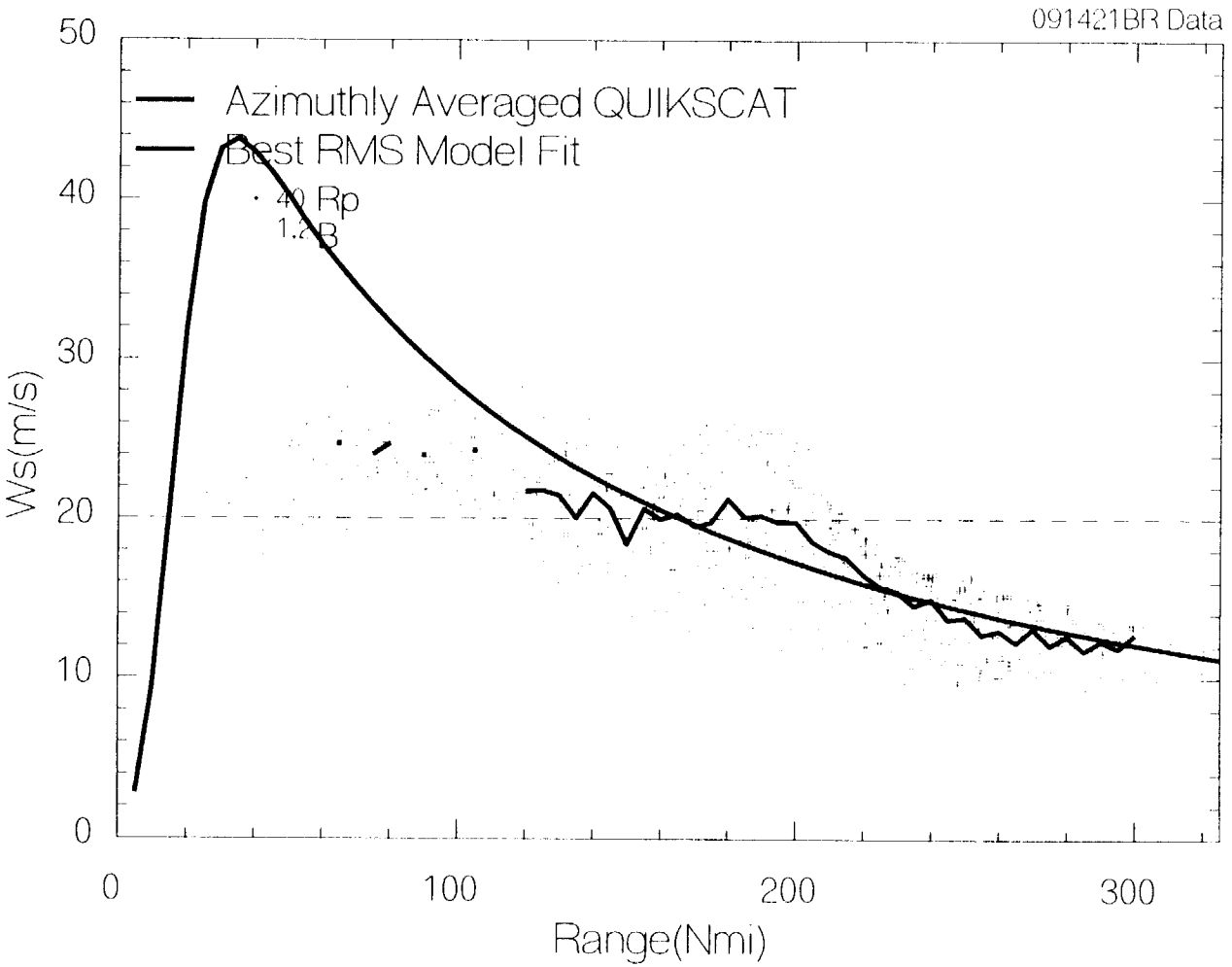

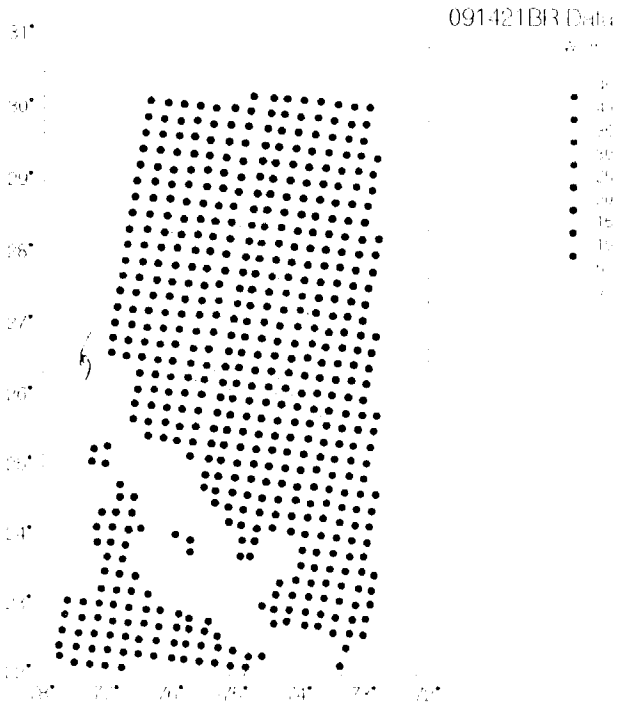

Quikscat Winds During Hurricane Floyd 1999

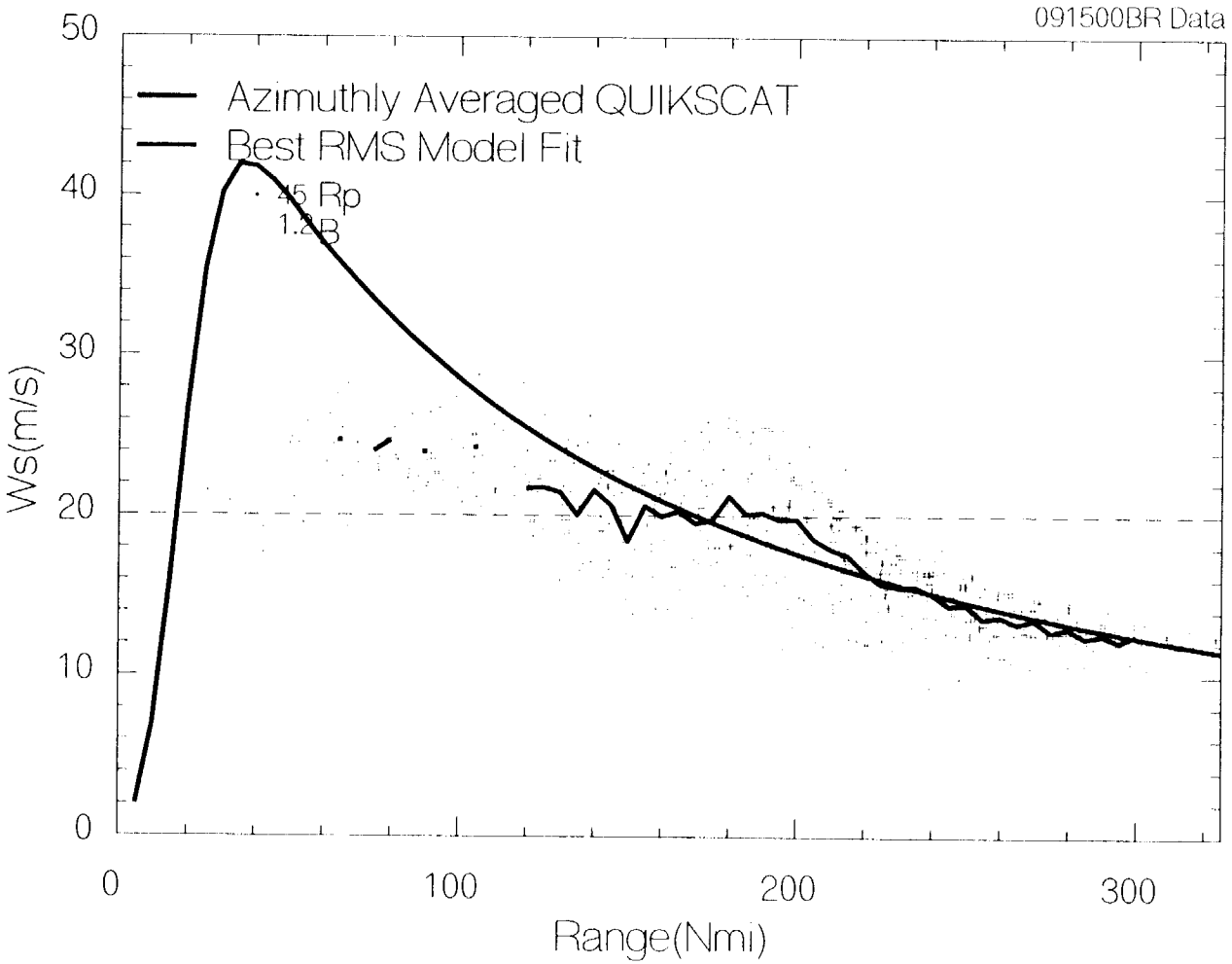

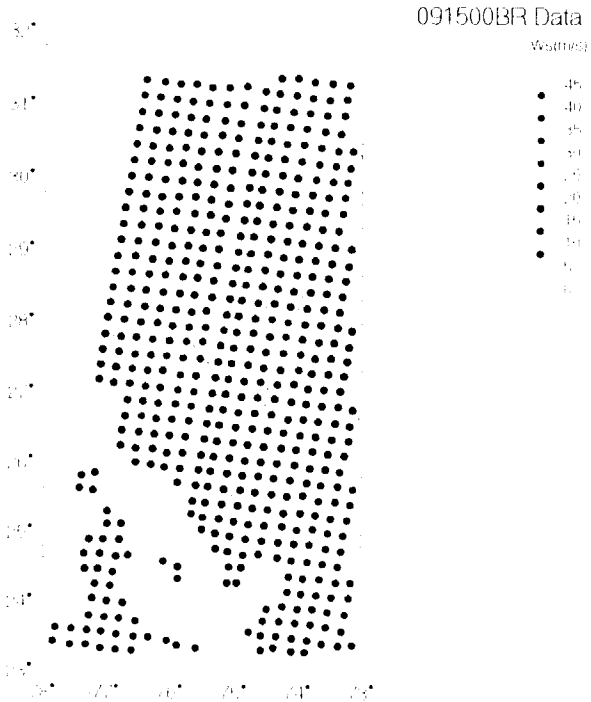

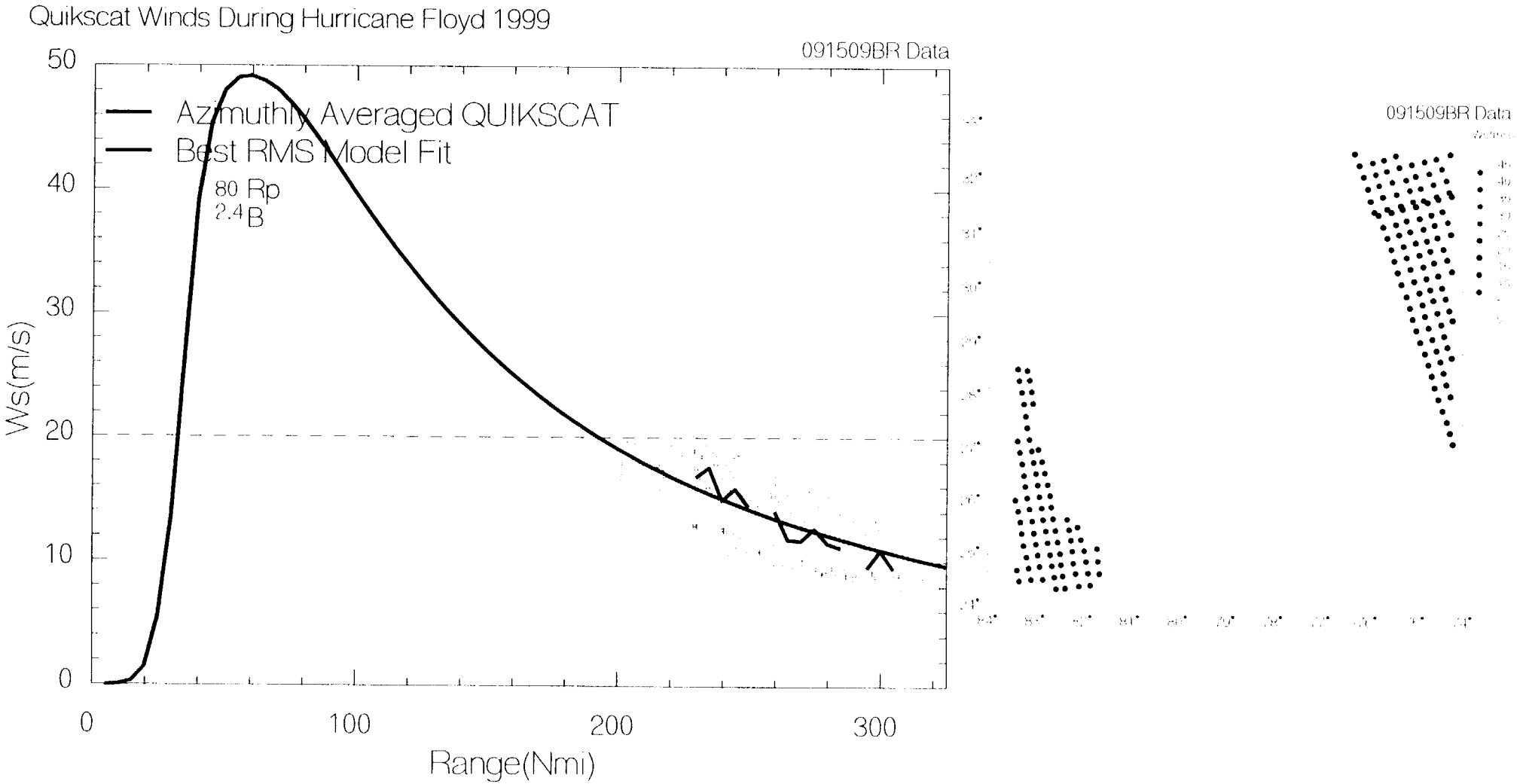
Quikscat Winds During Hurricane Floyd 1999
091509BR Data
Azimuthly Averaged QUIKSCAT
Best RMS Model Fit
80 Rp
2.4 B
Ws(m/s)
Range(Nmi)
0
10
20
30
40
50
0
100
200
300
091509BR Data

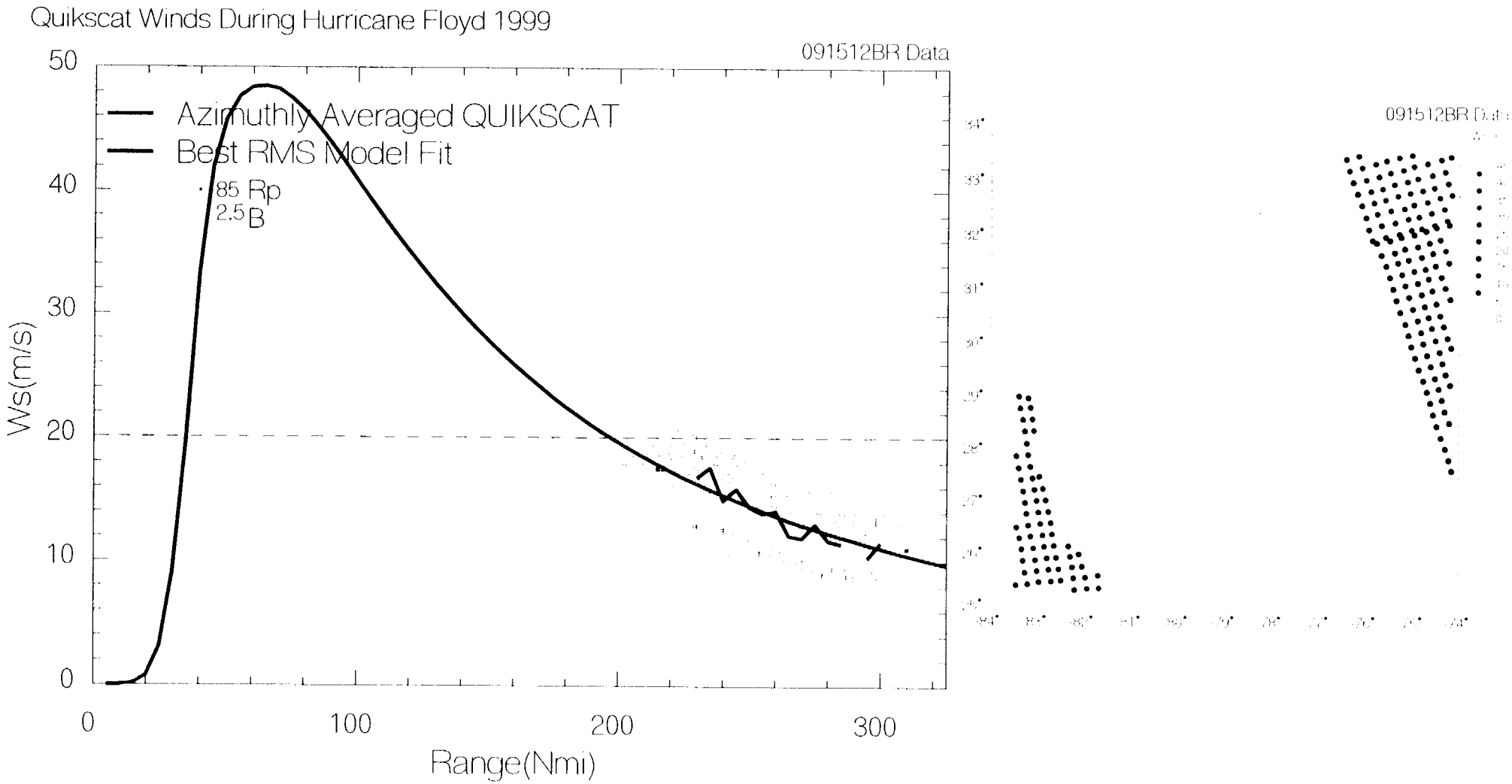
Quikscat Winds During Hurricane Floyd 1999
091512BR Data
Azimuthly Averaged QUIKSCAT
Best RMS Model Fit
.85 Rp
2.5 B
Ws(m/s)
Range(Nmi)
0
10
20
30
40
50
0
100
200
300
091512BR Data

Quikscat Winds During Hurricane Floyd 1999

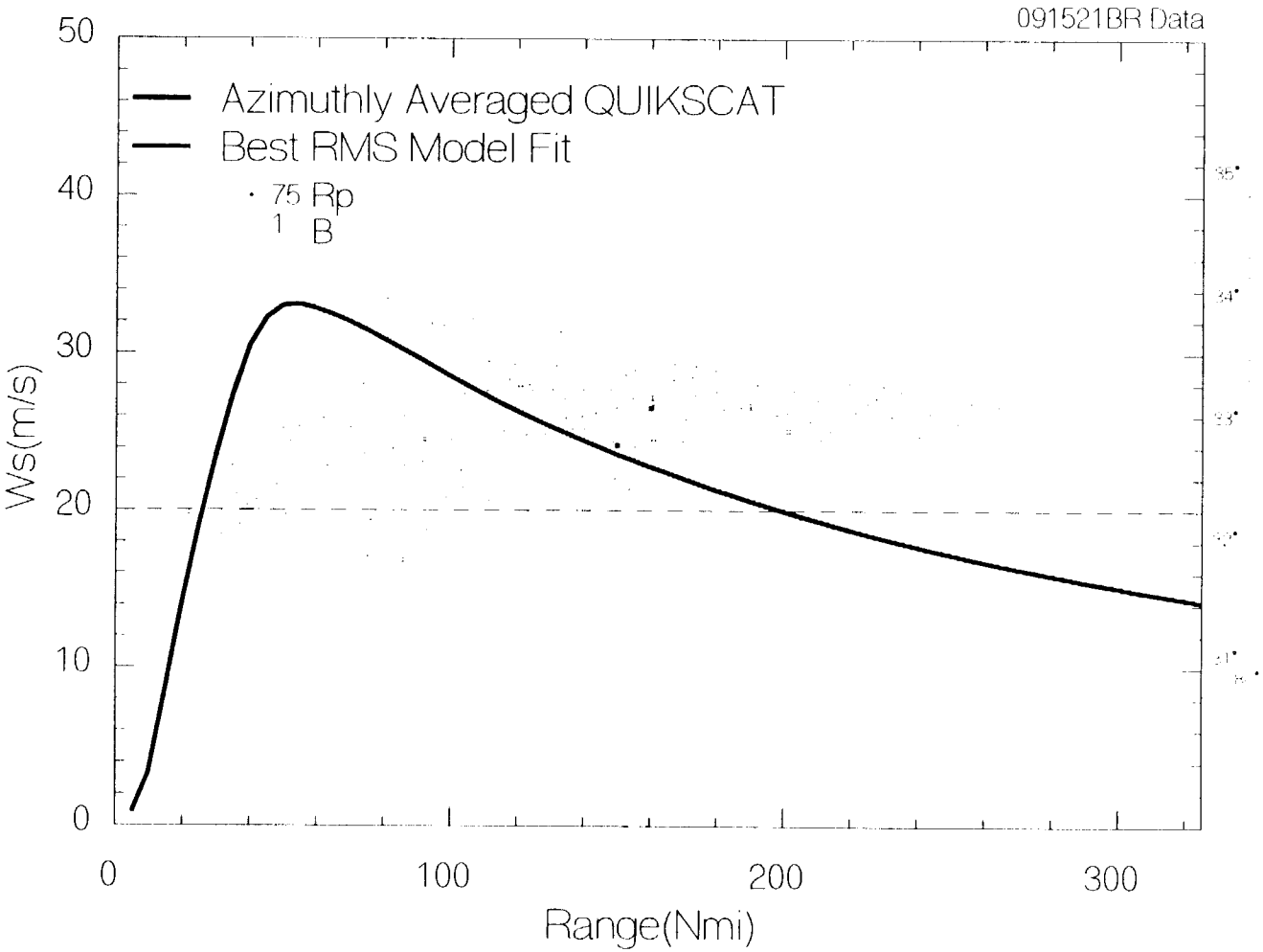

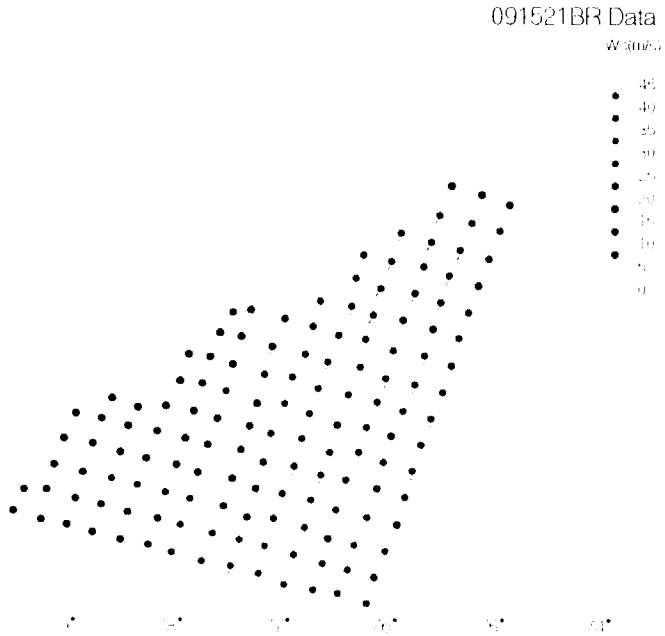

Quikscat Winds During Hurricane Floyd 1999

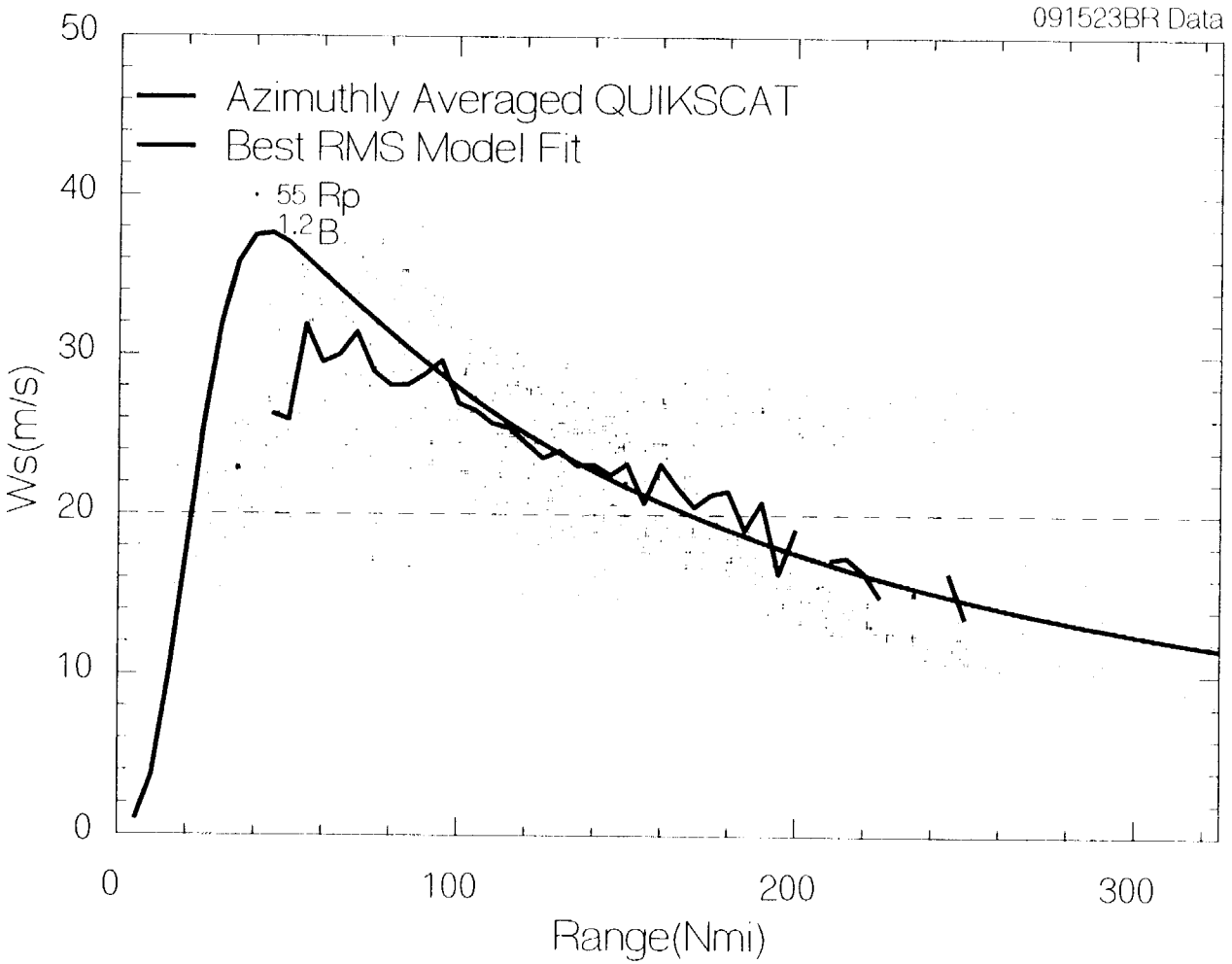

Quikscat Winds During Hurricane Floyd 1999

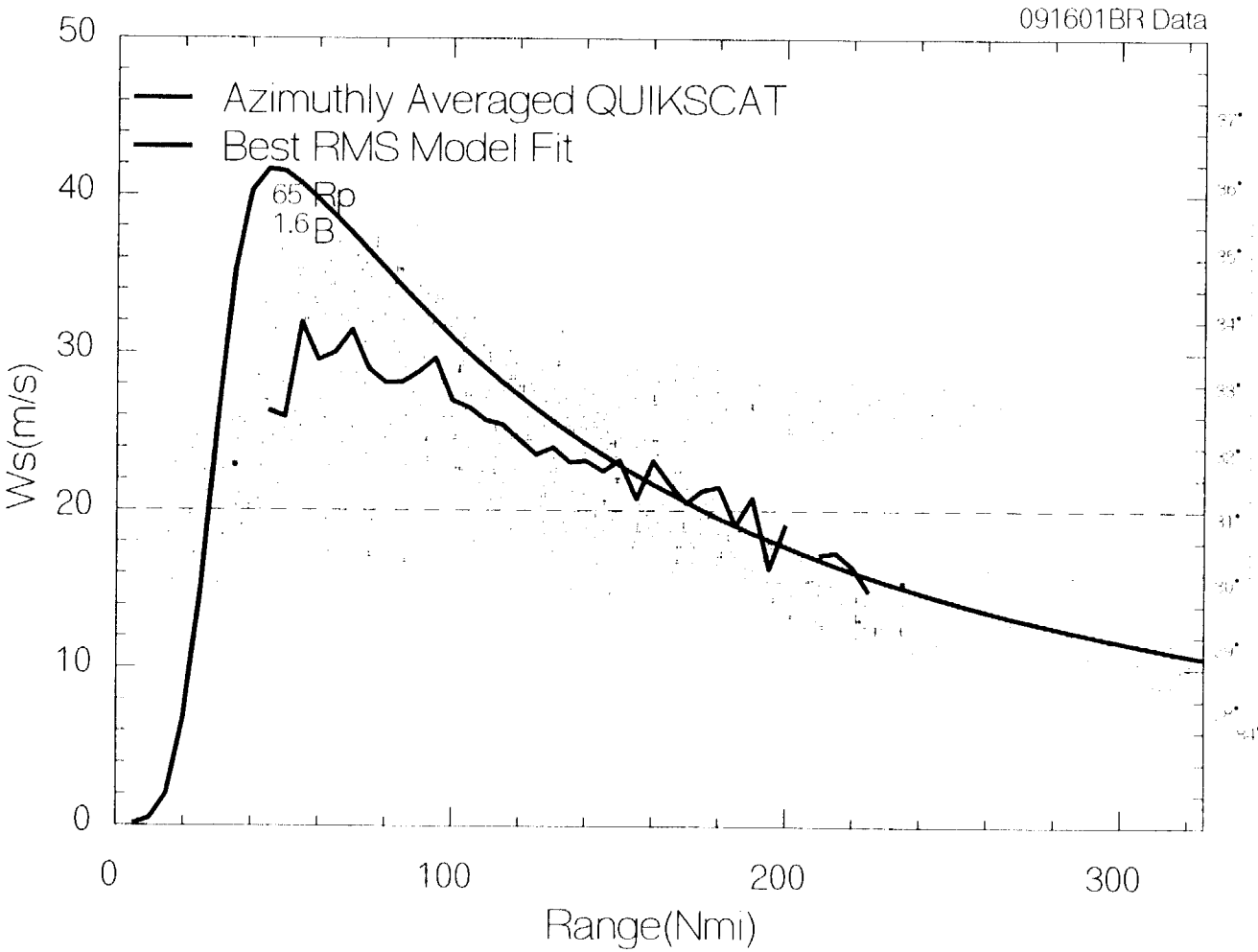

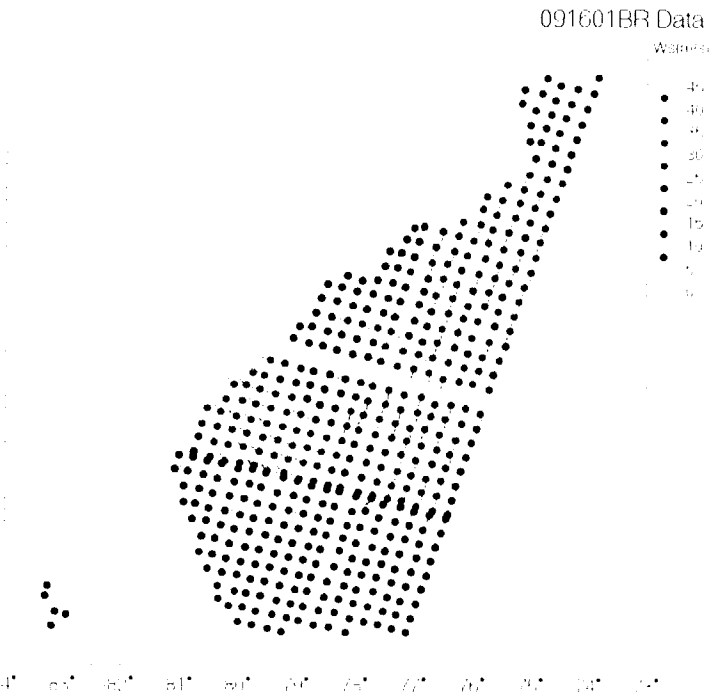

Quikscat Winds During Hurricane Floyd 1999

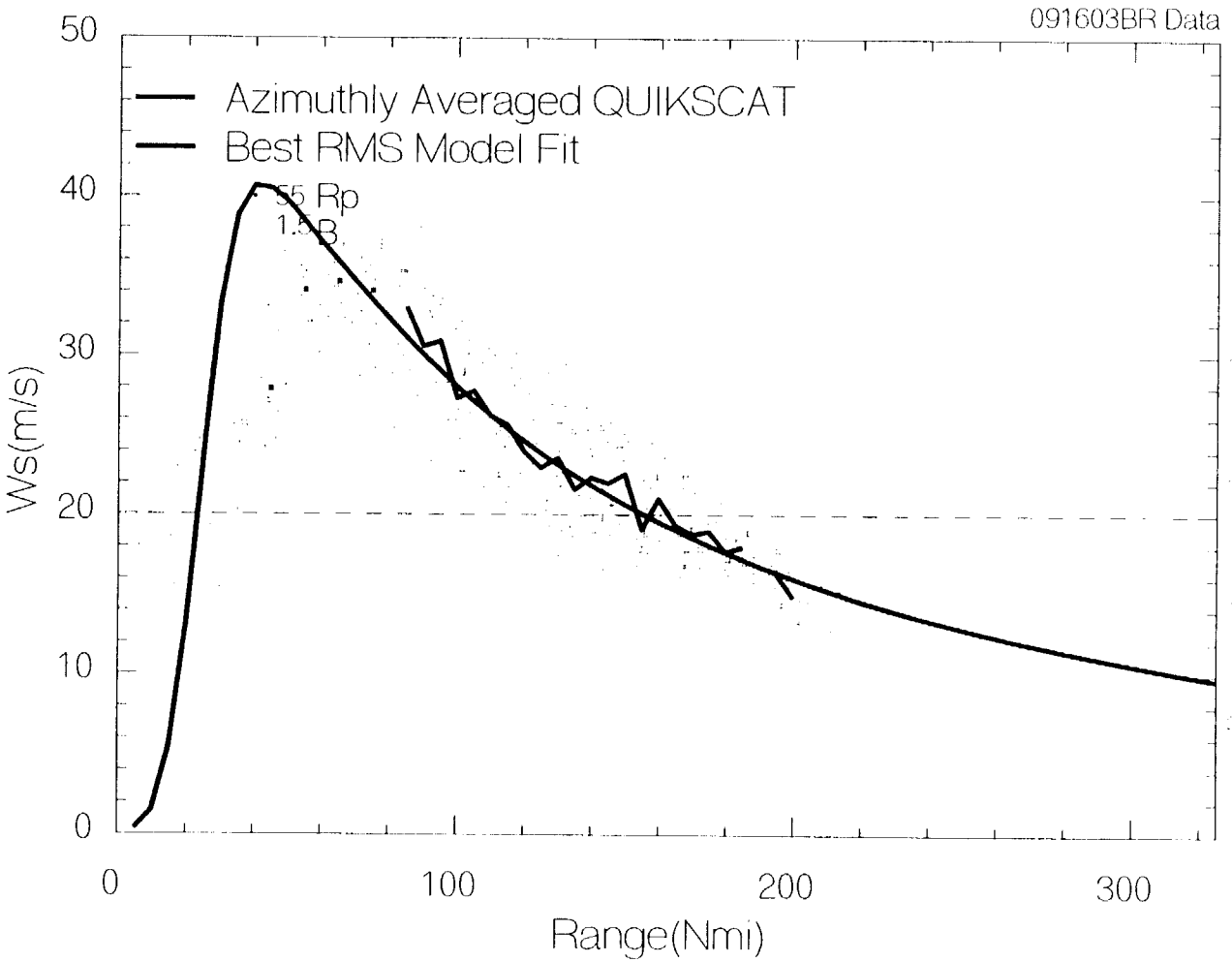

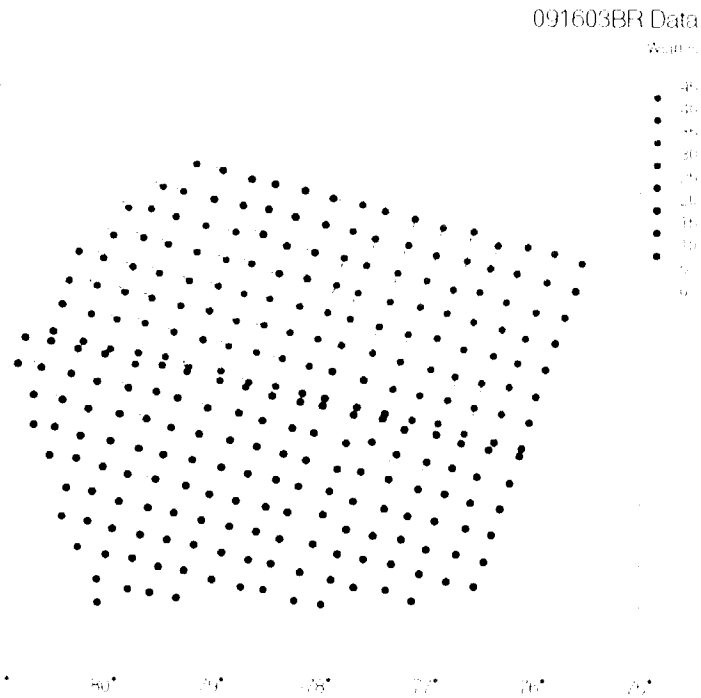

Quikscat Winds During Hurricane Floyd 1999

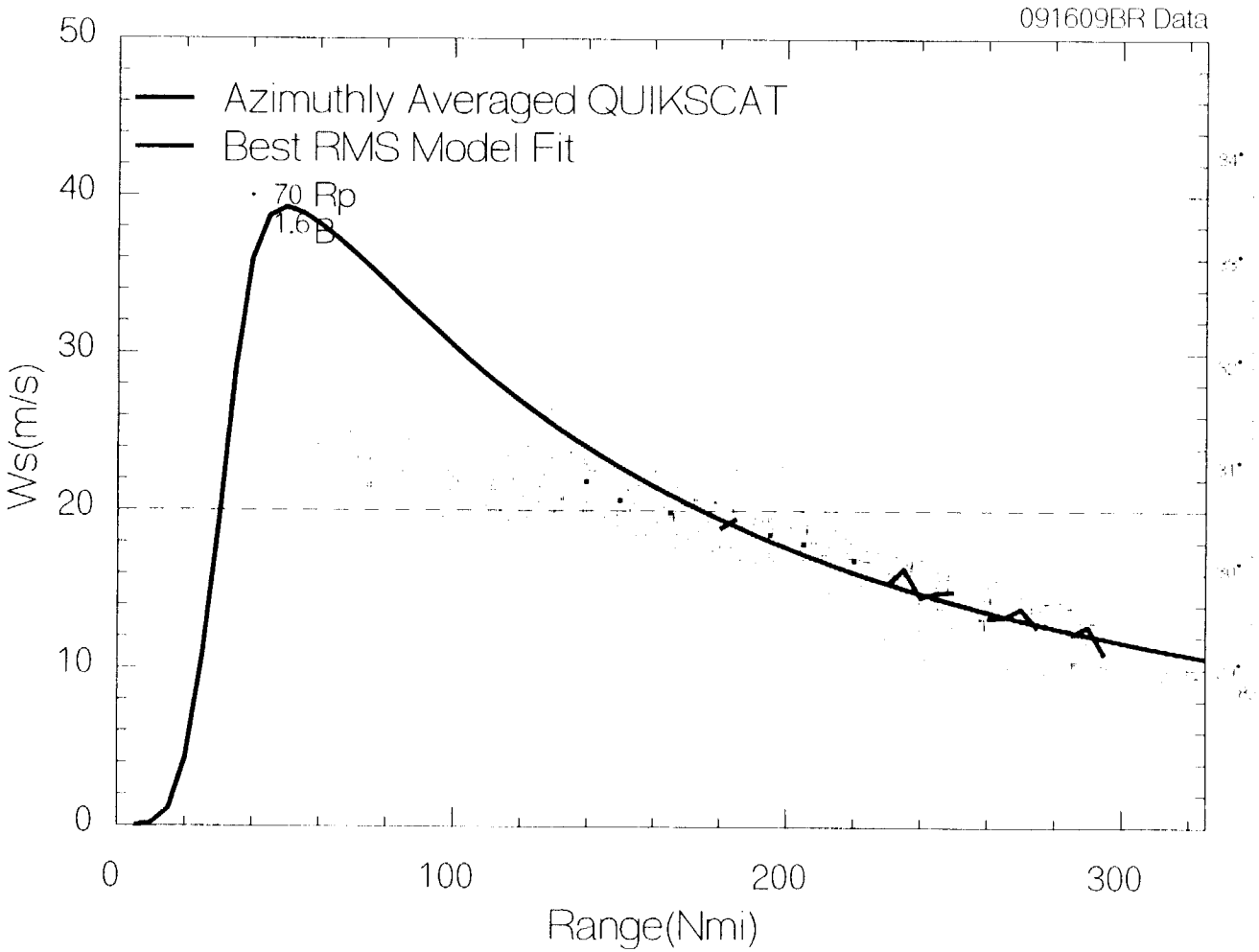

Quikscat Winds During Hurricane Floyd 1999

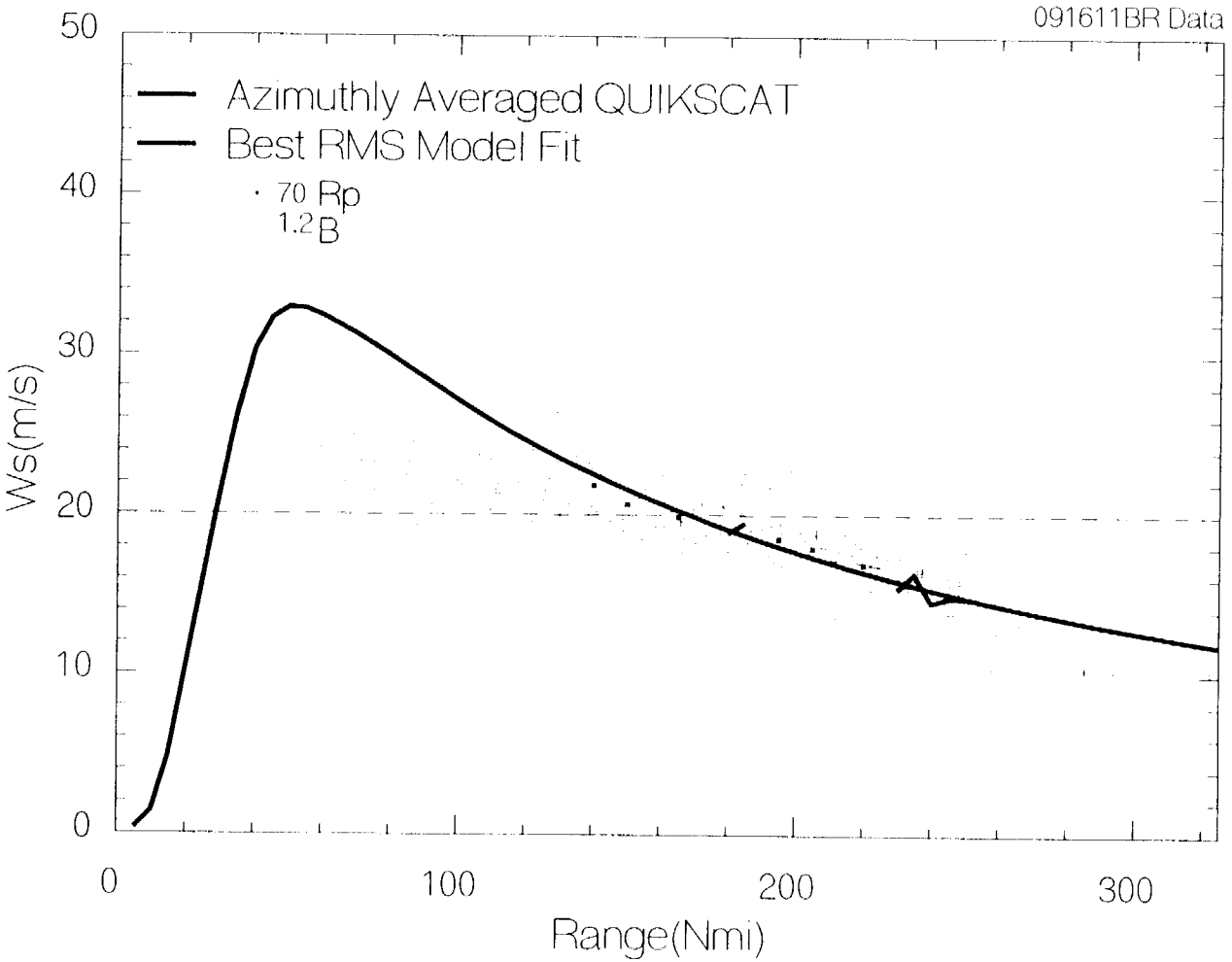

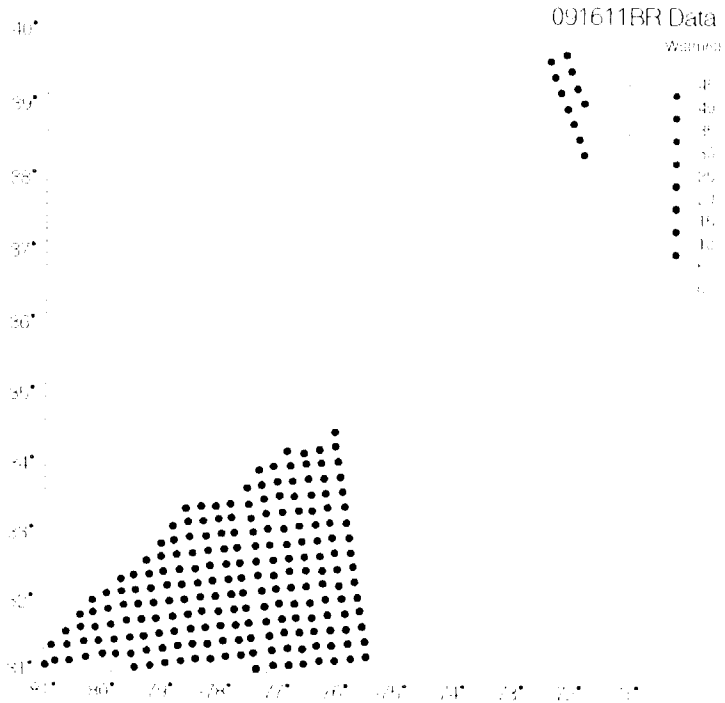

Quikscat Winds During Hurricane Floyd 1999

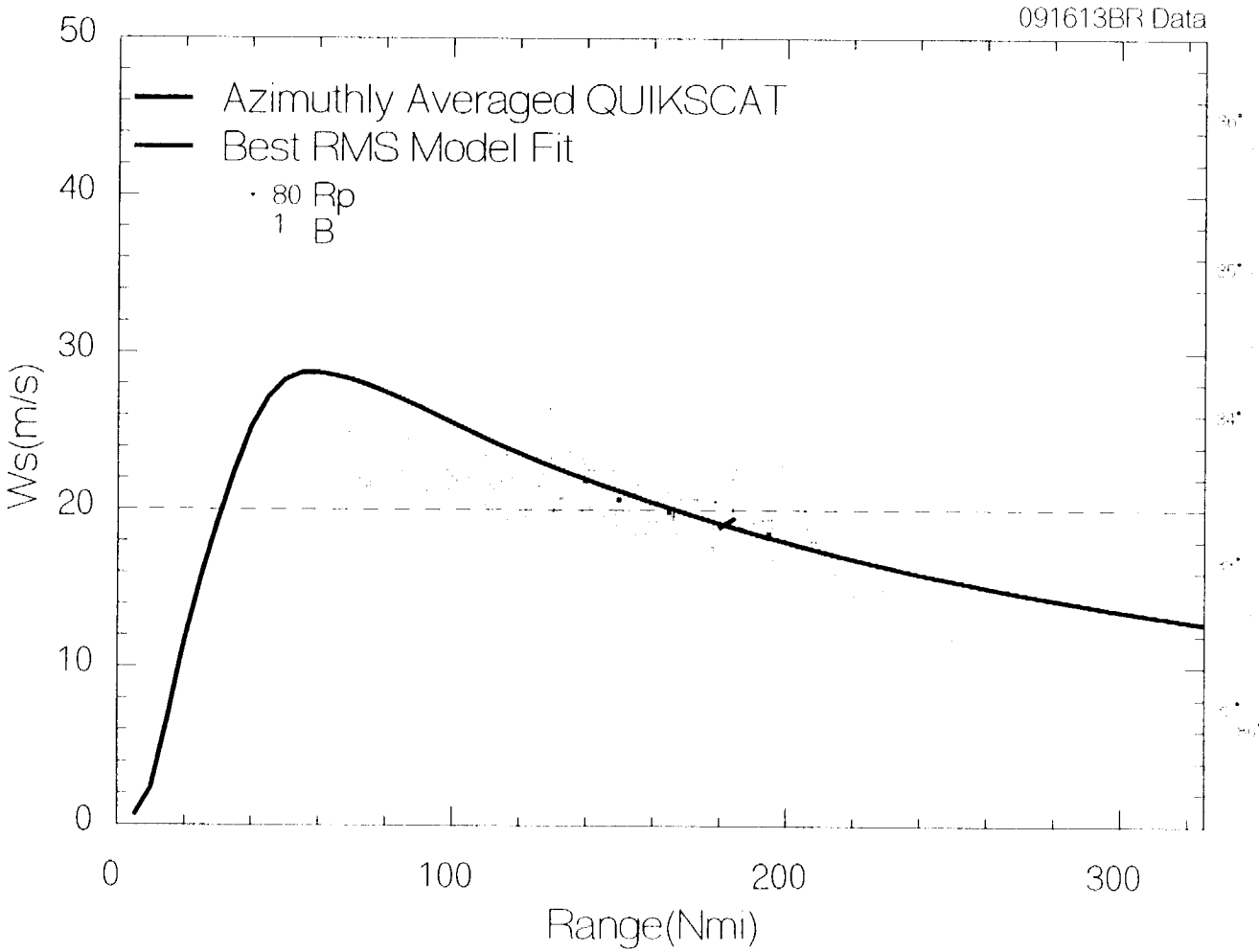

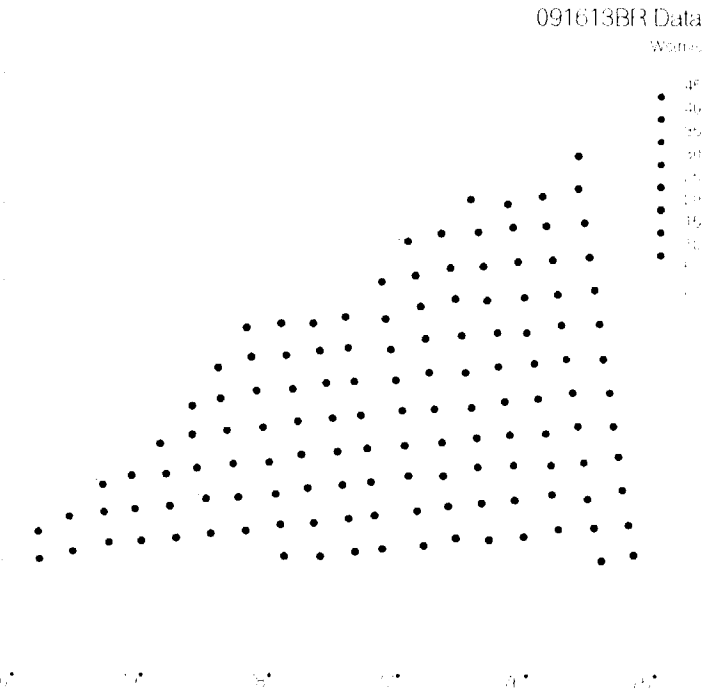

Quikscat Winds During Hurricane Floyd 1999

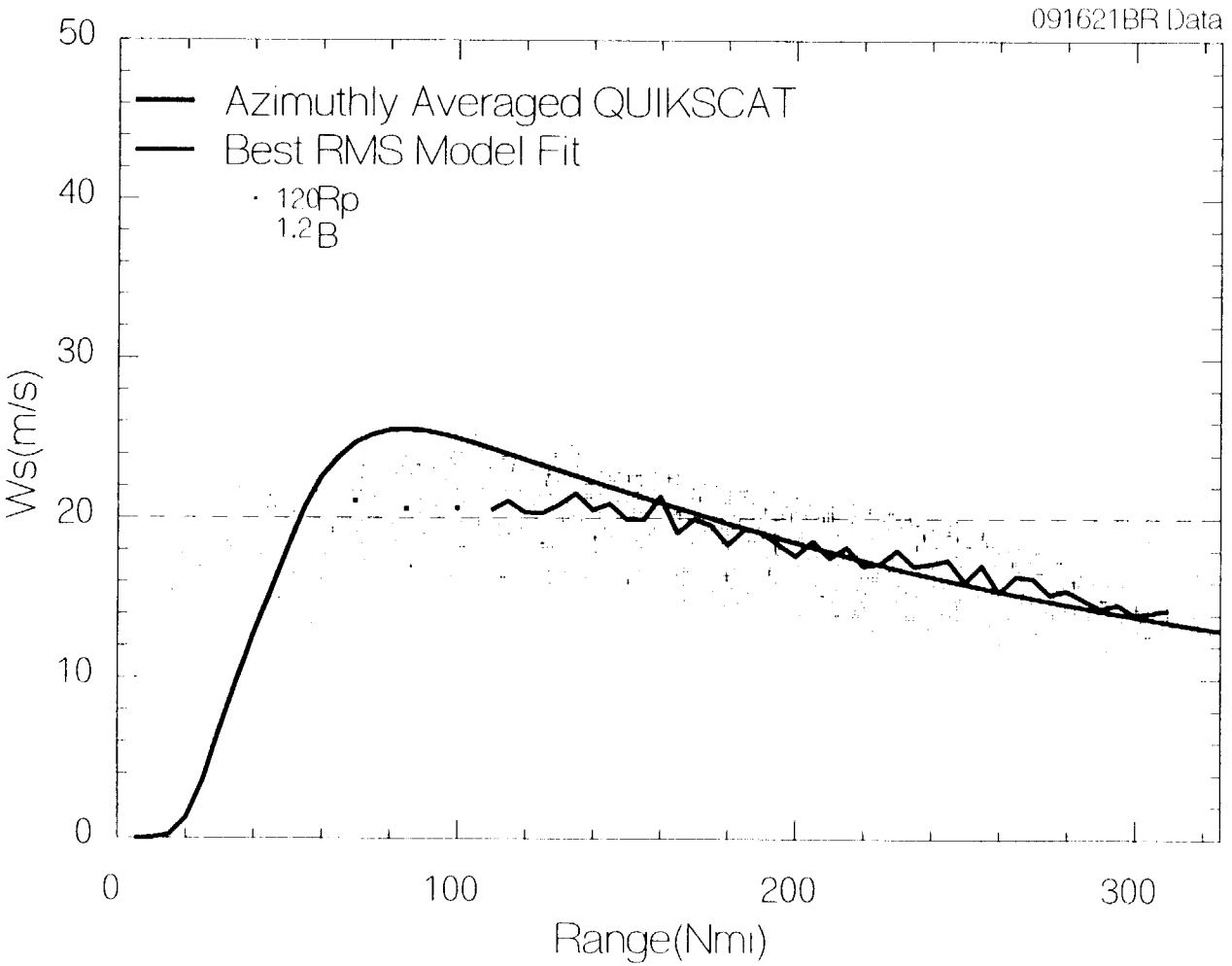

Appendix C. Comparison of OWI winds from inverse model and HRD snapshot wind fields at time of HRD snapshots. Color contours of wind speed differences

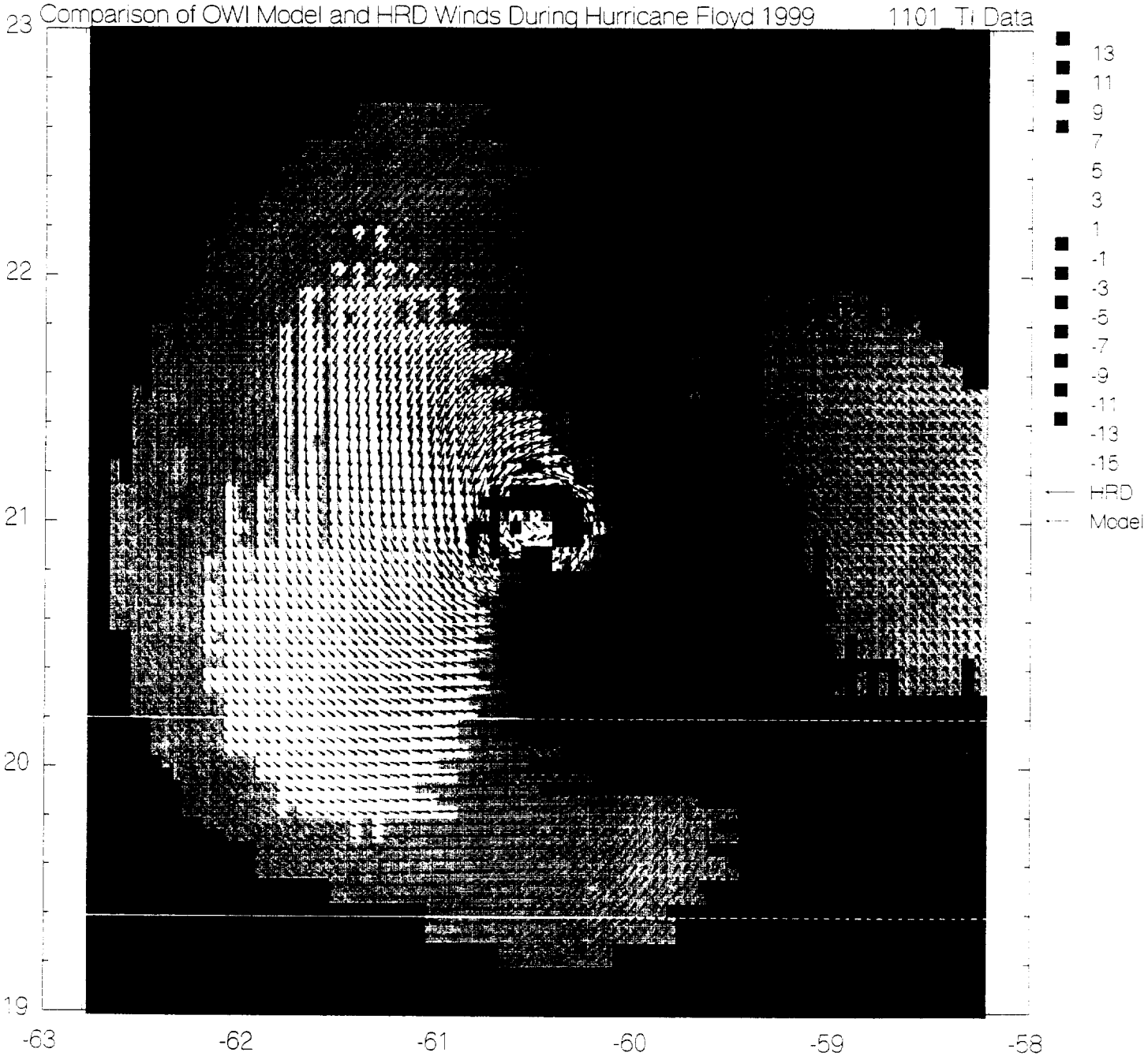
Comparison of OWI Model and HRD Winds During Hurricane Floyd 1999
1101_Ti Data
23
22
21
20
19
-63
-62
-61
-60
-59
-58
13
11
9
7
5
3
1
-1
-3
-5
-7
-9
-11
-13
-15
HRD
Model

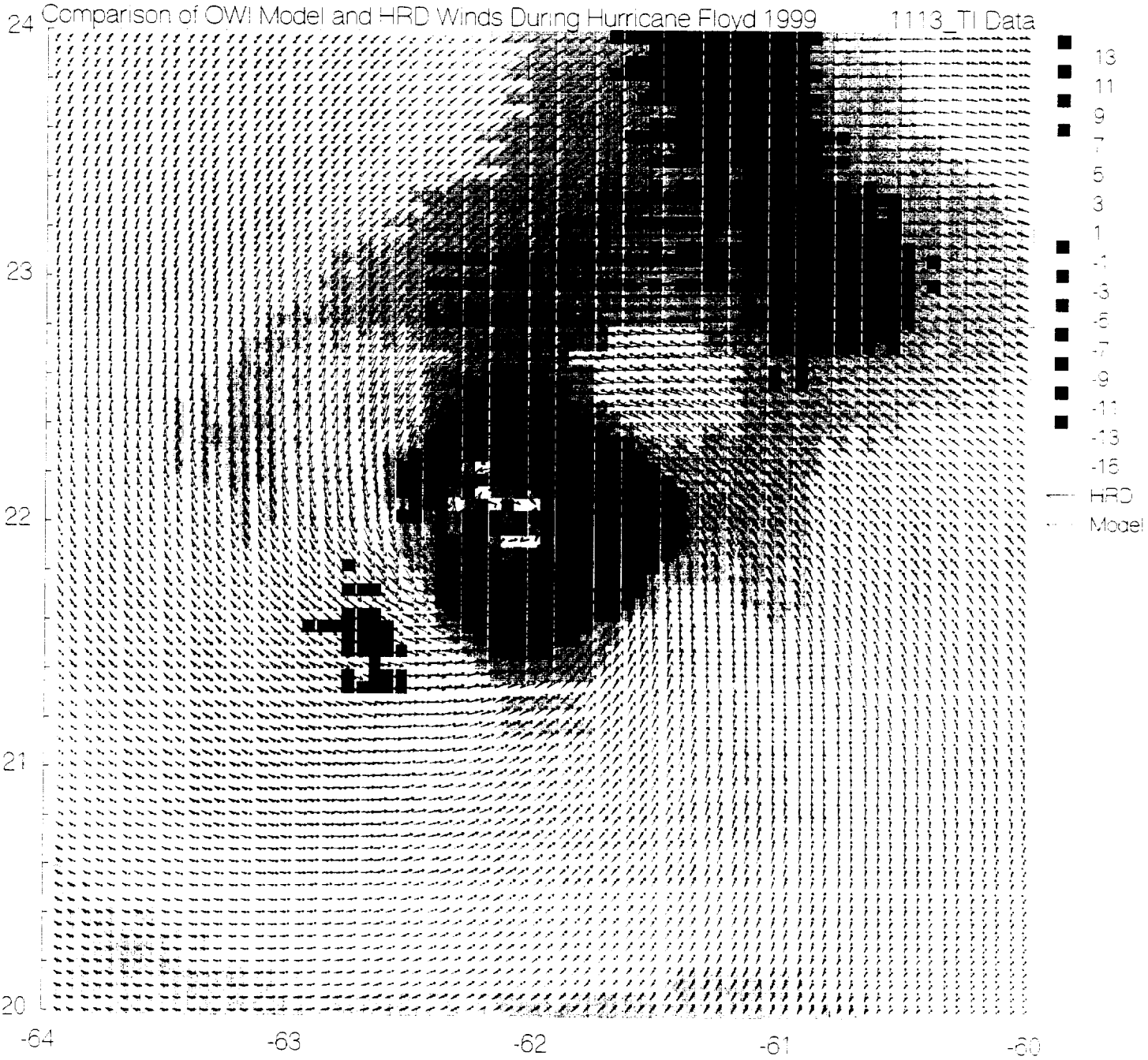
Comparison of OWI Model and HRD Winds During Hurricane Floyd 1999
1113_TI Data
24
23
22
21
20
-64
-63
-62
-61
-60
13
11
9
7
5
3
1
-1
-3
-5
-7
-9
-11
-13
-15
HRD
Model

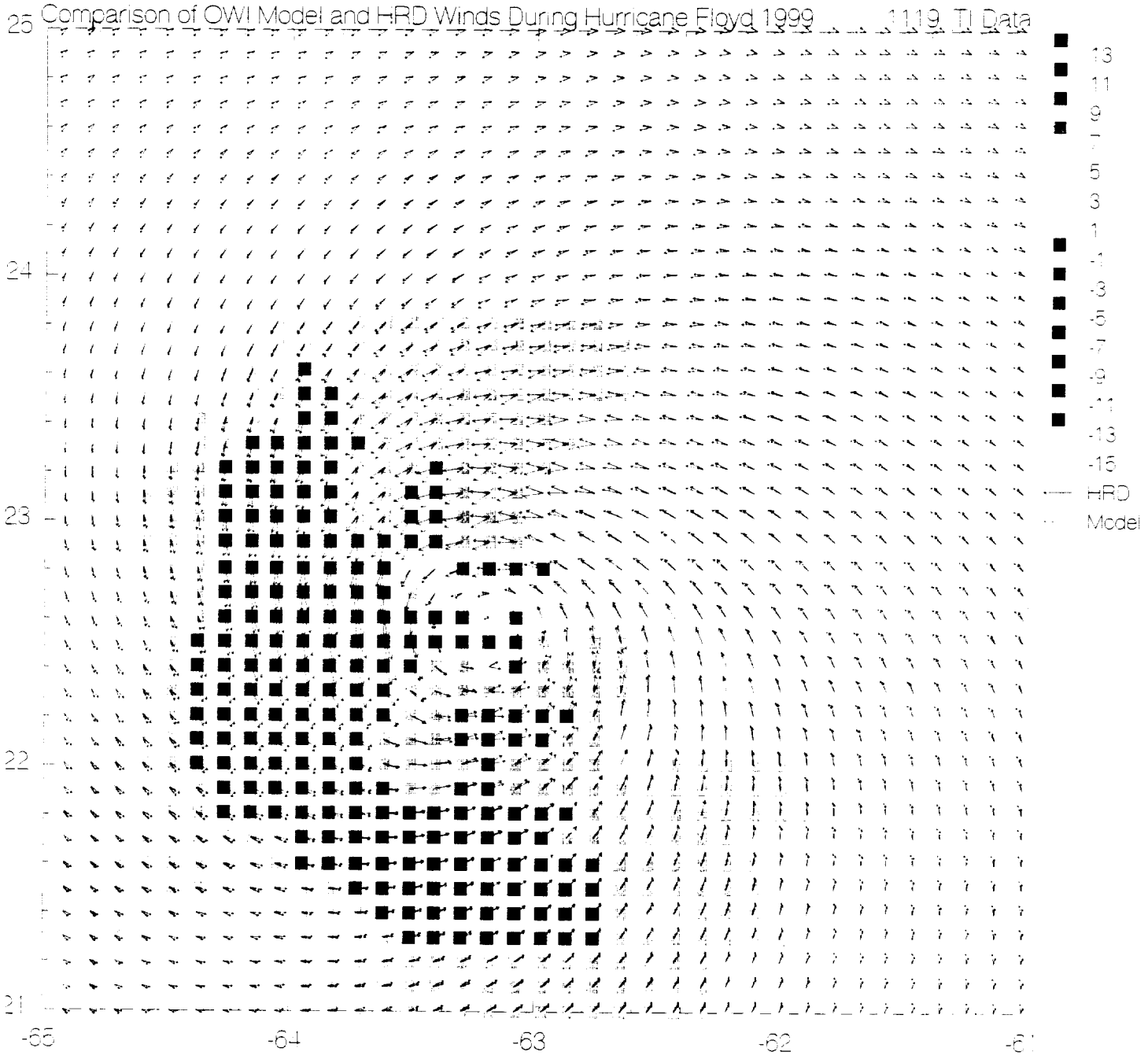
Comparison of OWI Model and HRD Winds During Hurricane Floyd 1999 1119 TI Data
25
24
23
22
21
-65
-64
-63
-62
13
11
9
7
5
3
1
-1
-3
-5
-7
-9
-11
-13
-15
HRD
Model

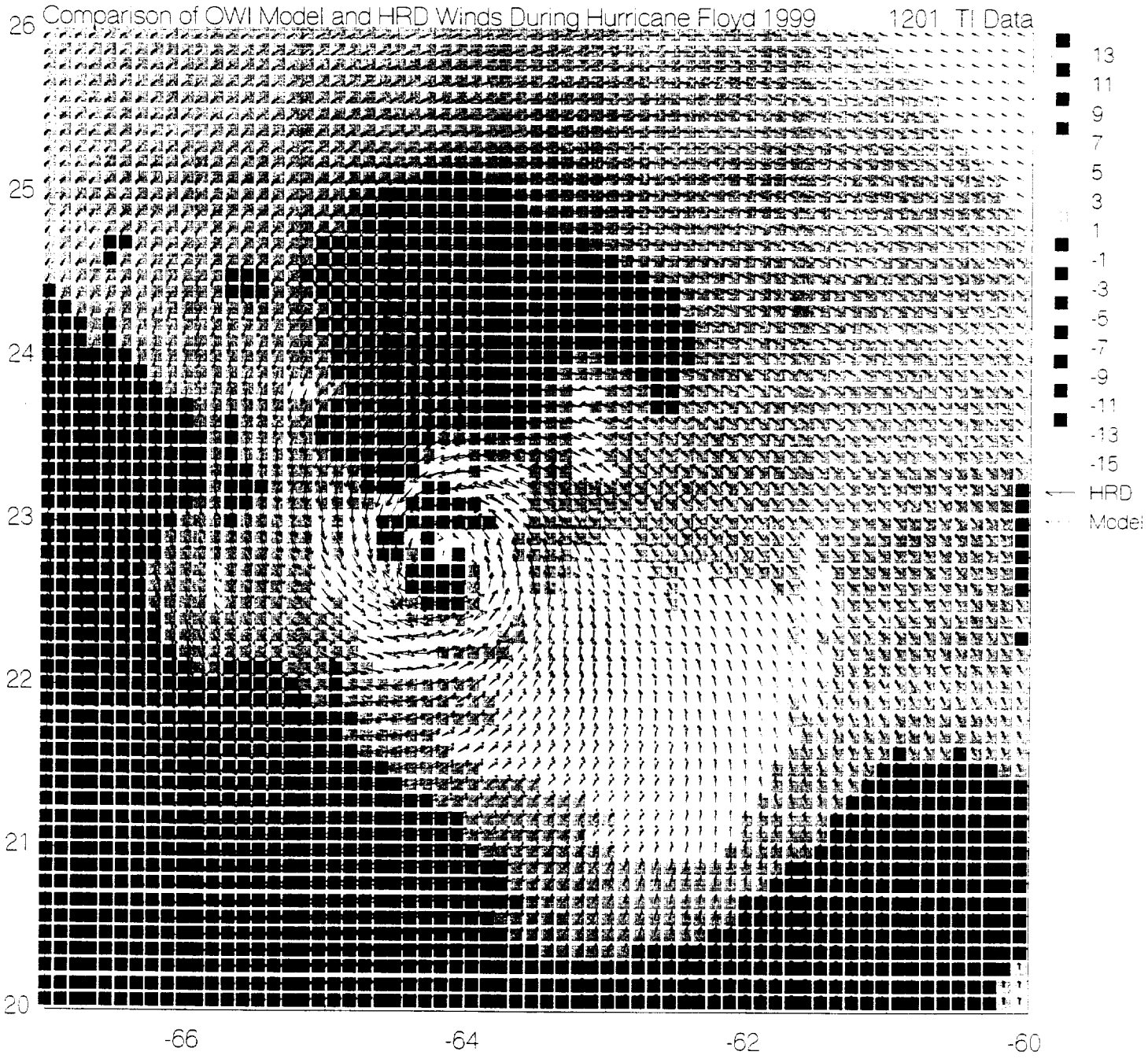
Comparison of OWI Model and HRD Winds During Hurricane Floyd 1999
1201 TI Data
26
25
24
23
22
21
20
-66
-64
-62
-60
13
11
9
7
5
3
1
-1
-3
-5
-7
-9
-11
-13
-15
HRD
Model

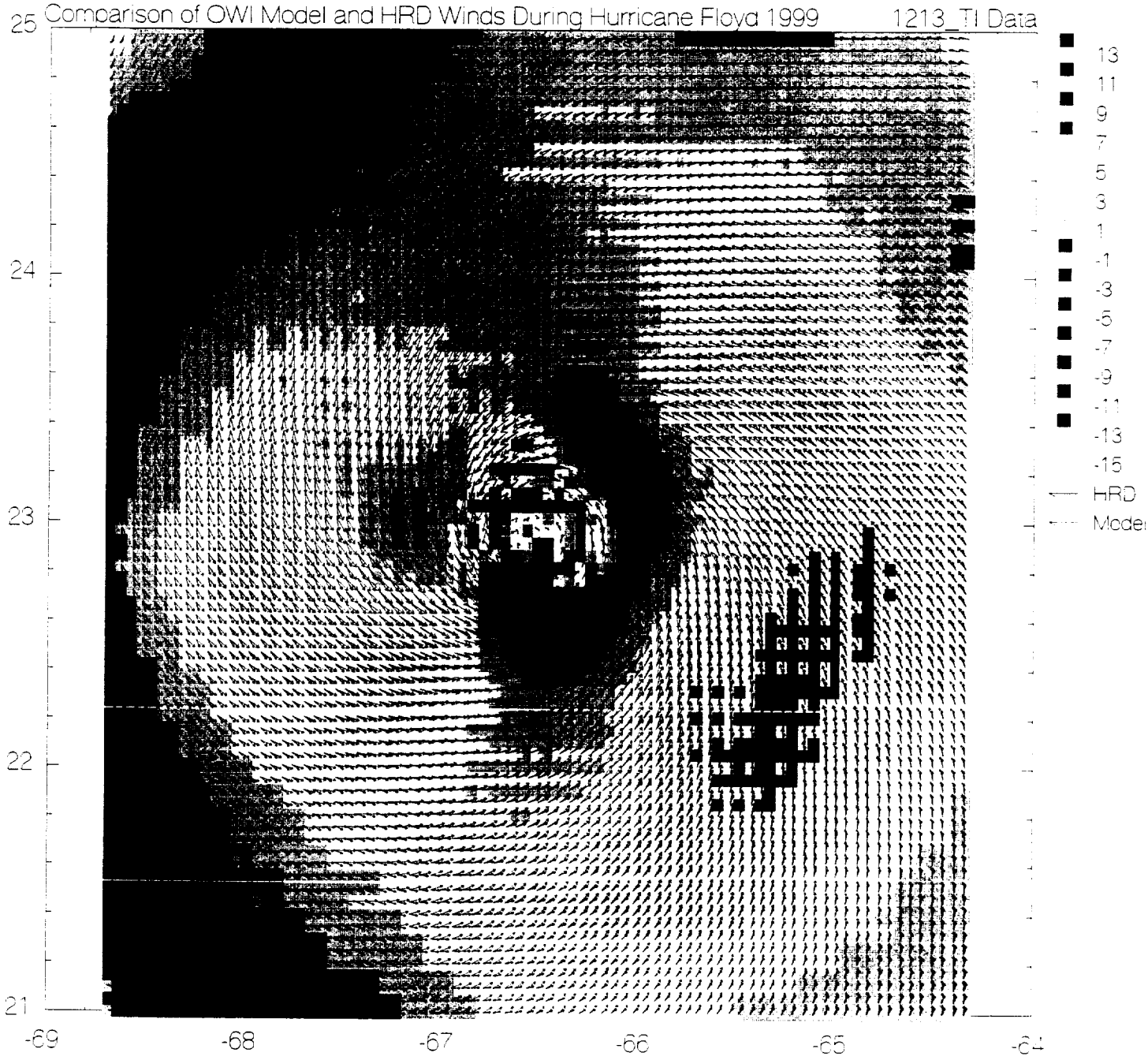
Comparison of OWI Model and HRD Winds During Hurricane Floyd 1999
1213_TI Data
25
24
23
22
21
-69
-68
-67
-66
-65
-64
13
11
9
7
5
3
1
-1
-3
-5
-7
-9
-11
-13
-15
HRD
Model

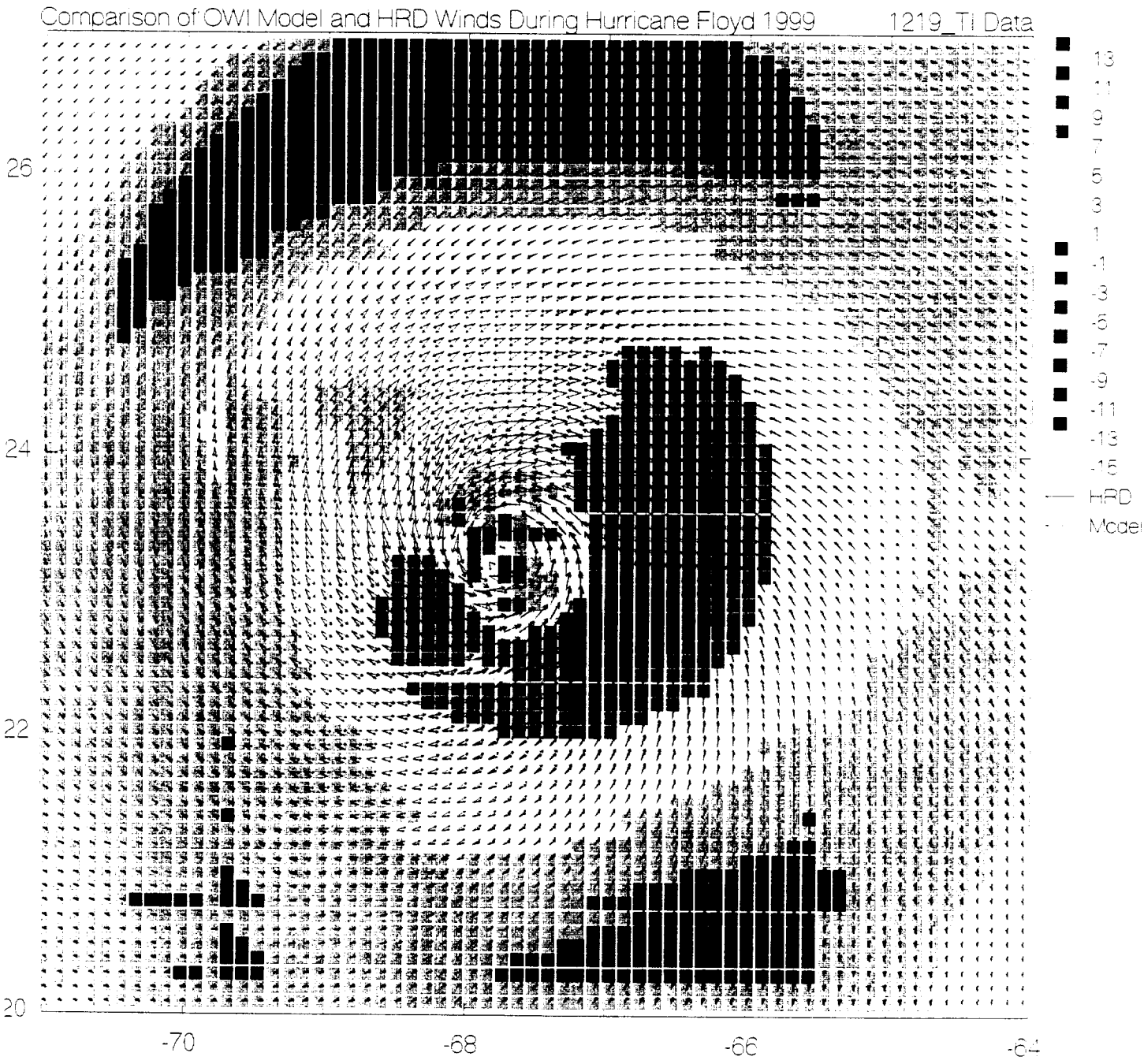
Comparison of OWI Model and HRD Winds During Hurricane Floyd 1999
1219_Ti Data
26
24
22
20
-70
-68
-66
-64
13
11
9
7
5
3
1
-1
-3
-5
-7
-9
-11
-13
-15
HRD
Model

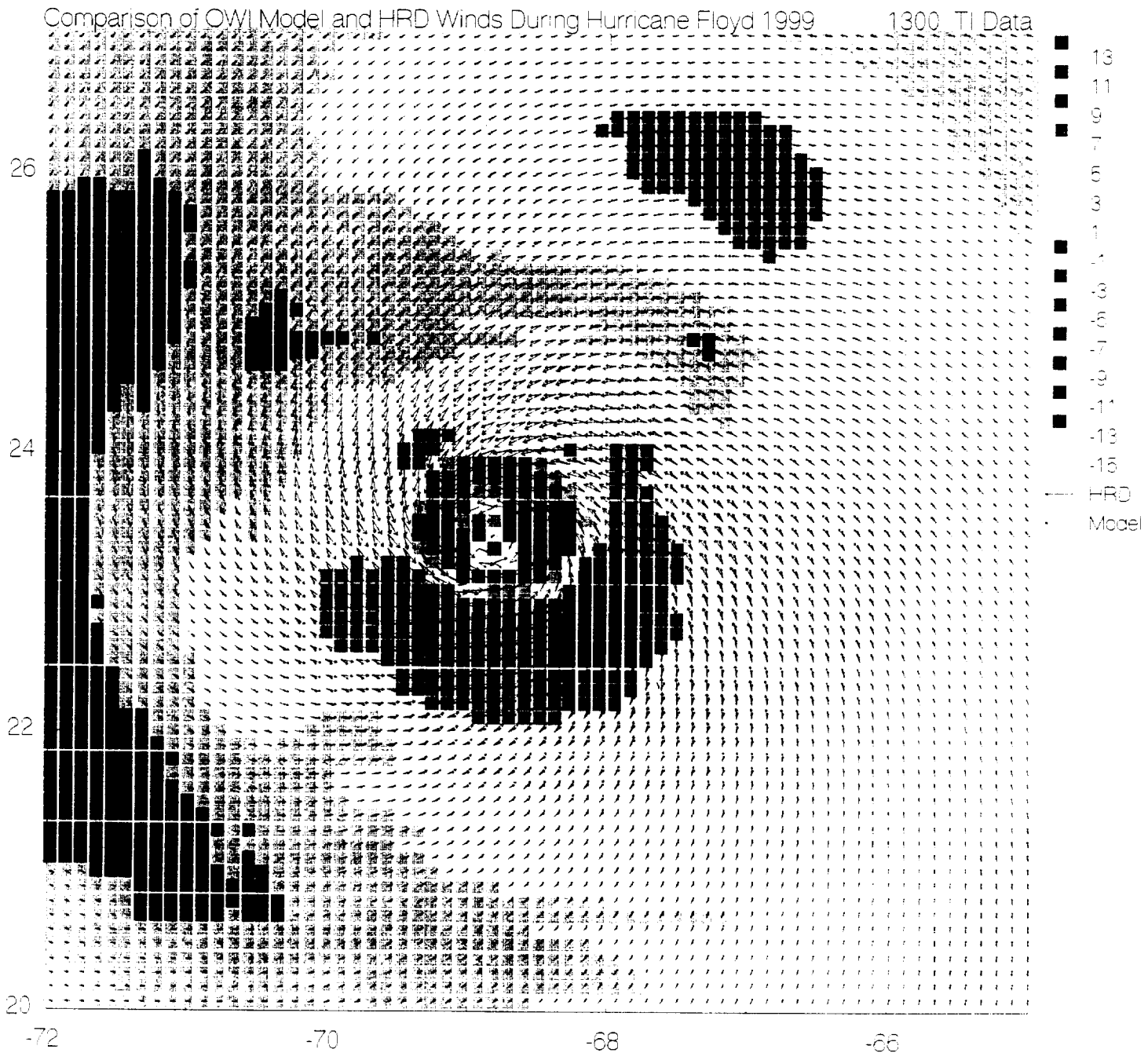
Comparison of OWI Model and HRD Winds During Hurricane Floyd 1999
1300 TI Data
13
11
9
7
6
3
1
-1
-3
-5
-7
-9
-11
-13
-15
HRD
Model
26
24
22
20
-72
-70
-68
-66

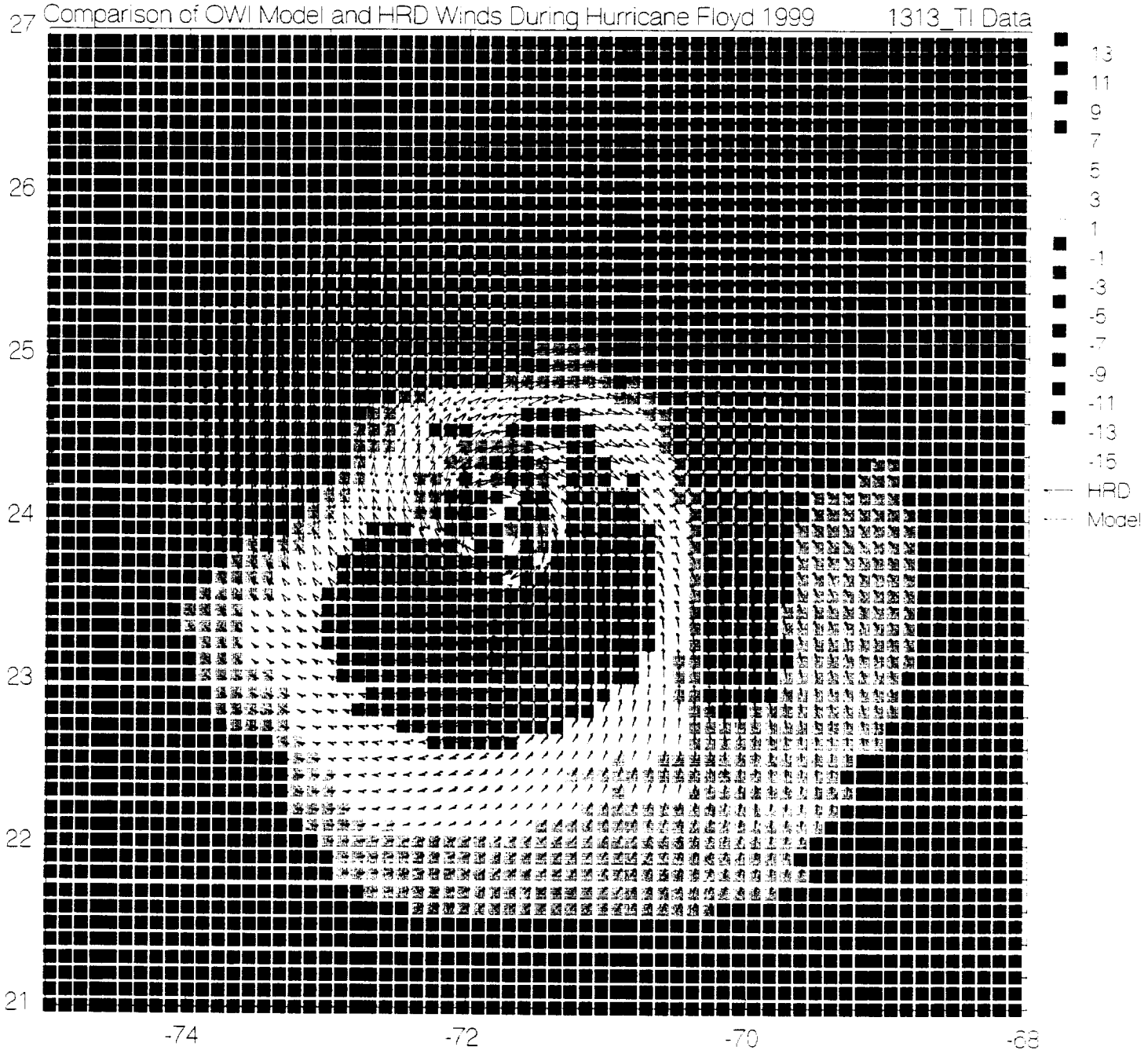
Comparison of OWI Model and HRD Winds During Hurricane Floyd 1999
1313_TI Data
27
26
25
24
23
22
21
-74
-72
-70
-68
13
11
9
7
5
3
1
-1
-3
-5
-7
-9
-11
-13
-15
HRD
Model

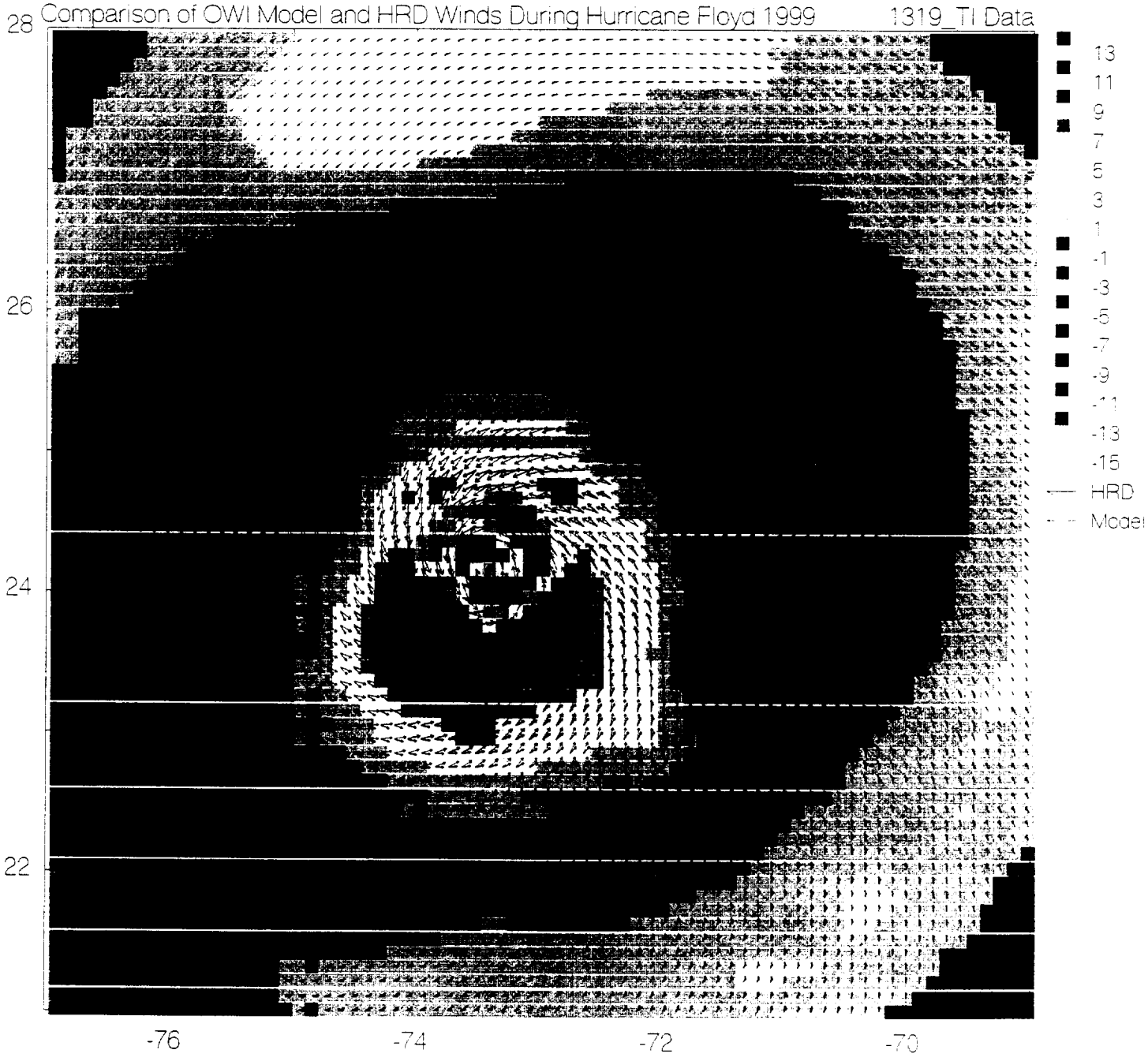
Comparison of OWI Model and HRD Winds During Hurricane Floyd 1999
1319_TI Data
28
26
24
22
-76
-74
-72
-70
13
11
9
7
5
3
1
-1
-3
-5
-7
-9
-11
-13
-15
HRD
Model

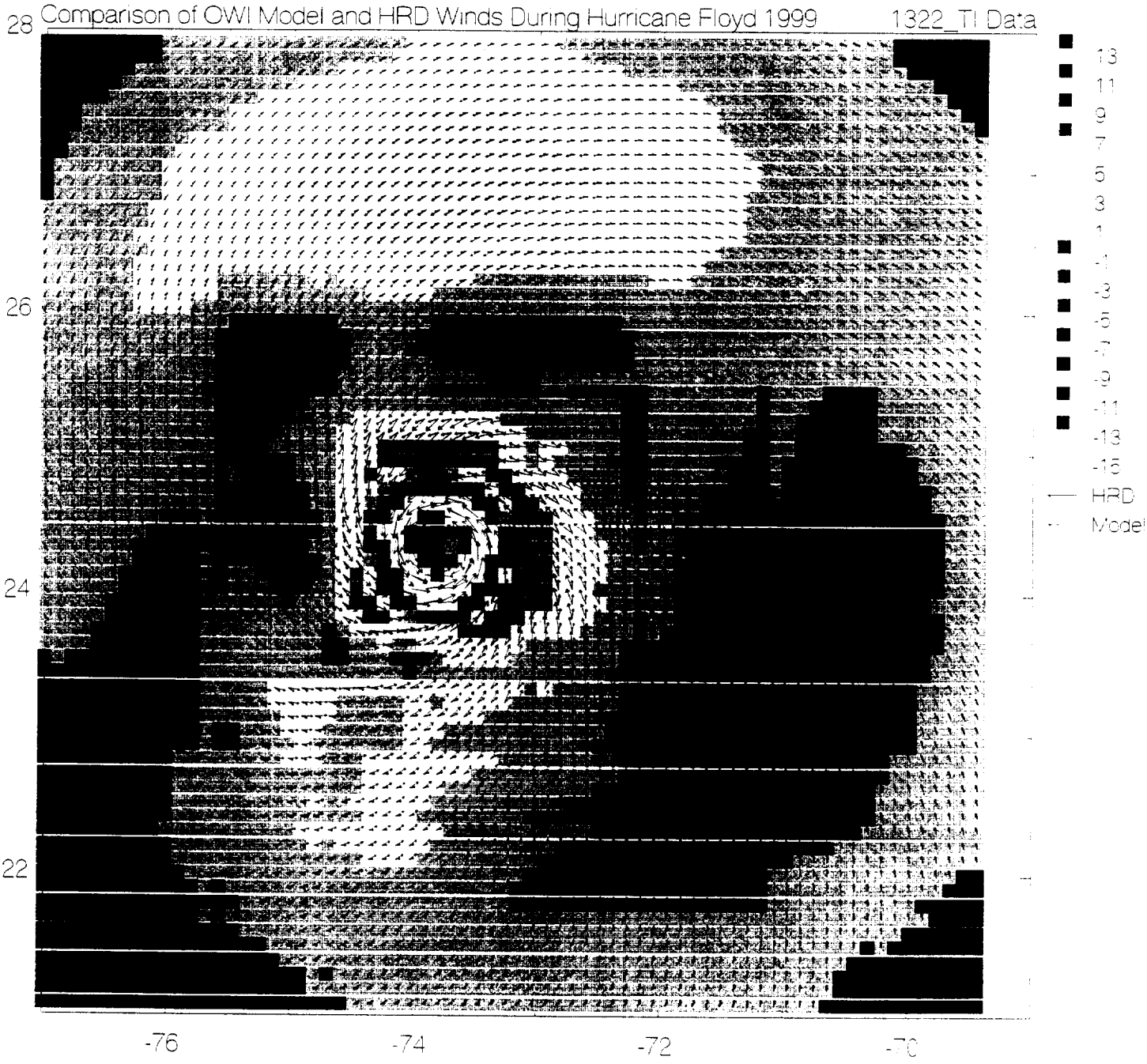
Comparison of OWI Model and HRD Winds During Hurricane Floyd 1999
1322_TI Data
28
26
24
22
-76
-74
-72
-70
13
11
9
7
5
3
1
-1
-3
-5
-7
-9
-11
-13
-15
HRD
Model

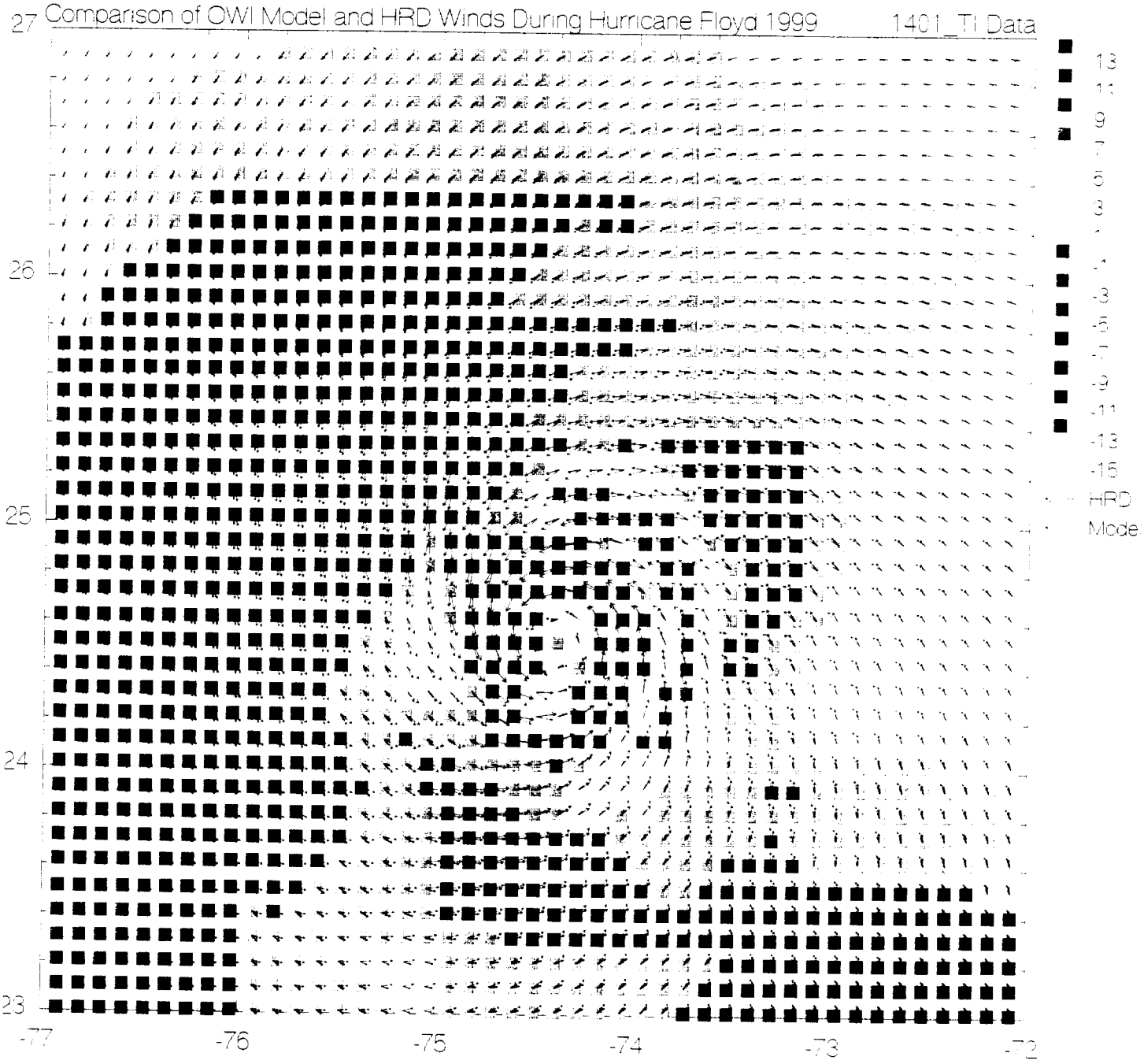
Comparison of OWI Model and HRD Winds During Hurricane Floyd 1999
1401_TI Data
27
26
25
24
23
-77
-76
-75
-74
-73
-72
13
11
9
7
5
3
-1
-3
-5
-7
-9
-11
-13
-15
HRD
Model

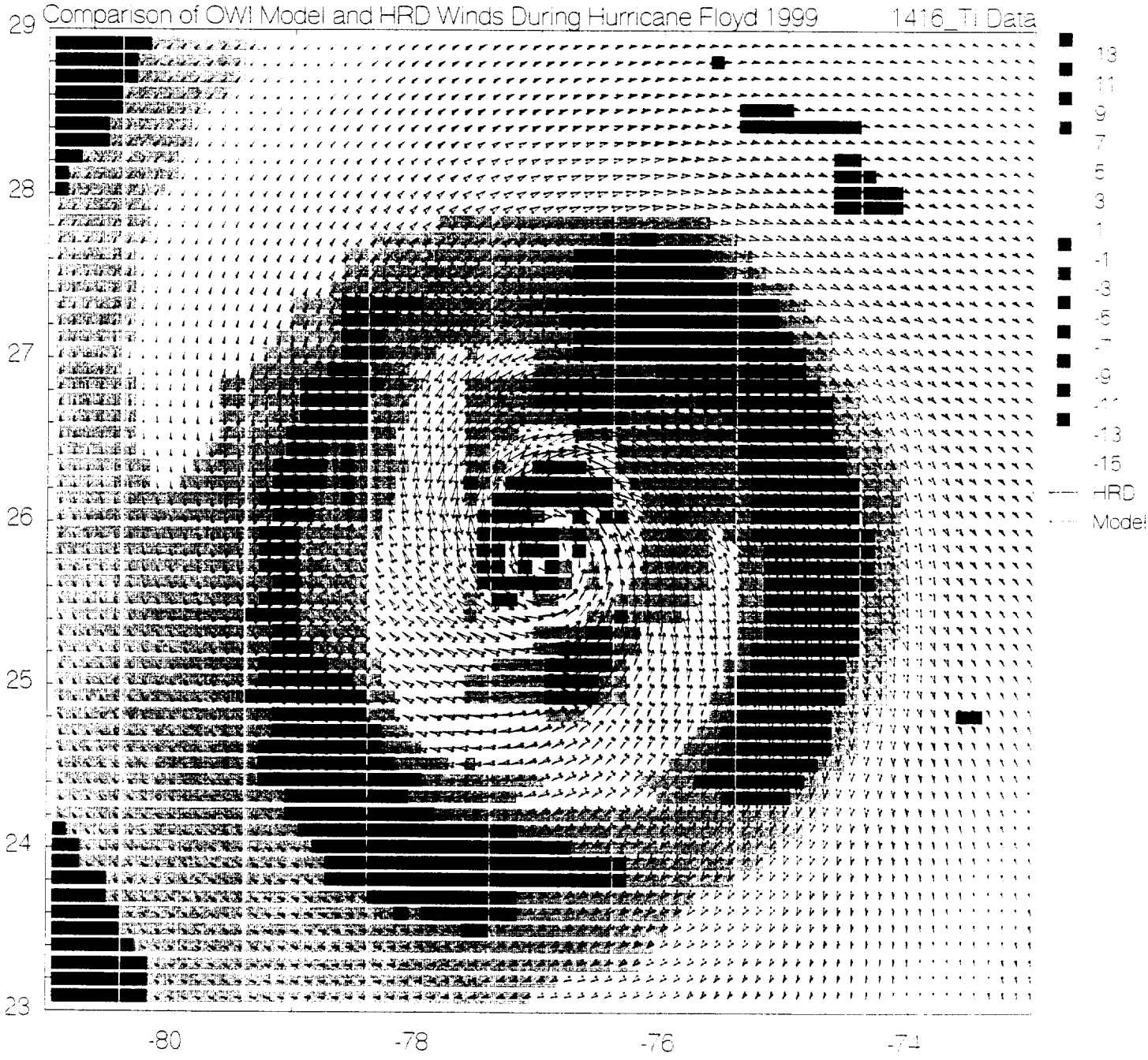
Comparison of OWI Model and HRD Winds During Hurricane Floyd 1999
1416_TI Data
29
28
27
26
25
24
23
-80
-78
-76
-74
13
11
9
7
5
3
1
-1
-3
-5
-7
-9
-11
-13
-15
HRD
Model

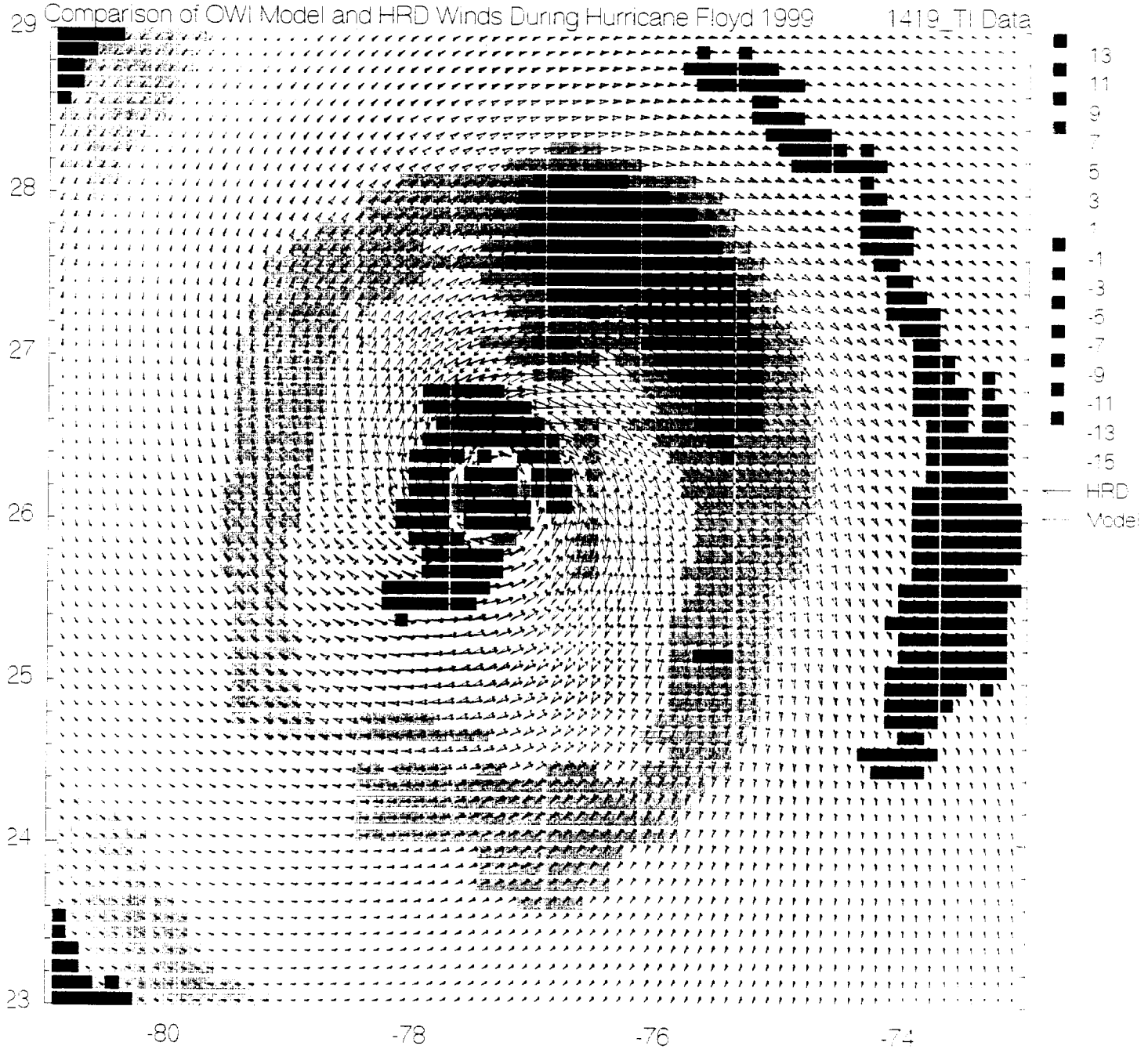
Comparison of OWI Model and HRD Winds During Hurricane Floyd 1999
1419_TI Data
29
28
27
26
25
24
23
-80
-78
-76
-74
13
11
9
7
5
3
1
-1
-3
-5
-7
-9
-11
-13
-15
HRD
Model

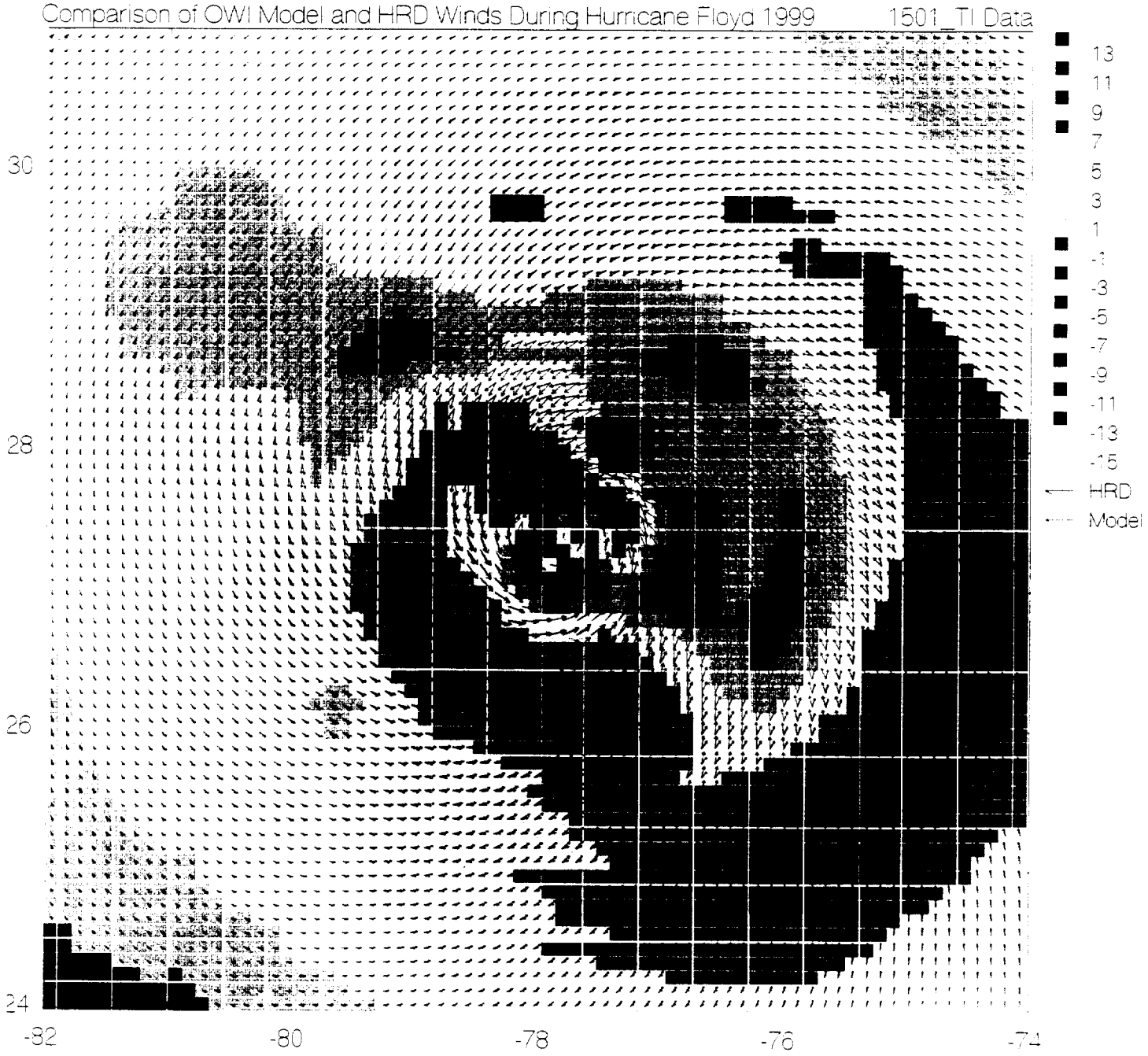
Comparison of OWI Model and HRD Winds During Hurricane Floyd 1999
1501_TI Data
13
11
9
7
5
3
1
-1
-3
-5
-7
-9
-11
-13
-15
HRD
Model
30
28
26
24
-82
-80
-78
-76
-74

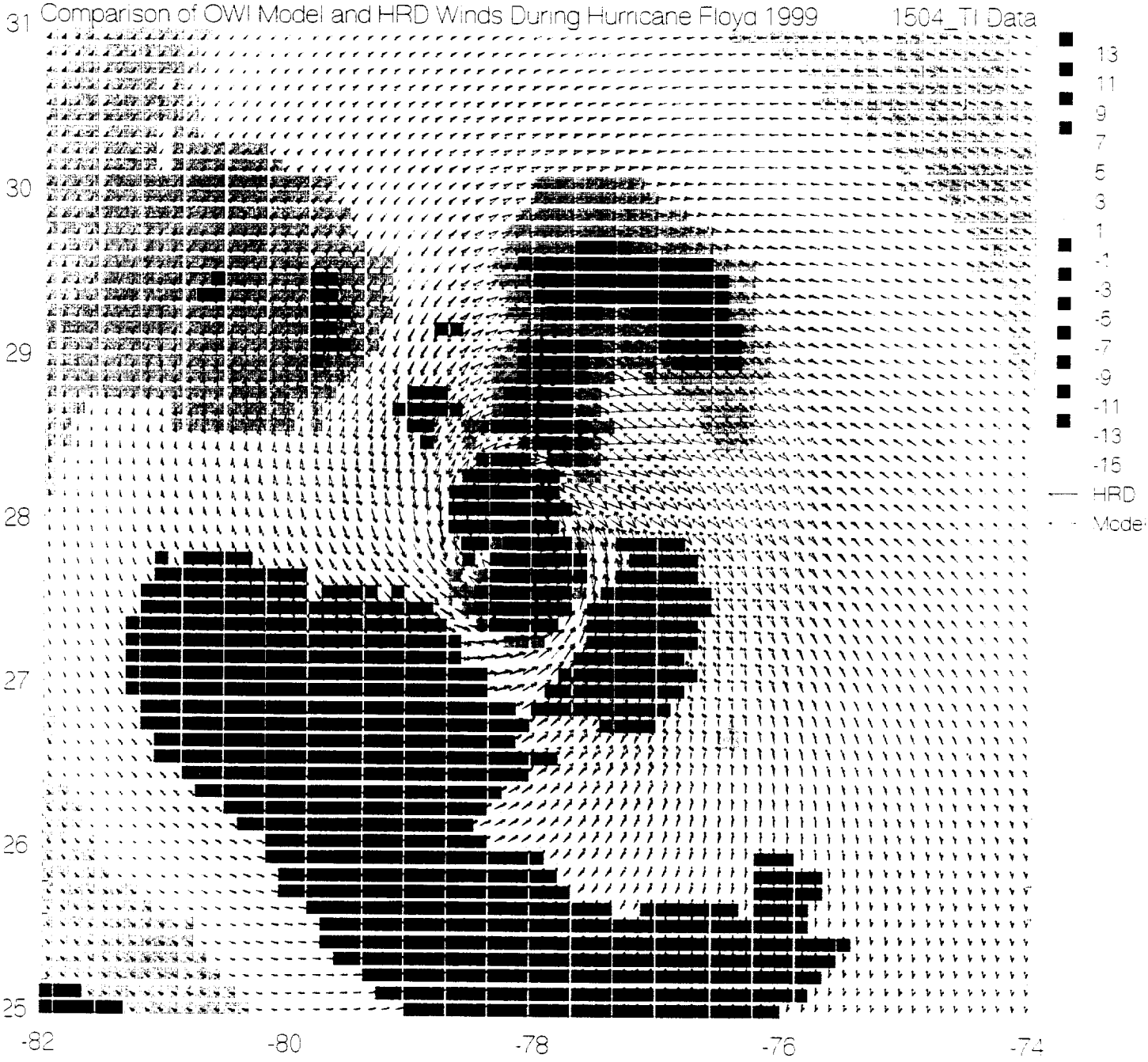
Comparison of OWI Model and HRD Winds During Hurricane Floyd 1999
1504_TI Data
31
30
29
28
27
26
25
-82
-80
-78
-76
-74
13
11
9
7
5
3
1
-1
-3
-5
-7
-9
-11
-13
-15
HRD
Model

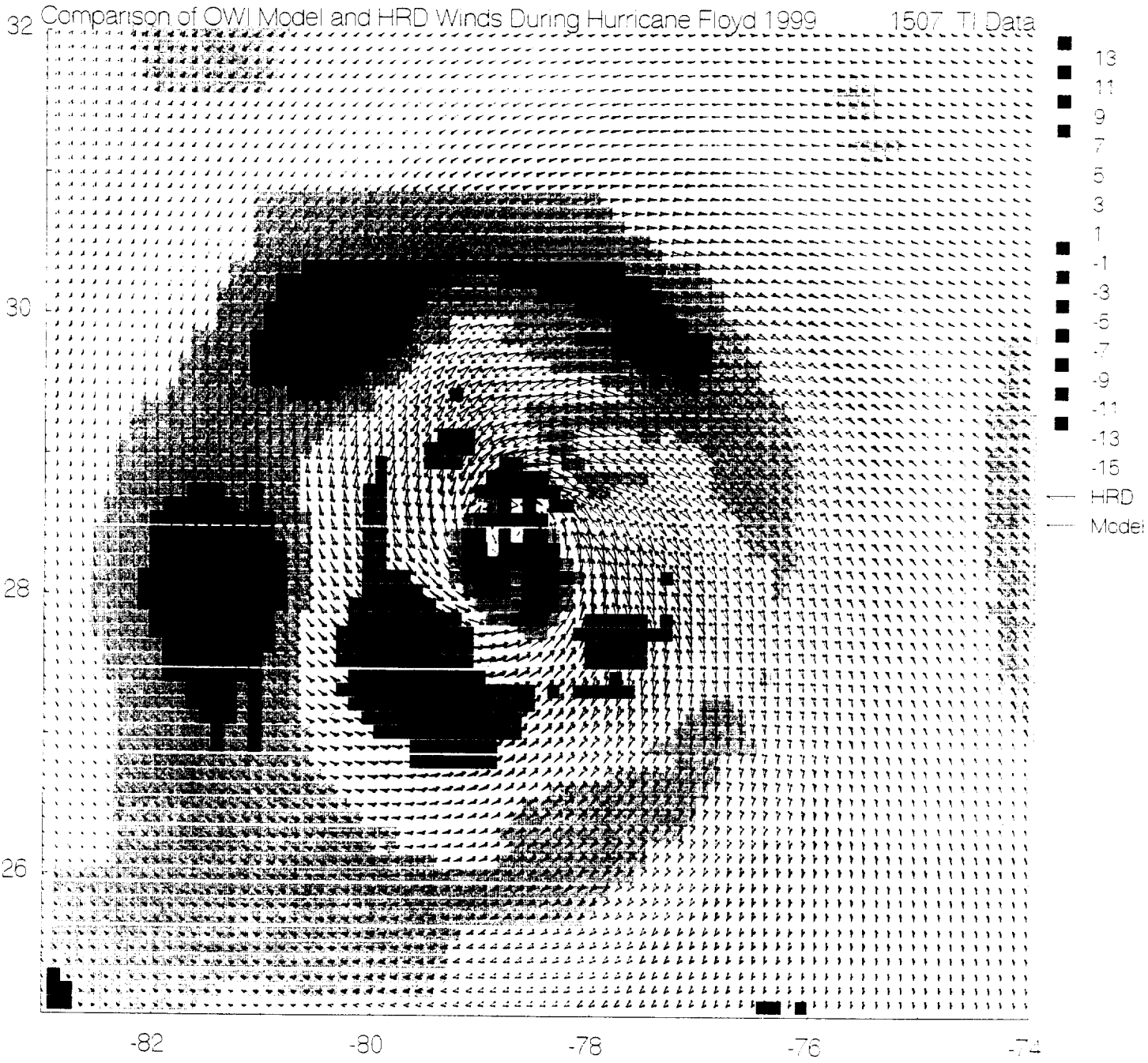
Comparison of OWI Model and HRD Winds During Hurricane Floyd 1999
1507 TI Data
32
30
28
26
-82
-80
-78
-76
-74
13
11
9
7
5
3
1
-1
-3
-5
-7
-9
-11
-13
-15
HRD
Model

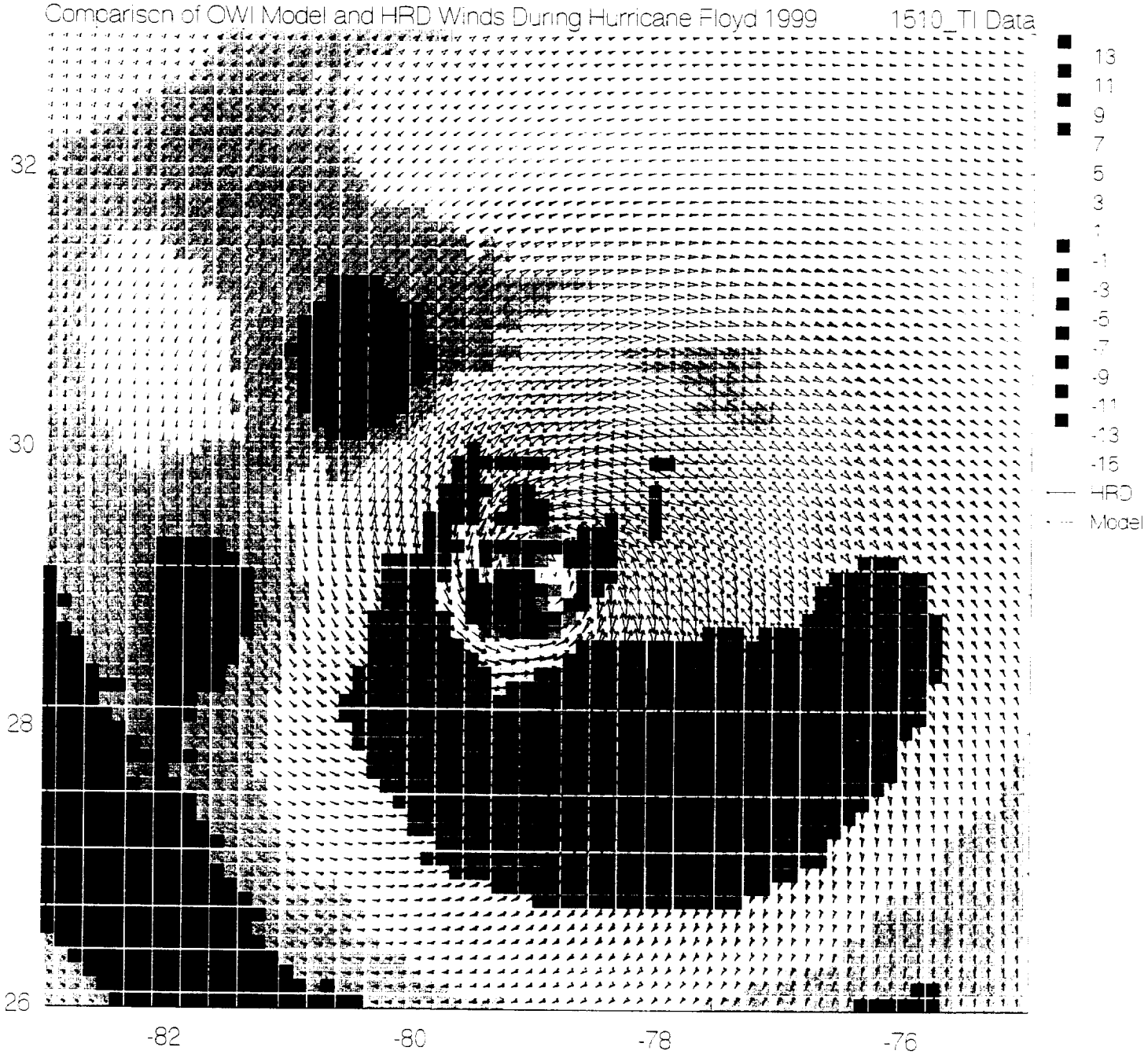
Comparison of OWI Model and HRD Winds During Hurricane Floyd 1999
1510_TI Data
13
11
9
7
5
3
1
-1
-3
-5
-7
-9
-11
-13
-15
HRD
Model
32
30
28
26
-82
-80
-78
-76

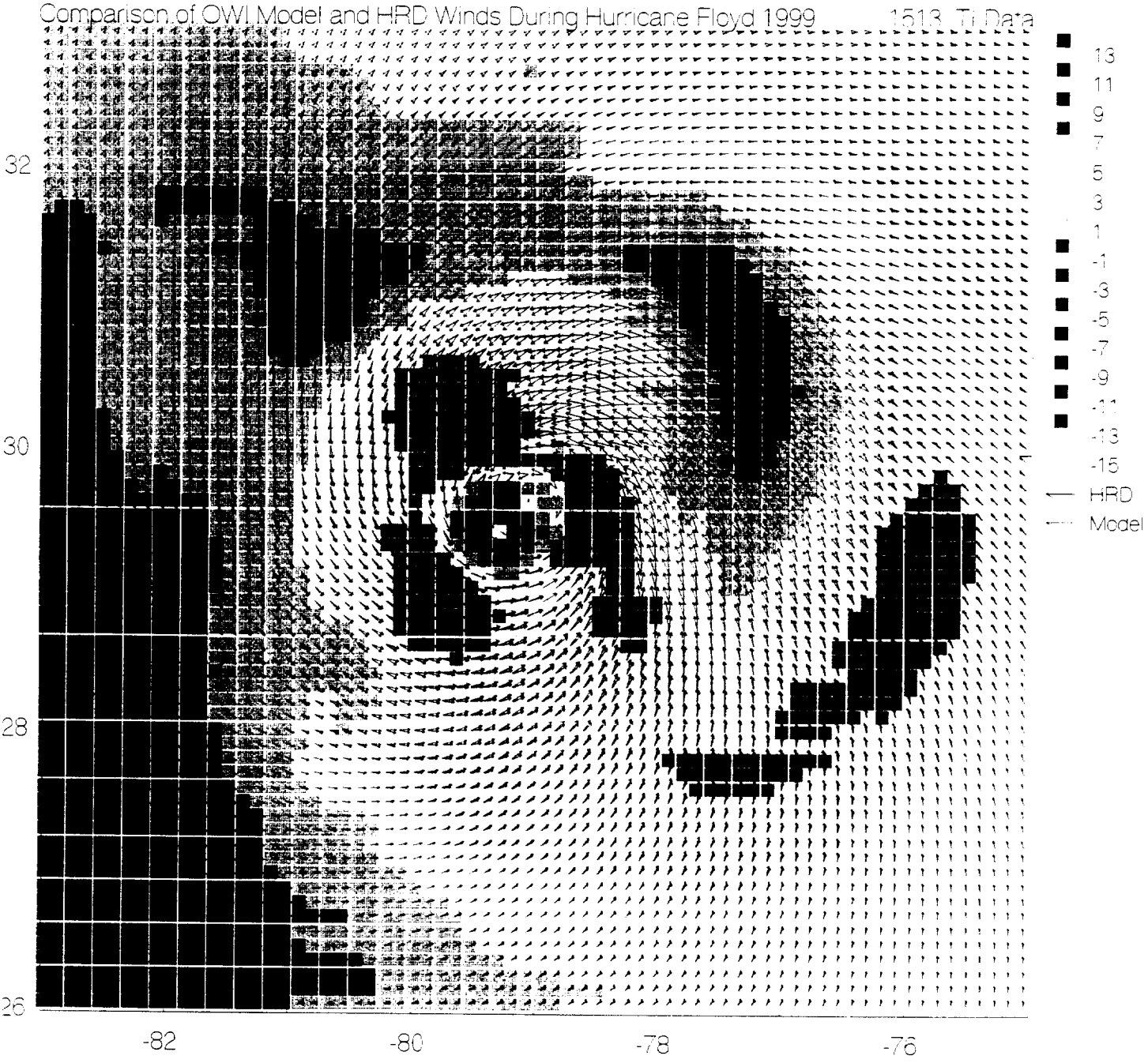
Comparison of OWI Model and HRD Winds During Hurricane Floyd 1999
1513 Tr Data
13
11
9
7
5
3
1
-1
-3
-5
-7
-9
-11
-13
-15
HRD
Model
32
30
28
26
-82
-80
-78
-76

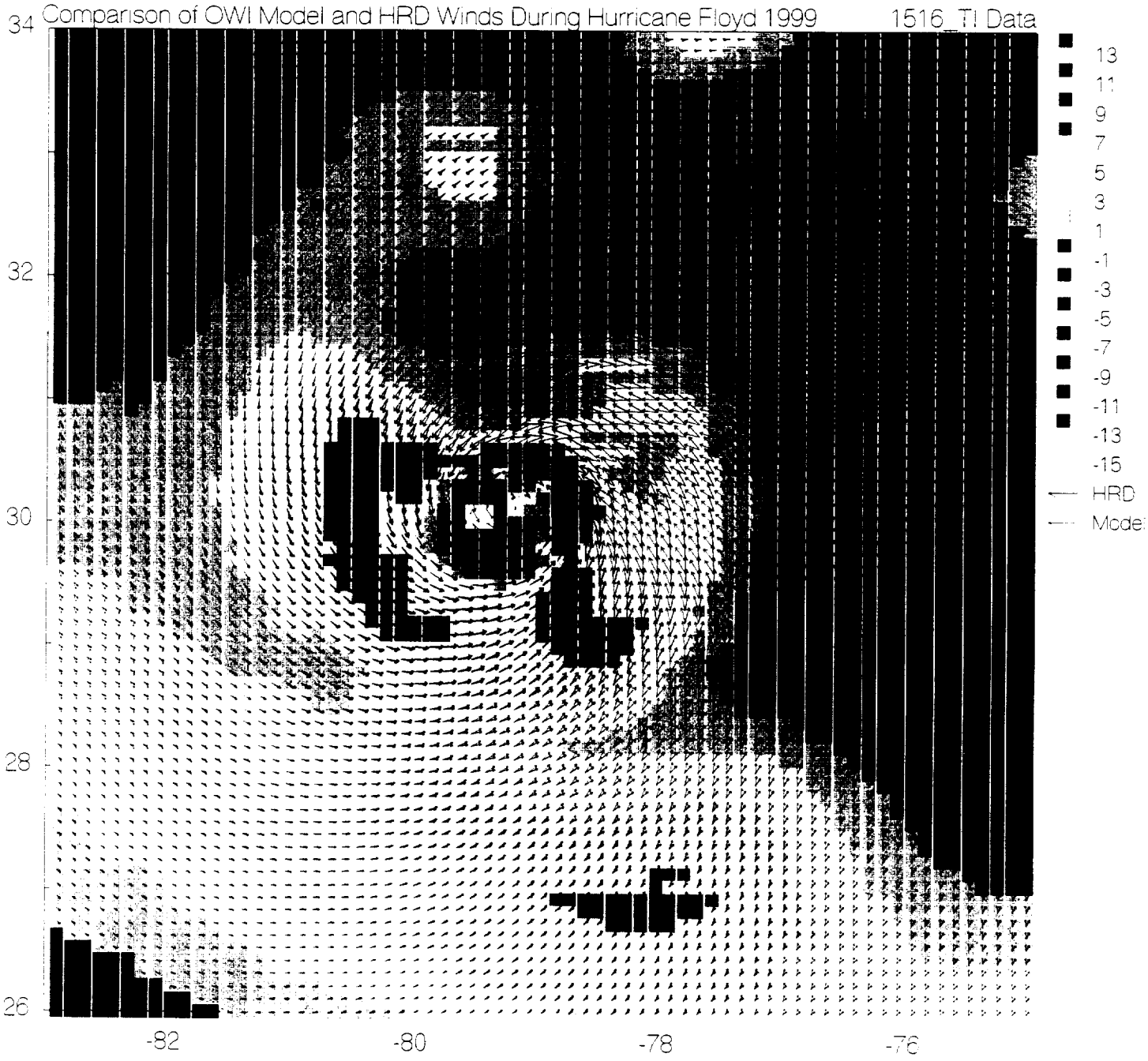
Comparison of OWI Model and HRD Winds During Hurricane Floyd 1999
1516_TI Data
34
32
30
28
26
-82
-80
-78
-76
13
11
9
7
5
3
1
-1
-3
-5
-7
-9
-11
-13
-15
HRD
Model

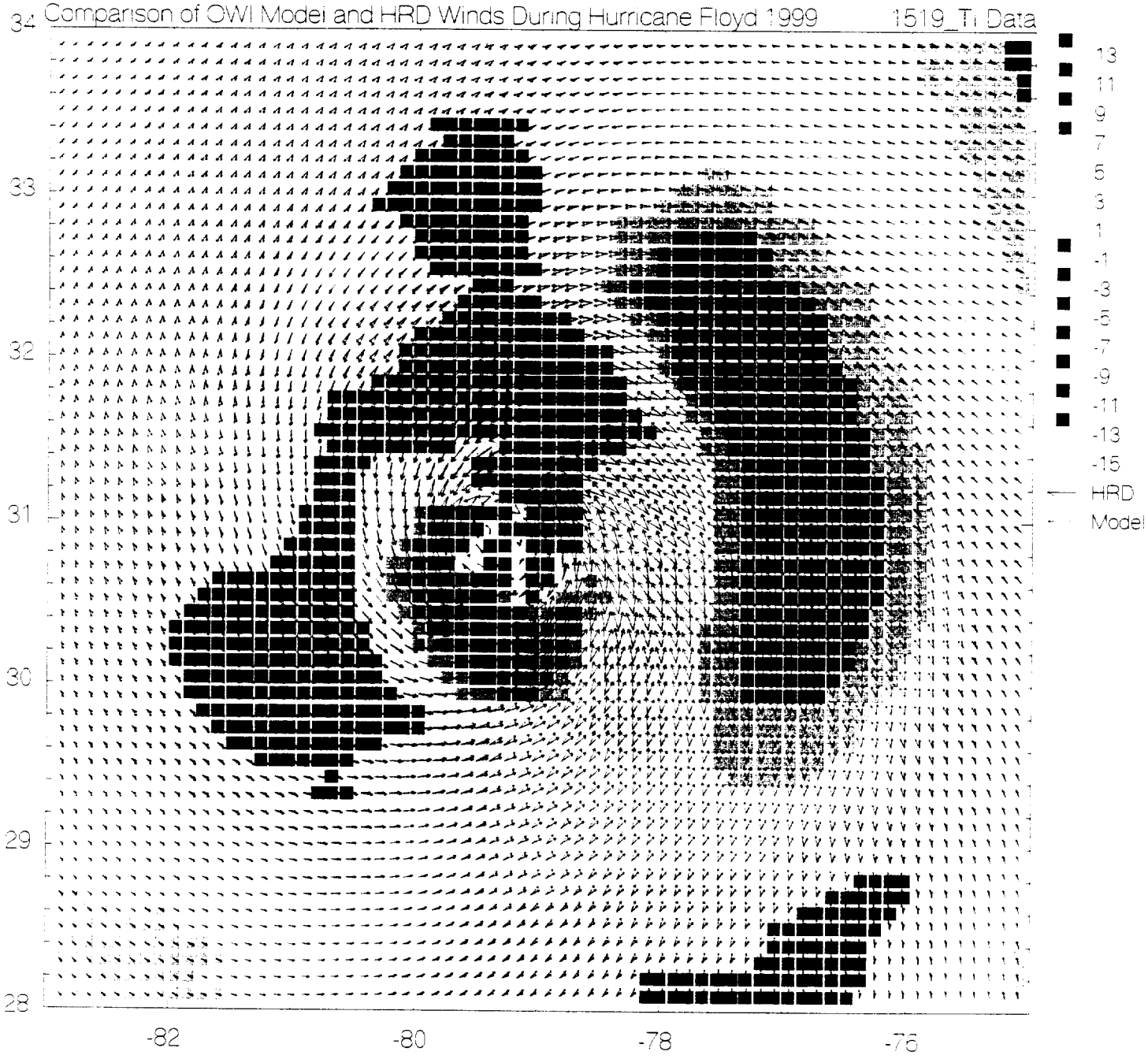
Comparison of OWI Model and HRD Winds During Hurricane Floyd 1999
1519_Ti Data
34
33
32
31
30
29
28
-82
-80
-78
-76
13
11
9
7
5
3
1
-1
-3
-5
-7
-9
-11
-13
-15
HRD
Model

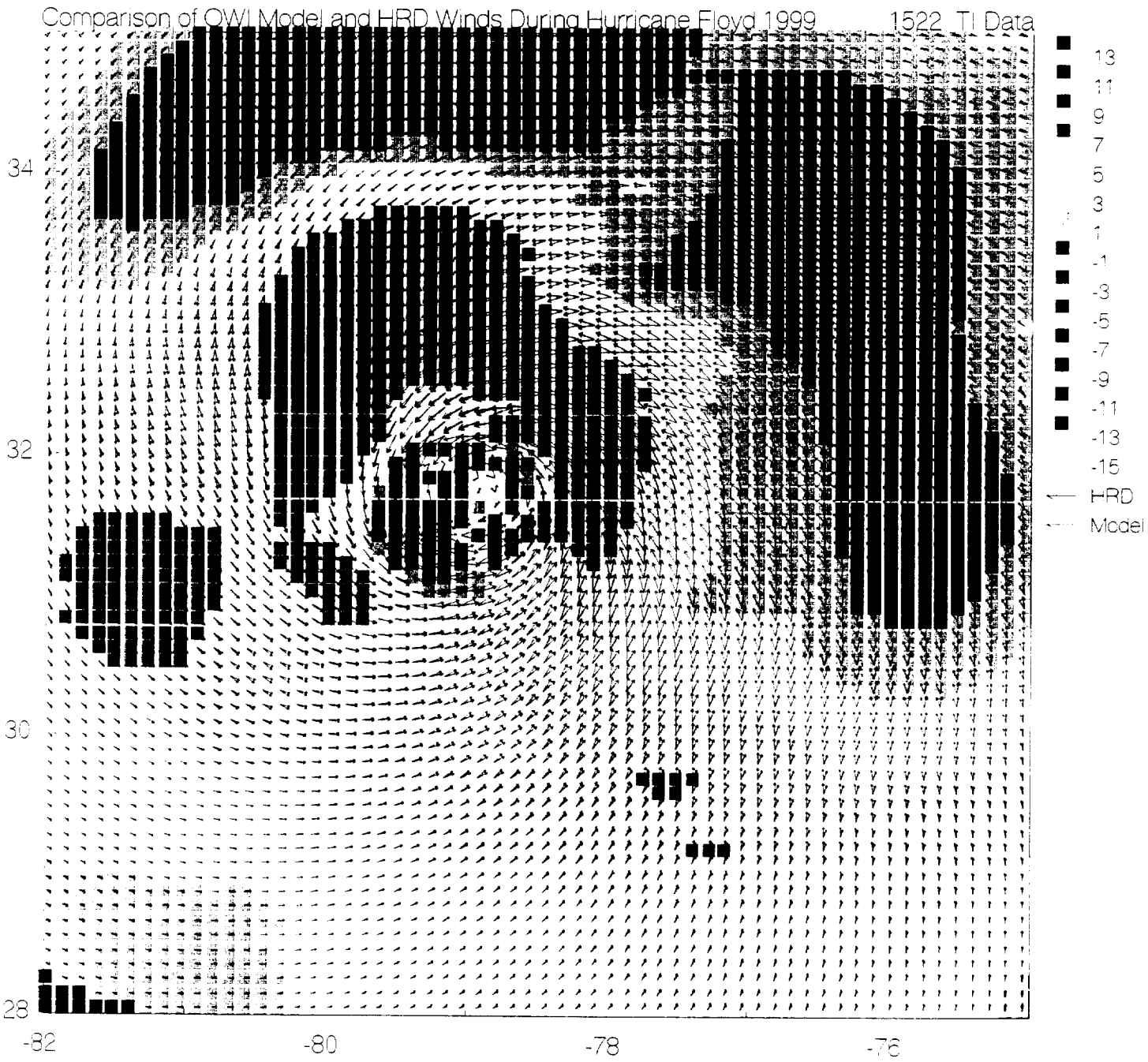
Comparison of OWI Model and HRD Winds During Hurricane Floyd 1999
1522 TI Data
13
11
9
7
5
3
1
-1
-3
-5
-7
-9
-11
-13
-15
HRD
Model
34
32
30
28
-82
-80
-78
-76

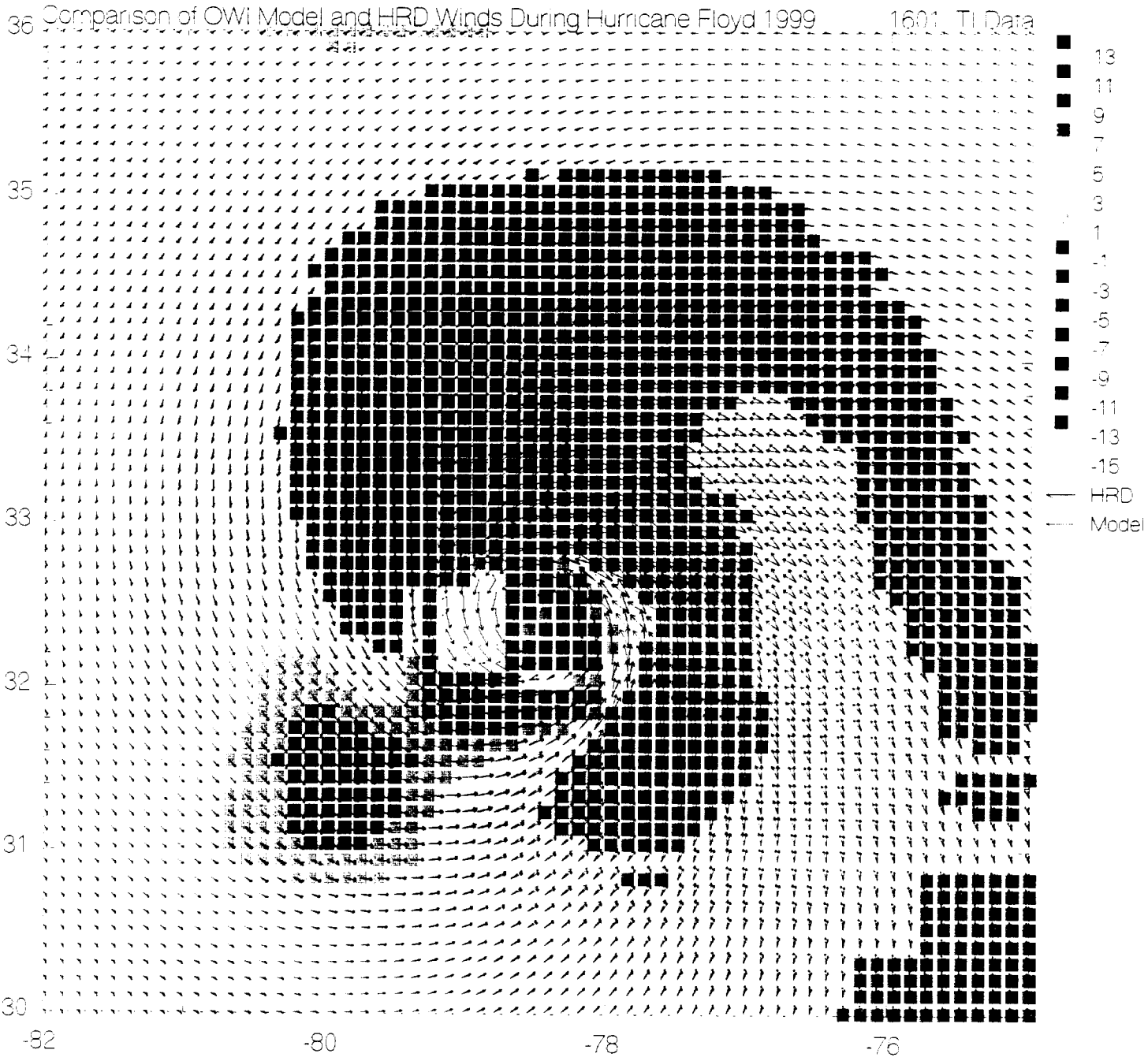
Comparison of OWI Model and HRD Winds During Hurricane Floyd 1999
1601 TI Data
36
35
34
33
32
31
30
-82
-80
-78
-76
13
11
9
7
5
3
1
-1
-3
-5
-7
-9
-11
-13
-15
HRD
Model

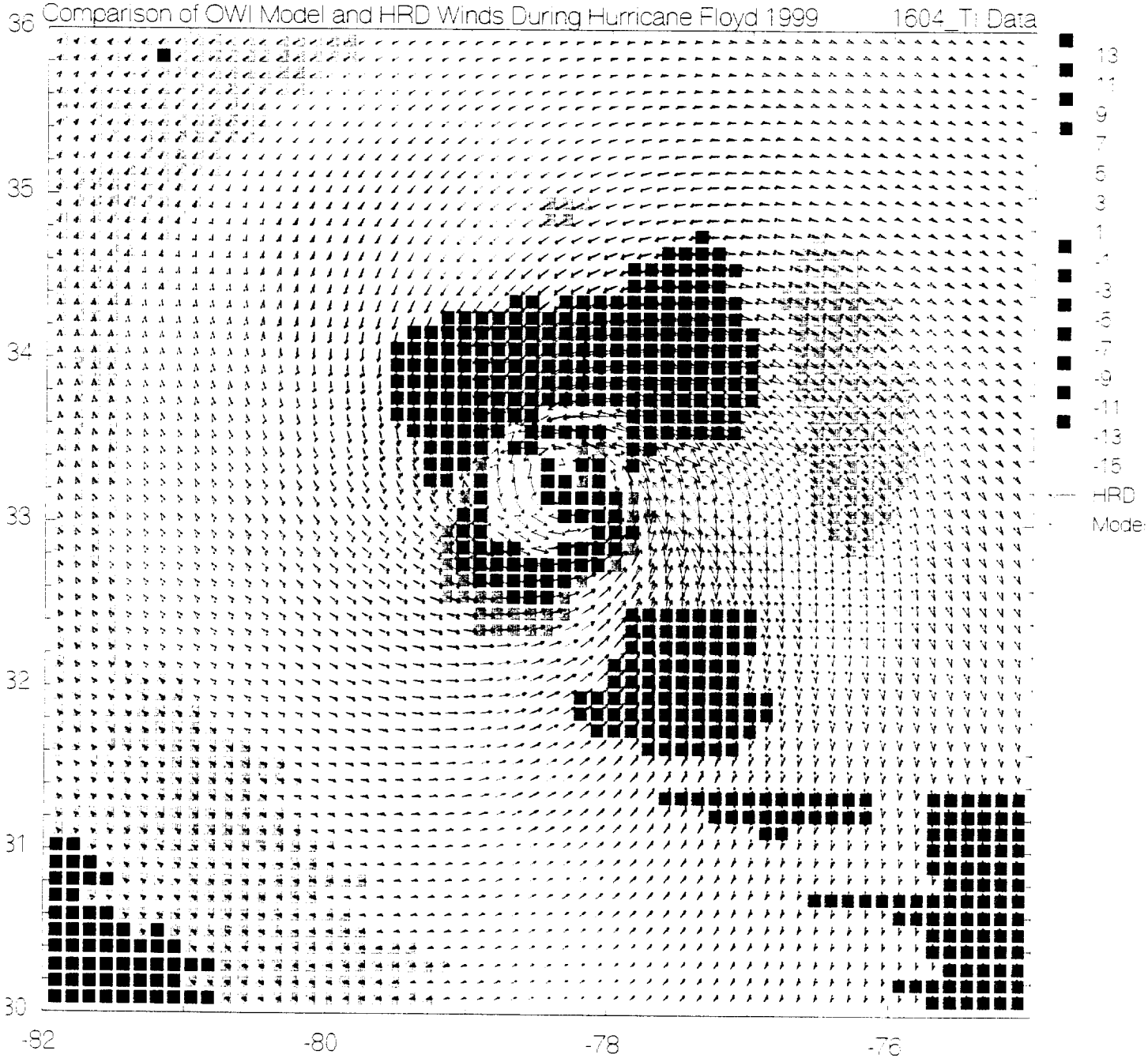
Comparison of OWI Model and HRD Winds During Hurricane Floyd 1999
1604_T: Data
36
35
34
33
32
31
30
-82
-80
-78
-76
13
9
7
5
3
1
-3
-5
-7
-9
-11
-13
-15
HRD
Mode

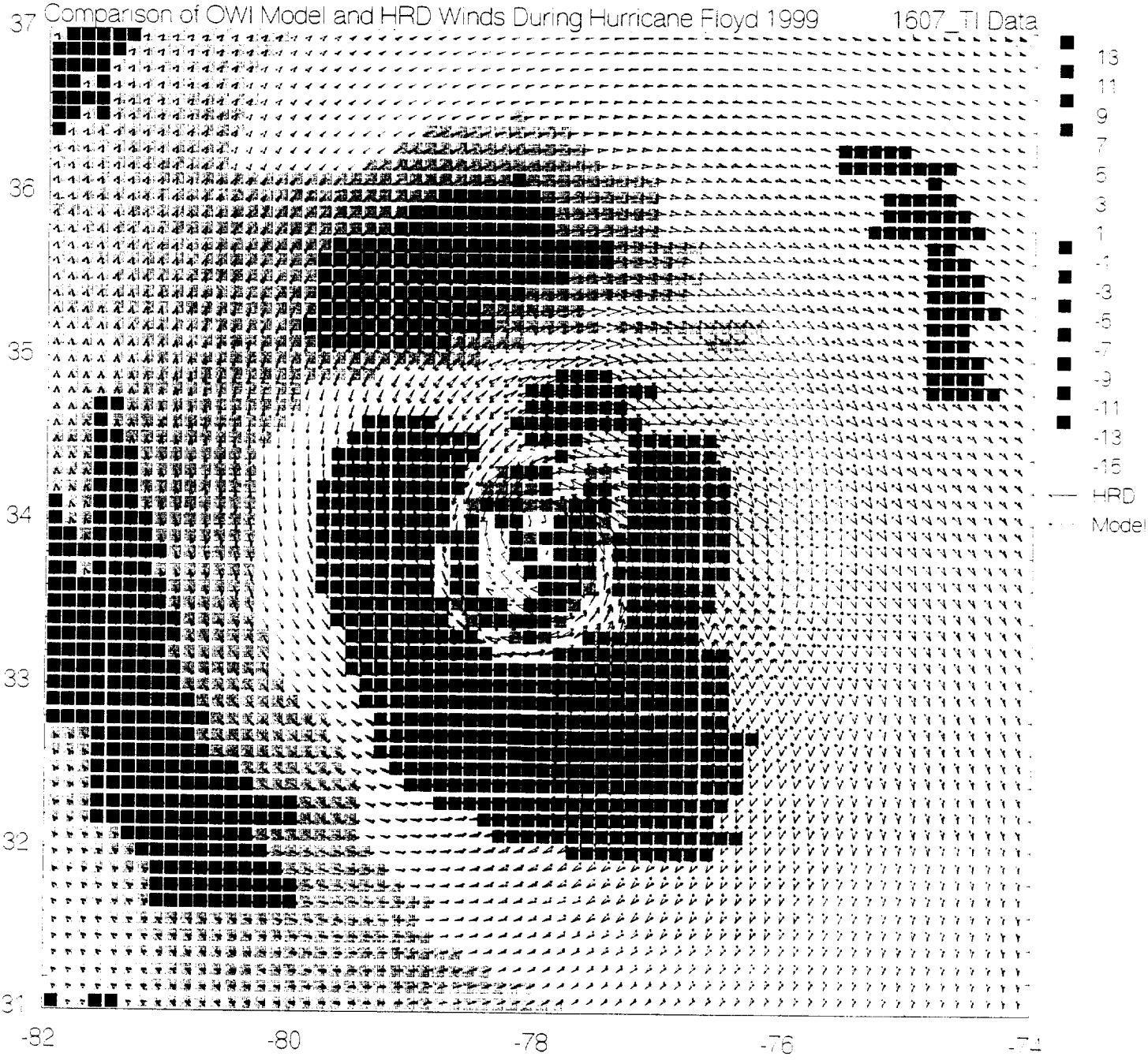
Comparison of OWI Model and HRD Winds During Hurricane Floyd 1999
1607_TI Data
37
36
35
34
33
32
31
-82
-80
-78
-76
13
11
9
7
5
3
1
-1
-3
-5
-7
-9
-11
-13
-15
HRD
Model

Appendix D. Abstract of paper to 2001 AMS Annual meeting:

Real Time Forecasting system of Winds, Waves and Surge in Tropical Cyclones: A Case Study with Hurricane Georges.

Real-Time Forecasting System of Winds, Waves and Surge in Tropical Cyclones: A Case Study with Hurricane Georges

Hans C. Graber, Mark A. Donelan and Michael G. Brown
Rosenstiel School of Marine and Atmospheric Science
University of Miami
Peter G. Black , Mark D. Powell and Sam H. Houston
NOAA/AOML Hurricane Research Division
Vincent J. Cardone, and Andrew T. Cox
Oceanweather, Inc.
Robert E. Jensen
US Army Corps of Engineers
Donald N. Slinn
Florida Atlantic University
John L. Guiney,
National Hurricane Center
Christopher Paluszek
Sun Microsystems, Inc.

The long-term goal of this partnership is to establish an operational forecasting system of winds, waves and surge impacting the coastline during the approach and landfall of tropical cyclones. The results of this forecasting system would provide real-time information to the National Hurricane Center during the tropical cyclone season in the Atlantic for establishing improved advisories for the general public and federal agencies including military and civil emergency response teams. As more people and societal infrastructure concentrate along coastal areas, the United States is becoming more vulnerable to the impact of tropical cyclones. Furthermore, it is not surprising that hurricanes are the costliest natural disasters because of the changes in the population and the national wealth density or revenue. A better understanding of both hurricane frequencies and intensities as they vary from year to year and their relation to changes in damages is of great interest to scientists, public and private decision makers and the general public.

The estimation of tropical cyclone-generated waves and surge in the coastal waters and nearshore zone is of critical importance to the timely evacuation of coastal residents, and the assessment of damage to coastal property in the event that a storm makes landfall. The model predictions of waves and storm surge in coastal waters are functionally related and both depend on the reliability of the atmospheric forcing. Hurricane Georges is an excellent example of an intense tropical cyclone with numerous landfalls and unexpected changes in intensity and movement. Results of real-time forecasting simulations for Hurricane Georges will be presented as the storm segment moved over the Florida Straits and then entered the Gulf of Mexico. As it approached the coast of the central Gulf of Mexico it gradually slowed. Georges made its final landfall near Biloxi, Mississippi early on 28 September with 105 mph winds. Results will include both the predicted wave heights and surge-induced water levels along the Mississippi/Alabama coastline prior and during landfall of Georges. We will also show the variability of these parameters for different forecasted tracks and how such information would impact the advisories.

REPORT DOCUMENTATION PAGE	Form Approved CMB No. 0704-0188

Public reporting burden for this collection of information is estimated to average 1 hour per response, including the time for reviewing instructions, searching existing data sources, gathering and maintaining the data needed, and completing and reviewing the collection of information. Send comments regarding this burden estimate or any other aspect of this collection of information, including suggestions for reducing this burden, to Washington Headquarters Services, Directorate for Information Operations and Reports, 1215 Jefferson Davis Highway, Suite 1204, Arlington, VA 22202-4302, and to the Office of Management and Budget, Paperwork Reduction Project (0704-0188), Washington, DC 20503

1. AGENCY USE ONLY *(Leave blank)*	2. REPORT DATE	3. REPORT TYPE AND DATES COVERED
	31 August 2000	**Final**

4. TITLE AND SUBTITLE
Objective Operational Utilization of Satellite Microwave Scatterometer Observations of Tropical Cyclones

5. FUNDING NUMBERS
Order No:
H-29389D, Amend No. 1

6. AUTHOR(S)
Vincent J. Cardone
Andrew T. Cox

7. PERFORMING ORGANIZATION NAME(S) AND ADDRESS(ES)
Oceanweather Inc.
5 River Road
Cos Cob, CT 06807

8. PERFORMING ORGANIZATION REPORT NUMBER
NA

9. SPONSORING/MONITORING AGENCY NAME(S) AND ADDRESS(ES)
George C. Marshall Space Flight Center
Marshall Space Flight Center, AL 35812

10. SPONSORING/MONITORING AGENCY REPORT NUMBER
NA

11. SUPPLEMENTARY NOTES

12a. DISTRIBUTION AVAILABILITY STATEMENT

12b. DISTRIBUTION CODE

13. ABSTRACT *(Maximum 200 words)*

This study has demonstrated that high-resolution scatterometer measurements in tropical cyclones and other high-marine surface wind regimes may be retrieved accurately for wind speeds up to about 35 m/s (1-hour average at 10 m) when the scatterometer data are processed through a revised geophysical model function, and a spatial adaptive algorithm is applied which utilizes the fact that wind direction is so tightly constrained in the inner core of severe marine storms that wind direction may be prescribed from conventional data. This potential is demonstrated through case studies with NSCAT data in a severe West Pacific Typhoon (Violet, 1996) and an intense North Atlantic hurricane (Lili, 1996). However, operational scatterometer winds from NSCAT and QuickScat in hurricanes and severe winter storms are biased low in winds above 25 m/s. We have developed an inverse model to specify the entire surface wind field about a tropical cyclone from operational QuickScat scatterometer measurements within 150 nm of a storm center with the restriction that only wind speeds up to 20 m/s are used until improved model function are introduced. The inverse model is used to specify the wind field over the entire life-cycle of Hurricane Floyd (1999) for use to drive an ocean wave model. The wind field compares very favorably with wind fields developed from the copious aircraft flight level winds obtained in this storm.

14. SUBJECT TERMS	15. NUMBER OF PAGES
Scatterometer Winds Tropical Cyclones NSCAT QuickScat	**119**
	16. PRICE CODE

17. SECURITY CLASSIFICATION OF REPORT	18. SECURITY CLASSIFICATION OF THIS PAGE	19. SECURITY CLASSIFICATION OF ABSTRACT	20. LIMITATION OF ABSTRACT
UNCLASSIFIED	**UNCLASSIFIED**	**UNCLASSIFIED**	**UL**